IN VITRO AND *IN VIVO* CHARACTERISATION OF A MURINE MODEL OF PULMONARY FIBROSIS

Sharon Ameena Ahmad, BSc., MSc.

A thesis submitted for the degree of Doctor of Philosophy

University of Edinburgh

2002

For my parents, for Sarah, for George,

with love

Declaration

I declare that all the work presented in this thesis is my own, and has been composed and performed by myself. All sources of information, including contributions by colleagues, are fully acknowledged in the text.

This work has not been submitted for candidature for any other degree or professional qualification.

Sharon Ahmad

"Nothing in the world will take the place of persistence. Talent will not, nothing is more common than unsuccessful men with talent. Genius will not, unrewarded genius is almost a proverb. Education will not, the world is full of educated derelicts. Persistence and determination alone are omnipotent. The slogan "press on" has solved and always will solve the problems of the human race."

Calvin Coolidge, 1872-1933

Table of Contents

Acknowledgements

I would like to thank my supervisors, Dr. Sarah Howie and Professor Jonathan Lamb, for their guidance, encouragement, and support through all stages of these studies.

I am very grateful for the technical support and advice from the staff of the Pathology Department and Centre for Inflammation Research, who were a tremendous help in accomplishing the work presented in this thesis. Particularly, Frances Rae, Su Haley, Andrew Jeske, Stuart McKenzie, and Anne Grant. A special thank you to June Stewart for her invaluable assistance with ELISAs and immunohistochemistry. Thanks also to Dr. Shirley O'Dea, who first introduced me to the exciting world of lung perfusions.

Thank you to the members of both the third floor office and the Lamb group, past and present, with whom I have greatly enjoyed working.

Thank you to my friends across the pond, Sheila and Ivana, who have always made the effort, and who lifted my spirits countless times with emails and phone calls.

For all the coffees, drinks, chats, films, advice and viciously competitive games in which I triumphed, thank you to Sharon S. (particularly for transforming me into the laid-back gal that I now am), Georgia, my running buddy Lucy, Armenika, Nicola, Kerry, Kathryn, Vjera, and everyone else I don't have space to mention.

Thank you to Rana, Adele, and Tarick, who make me laugh and remind me that, wherever I go, I'll never be alone. To Sarah, who does so much and to whom I will always be indebted, thank you for everything, including support, visits, trips, pressies, and being an Ahmad just like me.

Thank you to my parents for allowing me to choose my own path, and for always having faith in me. My gratitude and love are endless.

Finally, thank you to George, who makes it all worthwhile. Παντα στιν καρδια μου.

List of Abbreviations

AEC	Alveolar epithelial cell
AIP	Acute interstitial pneumonia
AM	Alveolar macrophage
APC	Antigen presenting cell
BAL	Bronchoalveolar lavage
BIP	Bronchiolitis obliterans with interstitial pneumonia
BSA	Bovine serum albumin
CCR	C-C chemokine receptor
CD	Cluster of differentiation
CD40L	CD40 ligand
CFA	Cryptogenic fibrosing alveolitis
conA	Concanavalin A
cpm	Counts per minute
DAB	Diaminobenzidine tetrahydrochloride
DC	Dendritic cell
DC1	Mature DC (MHC class II^{high}, IL-12-producing)
DC2	Immature DC (MHC class II^{low}, IL-10-producing)
DIP	Desquamative interstitial pneumonia
DMEM	Dulbecco's Modified Eagle's Medium
DMSO	Dimethyl sulfoxide
ECM	Extracellular matrix
ELISA	Enzyme-linked immunosorbant assay
FcR	Fc receptor
FCS	Foetal calf serum
FITC	Fluoroscein isothiocyanate
fs	Forward scatter
FSC	Forward scatter
GIP	Giant cell interstitial pneumonia
GM-CSF	Granulocyte-macrophage colony stimulating factor
H&E	Haematoxylin and eosin

H_2O_2	Hydrogen peroxide
ICAM-1	Intercellular adhesion molecule-1
IL	Interleukin
IL-1ra	Interleukin-1 receptor antagonist
IFN-γ	Interferon-γ
IPF	Idiopathic pulmonary fibrosis
LAd	Loosely adherent
LIP	Lymphoid interstitial pneumonia
MCP-1	Monocyte chemoattractant protein-1
MHC	Molecular histocompatibility complex
MIP-1α	Macrophage inflammatory protein-1α
MMP	Matrix metalloproteinase
NGS	Normal goat serum
NO	Nitric oxide
NSIP	Nonspecific interstitial pneumonia
OVA	Ovalbumin
$OVA_{323-339}$	OVA peptide, amino acids 323-339
PDGF	Platelet-derived growth factor
PGE_2	Prostaglandin E_2
PMN	Polymorphonuclear cell
RBILD	Respiratory bronchiolitis interstitial lung disease
SCID	Severe combined immunodeficiency
ss	Side scatter
SSC	Side scatter
TGF-β	Transforming growth factor-β
Th1	T helper Type 1
Th2	T helper Type 2
TIMP	Tissue inhibitor of metalloproteinases
TNF-α	Tumour necrosis factor-α
TP3	TO-PRO-3
UIP	Usual interstitial pneumonia

Abstract

Cryptogenic fibrosing alveolitis (CFA) is a chronic, progressive and usually fatal lung disorder of unknown aetiology, with a survival curve worse than for many cancers. As patients present in the later stages of this disease with no known natural history, elucidating the pathogenesis of CFA has proven to be very difficult. Thus, experimental animal models are essential in this process, providing much insight into the temporal, cellular and molecular mechanisms behind CFA. The work presented in this thesis is based on a modified murine model of fluorescein isothiocyanate (FITC)-induced pulmonary fibrosis.

The acute phase of the disease was characterised by FITC deposition surrounding the large and smaller airways and blood vessels, and in the alveolar walls, with a granulocytic infiltrate that was replaced over a week by a chronic mononuclear infiltrate. In the chronic phase, after a second dose of FITC, FITC deposition was often accompanied by thickening of the alveolar walls, deposition of fibrous tissue, and occasional B lymphocyte aggregates, all of which were found adjacent to areas of normal lung tissue. Immunohistochemical staining for cell surface proteins suggested that dendritic cells (DCs) may play a role in antigen presentation to lymphocytes in the aggregates, and thus may be the basis for a local humoral immune reaction. A system for scoring the lung fibrosis demonstrated higher levels of fibrosis in areas of FITC deposition compared to FITC-free areas. Moreover, the severity of fibrosis increased with time. Measurement of bronchoalveolar lavage (BAL) cytokine levels suggested that this model may resemble a Th2-like immune response, warranting further investigation.

Both DCs and alveolar macrophages (AMs) were isolated from FITC-treated and PBS control mice. FITC DCs in the chronic stages of the disease were less efficient T cell stimulators than PBS DCs, and may polarise T cells towards a Th2-type response *in vitro* by inducing the production of IL-13. BAL AMs were poorer T cell stimulators than DCs, consistent with published reports, although they were more efficient at T cell stimulation than those from control mice, and may also contribute towards a Th2 polarisation in the later stages of fibrosis.

Preliminary studies into the *in vitro* effect of FITC on lung epithelial cell lines suggest that alveolar epithelial cells (AECs) may be more susceptible to damage by FITC than bronchiolar epithelial cells.

The pathogenesis of CFA is poorly understood, and appropriate therapy relies on the correct understanding of the nature of the lung's response to injury. The FITC-induced model of pulmonary fibrosis characterised in this thesis, once optimised, will enable further study of fibrosis that develops through the inflammatory route. The data resulting from the evaluation of this model have provided insight into new directions for study that could ultimately lead to the development of novel and effective therapeutic interventions in the treatment of CFA.

CHAPTER 1

General Introduction

"Felix qui potuit rerum cognoscere causas"
(Lucky is he who can understand the causes of things)

Virgil 70-19 BC: Georgics

1.1 Alveolar Structure of the Lung

The normal adult lung contains 300 x 10^6 alveoli, which are grape-like structures that branch off terminal bronchioles [1] (Figure 1.1). The alveolar surface of the lung is covered primarily by two distinct types of epithelial cells in an almost balanced numerical proportion. Alveolar type I cells cover approximately 90% of the alveolar surface. They are thin, squamous epithelial cells that cover the pulmonary capillaries, and are required for effective gas exchange. Type II cells are cuboidal in shape and are found at junctions of alveolar septa and along the alveolar surfaces surrounding intrapulmonary vascular and airway structures. This places type II cells in close proximity to endothelial cells, AMs, fibroblasts and other interstitial cells, and implicates their immediate involvement in any processes that occur at the alveolar level [2]. Type II AECs have five known primary functions; first, they secret surfactant; second, they function as ion pumps and move fluid from the alveolar spaces into the subjacent interstitial spaces; third, as these cells represent the stem cell population for alveolar epithelium and can regenerate type I epithelium, they are responsible for repair following alveolar injury; fourth, type II cells control alveolar inflammation by secreting anti-inflammatory cytokines and antioxidants; and finally, they play a role in the metabolism of xenobiotics [3].

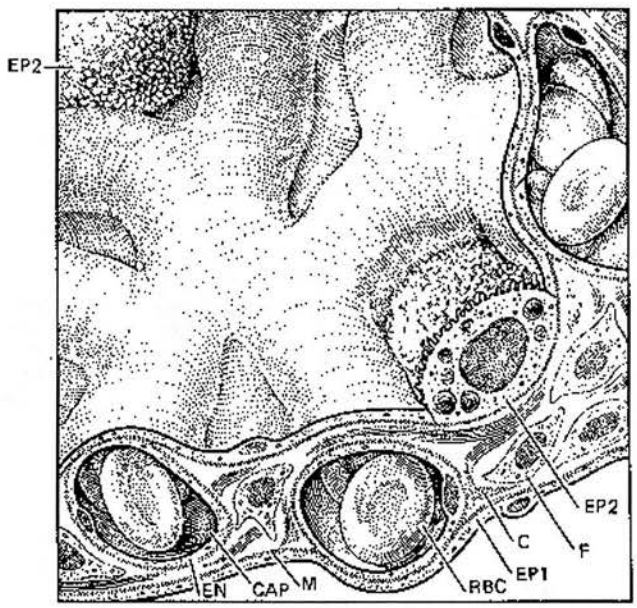

Figure 1.1 High power view of a normal alveolus. The cut surface demonstrates the type I (EP1) and type II (EP2) epithelial cells, endothelial cells (EN), basement membrane (M), red blood cells (RBC) in the capillaries (CAP), fibroblasts (F), and connective tissue (C). Inflammatory cells are not shown. Figure taken from Crystal *et al.* [1] with permission.

1.2 Lung Response to Injury

In most organs, tissue injury is followed by cycles of the normal physiologic response of inflammation and repair. Inflammation leads to matrix stimulation with mesenchymal cell proliferation and altered phenotype that stops the injury and provides temporary repair, and is often in the form of localised and transient scar formation. When the insult or injury is minimal, this is followed by matrix mobilisation, or fibrolysis and apoptosis of the repair cells, with eventual restoration of normal structure and function [4,5]. However, when injury is repetitive or larger in magnitude, the repair process is exaggerated and usually widespread, known as remodelling, and frequently results in scarring or fibrosis [4,6].

In the lung, shortly after injury the alveolar surface becomes denuded, followed by type II pneumocyte proliferation resulting in alveolar re-epithelialisation and the eventual return of the organ to normal function [2]. In chronic tissue injury however, many of the control mechanisms, which normally have a protective effect, are bypassed. A continuous cycle of repair distorts ECM deposition, proliferation of mesenchymal cells, and alteration of normal lung structure that effectively impairs gas exchange functions [7]. This is the fibrotic process (Figure 1.2).

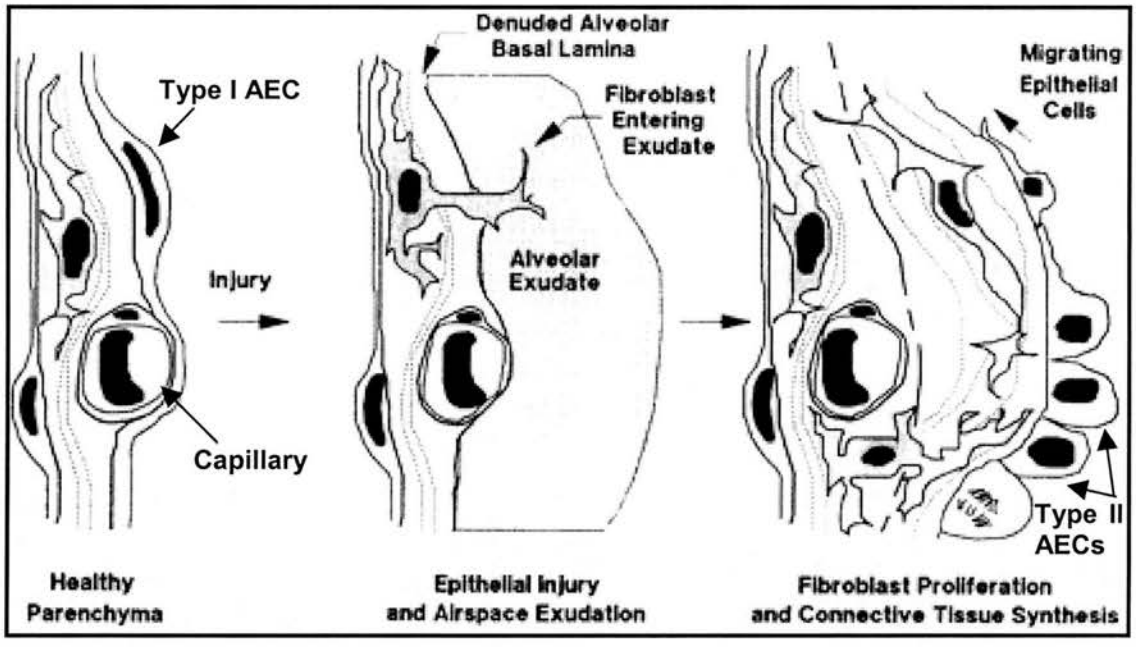

Figure 1.2 Early events in the pathogenesis of lung fibrosis. Figure taken from Crouch [8] with permission. Copyright © 1990 the American Physiological Society.

1.3 Cryptogenic Fibrosing Alveolitis

CFA, also known as idiopathic pulmonary fibrosis (IPF) in North America, is a chronic, diffuse, patchy, irreversible fibroproliferative lung disease of unknown aetiology, for which existing treatments are of limited benefit [5,9-12]. It is characterised pathologically by abnormal proliferation of lung mesenchymal cells, accumulation of excessive amounts of ECM proteins, and extensive lung parenchymal remodelling with accompanying evidence of injury and debatably, inflammation [13-15].

1.3.1 Classification

The interstitial lung diseases refer to a group of many acute and chronic lung disorders with variable degrees of pulmonary inflammation and fibrosis. CFA, now recognised as a distinct clinical disorder, is a subset of the interstitial lung diseases and is one of a family of idiopathic interstitial pneumonias [11,16] (Figure 1.3). Hamman and Rich [17] first described a series of patients who developed what is today considered a variant of CFA. These patients had what the investigators called an "interstitial fibrosis" of unknown cause. It was later called Hamman-Rich disease and was applied to most cases of pulmonary fibrosis at that time. That term is now reserved for acute interstitial pneumonia (AIP). Scadding [18] first introduced the term "fibrosing alveolitis" to define progressive lung disease that was characterised by two histological features present in varying combinations. These were thickening of the alveolar walls, which first appeared cellular but showed an early, and strong, tendency towards fibrosis, and the presence of large alveolar mononuclear cells in the alveolar spaces.

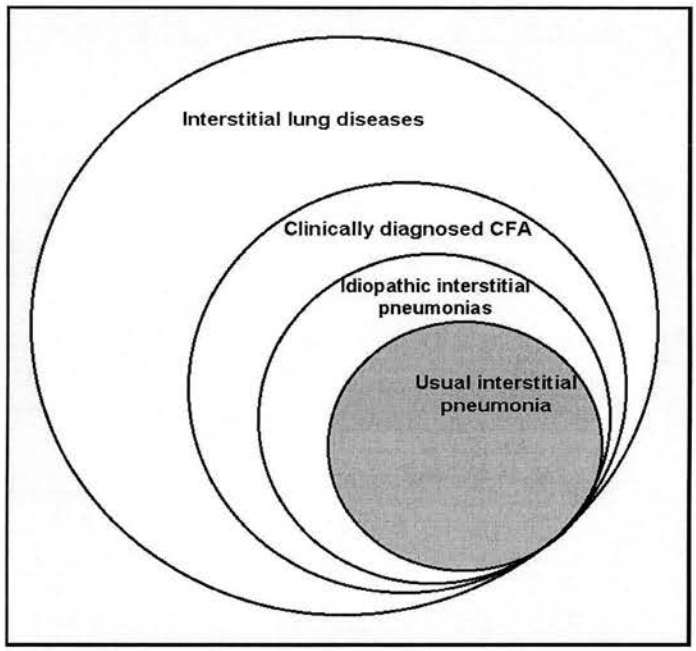

Figure 1.3 Relationships among usual interstitial pneumonia, idiopathic interstitial pneumonias in general, clinically diagnosed cryptogenic fibrosing alveolitis (CFA), and interstitial lung diseases. Usual interstitial pneumonia is the most common histologic pattern in cases previously defined as CFA. Figure adapted from Ryu *et al.* [19]

In 1975, Liebow [20] critically examined the pathologic features of the interstitial pneumonias and divided them into five groups based on specific histologic criteria (Table 1.1). These were usual interstitial pneumonia (UIP), desquamative interstitial pneumonia (DIP), bronchiolitis obliterans with interstitial pneumonia (BIP), lymphoid interstitial pneumonia (LIP), and giant cell interstitial pneumonia (GIP). Other investigators studying these same diseases suggested combining these groups into a single entity, but there was no consensus on the various terms proposed: diffuse interstitial fibrosis, CFA, IPF, classical interstitial pneumonitis-fibrosis, and diffuse fibrosing alveolitis [21-24].

ORIGINAL CLASSIFICATION OF IDIOPATHIC INTERSTITIAL PNEUMONIAS
Usual Interstitial Pneumonia (UIP)
Desquamative Interstitial Pneumonia (DIP)
Bronchiolitis Obliterans with Interstitial Pneumonia (BIP)
Lymphoid Interstitial Pneumonia (LIP)
Giant Cell Interstitial Pneumonia (GIP)

Table 1.1 Liebow classification of interstitial pneumonia. Data taken from Liebow [20].

In 1998, Katzenstein and Myers [10] suggested a revised classification scheme of four histologically distinct forms of idiopathic interstitial pneumonia that comprised the morphologic spectrum traditionally included under the designation CFA. This scheme maintained the UIP and DIP classifications from Liebow, and included AIP (previously Hamman-Rich syndrome) and nonspecific interstitial pneumonia (NSIP), as well as a more limited disorder resembling DIP, respiratory bronchiolitis interstitial lung disease (RBILD). LIP and GIP were excluded because they are not idiopathic, as well as BIP as pathologically it is a predominantly intraluminal rather than interstitial abnormality. These proposals by Katzenstein and Myers have evolved into the current classification system agreed upon in an international consensus statement jointly issued by the American Thoracic Society and the European Respiratory Society [11] (Table 1.2). This consensus statement thus defined CFA, "...as a specific form of chronic fibrosing interstitial pneumonia limited to the lung and associated with the histologic appearance of usual interstitial pneumonia (UIP) on surgical...lung biopsy. The etiology is unknown." Although recent data now suggest that some patients with CFA may also show a pattern of NSIP [25,26], UIP is considered to be the predominant histological pattern equating with CFA [27], and for the purposes of this thesis, the term CFA will refer to idiopathic interstitial pneumonia with a pattern of UIP.

REVISED CLASSIFICATION OF IDIOPATHIC INTERSTITIAL PNEUMONIAS
Usual Interstitial Pneumonia (UIP)
Desquamative Interstitial Pneumonia (DIP)
Respiratory Bronchiolitis-associated Interstitial Lung Disease (RBILD)
Acute Interstitial Pneumonia (AIP)
Nonspecific Interstitial Pneumonia (NSIP)
Idiopathic Bronchiolitis Obliterans Organizing Pneumonia (Idiopathic BOOP or Cryptogenic Organizing Pneumonia)
Lymphoid Interstitial Pneumonia (LIP)

Table 1.2 Current classification of idiopathic interstitial pneumonias.
Data taken from American Thoracic Society [11].

1.3.2 Epidemiology of CFA

There are few data available regarding the epidemiology of CFA. Estimates vary and can depend on the location of the sample population, or other factors such as racial and ethnic predictors, however, the data that do exist suggest that CFA is among the most common of the chronic interstitial lung diseases and may account for a majority of new interstitial lung disease cases [28].

1.3.2.1 Incidence, Prevalence and Mortality

The exact incidence, prevalence and mortality of CFA are not known, although all have been shown to increase with age [29-32]. Patients usually present between the

ages of 50 to 70 years, with two thirds of these patients over the age of 60 at the time of presentation, with a mean age at diagnosis of 66 years [22,23,33,34].

The incidence of CFA has been estimated at 10.7 cases per 100 000 per year for males, and 7.4 cases per 100 000 per year for females [30], although the criteria that provided the basis for these data are not precisely defined. This same population-based study, which focused on all interstitial lung diseases in the population of Bernalillo county, New Mexico revealed a prevalence of 20.2 cases per 100 000 for males and 13.2 cases per 100 000 for females with CFA [30]. In individuals over the age of 75 years, the prevalence exceeded 175 per 100 000. Mortality data estimate a 50 to 70% death rate at five years after diagnosis of CFA [11,25,35]. However, it is thought that mortality associated with CFA is likely to be grossly under-reported, and that epidemiologic data cannot define the high death rate of this chronic disease [12].

1.3.2.2 Genetic Predisposition

It is still unclear whether CFA has a single mechanism of pathogenesis or in fact has numerous causes. CFA appears to cluster in families in up to 3% of cases, suggesting the participation of genetic factors [36-38]. Providing additional compelling evidence for a genetic link is familial CFA, which is identical to the non-familial form of the disease, except that it has been shown to follow a pattern of autosomal dominant inheritance with variable penetrance [38-40].

Indeed, in the series of events leading to pulmonary fibrosis there are many points at which abnormal expression of any number of genes could potentially predispose to the development of pulmonary fibrosis by altering the immunological response to injury, or by modulating collagen metabolism in the lung. Bitterman and Crystal [41] hypothesised in 1980 that insult to the lungs of genetically susceptible individuals may result in CFA as they are unable to control immunologic or inflammatory processes, possibly because the genetic abnormalities could cause increased synthesis of matrix proteins or profibrotic mediators [37].

Pulmonary fibrosis similar to CFA is also frequently observed in autoimmune diseases, including rheumatoid arthritis and systemic sclerosis [42,43]. Humans often show a marked variation in responses to profibrotic agents even at similar levels of exposure, which may also suggest a predisposition to fibrosis [37]. Certain inbred stains of mice show profound differences in their susceptibility to profibrotic agents, and transgenic animals that either lack or overexpress genes involved in the expression of cytokines can develop lung fibrosis [44,45]. Moreover, polymorphisms have been observed in interleukin-1 receptor antagonist (IL-1ra), tumour necrosis factor-α (TNF-α), and major histocompatibility complex (MHC) loci [46,47].

However, there has been no systematic assessment made of CFA heritability and despite all the suggestions of such, there is as yet no clear evidence of a genetic basis for CFA [12,48].

1.3.2.3 Potential Risk Factors

Potential environmental risk factors have been examined in the investigation of the pathogenesis of CFA, with cigarette smoking being the most prevalent [49]. Up to 75% of index patients with CFA have been reported to be current or former smokers, and many of the inflammatory features of CFA are more strongly linked to smoking status than to the underlying lung disease [16]. Cigarette smoking is thought to alter pulmonary immune function, reduce clearance of inhaled agents, and increase respiratory epithelial permeability; it may also cause respiratory bronchiolitis, an entity histologically similar to DIP that may, in turn, lead to fibrosis [50]. However, it is still unclear whether CFA patients who are nonsmokers have a better prognosis than smokers, as conflicting findings have been reported in different series [51].

Several viruses, particularly those of the herpesvirus family, have been implicated in the pathogenesis of CFA, however, there is no clear evidence that convincingly points to a viral cause [52-56]. Other risk factors, such as environmental exposure to

dust [29], commonly prescribed drugs [57,58], gastroaesophageal reflux [59], and exposure to solvents [60] have been suggested. However, the studies which attempt to define these factors have often examined unconfirmed, or solely clinically diagnosed, cases of CFA [48,61].

1.3.3 Pathogenesis of CFA

It has been suggested that CFA is the consequence of sequential acute lung injury that results in irreversible damage to the alveolar surface of the lung; more specifically, it would appear that the ability of type II alveolar cells to restore damaged type I cells is seriously affected [2,16,62]. Supporting histological evidence in the lungs of CFA patients shows cuboidal-shaped hyperplastic type II cells, large reactive elongated epithelial cells which may represent transitional cells among type II and type 1 pneumocytes, microscopic areas of epithelial cell denudation, and areas of honeycomb lesions lined with bronchiolar epithelium [2].

1.3.3.1 The Inflammation Debate

Pulmonary fibrosis has been traditionally viewed as a consequence of chronic inflammation that injures the lung, modulates fibrogenesis, and leads to the end-stage fibrotic scar [10]. However this interpretation has been questioned in recent years because several of the key concepts that formed the basis for this hypothesis are deemed by some to be no longer valid [5,7,16,48,63,64].

The evidence to support the claim that inflammation does not play a major role in CFA pathogenesis is four-fold [48]. Firstly, inflammation is not a prominent histopathologic finding in UIP, but is usually mild, occurs mainly in areas of collagen deposition or honeycomb change, and rarely involves otherwise unaltered alveolar septa [10]. Moreover, foci of proliferating fibroblasts are more prominent

than evidence of inflammation in the lung tissue [65]. Secondly, there is some evidence, primarily from transgenic animal models, that inflammation is not required for the development of a fibrotic response. Adamson *et al.* [66] were able to induce a lung fibrotic response in a blood-free environment suggesting that epithelial injury does not require co-existing ongoing inflammation to stimulate the development of fibrosis; Sime *et al.* [67] showed that overexpression of a replication-deficient adenovirus expressing only active, rather than latent, transforming growth factor-β1 (TGF-β1) induced fibroblast proliferation and progressive ECM accumulation; silica instillation in IL-10-deficient mice induced greater lung inflammation but less fibrosis than wild-type mice [68]. Thirdly, most markers of inflammation fail to correlate with stage or outcome in CFA [48]. Finally, anti-inflammatory therapy does not improve disease outcome [69-71]. For these reasons, recent attention has focused on the ECM and molecules that normally regulate its homeostasis [15].

The new hypothesis suggests that unknown insults provoke multiple microscopic foci, or microenvironments, of epithelial damage and stimulation (Figure 1.4). Following the normal physiologic inflammatory response the altered mesenchymal cell phenotype, rather than being removed by fibrolysis and apoptosis, is retained by avoiding apoptosis. Matrix production persists and fibrolysis is reduced, while activated AECs continue to release factors inducing further fibroblast migration and proliferation and changes in cell phenotype. In the microenvironment of the lesion, myofibroblasts can induce epithelial cell apoptosis and basement membrane disruption, thus contributing to abnormal re-epithelialisation. Other areas outside these microenvironments remain normal in structure and environment. The final result is a patchy, aberrant remodelling of the lung parenchyma [4-7,64].

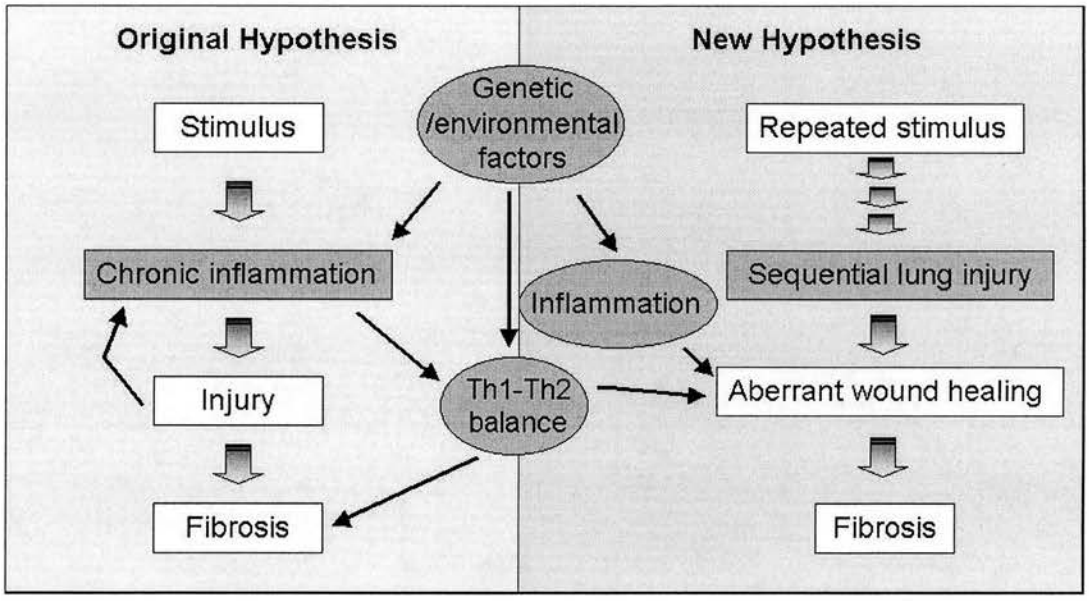

Figure 1.4 Original and new hypotheses for the pathogenesis of cryptogenic fibrosing alveolitis. Traditionally, CFA has been viewed as a result of self-perpetuating chronic inflammation that causes progressive parenchymal fibrosis. Newer theories suggest that CFA is the result of the wound-healing response to sequential lung injury. In both cases, several interacting factors could modify the fibrotic response: genetic background of the patient, the predominant inflammatory phenotype (Th1 or Th2), and environmental inflammatory triggers, such as cigarette smoking, viral infection, and respirable toxins. Figure adapted from Gross and Hunninghake [16].

This new hypothesis, however, is not without its faults. In a recent pro/con editorial on this subject, Streiter [5] raised some interesting points. Most importantly, Streiter suggested that UIP represents the end result of a continuous, untreated process that starts as NSIP and progresses in stages of disease. This is based on findings of interlobar and intralobar variability of idiopathic interstitial pneumonia, and the coexistence of chronic inflammation and fibrosis in a prospective study of patients with idiopathic interstitial pneumonia [26].

The arguments that clinical measurements of inflammation fail to correlate with UIP stage or outcome, and that conventional anti-inflammatory therapy is ineffective [48], imply that UIP is a unique disease rather than the end stage of a process. Streiter states that the evidence, however, supports UIP as being a manifestation of prolonged chronic inflammation and evolving fibrosis, progressing in stages from NSIP, to NSIP with fibrosis, and finally, to UIP [26]. Anti-

inflammatory/immunosuppressive agents in fact demonstrate efficacy in the treatment of NSIP, which represents the early stage of the process; the presence of pulmonary fibrosis itself is more related to the progression of the process making such treatments understandably less efficacious and dependent on the stage of disease of the patient.

Streiter also points to evidence showing that the ratio of T helper Type 1 (Th1):T helper Type 2 (Th2) cytokine expression polarises chronic inflammation [72,73], and suggests that a switch from an initial Th1 response to a Th2-dominated response could be induced by repeated and/or persistent episodes of injury, promoting dysregulated repair with chronic inflammation, fibrogenesis, and finally end-stage fibrosis. The importance of the Th1/Th2 response in pulmonary fibrosis is discussed in the next section.

Streiter's arguments are also supported by Majumdar *et al.* [74], who found evidence of a chronic inflammatory cell profile in a quantitative study of lung biopsies, and du Bois and Wells [51], who state that the histological appearances of advanced lung disease, in the form of "honeycomb" or "end-stage" lung, may be identical in any number of diffuse lung diseases as the lung has only limited responses to injury. It is earlier in disease, they suggest, that individual processes may be distinctive for the nature of the initiating factors and subsequent pathological response, whether this be immunological, inflammatory, or even fibrogenetic.

Thus, the original "inflammatory route" hypothesis suggests that an initial insult or injury to the lung leads to an influx of first acute, then chronic, inflammatory cells (Figure 1.3). The continuing presence of these cells maintains both immunological and inflammatory responses, and therefore is responsible for the progressive disease. In CFA, the number and activation levels of fibroblasts are increased, and as the disease progresses, the interstitial deposition of collagen and other connective tissue matrix proteins interferes with lung function [51,75-77].

The debate regarding the involvement, or lack, of inflammation in the pathogenesis of CFA continues, and indeed is beneficial as it provides potential new therapeutic targets. Perhaps the most insightful comment, however, has been made by Gauldie *et al.* [7], who state that "...inflammation appears necessary but not sufficient to explain the pathophysiology of fibrosis. This would appear more consistent with the suspected natural history of [CFA]."

While the pathogenesis of this disease is highly complex and still poorly understood, many factors, such as cytokines, growth factors, chemokines, and regulators of apoptosis have been implicated in its progression [15].

1.3.3.2 Th2 Cytokine Hypothesis of Fibrosis

Naïve T lymphocytes differentiate into distinct effector cells depending on the cytokine milieu they encounter during activation, and it is the heterogeneity of the responding $CD4^+$ T cell populations that is at least partially responsible for the type of immune response that develops in response to a foreign antigen [78]. Th1 and Th2 polarised inflammation represent two contrasting and mutually antagonistic responses of an organism to an immunogenic insult, in that individual cytokines are able to further stimulate and polarise the prevailing response [6,79]. Expression of these cytokine patterns is classically associated with generation of cell mediated (Th1) and humoral (Th2) immunity, however they are also likely involved in the repair processes that follow acute injury and the subsequent inflammation [6].

A simplified overview of the Th1/Th2 paradigm in the lung suggests that the Th1 response, characterised by cytokines including interferon-γ (IFN-γ), IL-2, IL-12, and IL-18, may be considered a favourable protective response, and is thought to promote repair with restoration of normal tissue architecture; in contrast the Th2 response, characterised by cytokines including IL-4, IL-5, IL-10, and IL-13, and monocyte chemoattractant protein-1 (MCP-1), may favour excessive fibroblast activation, proliferation, and ultimately the deposition of ECM protein and

fibrogenesis [6]. Indeed, in murine models of lung disease, animals whose response to tissue injury is predominantly of the Th2 type are more prone to pulmonary fibrosis after lung injury than those with a predominantly Th1 response [80].

Thus, the fact that Th1 and Th2 cytokines are expressed by many cells and have different functions suggests the potential importance of an imbalance in expression dictating different immunopathologic responses [81,82], and has led to the hypothesis that fibrosis occurs when such an imbalance exists between the Th1 and Th2 cytokines, shifting in a Th2 (type 2) direction [6,83] (Figure 1.5).

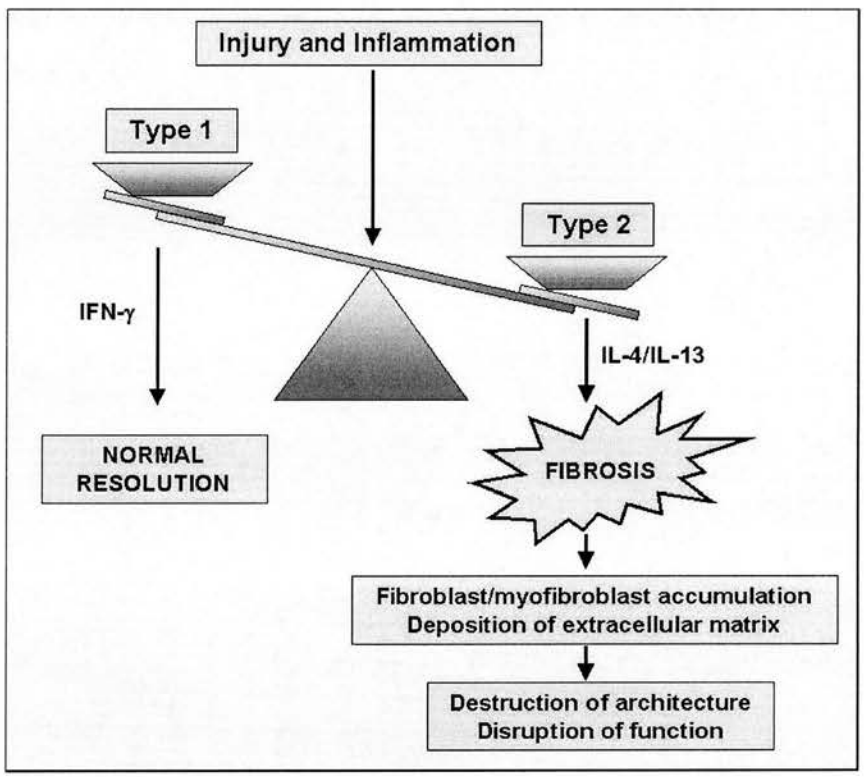

Figure 1.5 The basic premise of the Th2 cytokine hypothesis of the progression of CFA pathogenesis. If, after injury and inflammation, the prevailing cytokine response is shifted in the direction of the type 2 response, fibrosis can develop in the lung. The mechanism(s) by which Th2 inflammation generates tissue fibrosis is still poorly understood. Figure adapted from Sime and O'Reilly [6].

Data supporting the concept that fibrosis occurs when the cytokine balance shifts in favour of the Th2 response originate from both *in vitro* and *in vivo* studies. The inflammatory response in CFA is thought to closely resemble a Th2-type immune response. As in asthma, a classic Th2-mediated inflammatory disease, there are

eosinophils, mast cells, and increased amounts of the Th2 cytokines IL-4 and IL-13 [80,84-86]. Apart from lymphocytes, mast cells, macrophages, monocytes, epithelial cells, and activated fibroblasts have all been shown to produce significant levels of IL-4, IL-10, and IL-13 when appropriately stimulated [87,88] (Table 1.3).

Cell Type	Type 2 Cytokines Synthesised
Mast cells	IL-4, IL-5, IL-10
Epithelial cells	IL-10
Monocytes	IL-10
Macrophages	IL-10, IL-13
Fibroblasts	IL-10

Table 1.3 Non-T lymphocytes cell populations that can synthesise type 2 cytokines. Data taken from Lukacs *et al.* [89]

There is substantial evidence from both *in vitro* and *in vivo* animal studies demonstrating the importance of Th2 cytokines in activating fibroblasts and inducing their proliferation, and the resulting collagen production and deposition. For example, in a model of chronic *Aspergillus fumigatus*, the depletion of IL-13 (but not IL-4) had a beneficial effect on goblet-cell hyperplasia, mucus production, and subepithelial fibrosis [90], while the pulmonary overexpression of IL-13 in the airways of mice has been shown to cause a mononuclear and eosinophilic inflammatory response, mucus cell metaplasia, and airway fibrosis [79], and to induce tissue fibrosis by selectively stimulating and activating TGF-β1 [91]. In the bleomycin-induced model of pulmonary fibrosis, IL-5 and MCP-1 RNA have been reported to be increased, and neutralisation of these cytokines resulted in decreased inflammatory cell recruitment and pulmonary fibrosis [92-94]. Gene expression of IL-4 is also increased in this model [95], and IFN-γ-inducible protein-10 has been shown to inhibit bleomycin-induced pulmonary fibrosis [96]. Silica-induced fibrosis was significantly attenuated in an IL-10 knockout mouse [68], and finally, IL-12 has been shown to attenuate bleomycin-induced pulmonary fibrosis, most likely due to a concomitant increase in intrapulmonary IFN-γ [97].

Animal studies have thus provided much insight into a role for Th2 cytokines in the mediation of pulmonary fibrosis, but recent human studies have confirmed this profile in CFA. Hancock *et al.* [85] detected IL-13 protein in the BAL fluid in the majority of patients with CFA tested but in none of the control subjects, and the proportion of BAL purified AMs expressing IL-13 mRNA was increased in CFA patients. MCP-1 mRNA is strongly expressed in lung epithelial cells from patients with CFA, but not in cells from non-CFA patients [98], while MCP-1 levels are increased in the BAL fluid from CFA patients [99].

Perhaps most significantly, the presence of the Th2 cytokine IL-4 has been shown to predominate over the expression of IFN-γ in CFA patients [100,101]. Belperio *et al.* [102] speculate that this pattern of cytokine expression may suggest a potential role for the humoral response in CFA pathogenesis, or more likely, the inability of IFN-γ to tilt the balance away from a Th2-dependent profibrotic environment. This finding by Wallace *et al.* [100,101] was confirmed in a separate study, where it was also noted that Th2 cytokines were increased in CFA patients relative to systemic sclerosis patients [74]. The importance of this finding is noted [6] in that systemic sclerosis patients have lower levels of Th2 cytokines, as well as increased numbers of cells expressing Th1 cytokines, compared to CFA patients. As this is coupled with a less aggressive disease, it suggests the cause is a more favourable balance between the profibrotic Type 2 and antifibrotic Type 1 responses [6]. Further substantiation is found in the recent suggestion that IFN-γ treatment of CFA patients who failed to respond to glucocorticoids may be beneficial [103].

It must be mentioned, however, that in CFA one only sees end-stage disease, and therefore it must be with caution that the Th1/Th2 balance is emphasised. The early events in humans that result in disease are unknown, and while we can extrapolate from animal models, they too have their problems. Animal models of pulmonary fibrosis will be discussed further on.

1.3.3.3 *Autoimmunity in CFA Pathogenesis*

There are several factors that together, provide compelling evidence for an immunological pathogenesis for CFA. In patients with CFA, there have been reports of increased numbers of neutrophils, eosinophils, $CD4^+$ and B lymphocytes, and plasma cells [104,105], while stimulation of polyclonal B lymphocytes results in increased peripheral blood immunoglobulin concentration [106]. Increased B cell numbers have been associated with a poorer prognosis in CFA, and BAL fluid from CFA patients has increased B cell growth factor activity [107] and immunoglobulin [104] as compared to normal subjects. There are also immune complexes present in the blood, BAL fluid and tissue of CFA patients [108-112]. Non-organ-specific circulating autoantibodies have been found in approximately 40% of CFA patients [113], and include antinuclear and rheumatoid factor antibodies, anti-DNA topoisomerase II antibodies, and anti-cytokeratin 8 and 18 antibodies [111,112,114-118].

The variable expression of autoantibodies has led to the suggestion that they represent a non-specific consequence of lung inflammation and injury, and may not even be a primary cause of tissue damage, but rather augment the inflammatory response [106]. However, specific immunohistochemical data have shown the presence of circulating IgG autoantibodies to hyperplastic type II epithelial cells, and to a type II epithelial cell-derived cell line, in patients with CFA, which indicates an endogenous and lung-specific autoantigen and suggests a site where immunological injury could occur in CFA [119,120]. Wallace *et al.* [120] also noted that the distribution of the putative autoantigen in the lung tissue appeared to correlate with that described for immune complexes [121]. This group subsequently found that antibody raised against the autoantigen they had described induced increased secretion of profibrotic cytokine TGF-β, and tenascin, an ECM protein, in the type II epithelial cell line A549, and that decreased A549 cell numbers appeared to be a cytostatic effect [122,123]. Interestingly, they suggested that *in vivo*, the autoantibody could delay the re-epithelialisation of the damaged alveoli after lung

injury, which would provide a mechanism for promoting fibrosis by dysregulation of fibroblast activity [66,122,124].

Hapten immune pulmonary interstitial fibrosis is mediated by an immune response against hapten-modified self antigen, and with its abnormal regulation of inflammation in the lung and unresolved fibrosis, is a useful animal model for studying the autoimmune process in pulmonary fibrosis [125]. Work on this model has shown that the infiltration of immune inflammatory cells that contribute to the fibrogenic process is dependent on alteration of the suppressive phenotype of the resident AMs [126]. Investigation of the mechanisms that might restore the immunosuppressive phenotype of the AMs in the lung could lead to novel therapies for patients with autoimmune-regulated CFA. Furthermore, the participation of CD40/CD40 ligand (CD40L) interactions, which have been identified as important in lung injury models of pulmonary fibrosis mediated by oxygen or radiation [127,128], and more recently directly implicated in human CFA [6], were required to elicit the secondary immune responses that lead to pulmonary fibrosis in this model [129].

Finally, an interesting study by Kaneko *et al.* [130] recently demonstrated that the costimulatory molecules CD80 (B7.1) and CD86 (B7.2) were expressed without class II MHC molecules in AECs in lung tissue from CFA patients. They suggest that the dysregulation of these molecules in AECs may lead to the activation of autoreactive T cells, which might then contribute to CFA pathogenesis.

Although the pathogenesis of CFA remains elusive, the participation of the humoral immune response cannot be discounted. Further investigation is warranted to identify the exact role of the autoantigen specificities identified in sera from CFA patients. Questions remaining to be answered involve determining whether the autoantibodies represent evidence of ongoing injury or if they are initiating the injurious process, and if their presence is amplifying a cycle of inflammation and fibrogenesis that is already established [106].

1.4 Antigen Presenting Cells (APCs) in the Lung

Regardless of the role that inflammation may or may not play in CFA pathogenesis, there is certainly an immune response occurring in the lungs of CFA patients. As any T cell response depends upon activation by an APC, a role for these cells is indicated. There are many cells in the lung that could potentially act as APCs: epithelial cells, fibroblasts, endothelial cells, neutrophils, T and B lymphocytes, AMs, and DCs. The minor players in terms of antigen presentation are T cells, epithelial cells, fibroblasts and endothelial cells, which have inducible MHC molecules [131,132].

B lymphocytes are present in normal human lung tissue, but lymphoid aggregates containing B cells are scarce in the mucosa and are less well organised than in bronchus-associated lymphoid tissues described in other species [131]. B cells constitutively express MHC class II molecules, and play an important role in initiating immune responses [133]. They utilise antigen-specific membrane immunoglobulin and pinocytosis to effectively internalise antigen [134], although they have not been documented to migrate from tissues into draining lymph nodes bearing antigen as do DCs.

Thus, the vast majority of antigen presentation in the lung is the responsibility of the AMs, which police the alveolar surfaces in the deep lung, and the "professional" APCs, the DCs, which form a contiguous network within, and directly below, the airway epithelium and throughout the alveolar interstitium [135]. The airways and alveoli constitute a large surface that is continuously exposed to antigen. AMs are likely the first cells to encounter invading particles in the lung, and can release anti-inflammatory cytokines or inflammatory mediators. If the epithelial surfaces are disrupted, however, a local network of DCs is ready to take up antigens and migrate towards the lymph nodes to trigger T cells in the central immune response [135]. This review will focus on DCs and AMs. The isolation of lung APCs is discussed in Chapter 5.

1.4.1 DCs in the Lung

DCs originate from progenitors found in the bone marrow and, after circulating in the blood, migrate to all lymphoid organs and most nonlymphoid organs, including heart, liver, kidney, skin, gut and lung [136,137]. Upon arrival, DCs are in an immature state characterised by high antigen uptake capacity and low surface expression of MHC class II and T cell costimulatory molecules CD80 and CD86. [138]. In the tissues, DCs constantly sample their environment for antigen. Once in contact with antigen, and in the presence of "danger" signals [139], DCs begin to mature; antigen uptake and processing capacity decrease while MHC class II and T cell co-stimulatory molecules are upregulated on the surface of the cell.

In the murine lung, DCs form an extensive network in the airway epithelium, alveolar septae and in connective tissue surrounding pulmonary veins and airway vessels, from which they can sample the environment for antigen [140-143]. DCs are thought to have a high turnover rate at mucosal surfaces, where they are in constant contact with inhaled particles or organisms [144]; Holt *et al.* [145] have estimated a three day turnover for epithelial DCs in the rat, and this rapid rate is consistent with a surveillance or "sentinel" role for these cells. After antigen uptake in the airways, DCs migrate to the paracortical T cell zone in the draining lymph nodes of the lung, where they come into contact, and interact, with naïve T cells [146].

Under inflammatory conditions, immature DCs are thought to be recruited by inflammatory chemokines such as macrophage inflammatory protein (MIP-1α), MIP-3α, MCP 1-4, and TNF-α [147,148]. Maturation at the site of injury can be induced by the release of oxygen radicals, heat shock proteins, and changes in the balance between suppressive [IL-10, prostaglandin E_2 (PGE_2), nitric oxide (NO)] and inflammatory mediators [TNF-α, granulocyte-macrophage colony stimulating factor (GM-CSF), IL-1) [149]. Critically, DCs that have recognised and taken up foreign antigen must migrate to the draining lymph nodes, against chemotactic gradients that attract immature DCs into the inflammatory site. To achieve this, maturing DCs

produce inflammatory chemokines leading to ligand-induced downregulation of C-C chemokine receptor 1 (CCR1), 5, and 6, and upregulation of others [150]. The nonmigratory DCs situated around lung venules and within the alveolar wall, therefore, are responsible for presentation and amplification of effector T cell reactions during the effector and/or memory response.

1.4.1.1 Phenotypic Heterogeneity of Lung DCs

A phenotypically diverse population of DCs appears to exist in the lung [151]. Two distinct populations of DCs, lymphoid and myeloid, have been described in the murine spleen [152,153], however lung DCs do not completely correspond to either of these strict designations [154]. A number of groups have phenotyped DCs isolated from lung tissue with varying results, often reporting more than one distinct population, and depending on variables such as whether freshly isolated or cultured cells were phenotyped, or the method of isolation. Murine lung DCs utilise multiple accessory molecules to transmit activation signals to counter receptors on T cells, including CD11a, CD40, CD80 and CD86, and intercellular adhesion molecule-1 (ICAM-1) [154], and these markers, along with many others including CD11b, a marker of myeloid lineage [152] and possibly maturation [153], CD8α, a lymphoid-related marker [152], DEC-205, a lectin-like receptor shown to be involved in antigen processing by DCs [138,155], F4/80, a myeloid marker, and Fc receptor (FcR) [142], are used to identify and characterise murine lung DCs. A recurrent problem, however, is the lack of specific DC markers. Therefore, combinations of MHC class II and the integrin CD11c expression intensity are predominantly used as murine lung DC markers [156], again with variable results.

For example, Lipscomb and colleagues [154,155,157] showed that DCs isolated from the lungs of mice existed in two populations, differentiated on the basis of high and moderate MHC class II expression. They examined both populations for expression of accessory molecules on freshly isolated and cultured DCs. The majority of freshly isolated DCs expressed moderate levels of MHC class II and ICAM-1, and low

levels of CD80, CD86, CD40, and CD11a, all of which increased after culture. Expression of MHC class II on DCs seemed to coincide with the expression of several accessory molecules, with those expressing high levels of MHC class II having greater expression of CD80, CD86, CD40, CD11a, and ICAM-1 than DCs with moderate class II levels. Accessory molecule expression also increased after culture on class II high-expressing DCs. The majority of fresh DCs expressed moderate levels of CD11b that didn't change after culture, but those DCs with the highest levels of class II MHC also expressed the highest levels of CD11b.

Vermaelen *et al.* [138] selected only $CD11c^{+}$/low autofluorescence cells, and found the majority expressed MHC class II, although intensity was not reported. Interestingly, after an overnight adherence step without the addition of cytokines, they did not find any expression of CD8α, F4/80, CD80, CD86, or CD40. They suggested that this may be the result of the overnight adherence step. Moderate to high levels of expression were found for DEC-205, ICAM-1, CD11a, and CD11b.

Gonzalez-Juarrero and Orme [158] phenotypically identified three distinct lung DC populations after overnight culture in GM-CSF, based on cell surface expression of CD11c and MHC class II antigens analysed by flow cytometry. The first population was comprised of small cells [forward scatter $(FSC)^{low}$, side scatter $(SSC)^{low}$] that stained MHC class II^{low}, $CD11c^{low}$. The second population consisted of large cells with low granularity (FSC^{mod}, SSC^{low}) that stained MHC class II^{high}, $CD11c^{low}$. The third population was made up of larger and more granular cells (FSC^{high}, SSC^{high}) that stained MHC class II^{low}, $CD11c^{high}$. Most of the cells exhibited what is considered an immature phenotype ($CD11c^{mid\ to\ high}$ and MHC class II^{low}) [159,160]. A small number of more mature cells (MHC class II^{high}) [161] was also seen, as described by Lipscomb and colleagues (above) [157], and elsewhere [145]. After seven day expansion in GM-CSF, these lung DCs were MHC class II^{low} and $CD11c^{low\text{-}high}$. They were negative for CD8α, expressed low levels of F4/80, high levels of CD11a, CD11b, and ICAM-1. In addition, most cells expressed CD80, but only a small percentage expressed CD40 or CD86.

Finally, Gong *et al.* [151] examined rat lung and found that airway epithelial DCs constitute a distinct subset of pulmonary DCs. Airway DCs did not express ICAM-1 and only showed low expression of MHC class II. Greater than 50% of these cells displayed FcR. In contrast, the majority of parenchymal DCs were ICAM-1 positive, while less than 5% expressed FcRs, and all were intensely positive for MHC class II expression. Functionally, they also showed that the airway DCs were more effective stimulators of antigen-induced T cell proliferation than parenchymal DCs, while the latter were superior in stimulating proliferation of allogeneic T cells. Therefore, both groups were found to be heterogeneous, and the authors suggest that this reflects the continuous turnover that these cells undergo in the lung.

These studies show the considerable phenotypical and functional heterogeneity that exists in DCs, and reflect their different levels of maturity and function [145,151]. The capacity of DCs for antigen uptake and processing is highly dependent on the state of differentiation (Table 1.4).

	AM	**DC**	
		mature	**immature**
Lung Distribution	Alveoli	Tissue network	Nodes (tissue?)
Function			
Immunity	Innate immunity	Specific immunity	
Phagocytosis	++++	+++	+
TNF-α, IL-1 production	++++	+++	±
T cell activation	+	++	++++
Cell surface expression			
MHC class I	++	+++	++++
MHC class II	++++	+++	++++
Costimulatory molecules			
CD40	±	+	+++
CD80	±	+	+++
CD86	±	+	+++

Table 1.4 Phenotype and function of murine alveolar macrophages and dendritic cells. Table adapted from Nicod *et al.* [131].

1.4.1.2 *Immunoregulatory Functions of Lung DCs*

The mechanisms by which lung DCs activate the immune response, and how the cytokines produced by DCs themselves and their microenvironment could promote the development of deviant responses in the lung, have not yet been elucidated, and remain important questions to be answered [162].

DCs are unique in their capacity to induce primary immune responses, although this function is closely related to their maturational state. Consistent with the high antigenic load at these sites, respiratory and intestinal mucosal DCs are functionally specialised for antigen uptake [163]. However resident tissue DCs are predominantly functionally immature in terms of naïve T cell activation in order to prevent the initiation of potentially damaging immune responses, and generally do not acquire this capacity until they have left the tissue site and migrated to peripheral lymph nodes [136]. Precocious or unregulated *in situ* maturation of respiratory tract DC functional activity may lead to excessive T cell activation within the airway mucosa and to damaging local pathology in response to continuous environmental antigen exposure, a scenario that has been proposed for the aetiology of chronic asthma [164]. Studies correspondingly indicate that the majority of murine respiratory tract DCs express low levels of surface MHC class II, and produce IL-10 but minimal IL-12 - an immature phenotype that favours Th2 cell differentiation [165,166], although as discussed above, there is clearly a degree of heterogeneity. These DCs, which are predominantly of myeloid origin, are alternatively termed DC2s and preferentially stimulate Th2 cell development [167]. In contrast, mature DC1 cells isolated from peripheral lymphoid organs, express CD8α and stimulate the generation of Th1 cells through the production of IL-12 [166]. It should be noted that this concept was originally described for human DCs, in which there is a reversal of the murine system: DC1s are monocyte-derived cells and, therefore, of myeloid origin, whereas DC2s express T cell markers and are probably of lymphoid origin [168].

This evidence suggests two separate DC lineages, however Kalinski *et al.* [169] showed that subset-independent DCs can give rise to either a Th1 or a Th2 response, and demonstrated the importance of the microenvironment during maturation, suggesting that the ability of DCs to induce a particular type of Th response is predetermined in the tissues by the character of the local inflammatory response that induces the final DC maturation. Most likely, the solution will fall between the two theories, although there is not yet a final conclusion on this subject.

Th1/Th2 differentiation may also be influenced by the interactions of costimulatory molecules on APCs with their ligands on $CD4^+$ T cells. Studies in other organs have shown the importance of CD40-CD40L and CD80/CD86-CTLA-4/CD28 interactions in Th2 generation [170]. Furthermore, the cytokines present in the microenvironment, IL-4/IL-10/IL-13 vs. IL-12, play a decisive role in orchestrating the differentiation along the Th1 or Th2 lineage [171], and *in vitro* and *in vivo* data suggest that IL-12 production by DCs can also be modulated by microenvironmental tissue factors, as well as pharmacological agents. PGE_2 [169,172], β2-agonists [173], histamine [174], and NO [175] have all been identified as inhibitors of IL-12 production and thus favouring Th2 differentiation. Taken together, these findings support the theory that induction of either Th1 or Th2 differentiation depends on both the DC maturation state and on the influence of environmental factors [176] (Figure 1.6).

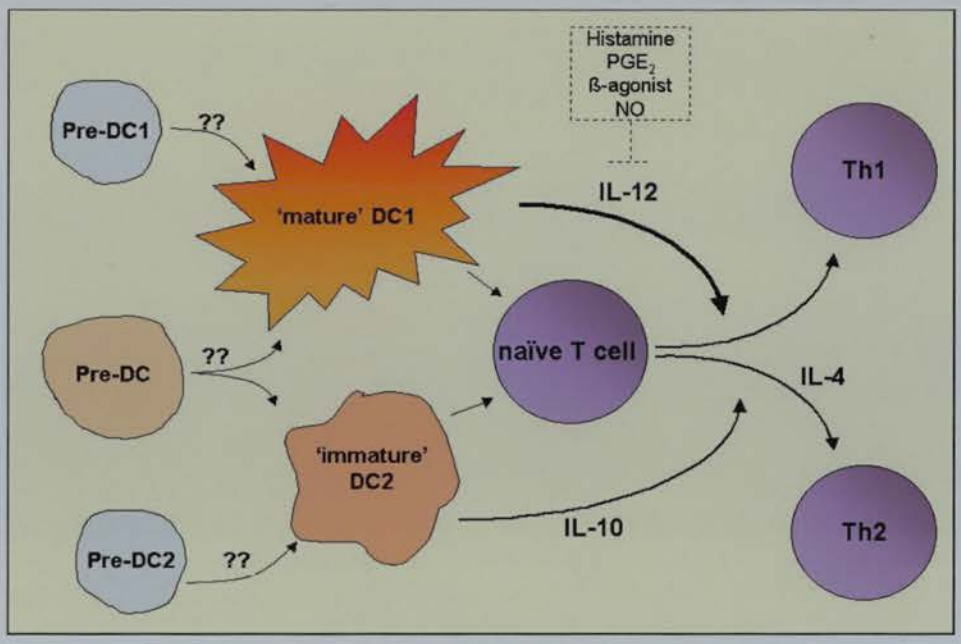

Figure 1.6 DC regulation of Th cell differentiation. Differentiation along the Th1 or Th2 pathway is triggered by stimulation with the antigen-MHC complex presented by the appropriate APC. The mature DC1, which may represent a separate lineage or share the same precursor as the immature DC, produces IL-12 that drives Th1 differentiation. The immature DC2, in contrast, does not produce IL-12, thus possibly providing a permissive environment for Th2 differentiation. Figure adapted from Sinigaglia and D'Ambrosio [176].

Presentation of antigen by DCs is not by itself sufficient to activate T cells. The potent capacity of DCs to activate immunologically naïve T cells is related to both their high constitutive expression of MHC class II and T cell costimulatory molecules, such as CD40, CD80, and CD86. Deficiency or absence of expression of these molecules reduces the APC function of DCs, and may render them potentially tolerogenic, and thus the T cells become unresponsive or fail to proliferate [177]. Recent studies suggest that *in vitro*-generated myeloid murine DCs with an "appropriate" surface phenotype (immature DC2s or "costimulatory molecule deficient") or $CD8\alpha^+$ lymphoid DC1s can subvert allogeneic T cell responses [178].

1.4.2 AMs in the Lung

Although ultimately macrophages derive from common haematopoietic precursors, they differ considerably in various tissues with respect to morphology, secretory products, surface phenotype and function [179]. In particular AMs, which comprise, by number, approximately 85% of free cells in the alveoli [144], are a distinctive cell type in a unique environment where they function to phagocytose and neutralise a large daily burden of foreign organisms and particles that reach the distal airways [180]. Clearance of these particles must be accomplished without excessive inflammation that could compromise gas exchange, suggesting that AMs are specialised phagocytes [179]. Indeed, AMs have been shown to differ from other macrophage populations in terms antigen-presenting capacity [181]; the better AMs are at phagocytosis, the poorer their antigen presenting capacity, and they are known to suppress T cell proliferation in the lung [144,182,183].

AMs reside within the airways at all levels of the respiratory tract, in the lamina propria, the interstitium, the alveolar regions and pleura, and within pleural spaces [184]. They are normally isolated from lungs by BAL [185], and this method is discussed further in Chapter 5.

1.4.2.1 Phenotype of AMs in the Lung

Pulmonary macrophages are both phenotypically and functionally diverse [184] (Table 1.4). Within subpopulations, AMs differ in expression of MHC class II, Fc and complement receptors, phagocytic capacity, cytokine production, and responses to chemotactic stimuli, and attempts to characterise them can exploit many of these factors [186-188]. Phenotypically, the majority of AMs have been shown to express high levels of cell surface CD11a, CD11c, and F4/80, with variable expression reported for MHC class II, CD11b, CD40, and other markers [131,179,184,189,190], and very little, if any, expression of accessory molecules such as CD80 and CD86

[191]. In some pathological states such as sarcoidosis, however, AMs express high levels of CD86 and CD40 [192], and this is despite their apparent end-stage differentiation state. In fact, similar changes have been found when murine AMs have been exposed to bleomycin [193].

1.4.2.2 Functions of AMs in the Lung

It is well established that resting AMs help to create an immunosuppressive environment in which the initiation of immune responses and the activation of antigen-specific T cells in the lung are limited [194]. Suppressed pulmonary immune responses, however, can be overcome by exposure to infectious agents or foreign antigens [195], and the suppressive activity of AMs specifically, can be inhibited by exposure to GM-CSF [196].

AMs phagocytose and neutralise foreign organisms and particles that reach distal airways, and produce oxygen radicals, cytokines, lysozyme, complement and many other substances. However, when AMs are exposed to bacterial products such as lipopolysaccharides, they release higher levels of cytokines such as TNF-α compared to peripheral monocytes, which release higher levels of IL-10 compared to AMs [197]. This demonstrates the higher inflammatory properties of AMs that may theoretically influence the phenotype and maturation stage of DCs in their vicinity. Nicod *et al.* [131] propose that AMs could influence neighbouring DC activation, and Th1/Th2 differentiation could be influenced when memory T cells migrate to the vicinity of interstitial DCs, while macrophages release either IL-10 or IL-12.

1.5 Animal Models of Pulmonary Fibrosis

Animal models are useful and necessary tools for investigating the factors involved in the pathogenesis and progression of pulmonary fibrosis. The majority of the animal models of pulmonary fibrosis have been produced in rodents, although rabbits, pigs, and primates have been used to a limited extent. Many rodent models, each with its own distinguishing features, have been produced, but this discussion will focus on the well-accepted models of silica-, ionising radiation-, and bleomycin-induced pulmonary fibrosis, as well as the FITC-induced model.

1.5.1 Silica-induced Model of Pulmonary Fibrosis

Silicosis is the fibrotic lung disease caused by the inhalation of damaging amounts of respirable free crystalline silica [198]. It is a progressive disease characterised by the persistence of pulmonary interstitial inflammation leading to increased proliferation of fibroblasts and exaggerated production of collagen [199,200]. Several cell types, including predominantly AMs, but also fibroblasts and epithelial and endothelial cells, play a central role in the inappropriate inflammatory lung response and in the development of silicosis by releasing a variety of mediators such as proinflammatory cytokines (e.g. TNF-α, IL-1, IFN-γ [201]) and factors that promote mesenchymal cell growth [68].

Although the mechanisms involved in the initiation of pulmonary inflammation and lung disease in silicosis are still under investigation [202], this model of has provided valuable insight into the complex role of the Th2 response in the development of pulmonary fibrosis. While increased Type 2 activity has been reported in the mouse silicosis model [203], the same group also found that the Type 2 cytokine IL-10 mediated different types of lung responses depending on the type of inflammatory cells involved, and suggested that when looking at human data, the stage of the

pulmonary disease needs to be carefully taken into account to interpret changes in IL-10 levels [68].

Similarly, while IL-9, a T cell-derived cytokine active on both T and B lymphocytes, has been shown to reduce the lung fibrotic response to silica and was accompanied by an expansion of lymphocytes in the lung as well as a reduction of the Th2 response to silica [204], production of IFN-γ, a Th1 cytokine, was also increased by lymphocytes in a mouse model of silicosis [205].

1.5.2 Radiation-induced Model of Pulmonary Fibrosis

The lung is particularly sensitive to cell injury induced by irradiation [206]. Relatively high and repeated doses of radiation often lead to pulmonary fibrosis, while continued doses of radiation produce continued pulmonary injury [207]. Endothelial cells have been identified as the predominant sites of cell injury induced by irradiation, and delayed repair following severe injury to the endothelium may cause an extended period of surface denudation with concomitant loss of fibroblastic control, resulting in cell proliferation and collagen deposition; it has been postulated that prolonged disruption of the normal endothelium-fibroblast control system is the crucial event in radiation-induced pulmonary fibrosis [206]. However, this is also accompanied by pulmonary oedema, death of type I alveolar cells, hyperproliferation of type II cells, and pneumonitis [207].

Radiation-induced pulmonary fibrosis has provided additional evidence of a role for the Th2 response. Both protein and gene expression of the prototypical Type 2 cytokine IL-4 have been reported in AMs [208] and $CD4^+$ T cells [209] in a rat model of the disease. Moreover, the finding that inbred strains of mice differ in their propensity to develop lung fibrosis after exposure to radiation [210] provides a useful model to identify genetic factors influencing this trait. Studies of the time course to develop lung damage in mice support the theory that there are strain differences in susceptibility [211], and research into this area could provide the basis for

determining similar events in the human form of the disease as there are currently no assays, either genetic based or otherwise, available to determine individual susceptibility to radiation-induced lung damage.

1.5.3 Bleomycin-induced Model of Pulmonary Fibrosis

Bleomycin is a cytotoxic agent used effectively in the treatment of various types of human cancer as it does not induce major myelosuppression or immunosuppression, however it soon became apparent that bleomycin exhibits a dose-dependent pulmonary toxicity and induces pulmonary fibrosis [58,212]. This toxic effect of bleomycin has been utilised advantageously in a number of experimental approaches to pulmonary fibrosis in animal models. The bleomycin model is the most used experimental model of pulmonary fibrosis, and is a paradigm of the inflammatory route [64].

Pulmonary toxicity due to bleomycin probably has multiple mechanisms, including direct tissue toxicity of the drug and indirect toxicity through amplification of pulmonary inflammation, which work both in sequence and simultaneously [58,213]. Bleomycin administration in rodents results in a dose-, route-, and strain-dependent pulmonary inflammatory response that is characterised by increased leukocyte accumulation, fibroblast proliferation, and lung collagen content [213-216]. During the initial stages of lung injury, bleomycin binds to DNA and iron which induces free radical formation, resulting in lung lipid peroxidation and injury [213,216,217].

Typically, intratracheal instillation of bleomycin causes a type I pneumocyte necrosis up to one day post-challenge, followed by acute alveolitis on day two or three, and an intense interstitial inflammation after 4-12 days [218-220]. In addition, initiation of fibroblast proliferation and synthesis of ECM occurs 4-14 days post-challenge, and a two-fold elevation in collagen content is found three weeks post-challenge [214,215,219]. Fibrosis is seen within the interstitium and the alveoli, leading to end-stage diffuse pulmonary fibrosis [214,219]. Thickening of the alveolar septa and

loss of lung elasticity result from these pathologic changes in pulmonary architecture, and lead to significant morbidity in the animal. As these features are similar to those seen in the lungs of humans with CFA, the rodent pulmonary inflammatory response to intratracheal bleomycin instillation is thought to constitute a representative model of human CFA [221,222].

However, the bleomycin model has recently been criticised as not resembling the human CFA [223]. A recent long-term study using bleomycin-induced lung injury in rats found that in the late chronic stages the model did not behave as a restrictive syndrome, nor was the histologic pattern compatible with the particular histologic pattern of UIP, which defines CFA in humans [223]. In addition, they noted that a number of animal studies have shown a reduction in histologic and biochemical markers of fibrosis in the bleomycin model with the use of anti-inflammatory and antifibrotic agents [224-227], whereas in humans CFA generally does not respond to treatment with these agents [10]. Additional problems with the bleomycin model are discussed in Chapter 3.

Although the features of bleomycin-induced lung injury are well established, the pathogenesis of its subsequent progression and evolution has not yet been determined [228,229]. Thus, many factors have been investigated which are relevant to the study of CFA pathogenesis.

TGF-β is thought to be one of the most important factors in pulmonary fibrosis, and production of this cytokine has been widely demonstrated in bleomycin-induced pulmonary fibrosis in mononuclear cells, fibroblasts, eosinophils, bronchial epithelial cells, and endothelial cells [230-232], although activated AMs are considered the predominant source [233-235].

TNF-α production has been reported to be increased [220,230] and also unchanged [236] in mice administered bleomycin, and the importance of C-C chemokines and their receptors [219,222,237], are coming to the forefront in bleomycin-induced pulmonary fibrosis research, as is the role of adhesion molecules [238,239]. The

administration of IL-12 leads to increased IFN-γ production and a decrease in pulmonary fibrosis in mice administered bleomycin, suggesting that a Th1 cytokine profile is beneficial in attenuating the fibrotic response [97].

As with radiation-induced pulmonary fibrosis, there are strain differences in sensitivity to bleomycin-induced fibrosis, with BALB/c mice considered to be a "resistant" strain [240,241]. Interestingly, Gur *et al.* [242] demonstrated only a mild and delayed increase in IFN-γ secretion in bleomycin-treated BALB/c mice, in contrast to C57BL/6 mice. Subsequently, this group showed that treatment with cyclosporin A, a potent immunosuppressive agent, augments the development of bleomycin-induced lung fibrosis in BALB/c mice, and that this was associated with increased secretion of IFN-γ [229]. Thus they suggest that the resistance of BALB/c mice to bleomycin-induced pulmonary fibrosis may be mediated in part by the prevalence of a Th2 response, and a decreased Th1 response, in this strain.

1.5.4 FITC-induced Model of Pulmonary Fibrosis

In 1995, Roberts *et al.* [243] described a novel model of pulmonary fibrosis induced in mice and rats by a single, surgical intratracheal instillation of the fluorescent haptenic antigen FITC. The FITC remained in the interstitium associated with the connective tissue for up to five months, at which time there was patchy pulmonary fibrosis. A chronic mononuclear interstitial infiltrate, dominated by T lymphocytes, was localised to areas of FITC deposition, and serum antibodies against FITC were demonstrated.

Further characterisation of this model [244] confirmed these findings in both BALB/c and C57BL/6 mice, and demonstrated quantifiable increases in lung collagen content. They also found that the development of fibrosis was independent of T cell-specific immunity, although they only evaluated the model in the short term (day 21). CCR2 knockout mice were subsequently shown to be protected from

fibrosis in the FITC model, suggesting that CCR2 activation leads to the generation of a variety of mediators involved in the fibrotic process [62,245]. The FITC-induced model of pulmonary fibrosis is discussed further in Chapter 3.

1.6 Lung Cytokines in Pulmonary Fibrosis

The development of lung fibrosis, and therefore CFA, appears to be associated with the *in situ* release of a broad range of cytokines that act as critical mediators of cell function and cell-cell communication by influencing many physiological cell properties, including proliferation, differentiation, and activation of other immunocompetent cells, chemotaxis, and connective tissue metabolism including increased synthesis of ECM proteins [83,246].

Numerous cytokines have been implicated in the progression of CFA, including IFN-γ, TGF-β, TNF-α, GM-CSF, the interleukins IL-1, IL-4, IL-8, IL-10, and IL-13, and C-C chemokines MCP-1 and MIP-1α, which will be discussed here.

1.6.1 IFN-γ

IFN-γ, the "classic" Th1 cytokine, is a 20kDa cytokine produced mainly by lymphocytes and macrophages, which plays a central role in the cellular immune response. Several potential anti-fibrotic actions have been reported for IFN-γ. These include inhibition of fibroblast proliferation and collagen synthesis and deposition, promotion of fibroblast apoptosis, and inhibition of the production and action of the fibrogenic cytokine TGF-β [247-254]. IFN-γ also attenuates bleomycin-induced lung fibrosis when administered to mice [255,256], and has been shown to downregulate TGF-β1 and procollagen I and III gene expression in this model [251].

Studies of lung tissue and blood from patients with CFA have found absolute and relative deficits in IFN-γ as compared with the Th2 cytokines [74,251,257], suggesting, as discussed previously, that a cytokine imbalance plays a role in CFA pathogenesis. Indeed, the increase in IL-4 and IL-5 expression in CFA appears to be concomitant with a reduction in IFN-γ expression [74,100,101]. Diminished IFN-γ reported in patients with CFA was also coupled with the observation that those patients with the lowest plasma levels of IFN-γ had the most marked deterioration in lung function on follow up, therefore, low IFN-γ levels could enhance collagen accumulation [250]. Interestingly, IFN-γ production has been demonstrated in the type II epithelial cells from patients with extrinsic allergic alveolitis and sarcoidosis, in which there is less frequent progressive fibrosis and a response to immunosuppressive therapy, but it was not expressed in CFA patients [100,101].

Recently, the potential importance of IFN-γ as a therapeutic immunomodulator was demonstrated in trials of IFN-γ administration to CFA patients undertaken in an attempt to switch the inflammatory response to a more protective Th1-type phenotype [103]. Lung function in these patients was significantly improved under IFN-γ and glucocorticoid treatment. Although this was a preliminary study, if confirmed it would represent a striking breakthrough in the treatment of CFA.

Despite the abundant evidence for an antifibrotic effect for IFN-γ, however, there are also reports of potentially profibrotic actions. Recently, Chen *et al.* [258] demonstrated the presence of elevated IFN-γ levels in the BAL of susceptible mice administered intratracheal bleomycin, and a reduced inflammatory response, and lower weight loss and mortality in IFN-γ knockout mice, suggesting that the inflammatory response to intratracheal bleomycin exposure is amplified by the local expression of IFN-γ in the lung. They suggest that IFN-γ may modulate the inflammatory and fibrotic response to bleomycin through its ability to enhance production of other proinflammatory mediators, such as TNF-α, and warn that the potential for toxicity related to enhancing proinflammatory processes should be realised in the clinical use of IFN-γ in pulmonary fibrotic disorders.

1.6.2 TGF-β

TGF-β is a pleiotropic cytokine that exists in five isoforms, three of which are expressed in mammals (TGF-β1, -β2, -β3) and these and their receptors are ubiquitously expressed in normal tissue and most cell lines [259]. Regulation of activity, however, is based on whether or not TGF-β is biologically active or latent. The latent form of the molecule is biologically inert, and signaling through TGF-β receptors requires exposure of the active site of the ligand, either through conformational change or through cleavage of the latency-associated peptide [260,261]. Regulation of the activity of the latent complexes is one of the principal pathways for regulating TGF-β effects, and the various mechanisms provide potentially useful therapeutic targets [12]. TGF-β1 is produced by T cells, monocytes/macrophages, platelets, fibroblasts and epithelial cells, and has emerged as a key cytokine in tissue repair and fibrosis, having important effects on both immune and structural cells [6,262,263].

TGF-β1 is chemotactic for fibroblasts, induces the synthesis and deposition of matrix proteins and glycoproteins through increased mRNA transcription and stability, and inhibits collagen degradation via inhibition of collagenase production and increased production of metalloproteinase inhibitors [262,264-266]. TGF-β1 exerts a growth-inhibitory effect on various cells, including AECs, suggesting that it is critical in the regulation of AEC growth [267]. However *in vitro*, bioactive TGF-β1 can be released from its latent form after damage to an epithelial cell monolayer and upregulation of activating molecules, and increases the speed of epithelial repair [261].

Both animal and human studies have provided much insight into the role(s) TGF-β1 may play in CFA pathogenesis, although the exact mechanisms of its actions have not been fully elucidated. *In vitro,* bleomycin has been shown to induce TGF-β1 mRNA expression and protein synthesis in endothelial cells and fibroblasts [268,269], while differential TGF-β1 gene expression, predominantly localised to

macrophages, has been demonstrated in murine bleomycin-induced lung fibrosis [235]. TGF-β1 gene expression and protein synthesis increase in several experimental models of pulmonary fibrosis [270,271]. However, evidence to implicate TGF-β1 as a direct effector of fibrogenic pathology came from the transient overexpression of active TGF-β1 by adenoviral gene transfer, which was shown to induce a severe, irreversible fibrotic reaction in the lungs, accompanied by extensive destruction of normal lung architecture and collagen deposition [67,272]. Moreover, neutralisation of TGF-β1 using antibodies significantly reduced experimental lung and kidney fibrosis [273,274].

Human studies have also generally supported a role for TGF-β1 in fibrogenesis, although there are conflicting reports. Local augmented tissue expression in epithelial cells and mRNA in AMs from lung biopsy specimens, and elevated TGF-β1 levels in BAL fluid and plasma, have all been reported in patients with CFA [275-281]. In early disease with minimal fibrosis, enhanced TGF-β1 expression was found primarily in AMs, but in advanced honeycomb fibrotic lesions typical of a UIP phenotype, TGF-β1 overexpression was localised to hyperplastic type II AECs [276]. However, decreased TGF-β1 production by AMs and normal BAL levels have also been reported [282].

Of all cytokines investigated to date, the TGF-β family has the most potent stimulatory effect on ECM deposition [263,283,284]. Gene expression and protein production are increased in the lungs of patients with pulmonary fibrosis [275-281], and inhibitors of TGF-β function attenuate fibrosis in animal models of the disease [273,274]. Coker and Laurent [285] have proposed that these three criteria be satisfied before anticytokine therapy is indicated, and as all three are fulfilled by TGF-β1, it makes an attractive therapeutic target. Indeed, pirfenidone, which inhibits TGF-β1-mediated collagen synthesis and fibroblast mitogenesis *in vitro* and TGF-β1 gene expression *in vivo*, appears to slow progression of CFA when administered to patients [286].

1.6.3 TNF-α

TNF-α is an important proinflammatory cytokine that is produced by different cell types in the lung, including activated monocytes and macrophages, neutrophils, and T cells, and when released in large amounts systemically, promotes neutrophil activation and adhesion to endothelial cells, with a local cytotoxicity leading to an increased capillary permeability with fluid leakage and shock [287,288]. However, a modest but persistent production of TNF-α may lead to chronic inflammation with fever, anaemia, bone resorption and wasting [289].

A role for TNF-α in the pathogenesis of CFA has been suggested through various *in vitro* and *in vivo* studies, although understanding of its precise role is still poor. TNF-α promotes fibroblast proliferation and collagen synthesis *in vitro* [220,277], although inhibitory effects on collagen gene expression have also been reported [290]. TNF-α mRNA expression is elevated in rodent bleomycin-induced lung fibrosis [220,230], and soluble TNF-α receptors reduce lung fibrosis in murine models [291]. Mice overexpressing TNF-α develop CFA-like fibrosis characterised by an increased expression of TNF-α by type II AECs [292]. There is also evidence that inhibition of early TNF-α expression with either anti-TNF-α antibodies or TNF-α antagonists inhibits fibrogenesis [220,291]. However, TNF-α upregulation has been documented in other inflammatory and immune lung pathologies in which normal lung repair processes occur without fibrosis [288,293], and Sime *et al.* [293] suggest that TNF-α may then act indirectly through upregulation of other fibrogenic molecules in fibrotic diseases such as CFA. As such, there is evidence that TGF-β1 upregulation occurs in some pathologies in which TNF-α is associated with the fibrosis but not in those where TNF-α expression leads to normal resolution [230,277,294]. Furthermore, Sime *et al.* [293] demonstrated that in normal adult rat lung, transient overexpression of TNF-α resulted in intense but transient inflammation and patchy interstitial fibrosis associated with secondary upregulation of TGF-β1 and induction of pulmonary myofibroblasts. In contrast, however, it is

also worth noting that high concentrations of TGF-β have been shown to moderately reduce TNF-α production by AMs [295].

In human CFA, compared with cells from normal lungs, TNF-α immunoreactivity is increased in hyperplastic type II cells [296]. In patients with CFA or asbestosis, BAL fluid-derived macrophages release increased amounts of TNF-α compared with controls [297], while AMs from patients with fibrosing alveolitis have also been shown to secrete more TNF-α than patients with nonfibrotic disease and normal individuals [298]. TNF-α, therefore, also fits the criteria proposed by Coker and Laurent [285] for determining suitability for anticytokine therapy, and indeed, promising results have been obtained by treating CFA patients with the same drug, pirfenidone, discussed above, which also has anti-TNF-α properties [286].

1.6.4 GM-CSF

GM-CSF regulates the proliferation and differentiation of cells in the granulocyte-macrophage lineage, and also has potent effects on the function of mature hemopoietic cells [299]. The lung is a rich source of GM-CSF, and studies in the context of pulmonary fibrosis indicate that GM-CSF may play an important but complex role in healing in the lung, likely determined by quantity, location and kinetics of expression [300].

Overexpression of murine GM-CSF induced by adenovirally-mediated gene transfer in the rat resulted in pulmonary fibrosis [301,302], and transgenic overexpression of GM-CSF in the lung under control of the surfactant protein C promoter results in enhanced lung growth and alveolar type II cell hyperplasia [303]. However neutralisation of GM-CSF, associated with a decreased number of macrophages in the alveolar space, in bleomycin-treated rats worsens pulmonary fibrosis, indicating that appropriate concentrations of this cytokine favour normal healing [300]. Similarly, Piguet *et al.* [304] found that administration of GM-CSF reduced

deposition of hydroxyproline, a measure of the lung collagen content, in response to bleomycin in mice. Christensen *et al.* [300] were also able to show that GM-CSF mRNA expression was diminished after intratracheal administration of bleomycin in rats before the development of pulmonary fibrosis, and that isolated type II cells from these animals demonstrated decreased expression of GM-CSF mRNA in response to *in vitro* stimulation with lipopolysaccharide. These data, they suggest, provide strong evidence that a defect in AEC expression of GM-CSF can play an important role in determining progression to fibrosis after lung injury, as GM-CSF has a protective role in bleomycin-induced pulmonary fibrosis [300]. Further support for a protective role for GM-CSF was shown by this group [305] in that mice with a targeted deletion of the GM-CSF gene had significantly enhanced fibrogenesis after bleomycin administration, and they indicated a possible mechanism for this effect could be impaired production of the potent antifibrotic eicosanoid, PGE_2.

1.6.5 IL-1

IL-1 has multiple roles, with effects on inflammation, the immune system and various cell functions [287]. Of the constituents of the IL-1 family, IL-1β is the more prominent in propagation of the inflammatory process [306]. IL-1β is present in chronically inflamed tissues and in tissues undergoing fibrogenesis, with accumulation of myofibroblasts and matrix deposition [230,307-309]. Inhibition of IL-1β at the initiation of animal models of fibrosis has been shown to attenuate the disease [310]. Finally, the transient overexpression of IL-1β in the epithelial cells of rodent lung using adenoviral gene transfer induces acute inflammation with alveolar tissue destruction resulting in progressive interstitial fibrosis, and this long-term effect coincides with sustained induction of TGF-β [306].

Interestingly, while normal BAL IL-1 levels have been observed in patients with CFA, concentrations of IL-1ra, which competes with IL-1 for its receptors and counteracts the proinflammatory functions of IL-1, are increased [311]. AMs from

patients with CFA also produce higher levels of IL-1ra *in vitro* than do those from healthy controls [312]. IL-1ra has been localised to hyperplastic type II cells, fibroblasts [311], and AMs [312]. The balance between IL-1 and IL-1ra is seen as a crucial ratio in destructive inflammatory disease [313].

There is also evidence for a protective role of exogenous IL-1ra in a number of animal models of acute lung injury. Targeted overexpression of IL-1ra to distal airway epithelium has been shown to give partial protection from IL-1β-induced airway inflammation and injury [314], and exogenous administration of IL-1ra can partially reverse changes of pulmonary fibrosis in bleomycin-induced fibrosis in mice [310].

1.6.6 IL-4

IL-4 is the prototypic Th2 cytokine produced by macrophages and Th2 cells, and while it is known to have anti-inflammatory effects, it can also promote fibroblast chemotaxis and proliferation, collagen gene expression, and collagen synthesis [315-317]. Notably, in other inflammatory interstitial lung diseases such as sarcoidosis and hypersensitivity pneumonitis, type II pneumocytes express both IL-4 and IFN-γ, but only profibrotic IL-4 appears to be detectable in the lungs of CFA patients [100]. However, there are conflicting reports about a role for IL-4 in CFA. Neutralising antibodies to IL-4 have been shown to prevent dermal collagen deposition in murine scleroderma [318], but IL-4 also modulates the expression of proinflammatory cytokines such as IL-1 and TNF-α, which are both involved in bleomycin-induced pulmonary fibrosis [242]. In addition, bleomycin-induced pulmonary fibrosis is not altered in either IL-4-overexpressing or -knockout mice [319].

1.6.7 IL-8

IL-8 is a chemotactic and activating factor leading to neutrophil migration and the release of their granule content, and while AMs are thought to be the major source of IL-8 in the lower respiratory tract in humans, many other cell types, including endothelial and epithelial cells, monocytes, fibroblasts and neutrophils, are capable of IL-8 synthesis and release [320]. In CFA, IL-8 is increased in the BAL fluid [99,321], and IL-8 mRNA is increased in AMs [322,323], suggesting a positive correlation between IL-8-specific mRNA in AMs and percentage of neutrophils in the BAL from patients with CFA.

There is some speculation that the intensity of IL-8 expression may be related to prognosis or disease activity in CFA, based on work showing less intense IL-8 expression in patients with fibrosing alveolitis associated with systemic sclerosis compared to patients with CFA, who have a worse prognosis [321]. Ziegenhagen *et al.* [320] confirmed this hypothesis by demonstrating that the degree of neutrophilic alveolitis in CFA is associated with increased serum levels of IL-8, and that serum IL-8 levels correlated significantly with impairment of lung function parameters. These findings may prove useful in the serological assessment of disease activity in CFA patients.

1.6.8 IL-10

IL-10 is produced by Th2 cells, B cells, monocytes, macrophages and keratinocytes, and has an anti-inflammatory and protective role in different pathologies [83]. IL-10 acts to reduce the synthesis of proinflammatory cytokines, including IL-1, IL-6, IL-8 and TNF-α and GM-CSF by monocytes/macrophages and neutrophils [83]. In addition, IL-10 can reduce macrophage free radical release and NO synthesis, and IFN-γ synthesis by T cells, as well as inducing apoptosis of activated neutrophils [4].

The role of IL-10 in fibrosis is unclear. IL-10 has been shown to have anti-inflammatory effects *in vivo* in a collagen-induced arthritic model [324]. It has reduced the production of Th2 cytokines and eosinophilia in allergic mice, however it also augmented airway reactivity [325]. In a silica-induced model of pulmonary fibrosis, IL-10 was shown to be anti-inflammatory, but also to exert pro-fibrotic activity [68]. Finally, IL-10 gene transfer into mouse lungs was shown to inhibit the development of pulmonary fibrosis by intratracheal bleomycin administration, partially through the reduction of TNF-α expression [326]. This study also found that constitutive and TGF-β-stimulated type I collagen mRNA expression was significantly reduced *in vitro* by IL-10, although IL-10 did not affect proliferation induced by platelet-derived growth factor (PDGF).

1.6.9 IL-13

IL-13 is a pleiotropic protein that is produced in large quantities by appropriately stimulated $CD4^+$ Th2 cells, as well as by B cell lymphomas, keratinocytes, mast cells and basophils [327]. IL-13 and IL-4 have overlapping effector profiles as their receptor complexes share the signal transducing IL-4E chain [327], but there are a number of important functional differences between IL-4 and IL-13. Most importantly, IL-4 directly induces both human and murine T cell proliferation and differentiation while IL-13 probably mediates its effects on T cells indirectly [328].

IL-13 can induce B cell proliferation, immunoglobulin production in primary immune cells, and acts as a chemoattractant for monocytes [329]. It can also inhibit the production of inflammatory cytokines by both macrophages and monocytes [330]. It is worth noting that, unlike IL-4, IL-13 is produced by DCs isolated from tonsillar germinal centres [331], and may contribute to DC regulatory functions of B cell proliferation and differentiation [327]. This suggests that IL-13 may play a role in maintaining the B cell aggregates often found in biopsies from patients with CFA.

IL-13 has emerged as a key component of Th2-mediated immunity, as it is known to contribute to the pathogenesis of asthma and other pulmonary diseases via its ability to generate myofibroblast proliferation and ECM deposition, mucus metaplasia, eosinophilic inflammation, and airway hyperresponsiveness [79,91,332-335]. IL-13 transgenic mice show that chronic expression of this cytokine manifests significant degrees of subepithelial and moderate amounts of adventitial fibrosis [79], and causes type II alveolar hypertrophy and surfactant lipid and protein accumulation in the setting of pulmonary fibrosis [336]. Interestingly, overexpression of IL-13 but not IL-4 in mouse lungs results in an overall increase in lung collagen content [91]. The potential for IL-13 to play a significant role in the pathogenesis of CFA is growing, as elevated mRNA levels have been found in BAL-derived AMs from patients with pulmonary fibrosis [85], and is discussed in more detail in Chapter 6.

1.6.10 C-C Chemokines: MCP-1 & MIP-1α

C-C chemokines are a family of chemotactic cytokines known to modulate cytokine production, adhesion molecule expression and mononuclear cell proliferation [222,337]. MCP-1 and MIP-1α are members of this supergene family, and because of their chemotactic activity and ability to activate mononuclear phagocytes, they have been implicated in the pathogenesis of pulmonary fibrosis. Eosinophils, macrophages, vascular smooth muscle cells, epithelial cells and myofibroblasts are the major cellular sources of MCP-1 in fibrotic lungs at different stages of disease [94,98,338], while macrophages appear to be the major source of MIP-1α [94,219]. Time-dependent upregulation of lung MCP-1 and MIP-1α mRNA expression has been shown in rodent bleomycin-induced pulmonary fibrosis, with peak expression preceding or overlapping the active fibrotic response [338].

Passive immunisation of bleomycin-challenged mice with anti-MIP-1α antibodies has been shown to reduce total lung inflammatory cell content by 35%, and to inhibit the fibrotic reaction [219,339]. It has also been postulated that TNF-α could

stimulate MIP-1α *in vivo*, as MIP-1α protein expression is decreased by 80% in bleomycin-challenged mice treated with soluble TNF receptor at two days post-challenge, which corresponds to the first MIP-1α expression peak [340]. In this same study mice treated later, at the second MIP-1α peak, demonstrate a modest 35% reduction in MIP-1α.

MCP-1 has been shown to increase type I procollagen synthesis *in vitro* [341]. MCP-1 antigens can also be detected in the BAL fluid from mice with bleomycin-induced pulmonary fibrosis [99]. MCP-1 signalling via the CCR2 receptor results in the generation of profibrotic signals in the FITC-induced model of pulmonary fibrosis, and mice deficient for CCR2 are protected from the fibrotic response induced by FITC [62]. MCP-1 has been implicated in the imbalance of Th1/Th2 regulation associated with pulmonary fibrosis. Neutralisation of MCP-1 in a Th2-type model of fibrosis has been associated with significantly reduced IL-4 and IL-5 generation, but treatment with MCP-1 neutralising antibody in a Th1-type model had no effect on cytokine production or inflammatory lesion size [342]. In addition, T cell activation in the presence of MCP-1 enhances IL-4 generation [343], and similarly, MCP-1 has been shown to directly contribute to the production of IL-4 by antigen-activated T cells in a variety of cell-to-cell interactions [344,345].

1.7 Lung Cells in Fibrosis

Alveolar epithelial and/or capillary cell injury occurs early in the sequence of events leading to pulmonary fibrosis, and promotes recruitment of circulating immune cells into the lung. These effector cells, including neutrophils, eosinophils, and lymphocytes, as well as resident lung cells such as AMs, alveolar epithelial and endothelial cells and fibroblasts, can then release a variety of factors that can influence the progression of CFA [83].

Although the various cell populations can closely interact in the pathogenesis of lung fibrosis, their involvement in lung injury and fibrogenesis will be discussed independently.

1.7.1 Neutrophils

Inevitably, the sequence of tissue injury is accompanied by a local inflammation predominantly comprised, within hours, of neutrophils. Neutrophils amplify the disruption of the tissue mainly by the release of oxidants, proteases and elastases that injure the local cells and extracellular components, thereby facilitating the development of pulmonary fibrosis [346], and while there can be little question of their key role in the initial injury to the lung, their role in the fibrogenic process is much less clear. Indeed, depletion of neutrophils from the lungs of rats [347] or hamsters [348] by administration of antineutrophil serum prior to intratracheal bleomycin gives rise to an increase in lung collagen content and in collagen synthesis rates.

However, neutrophils are considered to be major effector cells in CFA [349]. Pulmonary compartmentalisation of neutrophils (and eosinophils) may occur in chronic lung inflammation associated with CFA [323], with neutrophils representing up to 20% of BAL fluid cells [50]. The damaged cells and loss of normal pulmonary architecture that are histopathologically associated with CFA are also reminiscent of the kinds of derangements expected from extracellular degranulation of neutrophils [350]. Indeed, the BAL fluid of CFA patients shows markedly increased levels of enzymes released by neutrophils, including myeloperoxidase and collagenase, and neutrophils from these patients have been shown to release increased amounts of preformed proteins and toxic oxygen radicals, which may cause the parenchymal cell cytotoxicity [351,352]. Neutrophil elastase has also been implicated in bleomycin-induced pulmonary fibrosis [353]. Furthermore, reactive oxygen metabolites released by neutrophils have been shown to directly alter type II AEC function and induce cytotoxicity [354]. There are also immune complexes present in the blood,

BAL fluid and tissue of CFA patients [108-112], and their interaction with neutrophils has been shown to induce neutrophil activation, resulting in further lytic enzyme and oxygen radical release [355].

Finally, activated neutrophils are also a source of cytokines, such as IL-1, IL-8, and TNF-α, which further heighten the ongoing inflammatory response, and can contribute to the progression of the fibrotic process [356].

1.7.2 Eosinophils

The accumulation of eosinophils in both alveolar spaces and the parenchyma has been noted in CFA [357]. Increased numbers of these cells are usually found in the BAL of CFA patients [358], and raised concentrations of the granular eosinophil cationic protein have also been detected [359].

Two lines of evidence have suggested the importance of eosinophils in pulmonary fibrosis. First, these cells are now known to be a key source of cytokines with known inflammatory and fibrosis-promoting activities, including TGF-β1, IL-5, GM-CSF, IL-8, MIP-1α and TNF-α [360]. The recruitment of eosinophils to the lung for activation and participation in the pathogenesis of lung fibrosis in the bleomycin-induced model of pulmonary fibrosis appears to be in response to a significant increase in lung IL-5 mRNA and protein expression [93]. Of specific importance is the finding that eosinophils are the primary source of TGF-β1 and MCP-1, both profibrotic cytokines, in bleomycin-induced pulmonary fibrosis [94,232]. Eosinophils have also been found to localise to areas undergoing active fibrosis, and at these sites they were activated and expressing such fibrosis-promoting cytokines as TGF-β1 [232]. Secondly, the presence of eosinophils in lungs of patients with pulmonary fibrosis correlates with worst prognosis or resistance to therapy [358,361-363]. Thus there is compelling evidence to suggest that eosinophils may play an

important role in pulmonary fibrosis via their ability to elaborate the cytokines capable of driving the fibrogenic response.

1.7.3 Lymphocytes

T cells, through their unique capacity for primary antigen recognition, may play a larger role than originally considered in fibrosis. There have been conflicting reports, however, on the necessity for T cells in the fibrotic response. For example, one group reported that athymic nude mice, which are T cell deficient, were no different from normal mice in the induction of fibrosis by bleomycin [364]. Another group, however, showed lower cellular infiltration, fibroblast proliferation, collagen synthesis, and connective tissue accumulation after intratracheal bleomycin in nude mice compared to euthymic controls [215]. However, Th2 cells can modulate the proliferation and biosynthetic capacity of fibroblasts [365], largely because of their ability to generate IL-4, which recognizes specific receptors expressed by fibroblasts [317], and to stimulate them to proliferate and to undergo directed movement toward inflammatory stimuli [366].

T cells are therefore believed to influence fibrogenesis indirectly, through the release of a wide repertoire of cytokines, such as IL-1, IL-4, IL-5, IL-10, IL-13, and TNF-α [75], and as such play a role in the Th2-dominated environment of the fibrotic lung.

Of particular interest, T cells have been found to be the primary source of IL-5 in the fibrotic lung [367], and upregulation of IL-5 mRNA and protein by T cells and eosinophils at the site of active fibrosis have been shown in the bleomycin model [93]. IL-5 plays a major role in the chemotaxis of eosinophils and release of toxic mediators providing an additional role in the pathogenesis of lung injury and inflammation. A role for T cells in bleomycin-induced and other models of pulmonary fibrosis has been previously suggested [93], and may be mediated by T cell-derived IL-5 in those lesions characterised by eosinophil infiltration. Indeed,

this may be a mechanism by which neutralisation of TNF-α activity results in abrogation of pulmonary fibrosis [360].

Interestingly, a ratio of CD4/CD8 > 1 in the BAL fluid from CFA patients has been linked to a more benign course of disease [368], while another group showed that a low CD4/CD8 ratio in the BAL fluid from patients with NSIP may indicate that the alveolar structutre was not severely reconstructed by fibrosis [369].

B lymphocytes produce IgG, and IgG-containing immune complexes can be found in patients with CFA [108-112]. B cell aggregates have been demonstrated in the lungs of patients with CFA [105,370,371], and have been associated with a local humoral immune response [371]. The involvement of these aggregates in CFA pathogenesis is discussed in more detail in Chapter 4.

1.7.4 Lung DCs

The role of DCs in the pathogenesis of CFA has been largely overlooked, and will perhaps remain so as the focus moves towards structural cells in the lung. However, there is evidence to suggest that DCs have an integral role in the pathogenesis of this disease. Certainly, as discussed, DCs play a critical role in Th1/Th2 regulation in the lung, and as CFA has been shown to be a Th2-mediated disease, it suggests that DCs may be mediators of this phenomenon in CFA. Indeed, immunohistochemical analysis of murine lungs after bleomycin treatment showed increased staining of highly positive MHC class II cells, also suggesting a role for DCs in fibrotic lungs [237].

DCs may also be critical for the maintenance of chronic localised immune responses in the lung, and much evidence comes from the study of chronic asthma. It has been proposed that the presence of chronic inflammation and airway structural changes leads to local maturation of DCs and to antigen presentation occurring in the airways

[372], and this could certainly apply to CFA as well. The cytokines TNF-α, GM-CSF and IL-4 all have the potential to upregulate expression of DC costimulatory molecules, and all are expressed in both asthmatic epithelium and CFA [149,297,298,303]. Increased numbers of mast cells are thought to be important in asthmatic airways, as they express CD40L and produce cytokines that can activate DCs and prolong their survival in tissues [373,374]. Again, this could be applied to CFA, as numerous reports have documented increased numbers and hyperplasia of mast cells in pulmonary fibrosis [375-378], and specifically in fibrotic lesions [379], as well as increased histamine levels [378]. Finally, the process of airway remodelling in both asthma and CFA leads to the deposition of ECM components, such as collagens, fibronectin, and heparan sulphate, that have the capacity to enhance DC differentiation and costimulatory function [380,381].

Although there is no direct evidence for a role for DCs in CFA pathogenesis, the participation of this cell cannot be discounted, and warrants further investigation.

1.7.5 Alveolar Macrophages

The AM is the most prominent cell population obtained from the alveoli of individuals with CFA [75,382]. AMs are important regulators of the repair processes that are initiated following lung injury, and have the capacity to either increase tissue damage and fibrosis or to promote repair. The pathogenic potential of AMs comes from their ability to release mediators that amplify inflammation by recruiting other inflammatory cells such as mast cells, neutrophils, lymphocytes and other AMs [337,382,383], to increase cell injury by the production of reactive oxygen and nitrogen intermediates [354,384], or to increase the number and activity of fibroblasts by the production of growth factors [385,386]. AMs also have the capacity to release many cytokines, some of which are involved in the processes described above, including IL-1 [230], IL-8 [322], IL-13 [85], TGF-β [271], MIP-1α

[219], PDGF [385], and TNF-α [126,298], all of which have been implicated in CFA pathogenesis.

AMs, however, can also express molecules that inhibit fibrosis and promote repair in the proper milieu. These include substances that promote the clearance of fibrin matrix, such as urokinase [387,388], and downregulate inflammation, fibroblast proliferation and collagen deposition, such as PGE_2 or gelatinase B [248,389-392].

Therefore, the role of the AM in CFA pathogenesis is quite complex and requires further investigation to determine what drives the AM to exert its pathogenic effects rather than those promoting normal repair after injury.

1.7.6 Alveolar Epithelial Cells

AECs play a fundamental role in the resolution of inflammation. Following injury, type II cells are required to rapidly proliferate and differentiate into type I AECs to restore barrier integrity. Failure of type II AECs to carry out these tasks may determine whether or not progression to fibrosis occurs [66], and it appears that this process is seriously affected in CFA [2].

Type II AECs are an important source of enzymes, cytokines and growth factors, many of them profibrotic, which are known to be important in CFA pathogenesis. Most importantly perhaps, several studies have shown that in CFA, hyperplastic type II cells constitute the main site of synthesis of TGF-β1 and TNF-α [276,277,296,393]. Interestingly, Khalil *et al.* [276,278] demonstrated that in early fibrotic lungs (with inflammation and minimal fibrosis), TGF-β1 was found mainly in AMs, but in advanced fibrotic honeycomb lesions primarily seen in UIP, it was mainly present in AECs. Other cytokines, besides TGF-β and TNF-α, whose importance has been demonstrated in CFA have been found to be expressed by type II cells, including PDGF [394,395], IL-4 [100], GM-CSF [300], and MCP-1 [98].

The role of AECs as suppressors of fibroblast responses in the resolution of inflammation, and their failure in the progression to fibrosis, is becoming a popular focus for the investigation of CFA pathogenesis [48,396]. Evidence for such a role for type II cells comes from observations that in animal models of pulmonary fibrosis, failure of AEC proliferation or differentiation is a major factor in fibrotic, rather than reparative, responses to injury [66,397], and that AECs can inhibit fibroblast proliferation *in vitro* [398,399]. Two recent studies have elucidated some of the mechanisms involved in the suppression of fibroblast proliferation, demonstrating that the suppressive effects are regulated through MCP-1/CCR2 signalling, and mediated by PGE_2 [400], which in turn is dependent on cyclooxygenase-2 (prostaglandin synthase) [401].

1.7.7 Endothelial Cells

Injury to the epithelium and basement membranes appears to be necessary for the fibrotic process to occur [402], however it is thought that endothelial cell injury is the earliest lesion of bleomycin in pulmonary fibrosis [214,403]. Endothelial cells are able to secrete a variety of growth factors that theoretically have the potential to stimulate fibroblasts [404]. Stimulated endothelial cells can also produce inflammatory mediators such as IL-8 and MCP-1, and endothelial adhesion molecules are known to be reactive with counter-receptors expressed on leukocytes [14]. Recently, endothelial ICAM-1 was shown to be essential for abnormal leukocyte accumulation in capillaries and venules in bleomycin-induced pulmonary fibrosis [239]. Striking proliferation of endothelial cells may accompany the development of pulmonary fibrosis [405,406] and the ability of these cells to modulate fibrogenesis may merit further investigation [407].

1.7.8 Lung Fibroblasts

Fibroblastic foci are early morphological changes associated with progression to fibrosis, and occur in areas where the alveolar lining cells are destroyed and the epithelial basement membrane is denuded. Following injury to the lung, fibroblasts migrate to the area and are stimulated to secrete collagen and other matrix proteins. They also release various proteases that can degrade and remodel these matrix proteins. Dysregulation of this process can result in fibroblastic foci, followed by abnormal remodelling of the ECM and subsequent destruction of the lung architecture [64,396]

Fibroblasts from CFA patients show shifts in phenotype, from migratory, to proliferative, to profibrotic leading to production of abundant ECM components in the fibroblastic foci [64]. Myofibroblasts isolated from the lungs of CFA patients also show abnormal responses to, or release of, growth factors, other mediators and ECM proteins, including enhanced collagen and TGF-β1, giving them a profibrotic secretory phenotype [408]. Moreover, bleomycin-exposed lung fibroblasts secrete increased amounts of TGF-β1 protein as compared to normal lung fibroblasts [409]. The shifts in phenotype have been demonstrated in numerous studies on cell lines established from human and animal fibrotic tissue [410], and from Rel-B knockout mice with fibroblasts displaying sustained and persistent production of a wide array of inflammatory chemokines thereby regulating the switch from an acute resolving to a chronic persistent inflammation [411]. Most cells in the fibroblastic foci have been shown to be myofibroblasts aligned in parallel to one another and therefore probably contribute to active contraction and distorted architecture [412].

Matrix metalloproteinases (MMPs) and tissue inhibitors of metalloproteinases (TIMPs) are involved in the degradation of ECM, and their normal activation prompts clearance of the alveolar spaces after lung injury [48]. Several studies have shown profound changes in MMP and TIMP expression and localisation in CFA lung tissue. In particular, TIMP-2 expression is predominantly localised to myofibroblasts within the fibroblastic foci [413,414], suggesting enhanced

progressive accumulation of fibrillar collagens, and perhaps increased fibroblast survival as TIMP-2 is also able to induce proliferation [414]. Additionally, myofibroblasts from CFA patients synthesise the MMPs gelatinases A and B, which degrade basement membrane molecules, contributing to the failure of orderly type I cell repair and enhancing fibroblast/myofibroblast migration into the alveolar spaces [414].

Lung fibroblasts from CFA patients have also been shown to have a defect in cyclooxygenase-2 expression [389], and are unable to upregulate the TNF-α receptor [415], compromising their ability to synthesise antifibrogenic PGE_2, leading to their deficient production of eicosanoid autocrine inhibitors of proliferation, and ECM deposition [290]. In addition, fibroblasts and myofibroblasts from the lungs of CFA patients induce AEC death *in vitro* [416], possibly through the synthesis of angiotensin peptides [417], while *in vivo,* apoptotic AECs are detected primarily in areas immediately adjacent to underlying foci of myofibroblasts [418].

1.8 Hypothesis and Aims of Project

The work described in this thesis was undertaken with the goal of providing new insight into the pathogenesis of CFA. As such, these studies involved the characterisation of the murine FITC-induced model of pulmonary fibrosis, and the investigation of possible functional alterations in APCs from these lungs. As structural cells in the lung are becoming an increasingly popular focus in the study of CFA pathogenesis, preliminary studies were also conducted into the *in vitro* effects of FITC on lung epithelial cell lines.

1.8.1 Hypothesis

The hypothesis of this project was that APCs are altered by, and contribute to, the pathology of lung fibrosis, and that epithelial cell damage may have consequences for APC function in terms of cytokine production.

1.8.2 Scientific Questions

- *Chapters 3 & 4:* What are the acute and long-term pathological effects of FITC administration in mice, and how can they be measured quantitatively? How are these effects reflected in terms of cellular content and cytokine production in the BAL fluid?

- *Chapter 5:* What are the current methods in use for the isolation of lung DCs and BAL AMs from murine lungs? What are the most appropriate methods for use in this project? What are the phenotypes of the two isolated cell populations?

- *Chapter 6:* Do DCs and BAL AMs from the lungs of FITC-treated mice differ, from those of control mice, in their ability to induce antigen-specific T cell proliferation? Is this reflected in production of Th1 and Th2 cytokines?

- *Chapter 7:* What are the morphological effects of FITC treatment on the two murine lung epithelial cell lines? How does FITC affect their viability? Does FITC treatment induce cytokine production from these cell lines?

CHAPTER 2

Materials and Methods

Unless otherwise stated, all chemicals were obtained from Sigma Ltd (Poole, Dorset, UK) or Fisher Scientific Ltd (Loughborough, Leicestershire, UK). All tissue culture reagents and plastic ware were from Life Technologies Ltd (Paisley, Strathclyde, UK). Recipes for solutions described are shown in Appendix 1.

2.1 Tissue Culture

Sterile technique was used for all cell preparation and culture.

2.1.1 $CD4^+$ DO11.10 T Cell Purification

Using the MACS CD4 protocol (Miltenyi Bitoec GmbH, Bergisch Gladbach, Germany), this method, with some minor changes, was used to isolate antigen-specific $CD4^+$ DO11.10 T cells from the spleens of DO11.10 transgenic mice. These cells express a T cell αβ receptor specific for ovalbumin (OVA) peptide, amino acids 323-339 ($OVA_{323-339}$), presented on $I\text{-}A^d$ molecules [419]. The spleen and lymph nodes were removed from the mouse and placed on the ground-glass ends between two sterilised glass slides. The slides were continuously pressed together in a circular motion until only the capsule of the spleen and lymph nodes remained. The contents of the spleen and lymph nodes were washed with complete RPMI 1640 into a petri dish. Complete RPMI was prepared by the addition of 10% foetal calf serum (FCS) (Labtech International, Ringmer, East Sussex, UK), 2 mM L-glutamine, 100 U/ml penicillin/streptomycin, and $5x10^{-5}M$ β-2-mercaptoethanol. The isolate was then pushed through a 40 μm cell strainer using a syringe plunger to obtain a single cell suspension. The cells were washed twice in complete RPMI, layered on Lympholyte^M (Cedarlane Laboratories Ltd, Hornby, ON, Canada) and spun to remove red blood cells and cell debris. The cells were then washed twice and counted. As per the MACS protocol, 100 μl of CD4 beads was used to stain 10^7

cells. The cells were washed in MACS buffer, then a maximum of 10^7 cells were added to one pre-wetted miniMACS MS column on a miniMACS separator (Miltenyi Biotec). The $CD4^+$ T cells adhered to the magnetic beads in the column, and the cells were subsequently eluted. This method consistently yielded between approximately 30 – 50 x 10^6 $CD4^+$ T cells, to a purity of >88% as assessed by flow cytometry (Figure 2.1).

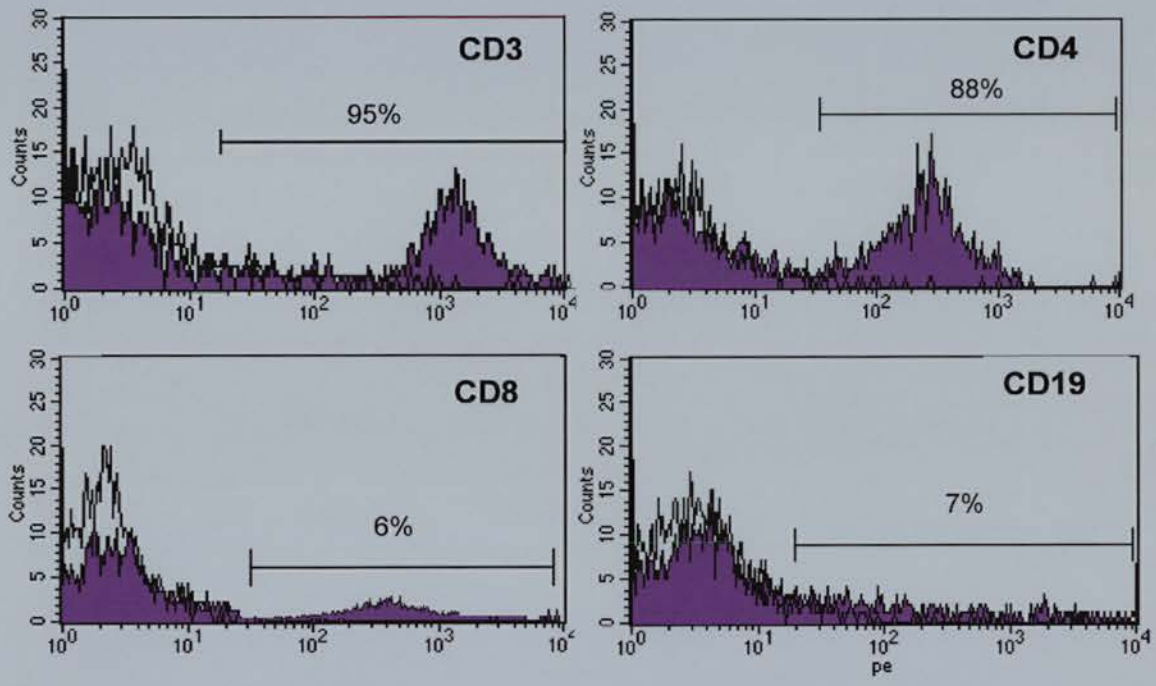

Figure 2.1 Cell surface phenotype of murine DO11.10 T cells. Flow cytometry histograms showing purity of $CD4^+$-enriched T cells isolated from the spleens of DO11.10 $OVA_{323-339}$ transgenic mice as described. Open histograms represent isotype-matched control monoclonal antibodies. The numbers shown on each histogram represent the % positive cells relative to the isotype control. CD3 , T cells; CD19, B cells.

2.1.2 [^{3}H]-thymidine Incorporation T Cell Proliferation Assay

This assay was used to measure the extent of T-cell proliferation. Antigen-specific (OVA/TCR) DO11.10 T cells were placed in 96 well tissue culture plates at a density of $1x10^5$ cells per well, in 200 µl of complete RPMI, in the presence of $3x10^4$

$CD11c^+$-enriched DCs or AMs that had been cultured overnight with 20 ng/ml GM-CSF (R&D Biosystems), then pulsed for two hours with $OVA_{323-339}$ peptide (Albachem, Edinburgh, UK). To determine the optimal concentration of $OVA_{323-3.39}$ peptide for use in the proliferation assays, $CD4^+$ DO11.10 T cells were cultured with APCs that had been pulsed for two hours with different concentrations of $OVA_{323-339}$ peptide from each batch synthesised. Although counts varied between experiments, optimal responses for batch one were obtained between 1 and 10 μg/ml $OVA_{323-339}$ peptide (Figure 2.2), and 10 μg/ml of peptide was used in all subsequent experiments with this batch of peptide.

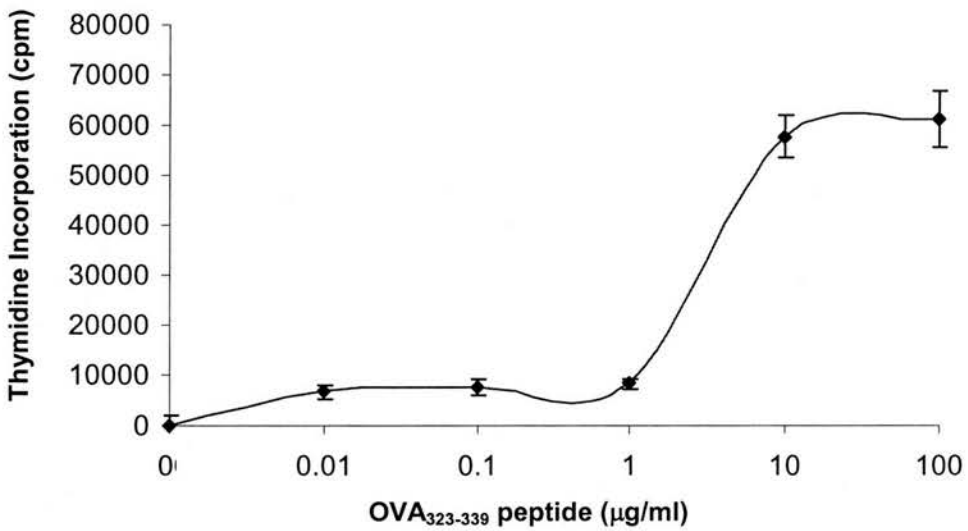

Figure 2.2 Representative $OVA_{323-339}$ peptide Batch 1 dose response curve. APCs (3 x 10^4 cells/well) which had been pulsed for two hours with 0 – 100 μg/ml of $OVA_{323-339}$ peptide and then washed, were cultured in round-bottom 96-well plates with $CD4^+$ DO11.10 T cells (1 x 10^5 cells/well). After three days, [^{3}H]thymidine (1 μCi/well) was added for the final 18 hours of culture to assess T cell proliferation, depicted as counts per minute (cpm). The data shown are the mean ± SEM of triplicate wells, and are representative of the trend seen in three independent experiments. T only, 695 cpm; T + 100 μg/ml peptide, 937 cpm.

A second batch of peptide was titrated in a similar fashion for use in later experiments. Again, counts varied, but with this batch optimal responses were obtained between 10 and 100 μg/ml $OVA_{323-339}$ peptide (Figure 2.3); 100 μg/ml of peptide was used in all subsequent experiments with this second batch of peptide

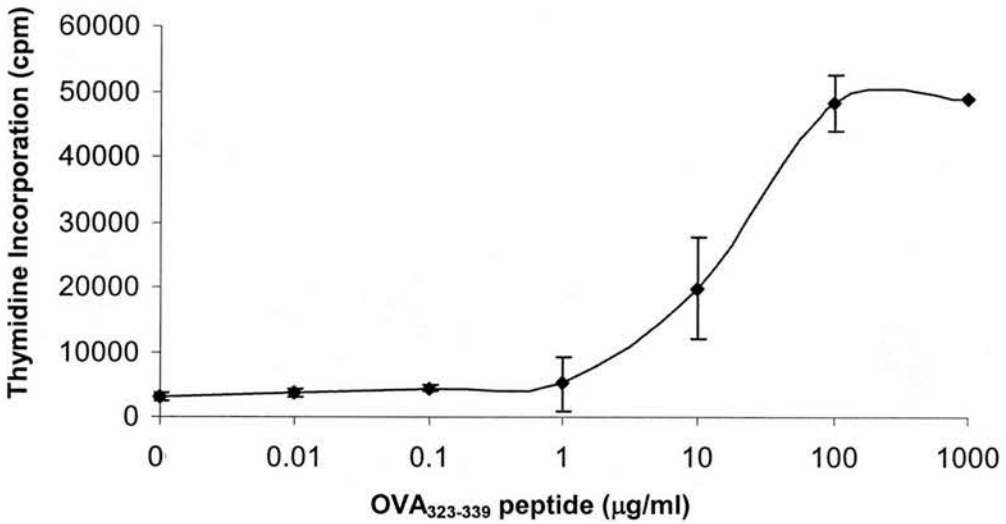

Figure 2.3 Representative $OVA_{323-339}$ peptide batch 2 dose response curve. APCs (3 x 10^4 cells/well) which had been pulsed for two hours with 0 – 100 μg/ml of $OVA_{323-339}$ peptide and then washed, were cultured in round-bottom 96-well plates with $CD4^+$ DO11.10 T cells (1 x 10^5 cells/well). After three days, [^{3}H]thymidine (1 μCi/well) was added for the final 18 hours of culture to assess T cell proliferation, depicted as counts per minute (cpm). The data shown are the mean ± SEM of triplicate wells, and are representative of the trend seen in three independent experiments. T only, 837 cpm; T + 100 μg/ml peptide, 1284 cpm.

2.1.2.1 Cell Stimulation

Cells were stimulated by the addition of $OVA_{323-339}$ peptide at 10 μg/ml (peptide batch 1) or 100 μg/ml (peptide batch 2), as determined by peptide titration (see above), or bovine serum albumin (BSA) as a negative control, or the T cell mitogen concanavalin A (conA) as a positive control (both at 1 μg/ml). To avoid background proliferation by any contaminating APCs in the T cell isolate, APCs were pulsed with $OVA_{323-339}$ peptide or BSA for two hours at 37°C, and the cells washed three times with PBS before the addition of the T cells. After the addition of $CD4^+$ T cells, the plates were incubated at 37°C with 5% CO_2 for four days. If required, 0.2 ml of medium was pipetted from each well after 72 hours for protein assays. This end-point was chosen as it allowed for maximum proliferation, and peak production of the highest number of cytokines. The supernatant was centrifuged at 300g for five

minutes to remove any cells, and was either assayed immediately or frozen at –70°C. Eighteen hours before the end of the stimulation, 1 μCi per well of 35 Ci/mmol [^{3}H]-thymidine (ICN, Basingstoke, Hampshire, UK) was added. At the end of the stimulation period, the cells were either immediately harvested or frozen at –20°C to arrest [^{3}H]-thymidine incorporation.

2.1.2.2 Cell Harvesting

Cellular nucleic acids were harvested onto filter mats (Wallac, Crownhill, Buckinghamshire, UK) using a 96 well Tomtec plate harvester (Wallac). The mats were dried in a 60°C oven for a minimum of one hour.

2.1.2.3 Scintillation Counting

Filter mats were sealed in plastic bags (Wallac) with 10 ml of 'Betaplate™ Scint' liquid scintillation fluid (Fisons, Loughborough, Leicestershire), placed into holding cassettes, and counted on a 1205 Betaplate™ liquid scintillation counter (Wallac) allowing 20 seconds of counting from each sample. Counts per minute (cpm), reflected T cell proliferation.

2.1.3 Cryopreservation of Cell Lines

Cell lines required for future use were harvested from tissue culture flasks using trypsin/EDTA (0.25% Trypsin, 1mM EDTA), washed, and resuspended in 1 ml FCS per flask, then mixed with an equal volume of 90% FCS/10% dimethyl sulfoxide (DMSO). A 1 ml volume of cells was then aliquoted into 1.5 ml CryoTubes, and frozen slowly by wrapping in cotton wool and placing in a polystyrene box in a

-70°C freezer for a minimum of 2 days. Cells were transferred to liquid nitrogen for longer-term storage. To thaw cells, CryoTubes were wrapped in aluminium foil and left at room temperature to defrost. The CryoTubes were washed with 70% ethanol before opening, and the cells then washed several times in medium to remove DMSO residue.

2.1.4 Maintenance of mtCC1-2 Epithelial Cell Line

The CC-10-expressing mouse Clara cell line, mtCC1-2, generated from the lungs of a transgenic mouse expressing the SV40 Large T antigen under the control of a Clara cell specific promoter [420], was kindly donated by Professor Franco DeMayo, Department of Molecular and Cellular Biology, Baylor College of Medicine, Houston, Texas, USA. The cell line was maintained in Dulbecco's Modified Eagle Medium (DMEM) 1X, supplemented with 10% FCS, 2 mM L-glutamine, 100 U/ml penicillin/streptomycin, at 37°C in 5% CO_2. mtCC1-2 cells were routinely maintained in 7500 mm^2 (T-75) tissue culture flasks. Cultures were started at passage 19, and continued until passage 30, before defrosting new stock. The cells were passaged once per week and while still in the growth phase. Passaging the cells involved removing the medium from the flask, and washing the cell monolayers with serum-free DMEM. Trypsin-EDTA was then added, and the flask was incubated at 37°C for 5-10 minutes. The detached cells were pipetted into a polypropylene tube with an equal volume of complete medium, and centrifuged for five minutes at 300g. The cells were resuspended in 6 ml fresh complete DMEM, and 2 ml of the cell suspension was added to each of 4 fresh T-75 tissue culture flasks containing 18 ml warmed complete DMEM.

2.1.5 Maintenance of CMT64/61 Epithelial Cell Line

CMT64/61 mouse C57BL/1CRF lung carcinoma epithelial cell line (ECACC, Salisbury, Wiltshire, UK, reference number 86082105) was maintained in Waymouth MB 752/1 medium, supplemented in the same way as for the mtCC1-2 cell line. CMT64/61 cells were routinely maintained in T-75 tissue culture flasks. Cultures were fed once per week, and were passaged every four to five days while still in the growth phase. The cells were passaged as described above, with the exception of 20-25 minutes of incubation with trypsin-EDTA as these cells were extremely adherent.

2.2 Cytospins

Immediately after isolation or taken directly from culture, cells were resuspended in complete RPMI or PBS with 10% FCS, at $2.5x10^5$ cells/ml. 200 µl of the cell suspension was added to each sample chamber. Poly-L-lysine-coated or BDH Superfrost plus glass slides were used. The cells were spun on a Shandon Cytopsin 3 (Shandon Inc, Pittsburgh, PA, USA) at 75g for three minutes. The slides were left to dry for approximately 10 minutes at room temperature, then fixed for two minutes in methanol, eosin stained in Diff-Quik®1 (Dade®, Gamidor Ltd., Abingdon, Oxon, UK) for two minutes, haematoxylin stained in Diff-Quik®2 for one minute, then immediately rinsed in water. After air drying for 10 minutes, cytospins were wetted in xylene, then mounted in Pertex mountant (Cellpath, Newtown, Powys, UK).

2.3 Cytokine Immunoassays

IL-10, IL-12, TGF-β1, IL-13, TNF-α, IFN-γ, MIP-1α, and GM-CSF levels were measured from cell culture supernatants or BAL fluid using DuoSet® enzyme-linked

immuno-sorbant assay (ELISA) Development System kits (R&D Systems Europe Ltd), following the manufacturer's instructions. Plates were washed using a HandyWash manual microplate washer (Dynatech Laboratories) and read at 450 nm on a Revelation 3.04 microplate reader (Dynex Tecnologies, Billinghurst, West Sussex, UK) with the correction wavelength set to 550 nm.

All standards were prepared in duplicate, as recommended by the manufacturer, while samples were prepared in triplicate. The plate reader software drew standard concentration curves and calculated cytokine concentrations of samples.

All samples were assayed neat, however samples for TGF-β1 determination required activation to liberate immunoreactive TGF-β1 from its latent complexes. As per the manufacturer's instructions, this was achieved by incubating the samples for 10 minutes at room temperature with 1N HCl, followed by neutralisation with 1.2N NaOH and 0.5M HEPES.

2.4 Flow Cytometry

Sample acquisition was performed on a Becton Dickinson FACScalibur. Analysis was completed using BD CellQuest Software.

Flow cytometry was used to phenotype the isolated cells and assess the purity of these populations. Cells for phenotyping, either from culture or directly after isolation, were placed in a round-bottomed 96-well plate in aliquots of approximately 10^5 cells per well, in 200 μl of medium. The plate was then centrifuged at 100g for two minutes, and the supernatant in each well discarded. The cells were washed by resuspension in 200 μl of chilled flow buffer, and centrifuged again. The supernatant was removed and the cells were resuspended in 50 μl of a 1:10 dilution of mouse serum, to block non-specific binding. The cells were blocked at room temperature for 10 minutes. Antibodies were then added directly to the wells in volumes of 5 or

10 µl, to obtain final dilutions of 1:100 or 1:50, respectively. Details of the specific antibodies and dilutions are listed in table 2.1. The cells were incubated with the primary antibody for 30 minutes on ice in the dark, and then washed in flow buffer, as described above, three times. After washing, the stained cells were resuspended in 200 µl of fresh flow buffer and transferred to labelled flow cytometry tubes containing an additional 200 µl of flow fix. Cells were run through the flow cytometer immediately.

Antigen	Clone	Supplier	Dilution	Isotype
CD3-PE	145-2C11	BD Pharmingen	1:100	HsIgG_1,κ
CD45R (B220)-PE	RA3-6B2	"	1:100	rIgG_{2a},κ
CD11b-PE	M1/70	"	1:100	rIgG_{2b},κ
CD11c-PE	HL3	"	1:50	HsIgG_1,λ
CD80-PE	16-10A1	"	1:50	HsIgG_2,κ
CD86-PE	GL1	"	1:50	rIgG_{2a},κ
CD54 (ICAM-1)-PE	3E2	"	1:100	HsIgG_1,κ
I-A^d / I-E^d-FITC	2G9	"	1:100	rIgG_{2a},κ
Ly-6G (Gr-1)-PE	RB6-8C5	"	1:100	rIgG_{2b},κ
CD19-PE	1D3	"	1:100	rIgG_{2a},κ
Isotype control-PE	A95-1	"	1:100	rIgG_{2b}
Isotype control-PE	A19-3	"	1:50	HsIgG
Isotype control-FITC	R35-95	"	1:100	rIgG_{2a}
Isotype control-PE	R35-95	"	1:100	rIgG_{2a}

Table 2.1 Primary antibodies used for phenotypic analysis. Monoclonal antibodies were all supplied by BD Pharmingen. Dilutions were made from supplied stock. All antigens listed above were either FITC- or PE-conjugated and did not require secondary reagents. Abbreviations in isotype column are as follows: Hs (hamster); r (rat).

2.5 Immunohistochemistry

All tissue sections, mounted on glass slides, were dewaxed in xylene for 10 minutes at room temperature, then rehydrated with one-minute washes in descending grades of alcohol (absolute, 74%, 64%) followed by a wash in deionised water. Vector Antigen Unmasking Solution (Vector Laboratories, Inc., Burlingame, CA, USA) was diluted 1:100 in deionised water in a covered plastic dish, and the slides were microwaved in this solution at 1000 watts for three sets of minutes each. The slide rack was turned after each five minute cycle. The slides were then cooled for 20 minutes in running tap water.

Next, to block non-specific staining, slides were incubated in a 0.15% solution of hydrogen peroxide (H_2O_2) in tap water at room temperature for 15 minutes, then washed twice in PBS for five minutes before being loaded onto a Shandon Sequenza staining rack (Shandon Inc, Pittsburgh, PA, USA). All volumes for solutions added to slides in these staining racks were 125 µl. The protocols from this point onward for the individual antibodies are described below.

After specific staining, all tissue sections were visualised using diaminobenzidine tetrahydrochloride (DAB) substrate solution (Dako Liquid DAB and large volume substrate chromogen solution) for five minutes, followed by a PBS wash. The DAB solution was prepared by according to the manufacturer's instructions: one drop (20 µl) added per ml substrate solution. The slides were removed from the Sequenza racks, and washed in running tap water. They were lightly counterstained in haematoxylin blue for 30 seconds, blued by dipping in Scott's tap water substitute for 30 seconds, and dehydrated in ascending grades of alcohol (64%, 74%, absolute). The slides were then cleared by short incubations in three changes of xylene and mounted in Pertex mountant.

2.5.1 Automated anti-FITC Staining of Tissue Sections

Following the H_2O_2 blocking, slides were washed for five minutes in a 1:20 dilution of OptiMax® concentrate in deionised water (OptiMax® buffer) (BioGenex, San Ramon, CA, USA). The slides were then marked with a grease pencil and loaded onto the BioGenex OptiMax®Plus consolidated staining system.

The following steps were automated, and the required solutions prepared in advance, at volumes determined by the OptiMax®Plus system, depending on the number of slides in the run. The slides were incubated in a 1:5 dilution of normal goat serum (NGS) in OptiMax® buffer, with four drops of Avidin D blocking solution (Vector) per ml, for 10 minutes. The positive slides were then incubated for 30 minutes in a 1:1000 dilution of rabbit anti-FITC primary antibody in NGS, with four drops of Biotin solution (Vector) per ml. The negative slides were also incubated for 30 minutes in the same solution, prepared without the primary antibody. Three rinses of OptiMax® buffer followed, and the slides were then incubated for another 30 minutes in a 1:300 dilution of goat anti-rabbit secondary antibody (Dako) in NGS. After three more washes in OptiMax® buffer, the slides were incubated in Vector R.T.U. Vectastain® Elite ABC Reagent for 30 minutes, and washed three times. The final step was a five minute incubation in DAB substrate solution (Dako, prepared as described in section 2.6.1) followed by three OptiMax® buffer washes.

The slides were then unloaded into more buffer, counterstained, blued, dehydrated, cleared and mounted as described.

2.5.2 CD3 Immunostaining

Tissue sections were blocked with Vector Avidin D blocking solution for 15 minutes, washed with PBS twice for 5 minutes, blocked with Vector Biotin solution, for 15 minutes, and washed twice again. The slides were incubated in Dako Chemate

Antibody Diluent (Dako Corporation, Carpinteria, CA, USA) for 10 minutes, followed by the CD3 primary antibody, (rabbit polyclonal, A0452, Dako) diluted 1:100 in Dako Diluent for the test slides or positive controls, or only Dako Diluent for the negative controls. The primary antibody was left on for 30 minutes at room temperature. The slides were then washed twice in PBS for five minutes, and then biotinylated goat anti-rabbit secondary (Dako), diluted 1:300 in Dako Diluent, was applied for 30 minutes. Two five-minute washes in PBS were followed by 30 minutes in Vector R.T.U. Vectastain® Elite ABC Reagent and another two five-minutes washes.

2.5.3 TGF-β Immunostaining

This assay required the use of freshly cut tissue sections. After being loaded onto the Sequenza staining racks, the slides were incubated Dako protein block for 10 minutes, followed by the TGF-β primary antibody, (chicken polyclonal, AF101-NA, R&D Systems) diluted 1:50 in Dako Diluent for the test slides or positive controls, or only Dako Diluent for the negative controls. The primary antibody was left on overnight at 4°C. After warming to room temperature, the slides were washed twice in PBS for two minutes, and then the goat anti-chicken secondary antibody (Vector), diluted 1:250 in Dako Diluent, was applied for 30 minutes. Two two-minute washes in PBS were followed by 30 minutes in Vector R.T.U. Vectastain® Elite ABC Reagent and another two five-minutes washes.

2.5.4 CD11c Immunostaining

The CD11c primary antibody (hamster anti-mouse) was adsorbed with a solution of 20% mouse serum and 20% rabbit serum in PBS for two hours at 37°C to inhibit non-specific binding. The adsorbed antibody was then centrifuged and decanted before use.

Once loaded onto the Sequenza racks, slides were blocked in a solution of 4 drops Vector Avidin D blocking solution per ml of 20% NGS in PBS for 10 minutes, then washed for two minutes in PBS, twice. The CD11c antibody was diluted 1:15 in 20% normal rabbit serum in PBS, and four drops of Vector Biotin block was added to this solution before it was applied to the tissue sections for 30 minutes at room temperature. Negative control slides received the same solution, without the primary antibody. Slides were then washed twice again, and incubated with the goat anti-hamster secondary antibody (Vector), which was diluted 1:150 in PBS, for 30 minutes at room temperature, and washed in PBS another two times. Vector R.T.U. Vectastain® Elite ABC Reagent was applied to 30 minutes, followed by another two five-minutes washes, and visualisation, counterstaining, clearing and mounting as described.

2.5.5 B220 Immunostaining

Tissue sections were blocked with Vector Avidin D blocking solution for 15 minutes, washed with PBS for three minutes, blocked with Vector Biotin solution, for 15 minutes, and washed again. The slides were incubated in Dako Chemate Antibody Diluent for 10 minutes, followed by the B220 primary antibody, (biotinylated rat anti-mouse, 011220A, Pharmingen) diluted 1:150 in Dako Diluent for the test slides or positive controls, or only Dako Diluent for the negative controls. The primary antibody was left on for 30 minutes at room temperature. The slides were given two two-minute washes with PBS, followed by 30 minutes in Vector R.T.U. Vectastain® Elite ABC Reagent and another two five-minute washes before completing as described.

2.5.6 MHC Class II Immunostaining

Tissue sections were blocked with Vector Avidin D and Biotin blocking solutions as described above. Following one three-minute wash in PBS, Vector M.O.M. mouse IgG block was applied for one hour at room temperature. The Vector M.O.M. immunodetection kit is designed specifically to localise mouse primary antibodies on mouse tissues, and was used as per the manufacturer's instructions. A two- minute PBS wash was followed by Vector protein concentrate for five minutes, and then the MHC class II primary antibody (mouse monoclonal, 06341D, Pharmingen), diluted 1:50 in PBS was left on overnight at 4°C. The slides were warmed to room temperature, then given two two-minute washes in PBS before incubating with Vector M.O.M. secondary antibody for 10 minutes. Following another two washes in PBS, Vector M.O.M. ABC was applied for five minutes, and the slides were given a final two five-minute washes in PBS before moving on to the final steps.

2.6 Statistics

Statistics throughout this thesis were calculated using GraphPad InStat (version 3.01, 32 bit for Windows 95/NT, GraphPad Software, San Diego California USA, www.graphpad.com), and followed the recommendations made by this program. Results were considered significant if $p<0.05$.

CHAPTER 3

Murine Model of FITC-induced Pulmonary Fibrosis: Acute Response

3.1 Introduction

The main hypothesis on which this thesis is based is that APCs are altered by, and contribute to, the maintenance of the chronic inflammation seen in interstitial lung diseases, such as CFA. In order to test this hypothesis it was necessary to use an animal model that best mimicked the pattern of the human disease. The following two chapters will outline the reasons for choosing the FITC model, and present data characterising the disease seen in mouse lungs after acute (Chapter 3) and long-term (Chapter 4) exposure to FITC.

3.1.1 Animal Models of CFA

As patients with pulmonary fibrosis most often present in the later stages of disease, animal models of CFA are essential in order to elucidate the early cellular events that lead to progressive disease. They allow research to be directed towards the understanding of the mechanisms that determine the induction, maintenance, and in some cases, resolution, of pulmonary fibrosis in humans. Various models have been produced, including those induced by the use of butylated hydroxytoluene and oxygen [397], cyclophosphamide [421], ionising radiation [206], paraquat [422], and phorbol myristate acetate [423]. The most commonly used and well-studied rodent model of lung fibrosis, however, is the bleomycin model [214,424-426].

3.1.2 The Bleomycin Model of Pulmonary Fibrosis

Bleomycin is a drug used successfully as a cytotoxic agent in the treatment of squamous cell carcinoma, testicular tumours, and lymphomas [216,427]. Although it was introduced largely because it has no major toxic effects on kidney or bone

marrow, bleomycin was soon found to cause pulmonary fibrosis in humans [212,427].

Animal models of bleomycin-induced pulmonary fibrosis have since been developed, and having many of the histological components of CFA [214,218], are thought to constitute a representative model of the human disease. However, as discussed in Chapter 1, a recent study by Borzone *et al.* [223] showed that while the early stages of bleomycin-induced lung damage resemble those of human pulmonary fibrosis, the later chronic stages do not resemble the histologic pattern of UIP that defines CFA in humans, nor was it restrictive. It is also difficult in the bleomycin model, as well as other models, to implicate specific immune responses to the initiating agent. As well, due to the severity of the response to bleomycin, the majority of studies only measure the response as far as three weeks after exposure [92,97,219,221,244,428,429]. This makes it difficult to study the long-term effects of progressive disease in this model.

3.1.3 The FITC Model of Pulmonary Fibrosis

Some of these limitations were addressed by a novel model of fibrosis developed in this laboratory [243]. This study demonstrated fibrosis in the lungs of both mice and rats given a single surgical intratracheal dose of FITC in PBS. An acute inflammatory response ensued, characterised by a granulocytic infiltrate which was replaced after one week by a chronic mononuclear cell infiltrate predominated by T lymphocytes. A chronic patchy fibrosis developed over several months, and was localised to sites of long-term FITC deposition, while adjacent lung tissue without FITC remained apparently normal. This study was carried out over a five month period. FITC is a known skin-sensitising agent shown to be capable of inducing specific immune responses [430]; specific immunity against the fluorescein hapten can also be measured in this model by the presence of anti-FITC serum antibodies [243].

This model was extended by Christensen *et al.* [244] who found that the single intratracheal dose of FITC, given to both BALB/c and C57BL/6 mouse strains, caused a reproducible lung injury, quantifiable increase in lung collagen content, and a specific immune response to the FITC. They also showed that the development of FITC-induced fibrosis is not dependent on T cell-specific immunity. However, this study was carried out over a maximum period of three weeks, and this group do not disagree that the immune response is important beyond their three week time limit, in the later, chronic stages of the disease (G.B. Toews, personal communication). Indeed, in the original paper, Roberts *et al.* [243] describe the appearance of lymphocytes in the BAL at seven days post-FITC, and frozen sections showed lymphocytic infiltrate at five months.

Thus the FITC-induced murine model of pulmonary fibrosis has several advantages over the traditional bleomycin model. Primarily, it produces a chronic persistent inflammation more in line with human pulmonary fibrosis, and allows for long-term evaluation of the mice. The use of the fluorescent hapten FITC itself is another advantage as it greatly facilitates the tracking of the ongoing response and the progression of the disease in the tissues, and allows measurement of a specific immune response.

The FITC-induced model of pulmonary fibrosis was further characterised for this body of work. The original FITC model, however, used a surgical method of intratracheal instillation. This was associated with a 30% mortality rate within 48 hours of instillation. Due to Home Office requirements for Reduction, Replacement and Refinement, the model was modified so that the FITC was introduced into the trachea by a non-surgical trans-oral method. This significantly reduced the mortality rate to less than 5% in the 48 hours following instillation.

3.1.4 Aims of Chapter

The principal aims of this chapter are to describe:

- the method, including modifications to the original method, of the FITC-induced murine model of pulmonary fibrosis
- the acute effects of FITC on murine lung tissue pathology
- a method of scoring the acute inflammatory response in the lungs of FITC-treated mice
- the acute effects of FITC on the BAL cells and fluid of murine lungs

3.2 Method of Intratracheal Instillation of FITC / PBS in Mice

Female BALB/c mice, between six and eight weeks of age and 10-22 grams in weight, were anaesthetised with 0.3 ml of Avertin given intraperitoneally. Each mouse was rested by its front teeth on the support shown in Figure 3.1A. A string with a weight suspended on the end was looped around the bottom teeth to hold the mouth open. A cold, fibreoptic light source was shone directly onto the throat to allow visualisation of the top of the trachea. A pipette was used to dispense 50 μl of the 2 mg/ml FITC solution or sterile, endotoxin-free PBS (for control mice) into a 1 ml syringe. A blunted 25-gauge needle was attached to the syringe and inserted into the trachea of the mouse. The FITC solution or PBS was carefully delivered into the trachea of the mouse (Figure 3.1B). The mouse was then removed from the support and laid on its side in the cage. Mice recovered from the anaesthetic within a couple of hours, and were monitored on a regular basis until required. Immediate death from the above procedure occurred extremely rarely, and greater than 95% of mice survived until the required time points.

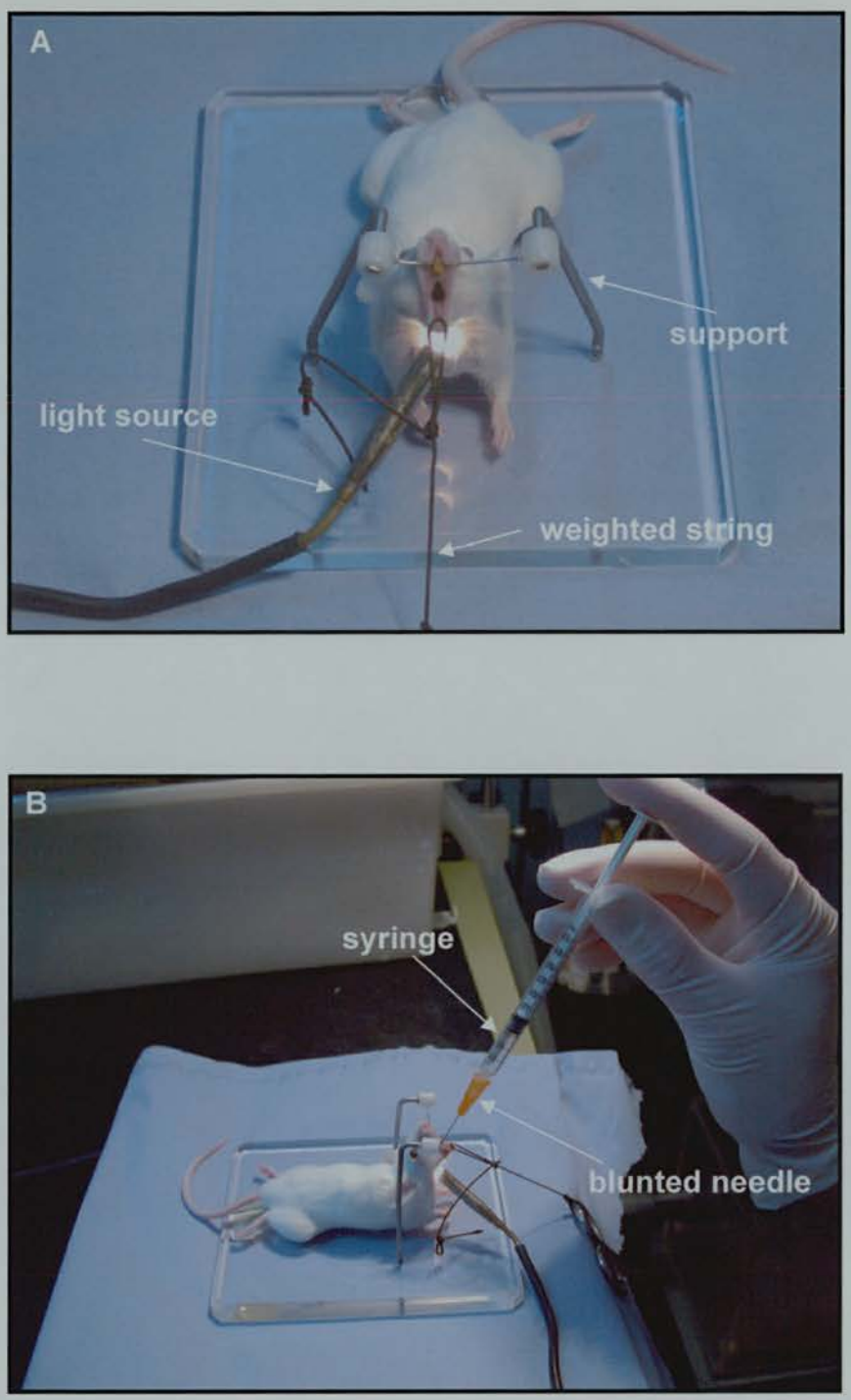

Figure 3.1 Intratracheal instillation of FITC/PBS dose. An anaesthetised BALB/c mouse rested on the support, with a weighted string holding the lower jaw open, and a light source illuminating the trachea (A). A 1 ml syringe with a blunted needle was used to instil the dose of FITC or PBS (B).

3.3 Acute Effects of FITC on Murine Lung Tissue Pathology

Murine lungs from mice given either FITC or PBS intratracheally were killed by intraperitoneal injection of 0.5 ml pentabarbitone (Sagatal) (Merial Animal Health, UK) at one, two, three, five, or seven days after treatment. Following perfusion and lavage, the lungs were fixed in formalin as described in section 5.3.3, and embedded and sectioned. Tissue sections were then stained with haematoxylin and eosin (H&E), and a second set were stained with anti-FITC antibody.

Of 12 pairs of mouse lungs examined on each of Days 1 and 2, after being given an intratracheal dose of FITC, 10 showed varying amounts of FITC deposition in the lungs, while two from each time point showed no FITC (Table 3.1). On Day 3, eight out of 12 mice were positive for FITC. On Day 5, all four mice given an intratracheal dose had FITC deposited in their lungs, while on Day 7, three out of four mice showed FITC deposition. All lung sections from PBS mice stained negatively for FITC at all time points.

# mice	Day 1	Day 2	Day 3	Day 5	Day 7
total	*12*	*12*	*12*	*4*	*4*
FITC +ve	10	10	8	4	3
FITC -ve	2	2	4	0	1

Table 3.1 Numbers of mice treated with FITC and assessed histologically and immunohistochemically. Mice were given a single dose of FITC intratracheally and assessed on Day 1, 2, 3, 5, or 7.

3.3.1 Distribution of FITC in Acute Lungs

Tissue sections (3 μm) stained with anti-FITC antibody were examined to determine distribution of the FITC in the mouse lungs. Although FITC staining could be variable, Figure 3.2 shows the typical distribution of FITC occurring at Day 1 and Day 5 after treatment. At Day 1, FITC was diffusely distributed around large (not shown) and small bronchi and blood vessels, and in the alveolar walls (Fig. 3.2A). Heavily stained macrophages could be seen in the tissues as well. In the PBS-treated mouse lung, however (Fig. 3.2B), the lung looked predominantly normal, although there could be mild cellular infiltrate. Five days after FITC instillation (Fig. 3.2C), some of the FITC had been cleared, presumably by the mucociliary apparatus, and macrophages that were still seen heavily stained for FITC, while PBS controls appeared normal (Figure 3.2D). However, much FITC still remained, particularly around the bronchi and blood vessels. Areas of thickened alveolar walls and cellular infiltrate were found, as well as anti-FITC antibody negative, normal-appearing areas of lung. A negative control section of Day 1 FITC-treated lung is shown in Figure 3.2E.

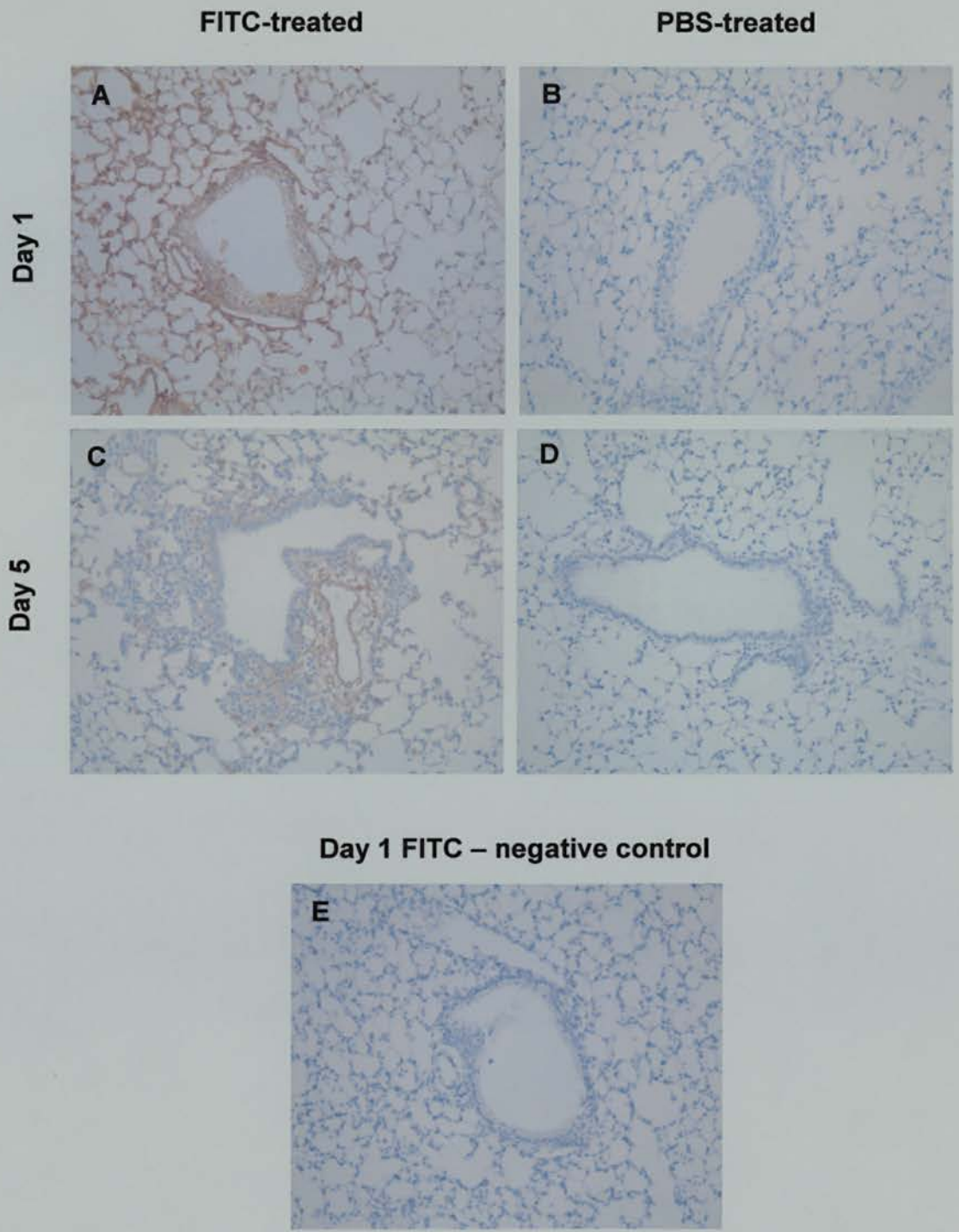

Figure 3.2 Anti-FITC antibody stained sections of mouse lung 1 and 5 days after treatment. Mouse lungs were fixed and processed as described. Lung sections from FITC-treated (A, C) or PBS-treated (B, D) mice on Day 1 (A, B) and Day 5 (C, D) were stained with anti-FITC antibody, while negative controls (E) received no antibody. Original magnification x200.

3.3.2 Scoring of Acute FITC-induced Damage

In order to assess the inflammatory reaction in the lungs and to compare the FITC-treated and control mice, a scoring system was devised. The scoring of peripheral lung inflammation was performed at x200 magnification over 10 random fields in which lungs were completely, but not overly, inflated, and where the field contained a complete transection of at least one bronchiole less than half a field width in diameter, and a blood vessel as well as an alveolar airway. Large bronchioles were ignored. As the lungs were all perfused and lavaged before fixation, no comment can be made on infiltrate in the alveolar airspaces. The scoring system is presented in Table 3.2.

Area scored (# of cells in)	Score			
	1	2	3	4
Perivascular Compartment*	no infiltration	<20 cells	<100 cells	>100 cells
Bronchiolar Epithelium	no infiltration	<5 cells	<10 cells	>10 cells
Peri-bronchiolar Alveolar Tissue§	no infiltration	<20 cells	<100 cells	>100 cells
Alveolar Walls†	no infiltration	2-3 cells	4-5 cells	>5 cells

* Cells around blood vessel walls

§ Defined as sub-bronchiolar tissue, beneath basement membrane and smooth muscle, not immediately adjacent to a blood vessel

† Scores indicative of focal expansion of alveolar walls by that number of cells

Table 3.2 Method for scoring peripheral inflammation in FITC- and PBS-treated murine lungs.

The highest score in each compartment per field set the score for that field. For each section 10 fields were scored. The scores for the 10 fields were averaged to give the score for the section. The scores for each compartment are given individually, but were also summated to give an overall score where:

- **4** = no infiltrate in any compartment
- **5-8** = overall mild infiltrate
- **9-12** = overall moderate infiltrate
- **13-16** = overall severe infiltrate

Statistics were calculated by taking the mean value of the 10 fields per section as the value for that animal at the time point. Using GraphPad InStat, the values for all animals at each time point after FITC treatment were then statistically compared to the values for all animals at the same time points after PBS treatment using a 2-tailed Mann-Whitney U test. Significance was assumed if $p < 0.05$.

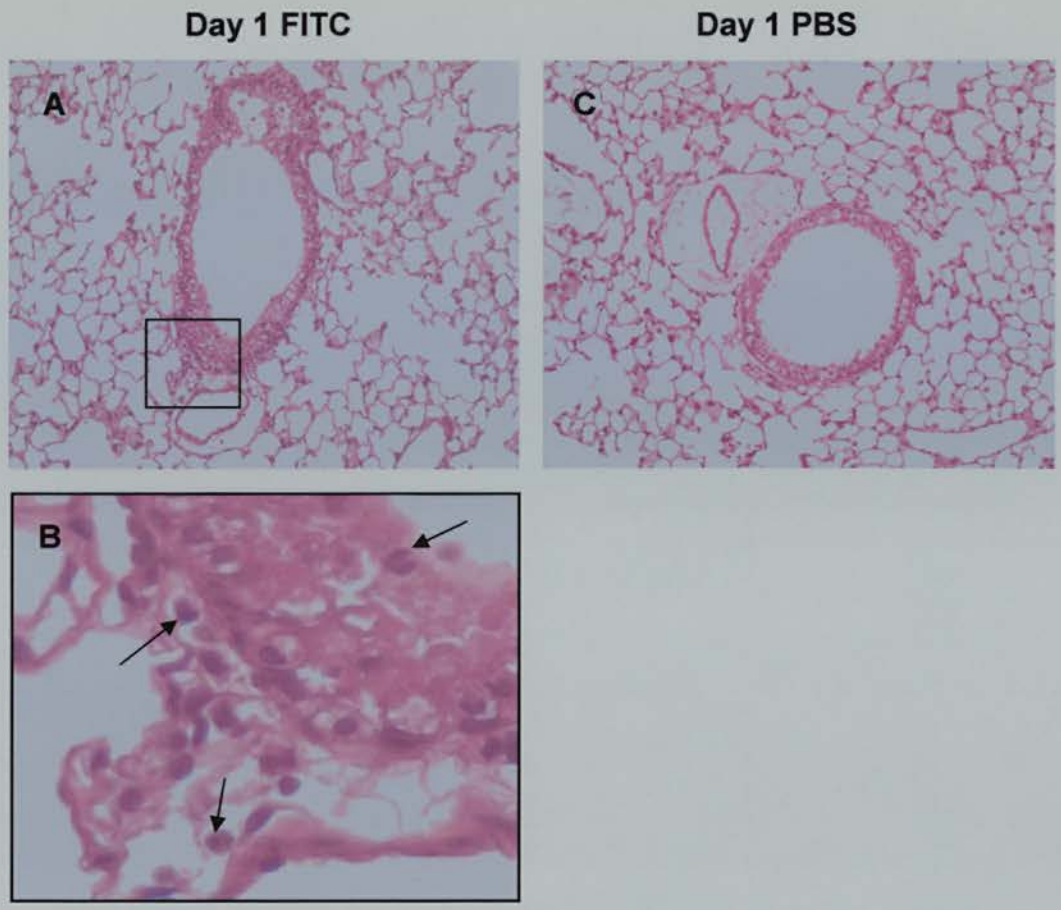

Figure 3.3 H&E stained sections of mouse lung one day after FITC (A, B) or PBS (C) instillation. Mouse lungs were fixed and processed as described. Sections were scored to assess damage to the lungs. Black box in A surrounds area of enlargement shown in B. Arrows indicate granulocytic cells with lobated nuclei. Original magnification x200. Enlargement approximately x800.

Figure 3.3 shows typical fields used to score acute FITC-induced lung damage. At x200 magnification (A and C), both fields fulfill all requirements: a complete transection of at least one bronchiole less than half the field width in diameter, a blood vessel, and an alveolar airway. Figure 3.2B shows that at Day 1 after FITC instillation, the cellular infiltrate is composed primarily of granulocytic cells.

At one day post-FITC treatment, the perivascular compartment in Figure 3.3A was given a score of "2" as there was cellular infiltrate, but there were fewer than 20 cells around the blood vessel walls. The bronchiolar epithelium was given a score of "3"

as there were more than five, but fewer than 10 cells in this area. In the peri-bronchiolar alveolar tissue, a score of "2" was given as there were fewer than 20 infiltrating cells. Finally, in the alveolar walls there was evidence of focal expansion by two to three cells, indicating a score of "2". A combined score of "9", calculated by adding all the scores in the field, was then given for that field, indicating an overall moderate infiltrate. This process would be repeated over nine additional random fields, and the mean scores would be calculated for the animal.

In Figure 3.3C, which shows a typical field from a section of PBS treated lungs after one day, the perivascular compartment showed fewer than 20 infiltrating cells (score = 2), the bronchiolar epithelium had fewer than 5 infiltrating cells (score = 2), the peri-bronchiolar epithelium shows no infiltrate (score = 1), and the alveolar walls showed evidence of focal cellular expansion by two to three cells in some areas (score = 2). This field was then given an overall score of "7", indicating overall mild infiltrate, which would be expected after introducing a substance into the lungs. As above, another nine random fields would be scored, and the mean score calculated for this animal.

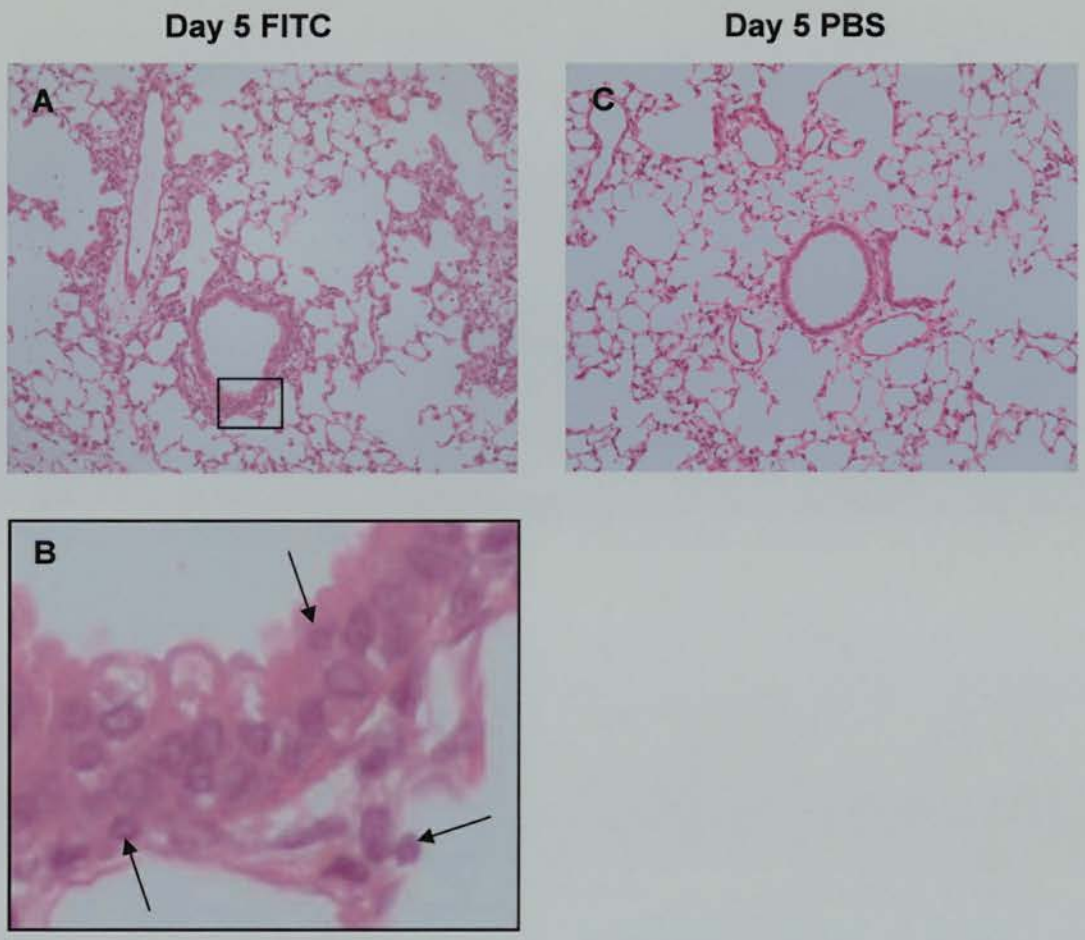

Figure 3.4 H&E stained sections of mouse lung five days after FITC (A,B) or PBS (C) instillation. Mouse lungs were fixed and processed as described. Sections were scored to assess damage to the lungs. Black box in A surrounds area of enlargement shown in B. Arrows indicate cells with a mononuclear appearance. Original magnification x200. Enlargement approximately x800.

Figure 3.4 shows typical fields from mice five days after intratracheal instillation of FITC (A,B) or PBS (C). The scoring for the Day 5 FITC section (Fig. 3.4A) was as follows: perivascular compartment = 2; bronchiolar epithelium = 2; peri-bronchiolar alveolar tissue = 2; alveolar walls = 2. This gave a combined score of 8, indicating overall mild infiltrate, bordering on moderate. This was similar to the combined score seen at Day 1, however the nature of the infiltrate was different. At Day 1 the infiltrate was primarily granulocytic (Fig. 3.3B), while at Day 5, it was predominantly mononuclear (Fig. 3.4B). This finding is consistent with that of the earlier model [243].

The scoring for the Day 5 PBS field in Figure 3.4C was as follows: perivascular compartment = 2; bronchiolar epithelium = 1; peri-bronchiolar alveolar tissue = 1; alveolar walls = 1. This gave an overall score of 5, which is at the low end of the overall mild infiltrate category. As mentioned previously, nine additional random fields would be scored for both the FITC- and the PBS-treated sections, and the means would be calculated. This would be repeated for each animal at each time point, and for each treatment.

Table 3.3 and Figure 3.5 summarise the results of scoring the acute FITC-induced or PBS control response in mouse lungs. Each of the four areas outlined in Table 3.2 were evaluated for each of the five time points (Days 1, 2, 3, 5, and 7).

In the perivascular compartment, the mean scores over each of the time points measured in the PBS-treated control mice indicated little cellular infiltrate, in contrast to those measured in the FITC-treated mice. The mean score for the FITC mice was highest at Day 7, but not significantly so. However, the mean scores of the FITC-treated mice in this compartment were significantly greater than those of the PBS control mice over each of the days measured ($p < 0.03$). In the bronchiolar epithelium, the scores were generally lower for both FITC- and PBS-treated mice, however the mean scores for the FITC-treated mice at Days 1, 2 and 3 were significantly higher than those of the PBS control mice ($p < 0.001$). Cellular infiltrate into the peri-bronchiolar alveolar tissue of the PBS-treated mice was minimal at all time points, but in the FITC-treated mice the cellular infiltrate consistently scored significantly higher than in the controls ($p < 0.03$), and had the highest score on Day 7. In the alveolar walls there was little, if any, cellular infiltrate in the PBS control mice, but again, in the FITC-treated mice the mean scores were significantly higher at each of the time points ($p < 0.03$). As in the previous compartment, the highest scores were seen at Day 7.

Time after treatment (# animals)	Perivascular compartment mean ± SEM [p, vs PBS]	Bronchiolar epithelium mean ± SEM [p, vs PBS]	Peri-bronchiolar alveolar tissue mean ± SEM [p, vs PBS]	Alveolar walls mean ± SEM [p, vs PBS]	Combined Score mean ± SEM [p, vs PBS]
Day 1 FITC (n=12)	2.13 ± 0.11 [p < 0.001]	1.92 ± 0.13 [p < 0.001]	2.03 ± 0.12 [p < 0.001]	2.15 ± 0.12 [p < 0.0001]	**8.23 ± 0.45** [p < 0.001]
Day 2 FITC (n=12)	2.22 ± 0.11 [p < 0.0001]	1.96 ± 0.12 [p < 0.0001]	2.29 ± 0.13 [p < 0.0001]	2.30 ± 0.13 [p < 0.0001]	**8.77 ± 0.45** [p < 0.0001]
Day 3 FITC (n=12)	2.33 ± 0.14 [p < 0.001]	1.34 ± 0.12 [p < 0.001]	2.51 ± 0.18 [p < 0.0001]	2.78 ± 0.20 [p < 0.0001]	**8.95 ± 0.59** [p < 0.0001]
Day 5 FITC (n=4)	2.3 ± 0.2 [p < 0.03]	1.28 ± 0.13*	2.33 ± 0.15 [p < 0.03]	2.4 ± 0.24 [p < 0.03]	**8.3 ± 0.7** [p < 0.03]
Day 7 FITC (n=4)	2.7 ± 0.2 [p < 0.03]	1.45 ± 0.13*	2.85 ± 0.14 [p < 0.03]	3.35 ± 0.30 [p < 0.03]	**10.35 ± 0.65** [p < 0.03]
Day 1 PBS (n=12)	1.48 ± 0.07	1.18 ± 0.09	1.26 ± 0.08	1.19 ± 0.10	**5.10 ± 0.33**
Day 2 PBS (n=12)	1.38 ± 0.05	1.06 ± 0.02	1.21 ± 0.06	1.16 ± 0.07	**4.80 ± 0.16**
Day 3 PBS (n=12)	1.35 ± 0.10	1.01 ± 0.01	1.20 ± 0.05	1.10 ± 0.04	**4.67 ± 0.14**
Day 5 PBS (n=4)	1.28 ± 0.06	1.02 ± 0.02	1.10 ± 0.07	1.05 ± 0.02	**4.42 ± 0.13**
Day 7 PBS (n=4)	1.40 ± .015	1.03 ± 0.03	1.10 ± 0.06	1.08 ± 0.05	**4.60 ± 0.27**

* p value not significant ($p > 0.05$)

Table 3.3 Peripheral lung inflammation scores in FITC-treated and PBS control mice. Statistics were calculated as described in section 3.3.2.

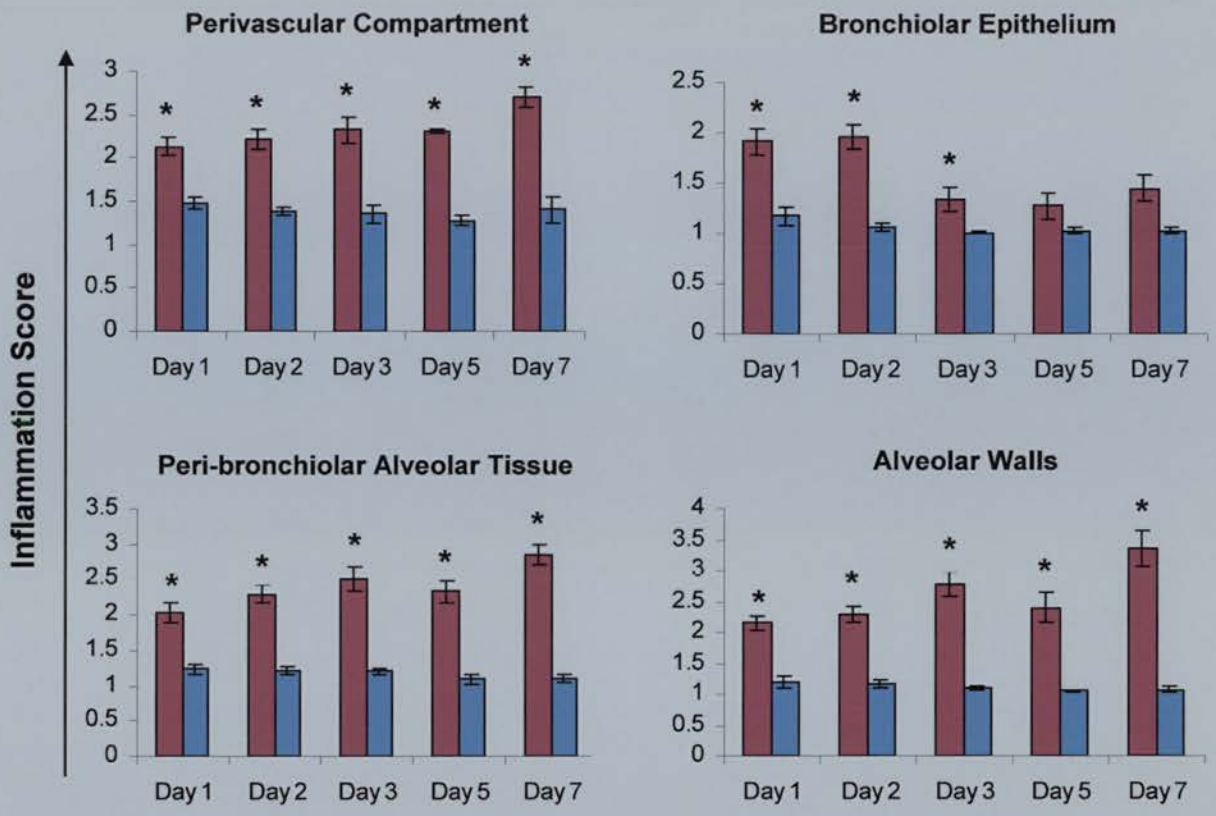

Figure 3.5 Inflammation scores on tissue sections of FITC-treated and PBS control mice over 7 days post-treatment. Tissue sections from FITC-treated (■) and PBS control (■) mice were scored as described. Data are presented as means ± SEM (n=12 at Day 1, Day 2, Day 3; n=4 at Day 5, Day 7).
*p<0.03 as compared to paired PBS value, by 2-tailed Mann-Whitney U test (see Table 3.3 for actual p values)

Figure 3.6 shows the combined scores for each of the five time points evaluated. The scores were calculated by adding the mean scores from each of the four compartments examined. In the PBS-treated mice, the combined score at Day 1 indicated an overall very mild infiltrate, but by Day 2, and through to Day 7, this dropped to a score indicating very little, if any, infiltrate measured in any compartment. In contrast, in the FITC-treated mice the combined scores over Days 1, 2, 3, and 5 indicated an overall mild infiltrate, bordering on moderate, and by Day 7 the score indicate an overall moderate infiltrate. As shown above, the infiltrate at Day 1 was primarily granulocytic, indicating an acute inflammatory response. By Day 5 the infiltrate appeared more mononuclear, suggesting a shift towards a chronic

inflammatory state. At each time point, the overall combined score for the FITC-treated mice was significantly higher than those of the PBS controls, indicating that the FITC did indeed cause an inflammatory reaction in the lungs of the mice that cannot be attributed to the carrier solution, PBS.

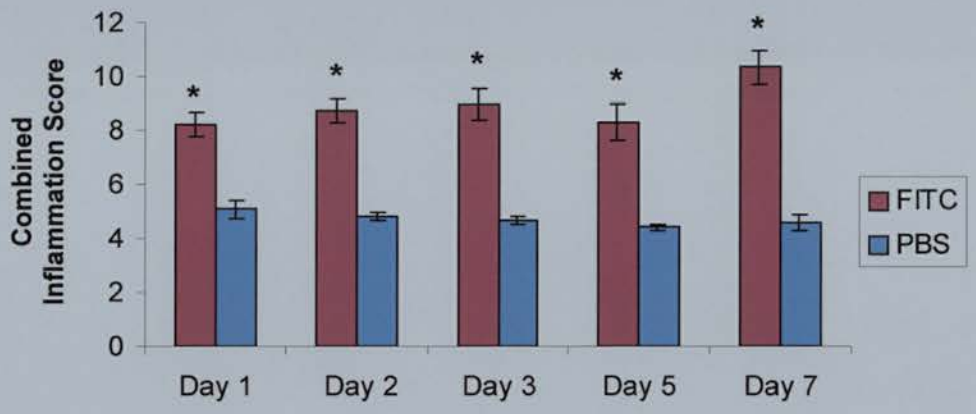

Figure 3.6 Combined inflammation scores on tissue sections of FITC-treated and PBS control mice over 7 days post-treatment. Tissue sections from FITC-treated and PBS control mice were scored as described. Data are presented as means ± SEM (n=12 at Day 1, Day 2, Day 3; n=4 at Day 5).
*p<0.03 as compared to paired PBS value, by 2-tailed Mann-Whitney U test (see Table 3.3 for actual p values).

3.3.3 Immunohistochemical Staining at Acute Time Points

Immunohistochemical staining for the cell surface protein CD3, to detect T lymphocytes, showed that T cells are present at similar levels in the tissues at Day 1 in both FITC- and PBS-treated mice (Figure 3.7A,E). Increased numbers of T cells were seen at Day 3 in the FITC-treated mice (B), but did not become prominent in the tissues until Day 5, and remained at Day 7 (C,D). In contrast, PBS-treated mice did not have increased numbers of T cells at Day 7 as compared to Day 1 (F,E). A negative control section in shown in Fig.3.7G.

B lymphocytes were detected immunohistochemically by staining with the B220 antibody. Unlike T cells, no influx in B cells was seen in FITC-treated mouse lungs up to Day 7, although numbers may have been slightly increased at Day 7, and particularly around potential cell aggregates (Figure 3.8A-D). This phenomenon will be discussed further in Chapter 4. Staining for B cells in PBS-treated mouse lungs showed no change between Day 1 and Day 7 (E,F). A negative control section is shown in Fig.3.8G.

TGF-β staining on tissue sections from FITC-treated mice appeared more abundant at Day 1 as compared to sections from PBS control mice (Figure 3.9A,E). Increased expression was seen at Day 3 (B), and appeared to peak at Day 5, with AMs being particularly strongly positive for the cytokine (C), with less staining evident at Day 7 (D). Staining for this cytokine was found on both alveolar macrophages and on the lung tissue itself.

CD11c cell surface protein was expressed on cells present in the tissue as well as on bronchial epithelium, but the AMs seemed to express more of this protein than other cell types. As will be discussed in Chapter 5, this correlates well with AMs from the BAL expressing very high levels of CD11c. No obvious change in the levels of CD11c protein expression was seen from Day 3 to Day 7 (Figure 3.10A-C), and PBS control mice expressed similar levels (D,E).

Cell surface staining for the MHC class II protein revealed that although there appeared to be more cells expressing MHC class II in the sections from FITC-treated mice than in PBS controls, these cells were by no means abundant (Figure 3.11A-D). The distribution of these cells was fairly localised, although not limited, to areas of alveolar thickening and dense cell clusters. As will be shown in Chapter 5, a subpopulation of DCs extracted from the lung tissue expressed high levels of this protein and indeed, examination of some of the heavily stained MHC class II-positive cells at high magnification *in situ* showed dendritic-like processes, suggesting that these are DCs (E).

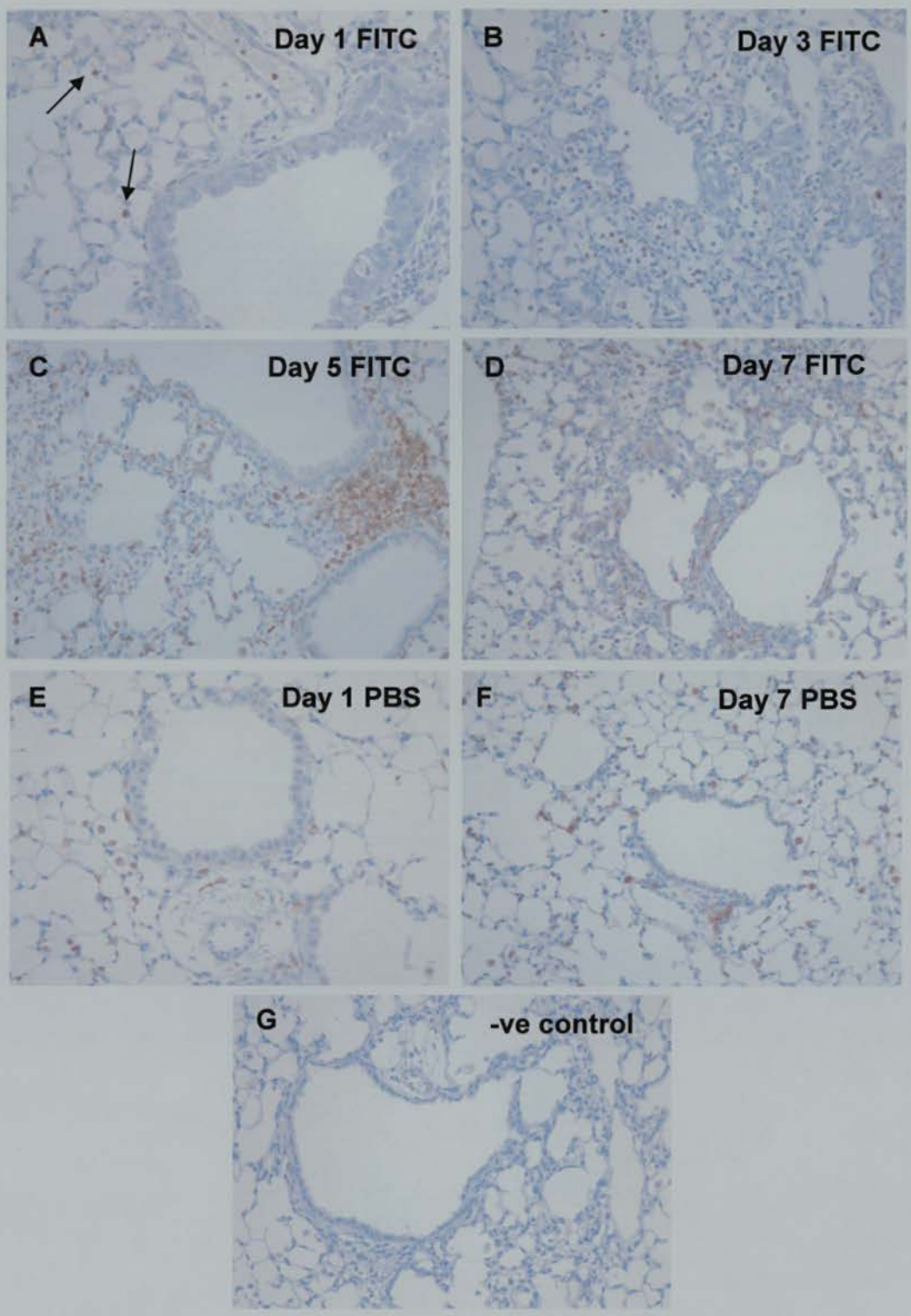

Figure 3.7 CD3 cell surface protein staining of lung tissue sections. Sections were stained by immunohistochemistry for CD3 to detect T lymphocytes. Sections are from FITC-treated mice on Day 1 (A) (arrows indicate positively-stained cells), Day 3 (B), Day 5 (C), Day 7 (D) after treatment, and from PBS control mice on Day 1 (E) and Day 7 (F) after treatment. A negative control from a Day 7 FITC-treated mouse is shown in G. Original magnification x200.

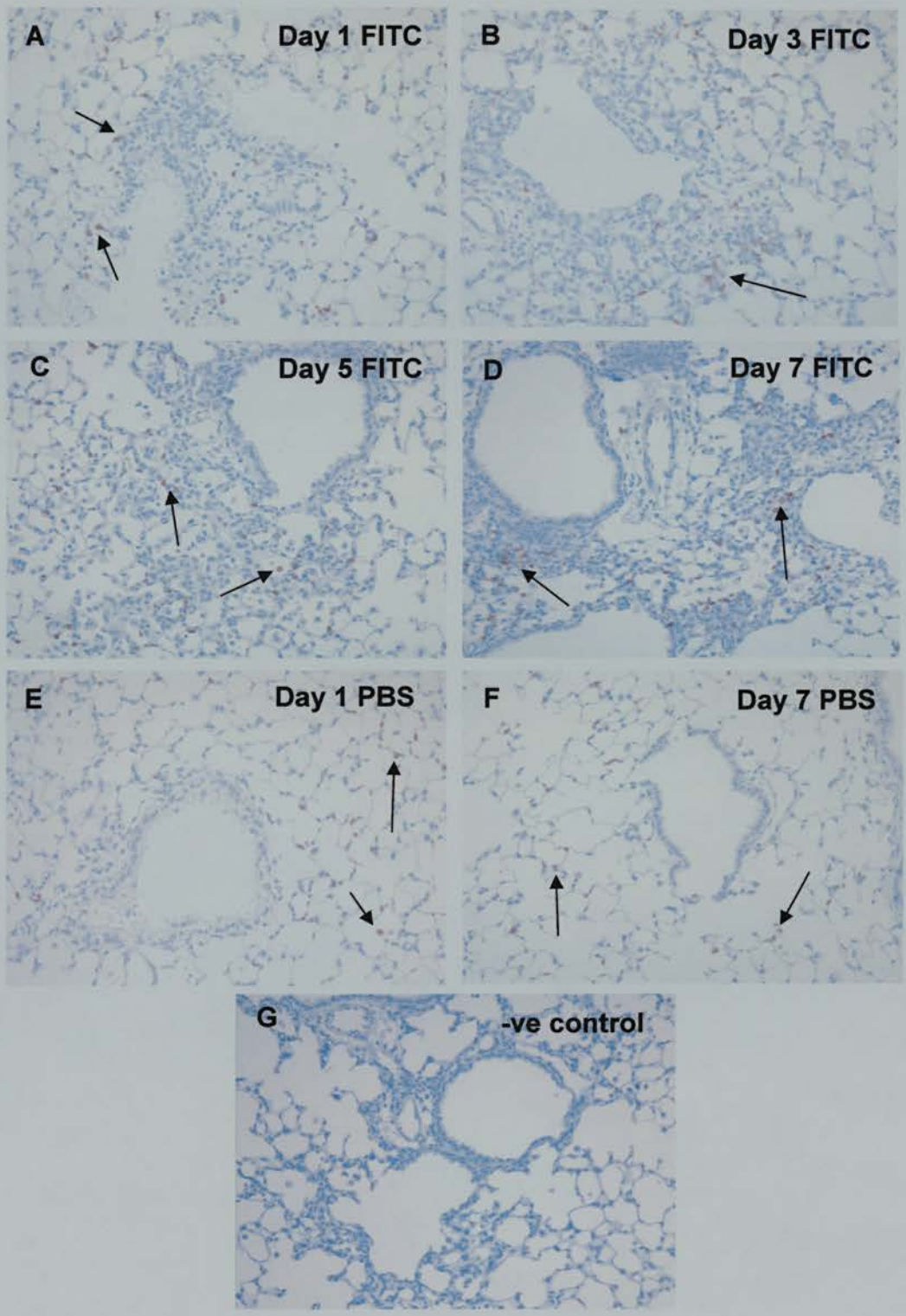

Figure 3.8 B220 cell surface protein staining of lung tissue sections. Sections were stained by immunohistochemistry for B220 to detect B lymphocytes. Sections are from FITC-treated mice on Day 1 (A), Day 3 (B), Day 5 (C), Day 7 (D) after treatment, and from PBS control mice on Day 1 (E) and Day 7 (F) after treatment. A negative control from a Day 7 FITC-treated mouse is shown in G. Original magnification x200.

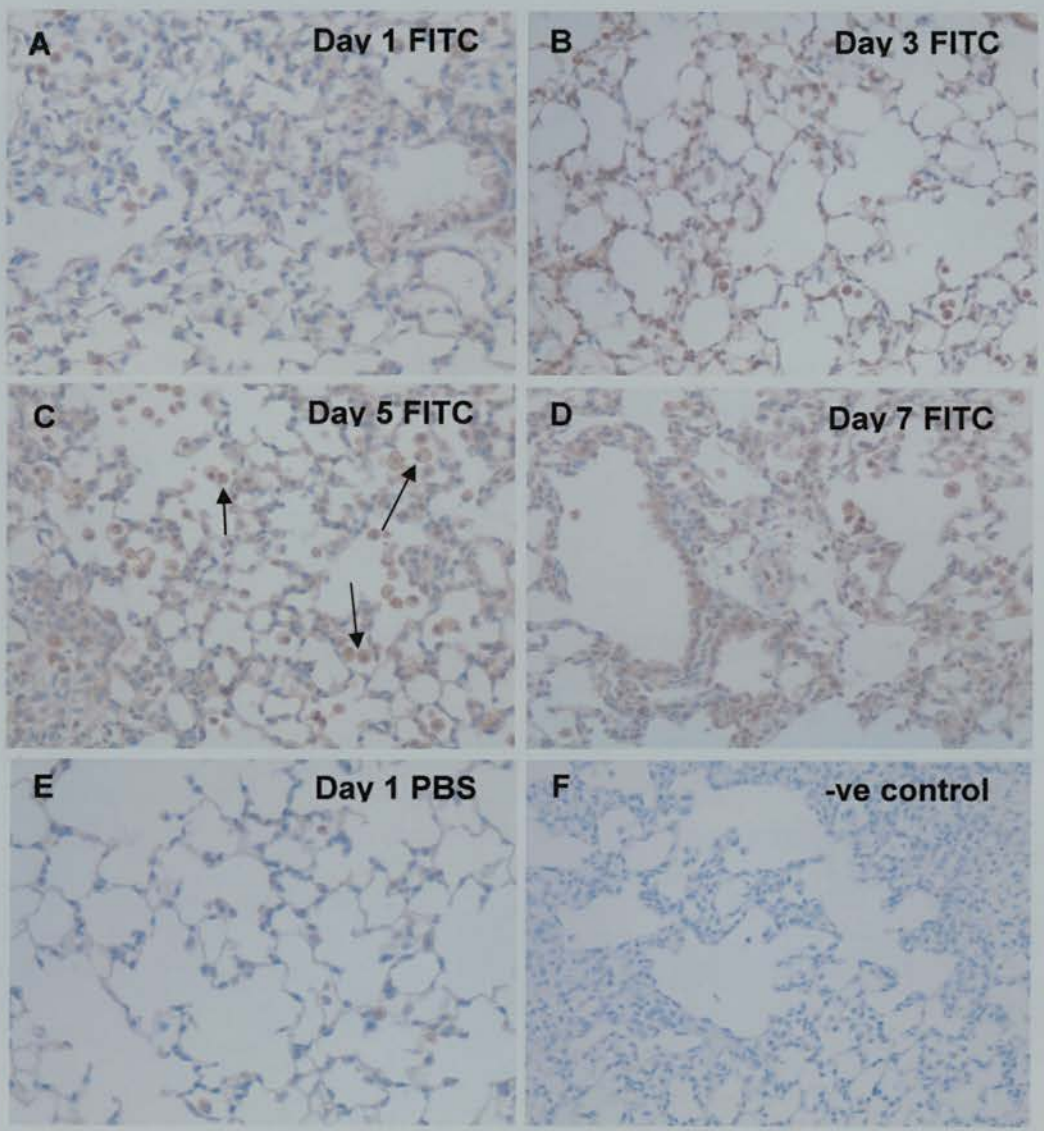

Figure 3.9 TGF-β protein staining of lung tissue sections. Sections were stained by immunohistochemistry for the cytokine TGF-β. Sections are from FITC-treated mice on Day 1 (A), Day 3 (B), Day 5 (C) (arrows indicate positively stained alveolar macrophages), and Day 7 (D) after treatment, and from PBS control mice on Day 1 (E) after treatment. A negative control from a Day 7 FITC-treated mouse is shown in F. Original magnification x200.

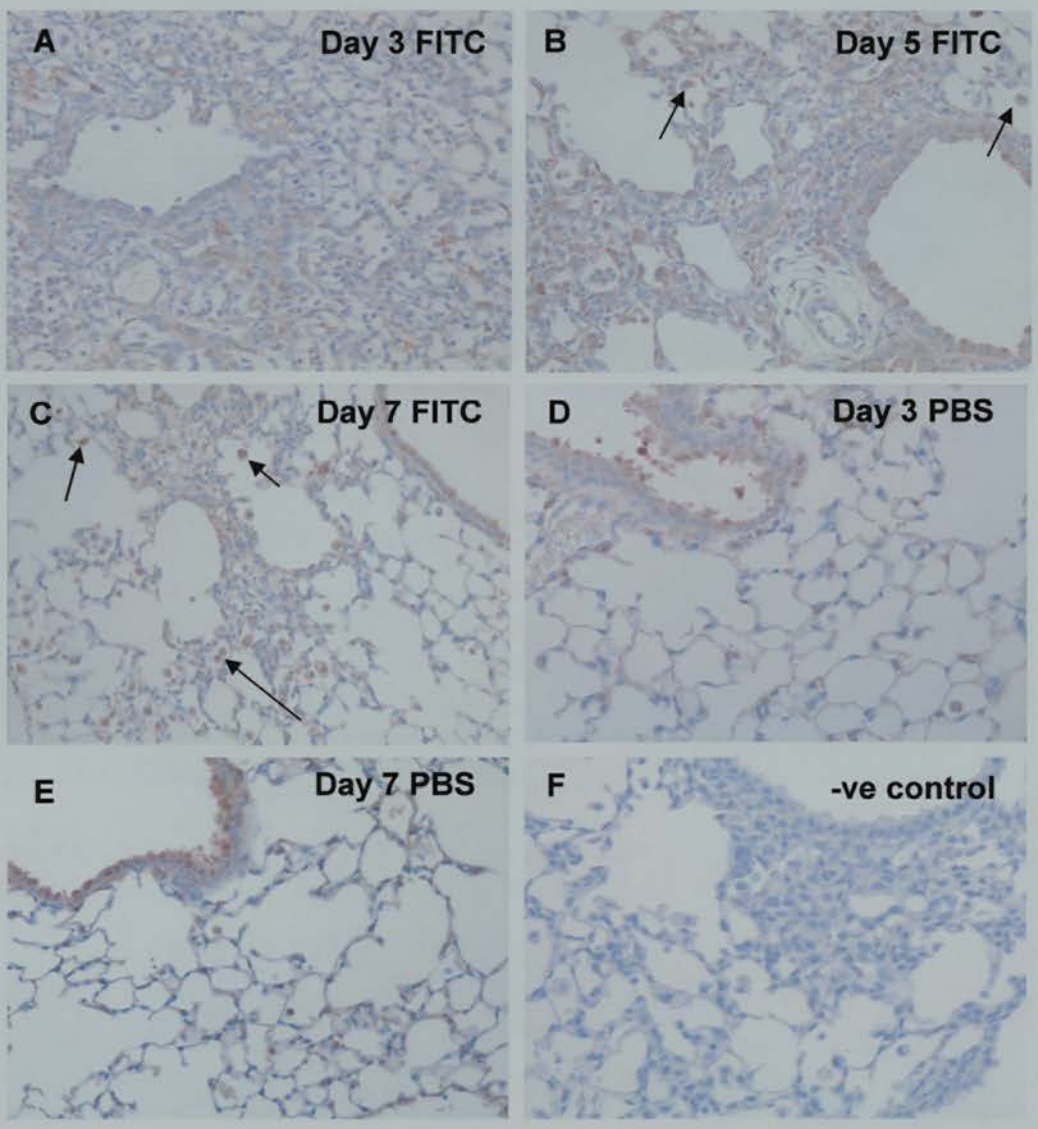

Figure 3.10 CD11c cell surface protein staining of lung tissue sections.
Sections were stained by immunohistochemistry for CD11c. Sections are from FITC-treated mice on Day 3 (A), Day 5 (B), and Day 7 (C) (arrows indicate positively stained alveolar macrophages) after treatment, and from PBS control mice on Day 3 (D) and Day 7 (E) after treatment. A negative control from a Day 7 FITC-treated mouse is shown in F. Original magnification x200.

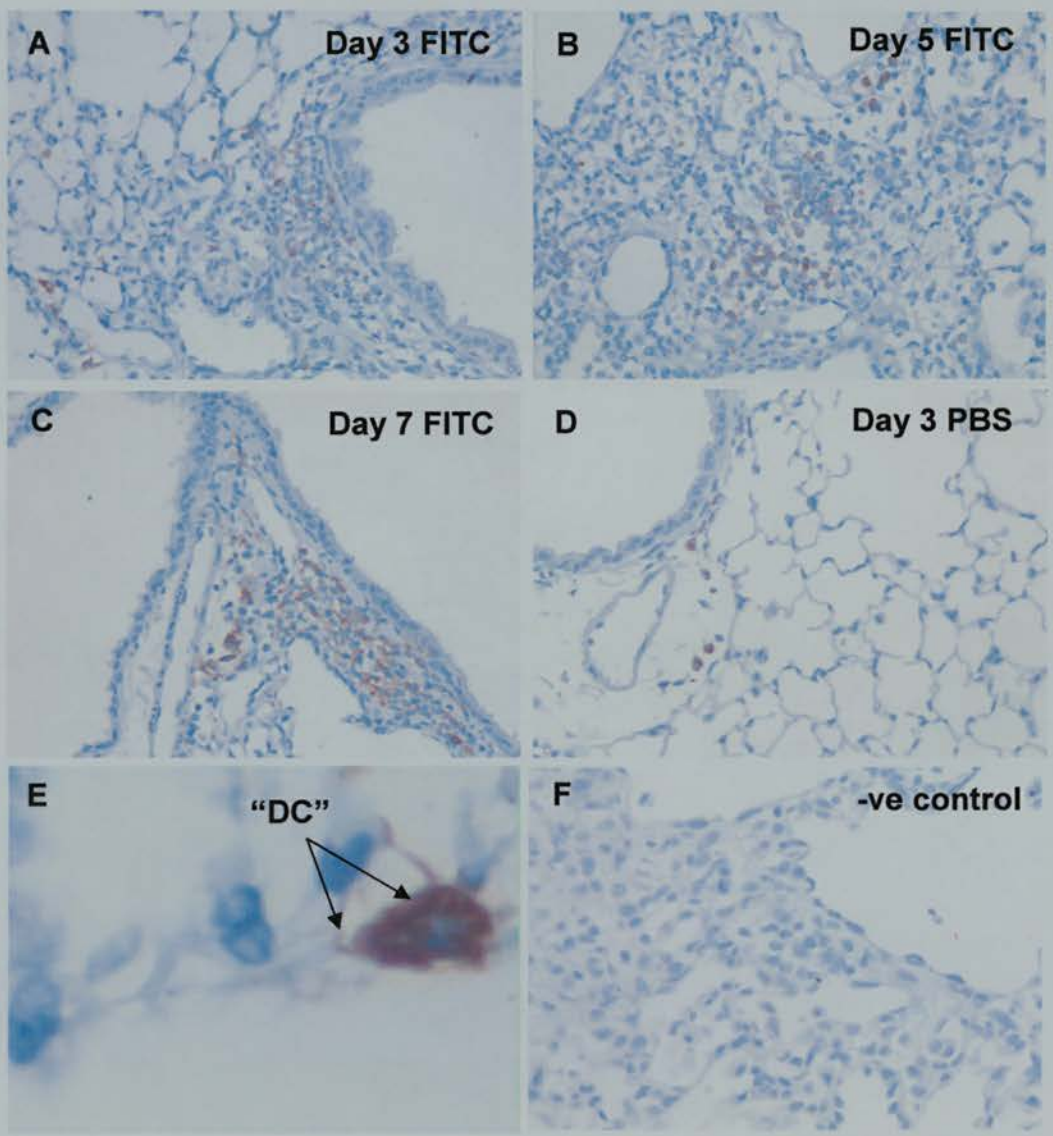

Figure 3.11 MHC class II cell surface protein staining of lung tissue sections. Sections were stained by immunohistochemistry for MHC class II. Sections are from FITC-treated mice on Day 3 (A), Day 5 (B), and Day 7 (C) after treatment, and from PBS control mice on Day 3 (D) after treatment. A heavily stained DC with classic dendritic processes (arrows) from a Day 3 FITC section is shown in E (magnification approximately x1000). A negative control from a Day 7 FITC-treated mouse is shown in F. Original magnification x200.

3.4 Acute Effects of FITC on BAL

In order to assess the acute effects of FITC on BAL cells and fluid, mice were killed one, two, three or seven days after receiving the FITC (or PBS for controls) intratracheally. BAL was collected and processed as described in section 5.3.2.

3.4.1 Total Cell Counts

Figure 3.12 shows the total cell count from BAL in PBS control vs. FITC-treated mice for all four time points. At one day post-instillation, the total cell count from the BAL was $0.97 \pm 0.05 \times 10^5$ in the PBS control mice vs. $1.27 \pm 0.17 \times 10^5$ in the FITC-treated mice (n=3). Two days post-instillation, cell counts increased in both groups of mice, but again, there were slightly more in the FITC-treated group: $1.90 \pm 0.21 \times 10^5$ PBS vs. 2.07 ± 0.27 FITC (n=3). After three days, total cell counts from the PBS-treated mice fell to near-normal levels ($1.35 \pm 0.00 \times 10^5$), while those from the FITC-treated mice dropped slightly, but were significantly greater ($1.86 \pm 0.05 \times 10^5$; $p < 0.02$) than those from PBS-treated mice (n=3). Finally, at seven days post-instillation, little difference was seen between the two groups, but cell counts had increased in both (n=8).

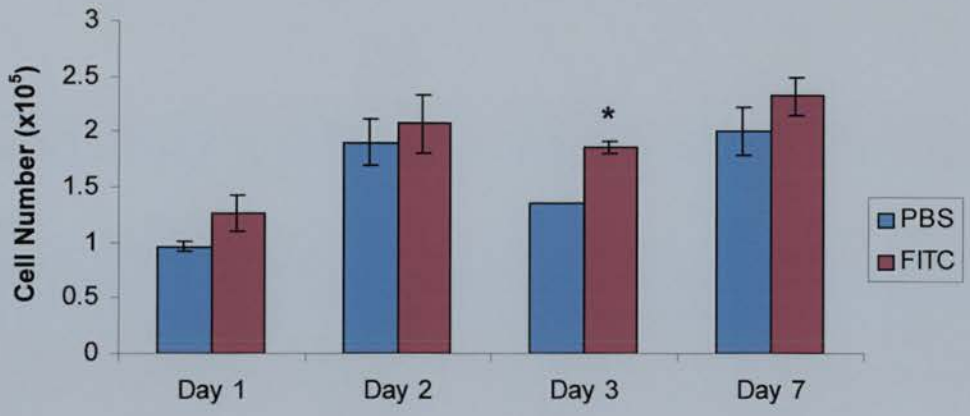

Figure 3.12 Total BAL cell counts measured 1, 2, 3, or 7 days after intratracheal instillation of FITC or PBS. BAL was collected at the time points indicated from both treated (FITC) and control (PBS) mice, and prepared as described. The data represent the means ± SEM (Day 1-3, n=3; Day 7, n=8).
* $p < 0.02$ as compared to paired FITC value, by paired Student's *t*-test.

3.4.2 Differential Cell Counts

In order to assess the types of cells present in the BAL fluid in treated vs. control mice, cytospin preparations of the BAL cells were made as described in section 2.2. Differential counts were performed by counting 300 cells per slide on random fields at x100 magnification. Figure 3.13 compares the values for FITC- and PBS-treated mice at each of the time points for macrophages, and Figure 3.14 compares values for polymorphonuclear cells (PMNs). Figures 3.15 and 3.16 show typical cytospin fields at each of the time points for both FITC- and PBS-treated mice. The remainder of the cells were lymphocytes, but as they comprised less than 1% of the population in all cases, numbers are not shown.

As will be discussed in section 5.4, a typical BAL cell population from a normal mouse is comprised of 98 ± 1% mononuclear cells; remaining cells were predominantly PMNs, and rarely, lymphocytes. Figure 3.13 shows that in the PBS-treated mice, macrophage levels in the BAL fluid dropped slightly one day after

treatment, and correspondingly, in Figure 3.14, their PMN levels rose, but by Day 2 levels of both cell types return to normal, and this is continued into Days 3 and 7.

In the FITC-treated mice, however, macrophage levels in the BAL dropped to 69.4 ± 3.2%, with a corresponding increase in PMNs (29.9 ± 3.2%), indicative of an acute inflammatory reaction. At Day 2 the macrophage numbers rose and PMNs decreased (90.8 ± 5.6% macrophages; 9.1 ± 5.7% PMNs), but even at Day 3, macrophage numbers remained slightly below those from the PBS-treated mice, and PMN numbers remained slightly higher. By Day 7, macrophage and PMN numbers had returned to normal value. These results demonstrated that the FITC did indeed cause an acute inflammatory reaction in the lungs, while the PBS did not.

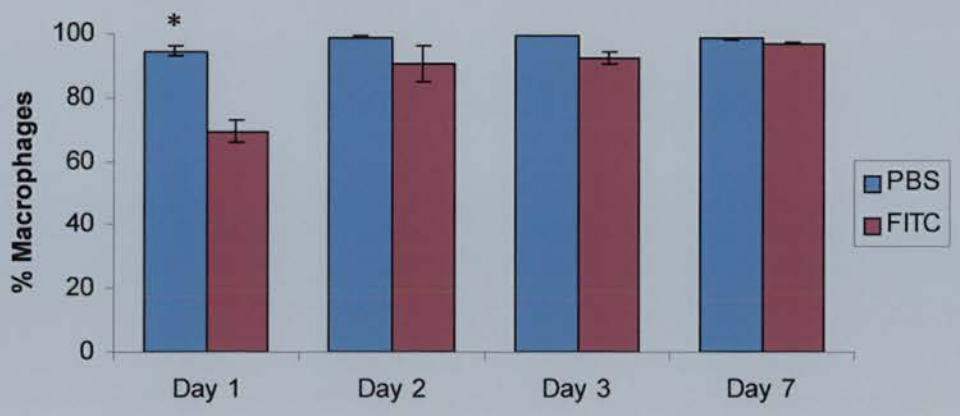

Figure 3.13 Percentage of BAL macrophages counted on cytospin preparations in treated (FITC) versus control (PBS) mice over four time points. Cytospins were prepared as described. Three hundred cells per slide were counted at x100 magnification. The data represent means ± SEM (Day 1-3, n=3; Day 7, n=8).
* $p < 0.01$ compared to paired FITC value, by paired Student's *t*-test.

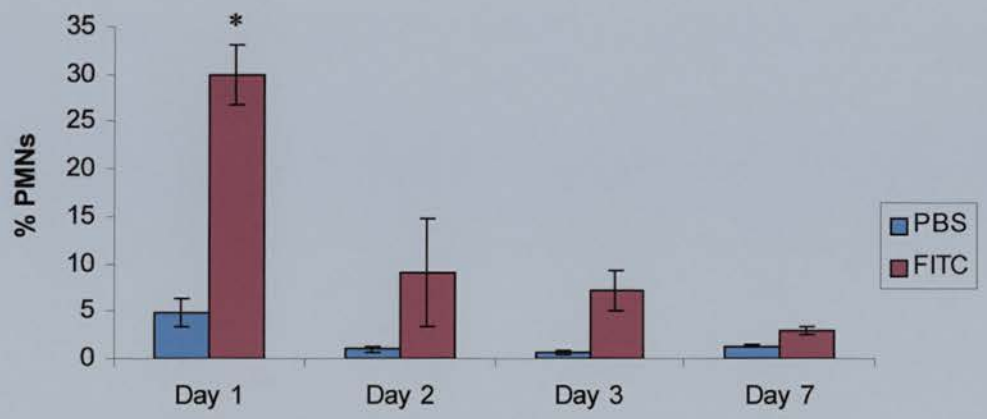

Figure 3.14 Percentage of BAL PMNs counted on cytospin preparations in treated (FITC) versus control (PBS) mice over 4 time points. Cytospins were prepared as described. Three hundred cells per slide were counted at x100 magnification. The data represent means ± SEM (Day 1-3, n=3; Day 7, n=8).
* $p < 0.01$ compared to paired PBS value, by paired Student's *t*-test.

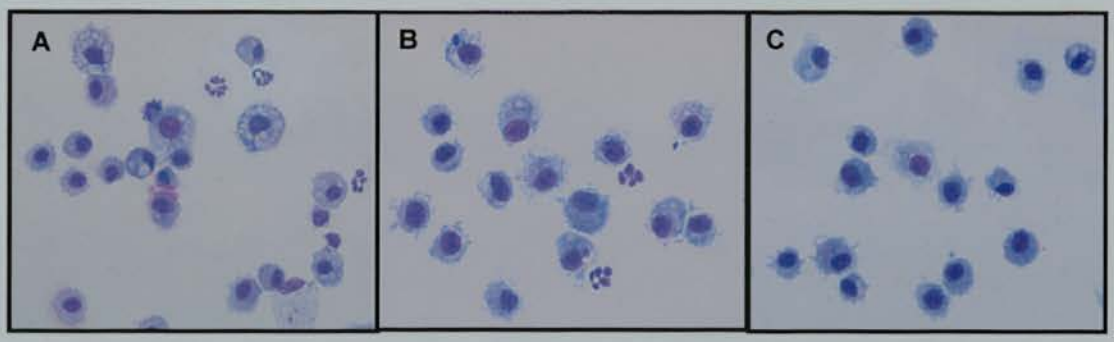

Figure 3.15 Typical microscope fields of BAL cells from PBS-treated mice used for differential counting. BAL was prepared as described, and 300 cells per slide were counted over random fields. A slight increase in PMN numbers is seen one day after PBS instillation (A), gradually reducing to normal levels by Day 2 (B), Day 3 (C) and Day 7 (not shown). The majority of cells are macrophages, with the occasional lymphocyte (not present in fields shown above).

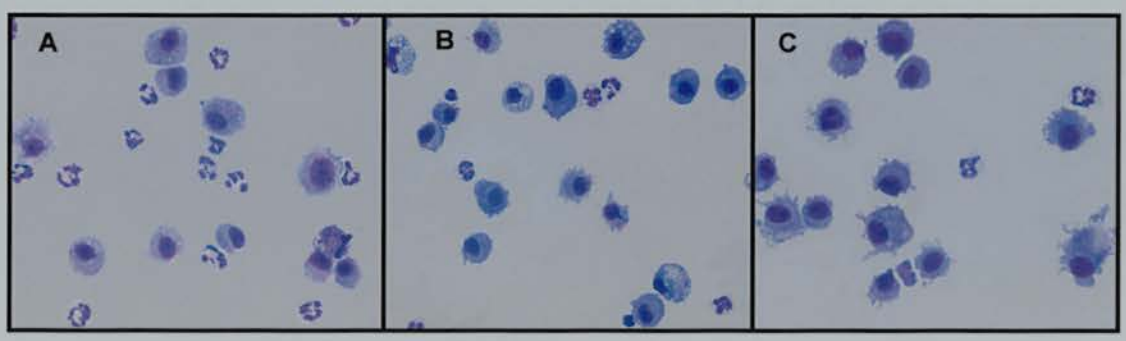

Figure 3.16 Typical microscope fields of BAL cells from FITC-treated mice used for differential counting. BAL was prepared as described, and 300 cells per slide were counted over random fields. A significant increase in PMN numbers is seen at Day 1 after FITC instillation (A), decreasing over Days 2 (B) and 3 (C), although levels remain higher than normal. The majority of cells are still macrophages, with the occasional lymphocyte. By Day 7 (not shown), differential count had returned to normal.

3.4.3 Cytokine Production

In order to compare cytokine production in between FITC-treated and PBS control animals, BAL fluid was collected and processed as described in section 5.3.2, and assayed by ELISA as described in section 2.3. The BAL fluid was assayed for TNF-α, the classic inducer of inflammatory responses, IFN-γ, which appears mainly after the induction of the adaptive immune response, and TGF-β, which plays a central role in wound healing and tissue repair, and is thought to play a major role in the initiation of pulmonary fibrosis [83,279,284]. As discussed in Chapter 1, TGF-β is secreted in a latent form, and only becomes biologically active after removal or conformational alteration of the non-convalently associated latency-associated peptide 1, to yield the active dimer [259,262].

3.4.3.1 TNF-α

Figure 3.17 shows that for both FITC- and PBS-treated mice, levels of TNF-α in the BAL fluid decreased over seven days. TNF-α production was measured at Day 1 in the PBS-treated mice at 20.0 ± 2.4 pg/ml. This level dropped below the level of detection of the R&D DuoSet ELISA assay (15.625 pg/ml) at Days 2, 3, and 7, the latter two being significant decreases as compared to the day one value ($p < 0.04$). In the FITC-treated mice, TNF-α was measured in the BAL fluid at Day 1 at 29.1 ± 6.5 pg/ml. This decreased only slightly by Day 2, and then significantly decreased to undetectable levels at Days 3 and 7, as compared to the Day 2 level ($p < 0.04$). Comparing the TNF-α levels between the two groups of mice shows that at both two and three days after treatment, TNF-α is significantly higher in the BAL fluid from FITC-treated mice than from PBS controls ($p < 0.03$).

BAL fluid from normal mice contains no detectable TNF-α [431]. As it is a potent proinflammatory mediator, its presence therefore, suggests the initiation of an inflammatory response. Detectable levels of TNF-α in the PBS control mice at Day

1 could be due to the intratracheal instillation process itself, and indeed, levels of the cytokine fell below the level of detection by Day 2. In the FITC-treated mice, however, TNF-α levels were consistently, and often significantly, higher than those of the control mice, and remained detectable until Day 3.

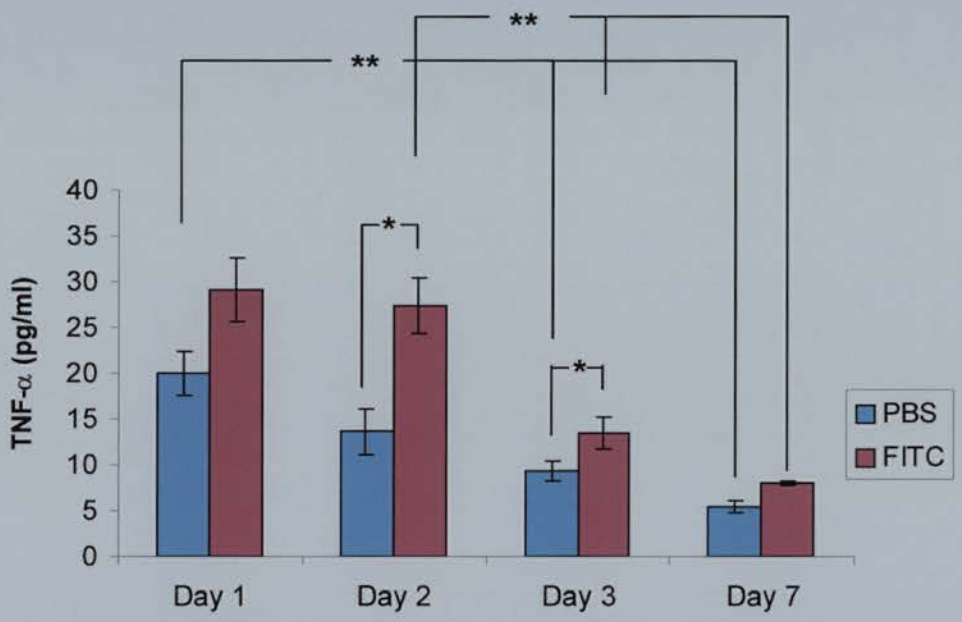

Figure 3.17 TNF-α production measured in BAL fluid from FITC-treated and control mice over 7 days. BAL fluid was collected, processed and assayed as described. Data are presented as means ± SEM (Day 1, 2, 3, n=12 PBS- and FITC-treated mice; Day 7, n=16 PBS- and FITC-treated mice)
*p<0.03 by paired Student's *t*-test, **p<0.04 by Student's *t*-test.

3.4.3.2 IFN-γ

IFN-γ production was measured in the BAL fluid as described. Figure 3.18 shows that there was no significant change in levels of IFN-γ production in PBS-treated control mice compared at Days 1, 2, 3, or 7. Although there was a slight drop in IFN-γ levels in FITC-treated mice at Day 3 as compared to Day 1 or 2, this decrease was not statistically significant. These data must be interpreted with caution as the detection level for the R&D murine IFN-γ DuoSet ELISA is 31.25 pg/ml, and as such, all values measured fell below that limit.

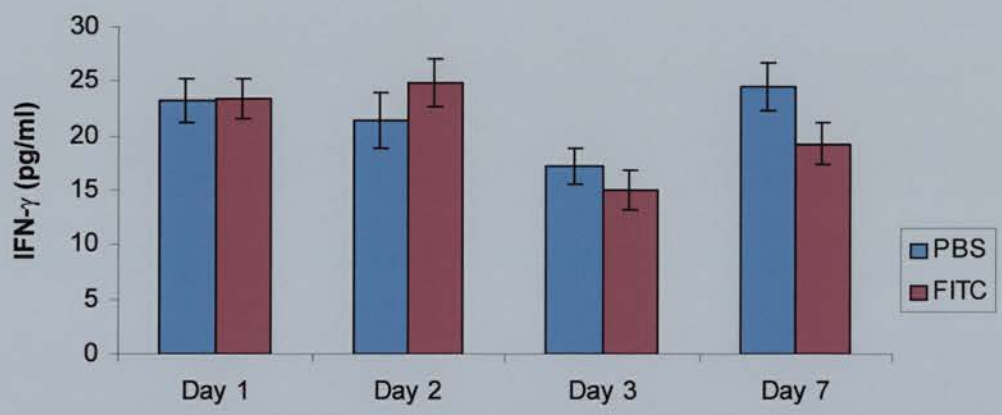

Figure 3.18 IFN-γ production in BAL fluid from FITC- and PBS-treated mice measured over seven days. BAL fluid was collected, processed and assayed as described. Data are presented as means ± SEM (Day 1, 2, 3, n=12 PBS- and FITC-treated mice; Day 7, n=16 PBS- and FITC-treated mice).

IFN-γ is one of the major Th1 cytokines, and has profound suppressive effects on the production of ECM, including collagen and fibronectin [247]. *In vivo* administration of IFN-γ may also cause a reduction of ECM in animal models of fibrosis [255], and even attenuates bleomycin-induced lung fibrosis in mice [256]. The inflammatory response in CFA is thought to most closely resemble a Th2-type immune response, and in murine models of lung disease, a predominantly Th2-type response to injury is more likely to develop into pulmonary fibrosis than a Th1-type response, due to the

profibrotic effects of many Th2 cytokines, such as IL-13 and MCP-1 [16,80]. As will be shown in the next chapter, the intratracheal administration of FITC did lead to pulmonary fibrosis, so the lack of IFN-γ in the initial stages was perhaps not surprising.

3.4.3.3 TGF-β

Both total (latent + active) and active TGF-β were measured in the BAL fluid samples as described in section 2.3. BAL fluid was also collected at five days after treatment from both FITC- and PBS-treated mice. Figure 3.19 shows total TGF-β levels present in the BAL fluid over seven days post-treatment. The detection limit for the R&D human TGF-β DuoSet ELISA is 31.25 pg/ml, so the results can only suggest possible trends as the values are all below this limit. It would appear that total TGF-β levels were slightly increased at Day 1 and possibly Day 2 after treatment in both PBS- and FITC-treated mice, falling to lower levels by Days 3, 5 and 7. Although not significant, at Day 2 total TGF-β was present at higher levels in the FITC-treated mice than in the PBS controls. Differences between the two groups were negligible at the other time points.

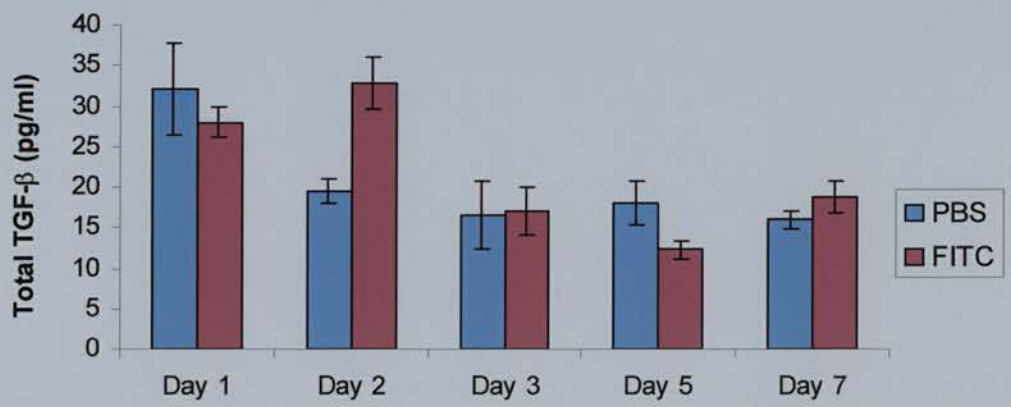

Figure 3.19 Total TGF-β levels measured in BAL fluid samples from FITC-treated and control mice at Days 1, 2, 3, 5, and 7 after treatment. Data are presented as means ± SEM (Day 1, 2, 3, n=12 PBS- and FITC-treated mice; Day 7, n=16 PBS- and FITC-treated mice).

Active TGF-β was also measured (Figure 3.20), and again the results must be interpreted with caution as the values all fall below the ELISA detection limit. In the PBS control mice, there was no detectable active TGF-β over the seven days. At Day 2 in the BAL fluid from the FITC-treated mice, however, there was a detectable level of TGF-β, and it was significantly higher than the corresponding PBS control at the same time point ($p < 0.05$). This mimics the trend seen in the samples measured for total TGF-β, although in that case the difference was not significant.

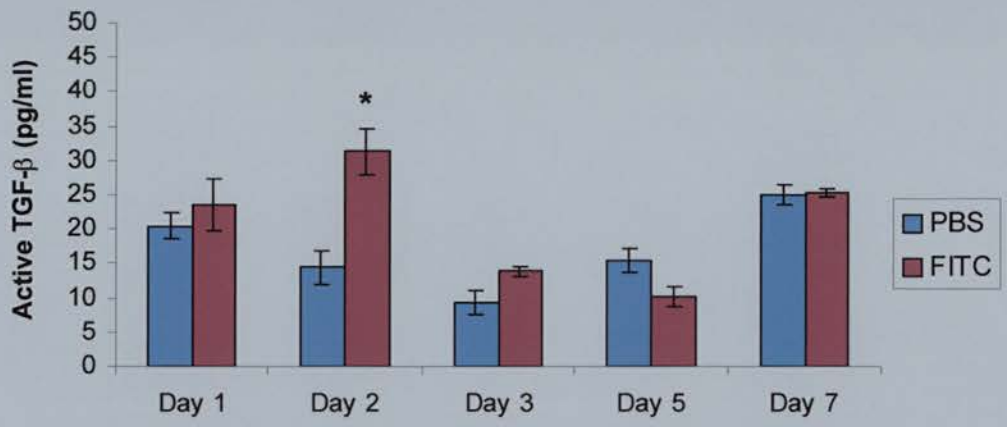

Figure 3.20 Active TGF-β measured in BAL fluid samples from FITC- and PBS-treated mice at Days 1, 2, 3, 5 and 7 after treatment. Data are presented at means ± SEM (Day 1, 2, 3, n=12 PBS- and FITC-treated mice; Day 7, n=16 PBS- and FITC-treated mice)
*$p < 0.05$ as compared to paired PBS value, by Student's *t*-test.

Khalil *et al.* [279] have shown that AMs from patients with CFA secrete biologically active TGF-β, while those from normal lung secrete only the latent form of the molecule. These observations are consistent with the bleomycin model in the rat which shows that active TGF-β from AMs is critical to the pathogenesis of inflammation and fibrosis [233,432,433]. In the model described here, however, very little total (and therefore latent) TGF-β is secreted in the BAL fluid of PBS- or FITC-treated mice, and only on Day 2 after FITC treatment is any active form of the molecule found. These findings are not consistent with published data regarding CFA, and may be unique to this model. Further discussion will be found at the end of Chapter 4.

3.5 Conclusions and Discussion

The FITC model of murine pulmonary fibrosis was originally developed to study the involvement of the immune system in the development of this disease [243]. Initially, FITC was delivered in one dose by surgical instillation. Home Office requirements, however, necessitated a new method of delivery. As described in section 3.2, this method involves non-invasive intratracheal instillation of the FITC in two doses, spaced six weeks apart. This chapter has described the acute effects of FITC on murine lungs from one day to seven days after the initial FITC dose.

Lung sections stained with anti-FITC antibody showed that FITC was successfully deposited in the lungs of the majority of mice at all time points (Table 3.1). As will be discussed in section 4.4.3, however, much of this FITC may be cleared from the lungs, and the remainder may not be sufficient to cause fibrosis. One day after instillation, the FITC was widely distributed throughout the blood vessel walls, larger and smaller airways, and reached the alveolar walls in some areas (Figure 3.2). Macrophages heavily stained for FITC were evident throughout the lung. Much of the FITC was cleared by Day 2, presumably by these macrophages and the mucociliary apparatus, and by Day 5 FITC showed a patchy deposition. There was focal evidence of alveolar oedema, particularly at Day 5, and of an acute inflammatory response (Figure 3.4). The cellular infiltrate on Days 1 and 2 was predominantly granulocytic (Figure 3.3), gradually becoming more mononuclear over Days 3 – 7 (Figure 3.4), indicating a shift from an acute to a chronic inflammatory response.

In order to measure the inflammatory response to FITC, a scoring system was developed by giving numerical scores for the cellular infiltrate seen in each of 10 fields, in four separate compartments, which were evaluated for each lung section. These scores were then combined to give an overall score which rated the severity of infiltration.

The individual compartment scores showed that there was significantly more cellular infiltration in the lungs of the FITC-treated mice in each of the perivascular compartment, the peri-bronchiolar tissue, and the alveolar walls over Days 1-7, as compared to the lungs of the PBS control mice (Figure 3.5). In the bronchiolar epithelium, the difference was significant over Days 1-3. This demonstrates that the inflammatory process is dynamic, and that different compartments of the lung are involved at different times.

The combined inflammation scores showed that the FITC-treated mice had an overall mild, bordering on moderate, infiltrate up to Day 5, which became moderate by Day 7 (Figure 3.6). These scores were all significantly higher than those of the PBS control mice which had scores indicating very mild, if any, cellular infiltrate. Encouragingly, no severe inflammation was seen, correlating well with the mild onset of clinical CFA in which patients normally present at a late stage of disease. This scoring system allows for direct measurement of the cellular infiltrate in the lungs of mice after injury, and is ideal for comparing the severity of the inflammatory reaction caused by the intratracheal instillation of FITC or PBS.

Immunohistochemical staining of paraffin lung sections for the T cell marker CD3 showed that T cell numbers increased in the FITC-treated lungs over the first week, becoming very prominent in the tissues by Day 5 and particularly in areas of alveolar thickening (Figure 3.7). T cell numbers in PBS-treated lungs remained low. B cells were stained with the B220 antibody and in contrast to the T cells, did not become prominent in the FITC-treated lungs at any time point (Figure 3.8). Slightly increased numbers of B cells may have been present at Day 7 in areas of alveolar thickening and cell aggregates. PBS control mouse lung sections showed no change in B cell numbers from Day 1 to Day 7. Sections were also stained for the profibrotic cytokine TGF-β (Figure 3.9). TGF-β protein was expressed on AMs, bronchial epithelium and alveolar walls in the FITC-treated mice. Expression in the PBS control mice was mainly on AMs. TGF-β protein expression appeared higher in FITC-treated mice at Day1 than in PBS-treated mice, and peaked at Day 5. Staining for the CD11c cell surface protein was evident on both cells and the bronchial

epithelium in both FITC- and PBS-treated mice, with the strongest expression seen on the AMs (Figure 3.10). There was no obvious change in CD11c expression between time points in either group of mice. Finally, cell surface staining for the MHC class II protein was limited to specific cells that were strongly positive and, on closer examination, often showed dendritc-like processes, suggesting that they were DCs (Figure 3.11). More positive cells were seen in the sections from FITC-treated mice, and seemed to be localised to areas of alveolar thickening and cell aggregation.

Examination of the cellular components of the BAL fluid in FITC-treated and control mice showed that while total cell counts did not vary much between groups over the seven days (with the exception of Day 3, at which FITC-treated mice had significantly more cells in their BAL fluid than the control mice) (Figure 3.12), the proportions of cells were variable (Figures 3.13, 3.14). At Day 1, the BAL fluid of the FITC-treated mice had significantly more PMNs, and proportionally fewer macrophages than the PBS-treated mice. Although not significantly different from controls, the percentage of PMNs in the BAL fluid of FITC-treated mice remained consistently higher over the seven days. This would indicate that a classic acute inflammatory response occurred in the lungs of the FITC-treated mice, as opposed to the reaction seen in the PBS controls.

Inflammatory cells, including AMs, participate in the lung tissue injury and repair process by secreting various mediators that play a host of roles. The cytokines examined for this body of work were TNF-α, IFN-γ, and TGF-β, and the profile obtained by ELISA analysis of the BAL fluid was mixed.

As expected, production of the proinflammatory mediator, TNF-α, was significantly higher in the FITC-treated mice than in the PBS controls (Figure 3.17). Levels were highest at Day 1, and gradually decreased over the seven days. No detectable IFN-γ was found in the BAL fluid from either of the groups of mice (Figure 3.18), which might suggest the absence of a Th1 cytokine profile, mirroring other animal and human studies [16]. In fact, IFN-γ has been used as a therapeutic agent in a study of CFA patients, with promising results [103].

Both latent and active TGF-β levels in the BAL fluid were undetectable in both groups of mice at all time points, with the exception of Day 3, at which detectable latent and active levels were measured in the BAL fluid from the FITC-treated mice alone (Figures 3.19, 3.20). This is surprising, as TGF-β has been measured in the murine bleomycin model at 24 hours [216,235,434]. This may be a finding unique to the FITC model of pulmonary fibrosis, and will be discussed further at the end of Chapter 5.

The examination of the acute response to the intratracheal instillation of FITC in mice has shown that an acute inflammatory reaction, predominated by neutrophils, occured at Day 1, and gradually shifted towards a more chronic inflammatory state by Day 7. Quantification by scoring the cellular infiltrate showed that the acute response seen in the lungs of the FITC-treated mice was significantly greater than that seen in the PBS control mice, and thus the response could not be attributed to the PBS alone. The presence of TNF-α and absence of IFN-γ in the BAL fluid suggested an inflammatory state that was not of the Th1 type, correlating with published data on CFA in both humans and animals. The absence of the profibrotic cytokine TGF-β requires further examination.

The next step in the characterisation of the murine FITC model of pulmonary fibrosis is to examine the longer-term effects of FITC on the mouse lungs, and the results presented above will be discussed further in that context at the end of the subsequent chapter.

CHAPTER 4

Murine Model of FITC-induced Pulmonary Fibrosis: Long-term Response

4.1 Introduction

This chapter will describe the long-term effects of the intratracheal instillation of FITC into murine lungs. Work in the Immunobiology Group (Gareth Stewart, PhD thesis, University of Edinburgh, 2002) had shown that, unlike the original model, using the modified nonsurgical method of FITC instillation did not induce fibrosis after a single instillation. This is most likely due to the difference in the lung penetrance between the two methods. A second dose given six weeks after the initial dose was therefore necessary.

4.1.1 Aims of Chapter

The principal aims of this chapter are:

- To describe the long-term pathological effects of FITC-instillation on murine lung tissue in terms of histology and cell surface protein staining
- To describe a method of obtaining quantitative data that reflects the chronic inflammatory and fibrotic changes in the lungs of FITC-treated mice
- To describe the long-term effects of FITC on murine lungs as reflected by cytokine production measured in the BAL fluid
- To discuss the implications of the acute inflammatory process, which is followed by a progressive, chronic pulmonary fibrosis induced in the lungs of mice by FITC instillation in terms of application to the human disease

4.2 Long-term Effects of FITC on Murine Lung Tissue Pathology

In order to assess the longer-term pathological effects of FITC on murine lungs, mice were given an intratracheal dose of FITC or PBS as described in section 3.2. Some mice were killed at six weeks after the first dose. Remaining mice were given a second intratracheal dose at six weeks, and were killed seven days, six weeks or 14 weeks after this second dose (Figure 4.1). Three different series of mice were set up in this fashion, and will be identified as Series 2, 3 or 4. Series 1 mice were groups of mice that were set up specifically for one time point, e.g., four FITC-treated and four PBS-treated mice set up just for a six week time point. Series 2 and 3 mice were each set up from one large group of mice, and the required number of mice were randomly selected at each time point.

The numbers of FITC-treated mice at each time point, which included animals taken from all series of mice, are presented in Table 4.1. At six weeks after the first dose, of nine mice given FITC treatment, only four showed FITC-positive stained lung sections, while the remaining five were negative for FITC. None of the mice showed any sign of fibrotic disease. Although a single dose of FITC did induce inflammation, as shown in Chapter 3, it was not sufficient to induce fibrotic changes. Six weeks after the initial dose, most of the FITC that managed to penetrate into the deep lung had been cleared, most likely by the macrophages. Thus, a second dose was given to the mice, six weeks after the first.

Of eight pairs of lungs examined three days after the second dose, five stained positively with the anti-FITC antibody, while only three were negative (Table 4.1). Of the five positives, all showed signs of disease on histological examination. Seven days after the second dose, eight out of 13 mice had FITC present in their lungs, and all eight scored positive for disease. Again at six and 14 weeks after the second dose of FITC, the majority of mice given FITC had FITC present in their lungs, and all FITC-positive lung sections were also positive for disease. Importantly, no mouse given PBS developed any sign of disease at any time point. Administration of the

second dose, then, was sufficient to induce disease in the lungs of the majority of mice. Of those mice given FITC that did not develop disease, possible explanations include clearance from the lungs or technical failure of the FITC instillation. Further discussion will follow in section 4.4.3.

# of Mice	6 wks	2^{nd} + 3d	2^{nd} + 7d	2^{nd}+ 6 wks	2^{nd} + 14 wks
total	*9*	*8*	*13*	*11*	*4*
FITC +ve	4	5	8	8	3
FITC –ve	5	3	5	3	1
+ve with disease	0	5	8	8	3
-ve with disease	0	0	0	0	0

Table 4.1 Numbers of mice treated with FITC and assessed histologically and immunohistochemically. Mice were given one dose of FITC intratracheally and were assessed after six weeks. Remaining mice were given a second dose at six weeks and assessed after three days (2^{nd} + 3d), 7 days (2^{nd} + 7d), six weeks (2^{nd} + 6wks), and 14 weeks (2^{nd} + 14 wks). Numbers of mice that were FITC-positive (+ve), FITC-negative (-ve), FITC-positive with signs of disease (+ve with disease) and FITC-negative with signs of disease (-ve with disease) are shown.

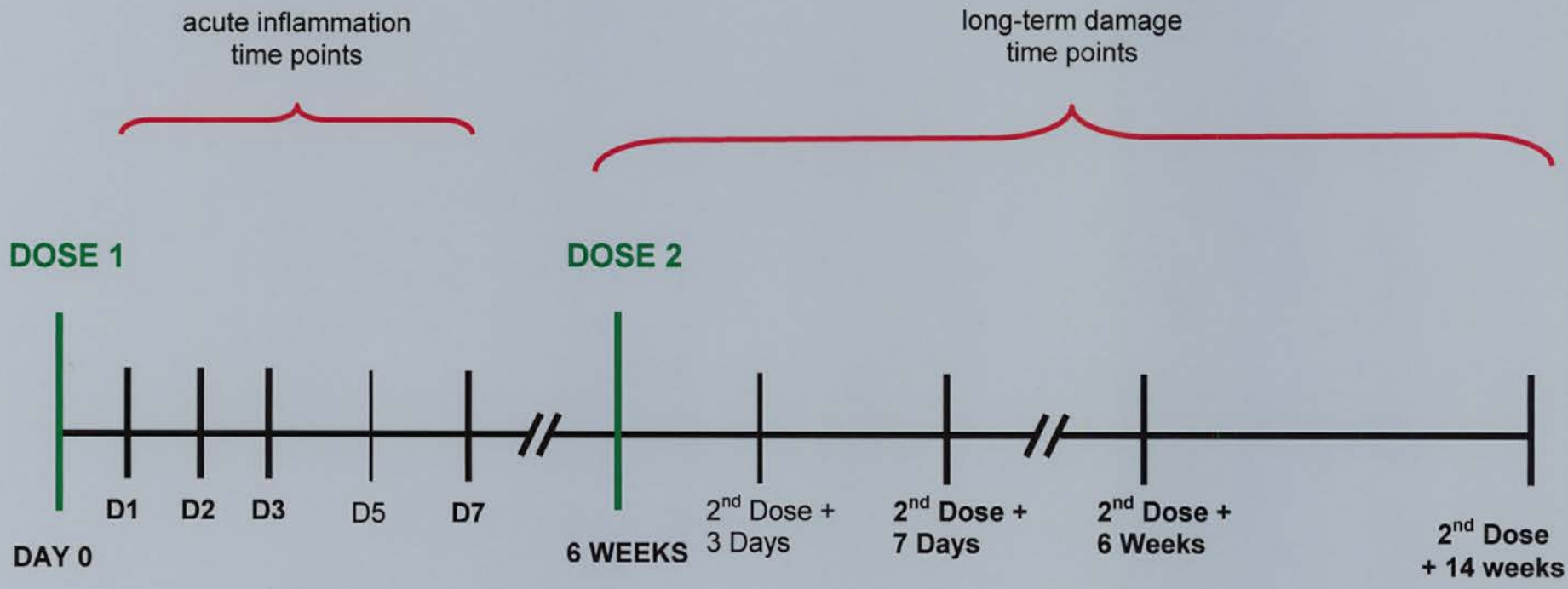

Figure 4.1 Timeline of FITC or PBS dosing and time points examined. Anaesthetised female BALB/c mice were given one 2 mg/ml dose of FITC in PBS, or PBS alone, on Day 0. Acute inflammation was evaluated in the lungs on Day 1, Day 2, Day 3, Day 7, and in some cases Day 5. Longer-term damage was evaluated at 6 weeks after the first dose. A second dose of FITC or PBS was given after 6 weeks, and mice killed for evaluation after 3 days, 7 days, 6 weeks or 14 weeks after this second dose.

4.2.1 Six Weeks Post-Dose 1

Six weeks after the initial dose, examination of full lung sections revealed some deposition of FITC was still evident in the tissue, along with evidence of chronic inflammation in some areas (Figure 4.2). Both the FITC deposition and the inflammation, however, were not widespread, and in some mice were not evident at all. As mentioned, previous work in the laboratory had shown that mice given only a single FITC dose did not go on to develop fibrosis, so a second dose was given to the mice six weeks after the first dose.

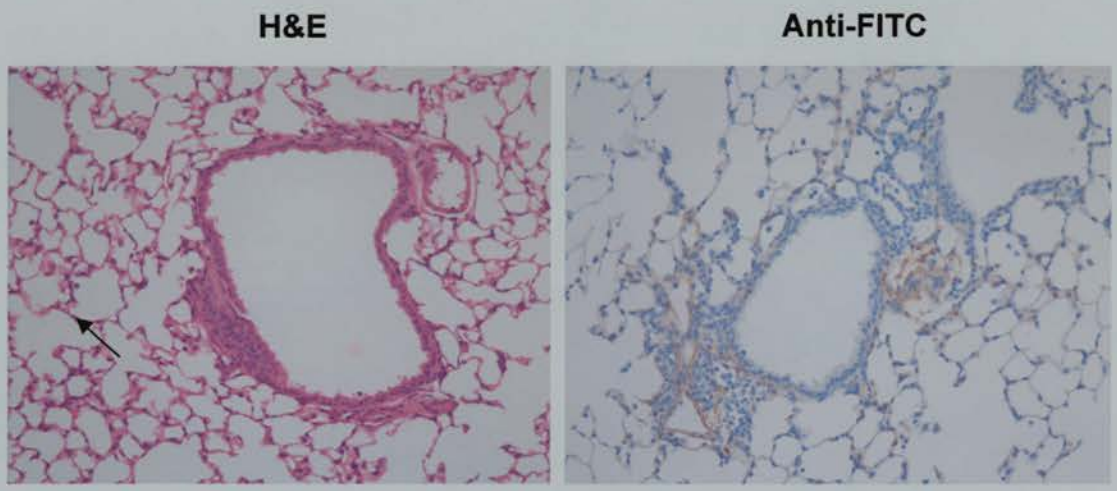

Figure 4.2 H&E and anti-FITC stained sections of mouse lung 6 weeks after single dose of FITC. H&E section shows mononuclear inflammation around airway and small areas of thickened alveolar walls (arrow). Anti-FITC section shows moderate inflammation in areas of FITC deposition. Original magnification x200.

4.2.2 Second Dose + Seven Days

Seven days after a second intratracheal dose of FITC was administered, areas of inflammation could be seen around many airways (Figure 4.3A), similar to that seen at seven days after the initial dose, and in contrast to the PBS control mice (Fig. 4.3B). FITC deposits were quite dense in these inflamed areas (Fig. 4.3C).

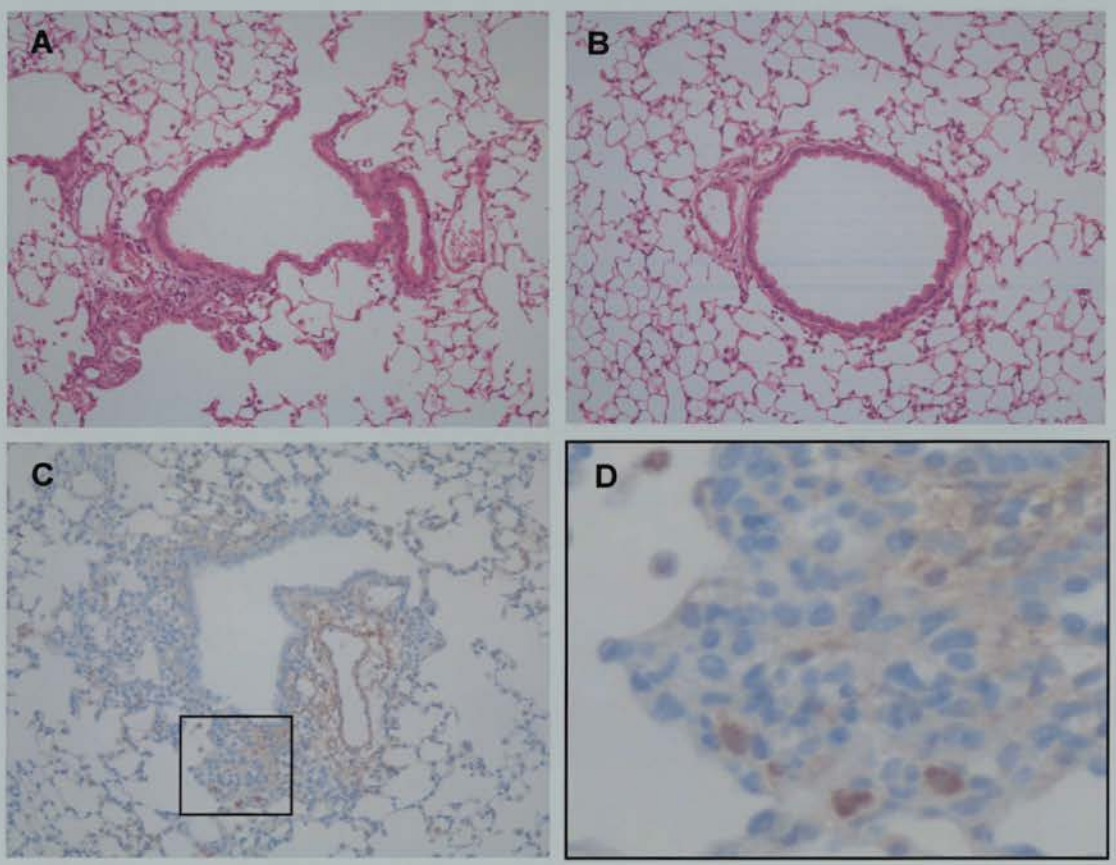

Figure 4.3 H&E and anti-FITC stained sections of mouse lung seven days after the second FITC dose. H&E stained section of FITC-treated mouse lung (A) shows inflammation around the airway, in contrast to the PBS-treated lung (B). FITC-treated mouse lung stained with anti-FITC antibody shows deposition around airway (C). Black box surrounds enlargement shown in (D), which shows FITC deposition in tissues, surrounded by cellular infiltrate, and present in macrophages. Original magnification x200. Enlargement approximately x800.

The inflammatory cells were mostly mononuclear at this time point, including many T cells (Figure 4.4A) and some B cells (Fig. 4.4B). Although several cell types express CD11c, the macrophages/DCs stained strongly for this protein (Fig. 4.4C). MHC class II staining revealed a small number of strongly stained cells (Fig. 4.4D). As will be shown in Chapter 5, macrophages isolated from the lung typically expressed high levels of CD11c, and moderate MHC class II, while DCs expressed low levels of CD11c but very high levels of MHC class II. Antibodies for immunohistochemical staining of F4/80 (primarily found on macrophages, but also on DCs) and costimulatory molecules CD80 and CD86 were not available. Finally, TGF-β stained sections showed that abundant amounts were present in the lungs at this time point, with the macrophages staining very strongly (Fig. 4.4E).

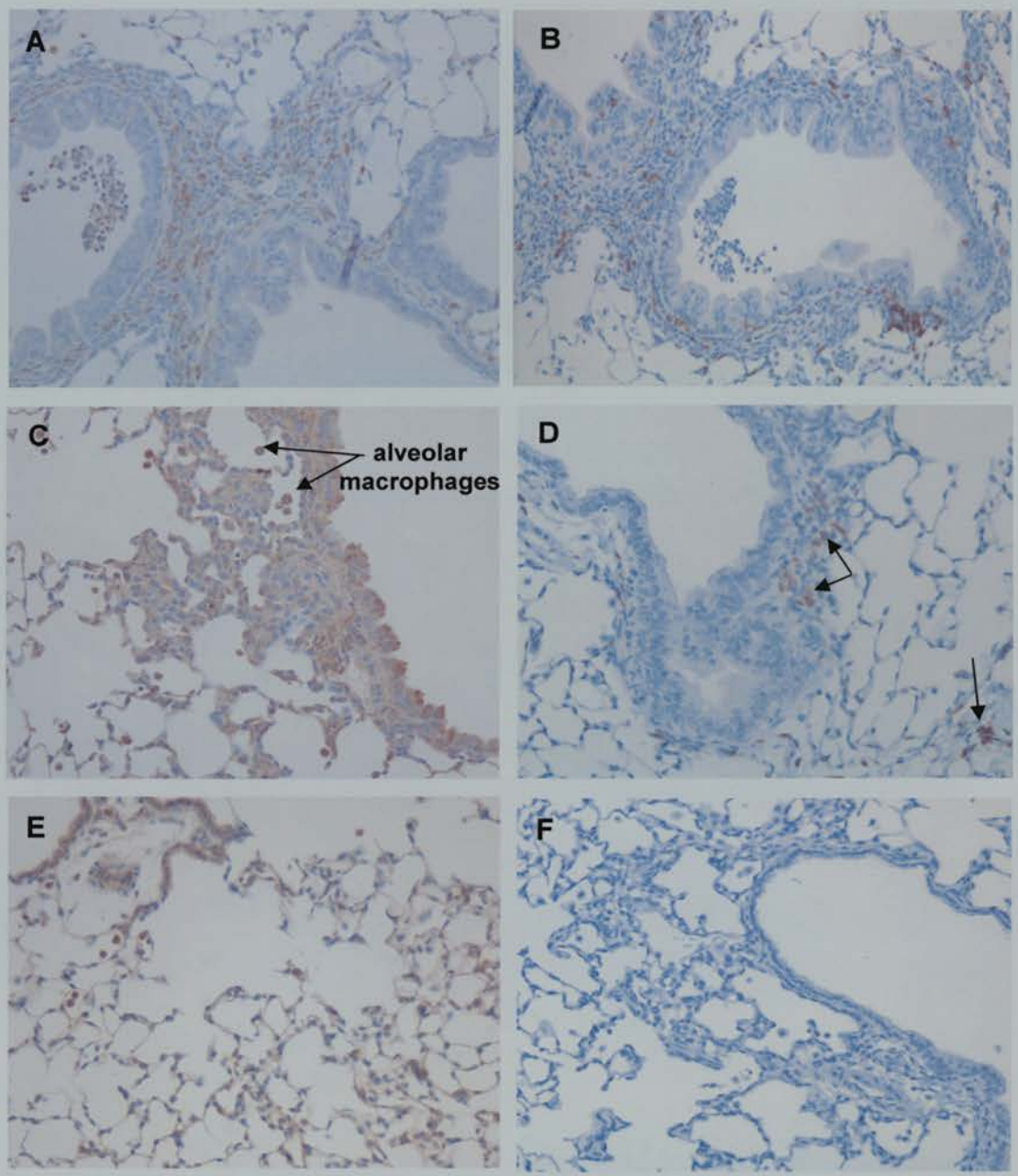

Figure 4.4 FITC-treated mouse lung sections at seven days after the second FITC dose stained for cell surface proteins. Sections were stained by immunohistochemistry for CD3, to detect T cells (A), B220, to detect B cells (B), CD11c and MHC class II, both found on macrophages and DCs, among other cells (C, D, respectively) (arrows in D indicate positive cells), and TGF-β (E). Representative MHC class II negative control shown in F. Original magnification x200.

4.2.3 Second Dose + Six Weeks

Six weeks after the second dose of FITC, many areas of the lung had thickened alveolar walls, occasionally with loss of architecture, and continued cellular infiltration (Figure 4.5A). Loss of architecture was evident particularly in areas of FITC deposition (Fig. 4.5B). Much of the FITC had been cleared, presumably by the macrophages, but it was still evident in the tissues, diffuse in some areas (Fig. 4.5C), and sparingly in others (Fig. 4.5E). Large aggregates of mononuclear-type cells were also evident (Fig. 4.5D).

The inflammatory cells at this time point consisted of primarily T cells, which were spread fairly evenly throughout the damaged tissue (Figure.4.6A), and B cells (Fig. 4.6B). MHC class II staining showed strongly positive cells spread throughout the tissue, and interestingly, some in the mononuclear cell aggregates (Fig. 4.6C). TGF-β staining showed even more diffuse staining than at the previous time point (Fig. 4.6D).

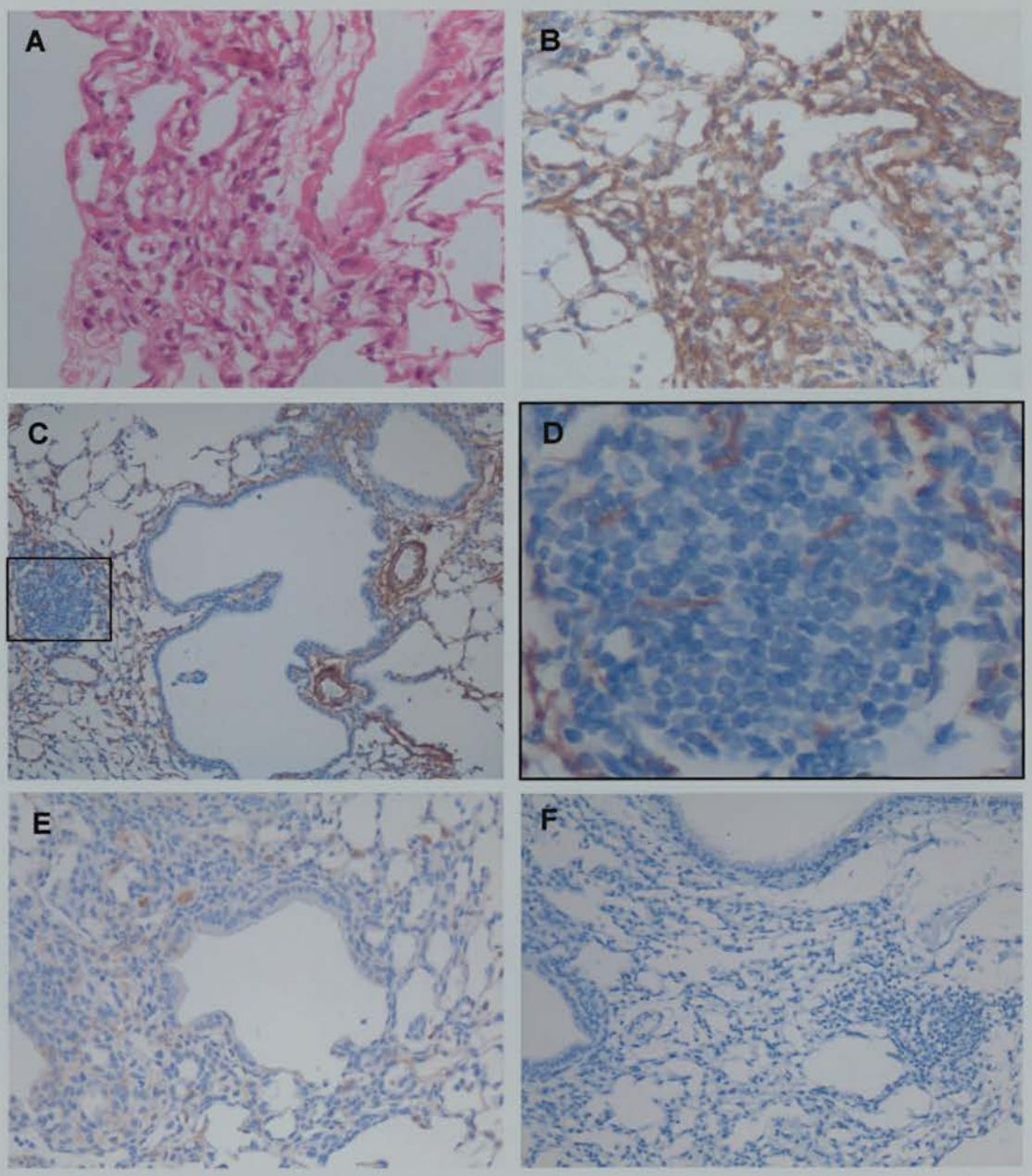

Figure 4.5 H&E and anti-FITC stained sections of mouse lung six weeks after the second dose of intratracheal FITC. Enlarged H&E section shows extensive thickening of alveolar walls, and evidence of continued inflammation (A). Anti-FITC staining in B depicts loss of alveolar wall architecture in areas of FITC deposition. Heavy (C) and light (E) FITC staining are both evident at this time point. Black box in (C) surrounds enlargement shown in (D), which depicts mononuclear nature of cellular aggregate. Anti-FITC negative control (FITC-treated mouse lung) is shown in F. Original magnification x200. Enlargement approximately x800.

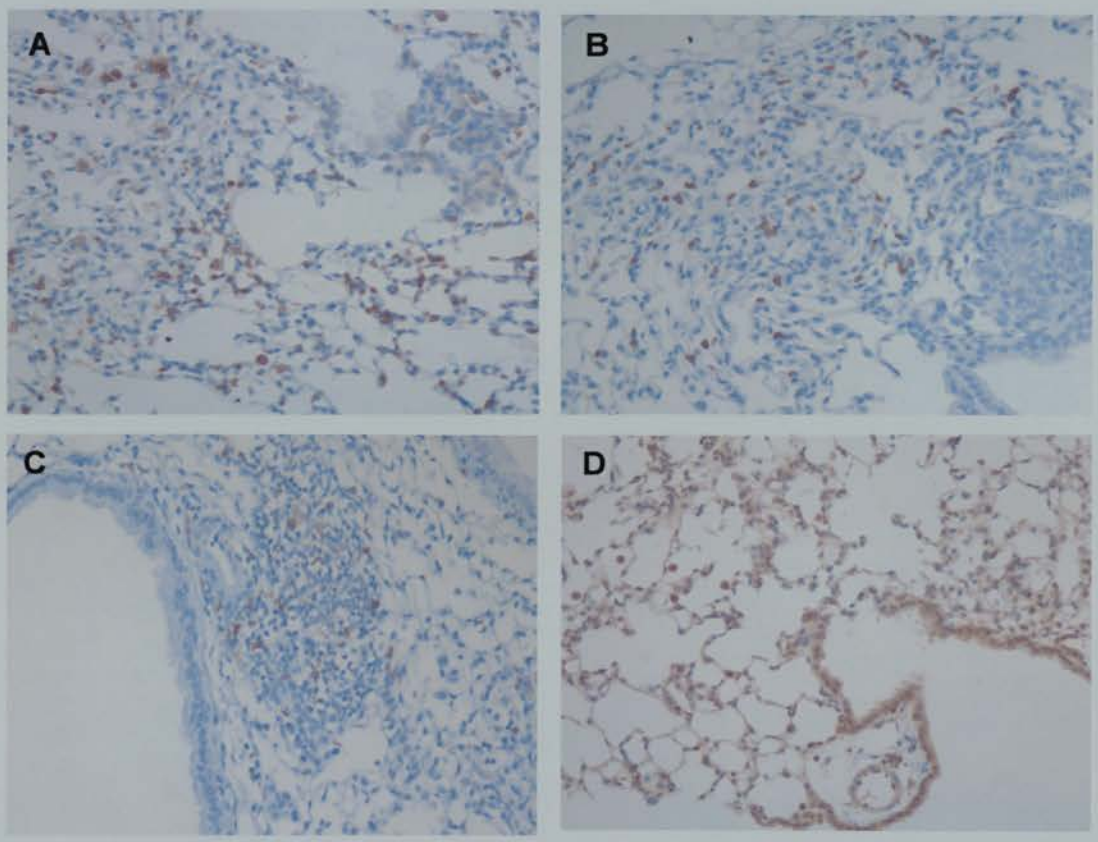

Figure 4.6 FITC-treated mouse lung sections at 6 weeks after the second FITC dose stained for cell surface proteins. Sections were stained by immunohistochemistry for CD3 (A), B220 (B), MHC class II (C), and TGF-β (D). Original magnification x200.

4.2.4 Second Dose + 14 Weeks

The final time point examined was 14 weeks after the second FITC dose, or five months and two doses in total. Areas of severe fibrosis with obliteration of alveolar wall architecture and large fibrous deposits were found adjacent to areas of normal lung tissue (Figure 4.7A,B). Areas of chronic inflammation were also evident. Although the majority of FITC had been cleared away, some was still evident with accompanying fibrosis of the alveoli (Fig. 4.7C,D).

T lymphocytes, bearing the CD3 cell surface protein, were still present, but in lower numbers than at previous time points, and their distribution was more localised (Figure 4.8A). B220-positive B lymphocytes were relatively few in number, and did not seem to be located in the fibrotic areas of the lung (Fig. 4.8B). CD11c-bearing cells showed the same pattern as seen at previous time points, indicating the presence of possibly both macrophages and DCs (Fig. 4.8C). MHC class II stained cells were distributed sparingly throughout the tissue, and were again found in the mononuclear cell aggregates (Fig. 4.8D). Finally, TGF-β staining indicated that much of this cytokine was still being produced in the lungs of mice after five months (Fig. 4.8E). A representative negative control section is shown in F.

The mononuclear cell aggregates that became evident from six weeks after the second FITC dose were comprised mainly of $B220^+$ B lymphocytes (Figure. 4.9A), but also contained $CD3^+$ T lymphocytes (Fig. 4.9B), and MHC class II^+, possibly DCs (Fig. 4.8D). These aggregates appeared to be similar to those described by Wallace *et al.* [371] in patients with CFA. They suggested these aggregates might be evidence of a local humoral immune reaction. Further discussion of these aggregates can be found in section 4.4.1.

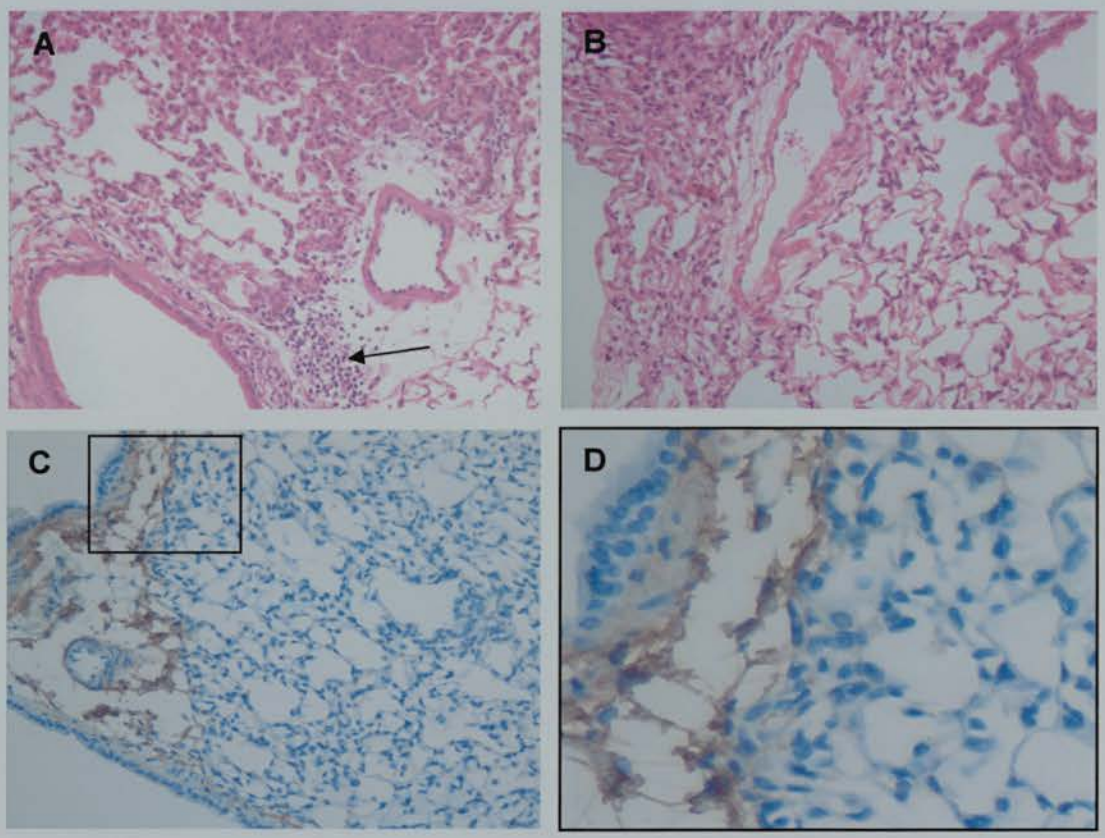

Figure 4.7 H&E and anti-FITC stained sections of mouse lung 14 weeks after the second FITC dose. H&E stained sections show extensive fibrotic changes (A) with inflammation (arrow), and loss of architecture with fibrous deposits next to normal lung tissue (B). Anti-FITC staining is less extensive than seen at previous time points (C). Black box surrounds enlargement shown in D, which displays thickened alveolar walls next to FITC-stained tissues. Original magnification x200. Enlargement approximately x800.

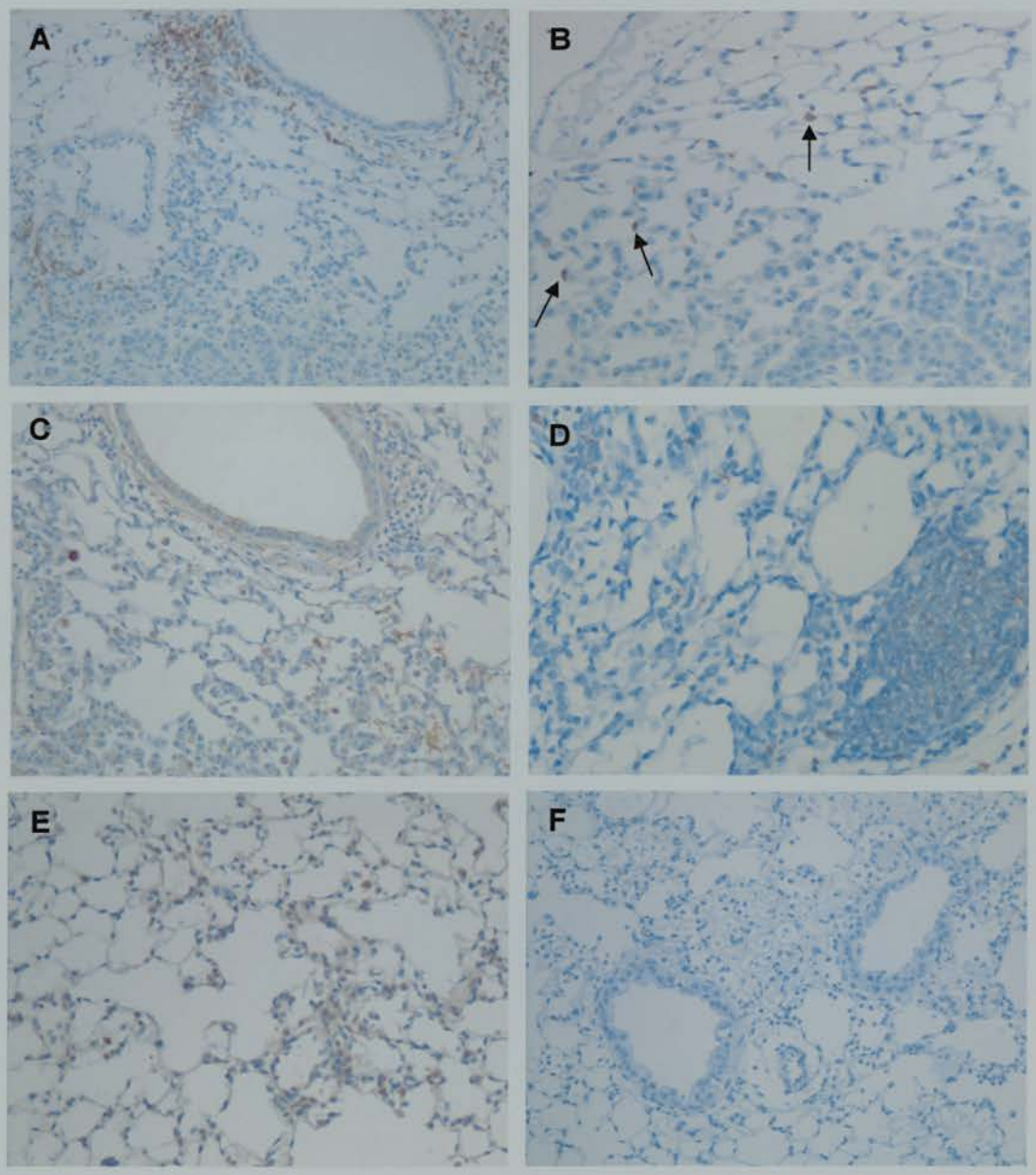

Figure 4.8 FITC-treated mouse lung sections at 14 weeks after the second FITC dose stained for cell surface proteins. Sections were stained by immunohistochemistry for CD3 (A), B220 (arrows indicate positively stained cells) (B), CD11c (C), MHC class II (D), and TGF-β (E). Representative B220 negative control is shown in F. Original magnification x200.

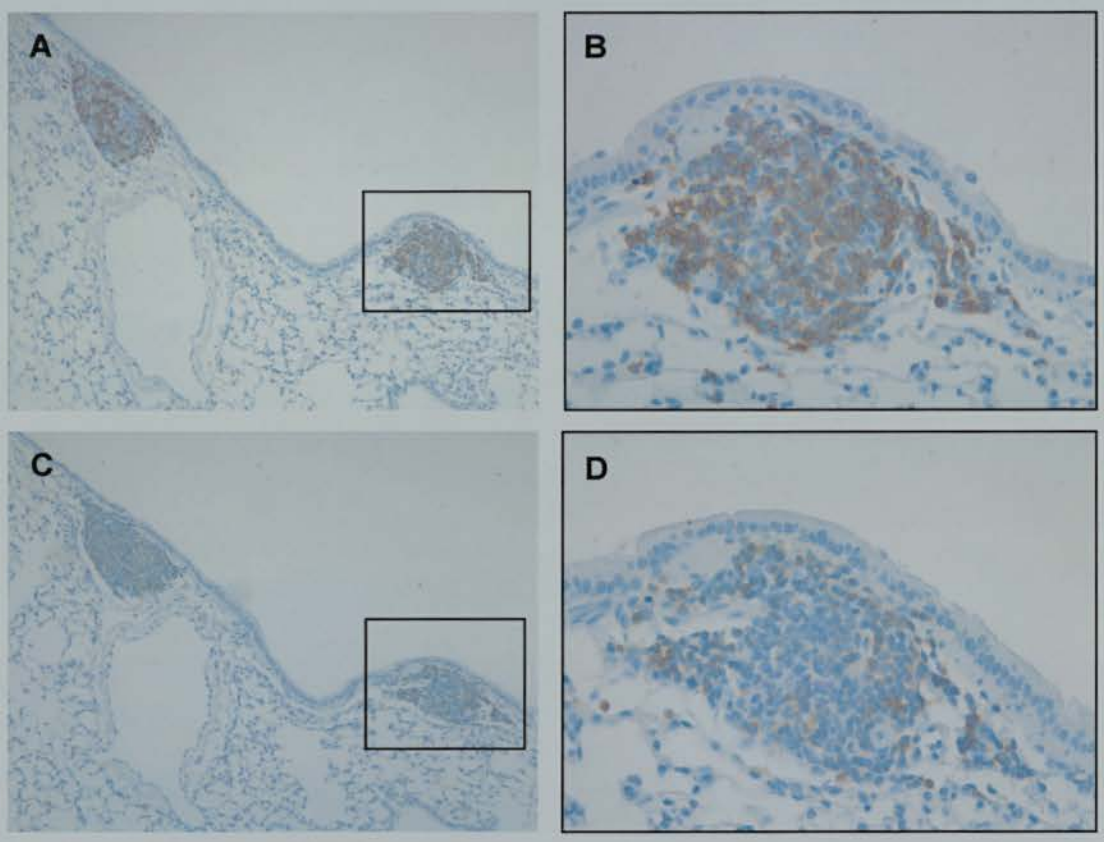

Figure 4.9 B220 and CD3 stained lung sections at 14 weeks after the second dose of FITC, showing mononuclear cell aggregates. Mononuclear cell aggregates in lung tissue on same section contain predominantly B cells, which stain for the B220 protein (A,B), also T cells, which are CD3 positive (C,D). Black boxes surround enlargements shown to the right of original picture. Original magnification x200. Enlargements approximately x800.

4.2.5 Scoring of FITC-induced Damage

In order to assess the damage caused by the intratracheal instillation of FITC, and to compare between FITC-treated and control animals, and between different time points, a scoring system was devised based on the system of Ashcroft *et al.* [435]. They proposed a continuous numerical scale of fibrosis in human lung samples based on microscopical examination of randomly selected fields. In each field, the score was applied to the degree of fibrosis that occupied more than 50% of the field, excluding fields predominantly occupied by malignant tumour deposits, portions of large bronchi or blood vessels, or inflammatory exudates in air spaces. Table 4.2 outlines the criteria used to determine scores.

Grade of fibrosis	***Histological features***
0	Normal lung
1	Minimal fibrous thickening of alveolar or bronchiolar walls
2	
3	Moderate thickening of walls without obvious damage to lung architecture
4	
5	Increased fibrosis with definite damage to lung structure and formation of fibrous bands of small fibrous masses
6	
7	Severe distortion of structure and large fibrous areas; "honeycomb lung" is placed in this category
8	Total fibrous obliteration of the field

Table 4.2 Ashcroft criteria for grading of human lung fibrosis.

The system described above was devised for use on human biopsies, although many groups have used it to assess murine lung fibrosis [96,239,325,428,436-446]. Several modifications were made to adapt it to use on mouse lung tissue sections for these studies.

Ashcroft *et al.* [435] examined the human tissue sections at x10 magnification; this was changed to x40 magnification to allow for the difference in size between human and murine acini. To allow for differences between FITC-positive and FITC-negative areas of the lung, sections stained with the anti-FITC antibody were chosen for examination. A field was therefore considered FITC-positive if more than 50% of the tissue within that field was stained, and negative if less than half the field was stained. Following the proposal of Ashcroft *et al.* [435], damage was assessed by firstly trying to assign fields to an odd number on their scale, and only using even numbers if there was difficulty deciding between two odd numbered grades. The recommended number of fields scored per biopsy was 40 – 50. On the mouse lung sections, 36 FITC-positive and 36 FITC-negative fields were found to cover nearly the entire section, proceeding from one outside edge in non-overlapping rows. Areas in which there was poor inflation or overinflation (usually at lobe margins) were ignored. The sections were scored on a multiheader microscope, and a consensus score was reached between observers for each field. The mean score for fibrosis was determined for both the FITC-positive and the FITC-negative areas.

Examination of the Ashcroft scores of the lung sections at each of the time points clearly showed that two intratracheal doses of FITC do cause pulmonary fibrosis in mice (Figure 4.10). Six weeks after the initial dose, scores from both FITC- and PBS-treated mice indicated very little change from the normal, with no significant differences between fields. Three days after the second intratracheal dose, however, the FITC-positive fields from the sections of the FITC-treated mouse lungs had an mean score of 0.99 ± 0.01, indicating minimal fibrous thickening of the alveolar or bronchiolar walls. This Ashcroft score was significantly greater than the scores for the FITC-negative fields of those same sections, and for the PBS controls ($p < 0.001$). At each of the remaining time points, the FITC-positive fields scored significantly higher scores than the corresponding FITC-negative fields and the PBS controls ($p < 0.001$).

The scores of the FITC-positive fields increased with each successive time point, reaching a high score of 3.26 ± 0.16 at 14 weeks after the second dose of FITC,

indicating that these mouse lungs showed moderate thickening of the walls without obvious damage to the lung architecture. As the scores for each lung were obtained by taking the mean of the scores for each of the 36 FITC-positive fields, many fields had much higher scores, indicating more severe fibrotic damage. As these areas were also found surrounded by normal areas of lung, it demonstrates the patchy nature of the FITC-induced disease, which parallels that of the human disease.

Figure 4.11 compares the Ashcroft scores at each time point in terms of percentage of FITC-positive fields. At six weeks after the first dose, 99% of FITC-positive fields had an Ashcroft score of "0", indicating normal lung. Three days after the second dose, 55.1% of FITC-positive fields had a score of "1", indicating most positive fields showed only minimal signs of disease, and no fields received scores higher than "3". Seven days after the second dose of FITC, most positive fields were scored at either "0" or "1", again indicating few signs of disease, but by this time point, approximately 25% of FITC-positive fields received scores of "2-3" or higher. At six weeks after the second dose of FITC, 55% of the positive fields received Ashcroft scores of "1", and 35% of remaining fields were scored at "2-3" or above. Finally, at 14 weeks after the second FITC dose, 61% of FITC-positive fields were scored at "2-3", indicating moderate signs of fibrotic change. Score of "4-5" were given to 23% of positive fields, and 3% received scores of "6-7", the range in which "honeycomb" changes are placed. Only 13.2% of positive fields were scored at "1", and no fields at this time point received a score of "0".

Thus, the severity of fibrosis in FITC-positive fields increased with time. It is also important to note that all sections from all PBS control mice received Ashcroft scores of "0" at each time point, as did the three and seven day time points.

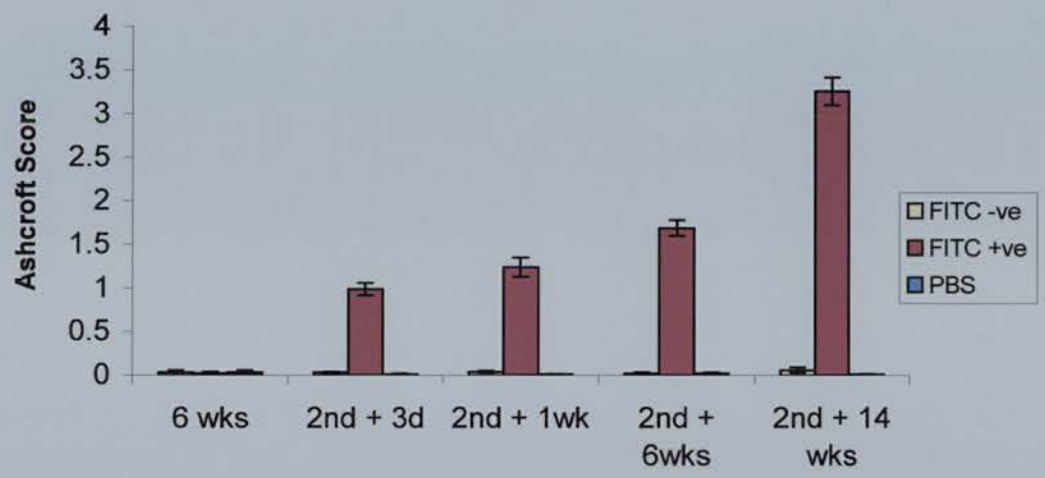

p values	6 wks	2nd + 3d	2nd + 1 wk	2nd + 6 wks	2nd + 14 wks
+ve : -ve	ns	< 0.001	< 0.001	< 0.001	< 0.001
+ve : PBS	ns	< 0.001	< 0.001	< 0.001	< 0.001
-ve : PBS	ns	ns	ns	ns	ns

Figure 4.10 Ashcroft scores comparing severity of fibrosis in FITC- and PBS-treated mice at various time points. Mice were given one intratracheal dose of FITC or PBS, and their lungs were scored six weeks later. Remaining mice were given a second dose after six weeks and lungs were scored on Days 3, 7, or Weeks 6 or 14 after this second dose. Lung sections were scored as described. "FITC +ve" and "FITC -ve" indicate scored sections of lung from FITC-treated mice that did, or did not, stain with the anti-FITC antibody, respectively. "PBS" indicates anti-FITC stained, scored lung sections from PBS-treated mice. Table shows p values comparing the different sections scored for each time point. "ns" = not significant. See Table 4.1 for numbers of mice in each group.
P values were calculated by the Kruskal-Wallis test (nonparametric ANOVA) with Dunn's multiple comparisons post-test.

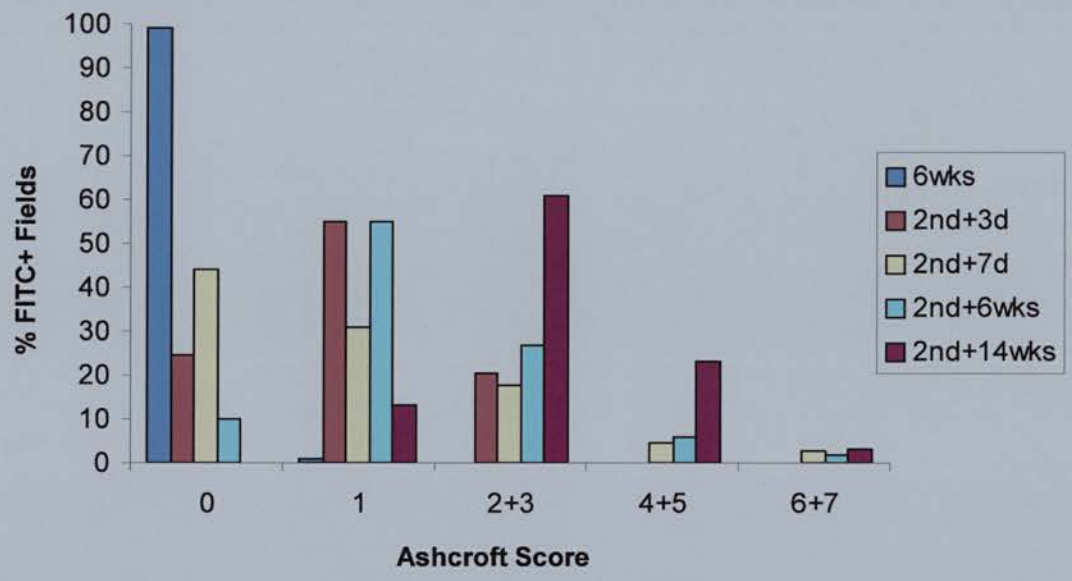

Figure 4.11 Comparison of Ashcroft scores as a percentage of FITC-positive fields for each long-term time point. Ashcroft scores were measured as described. The percentage of FITC-positive fields receiving each degree of Ashcroft score were calculated from all scores from all long-term time points. 6wks, n=56 fields; 2^{nd}+3d, n=138; 2^{nd}+7d, n=243; 2^{nd}+6wks, n=237; 2^{nd}+14wks, n=76.

4.3 Long-term Effects of FITC on BAL Fluid

BAL fluid was collected and processed as described in section 5.3.2 from the mice at each of the time points indicated.

4.3.1 Total Cell Counts

No significant changes in the total mean cell count in the BAL fluid were seen between the FITC- and PBS-treated mice at any of the time points examined, although the counts for the first two time points up to and including 2nd dose + 7 days were slightly increased as compared to normal counts from untreated mice (Figure 4.12). At the 2nd dose + 6 week time point, the cell count in the BAL fluid of the FITC-treated mice was decreased as compared to the PBS control, but not significantly so. At 14 weeks after the second dose the counts for both groups dropped back to normal levels, however again, this difference was not significant.

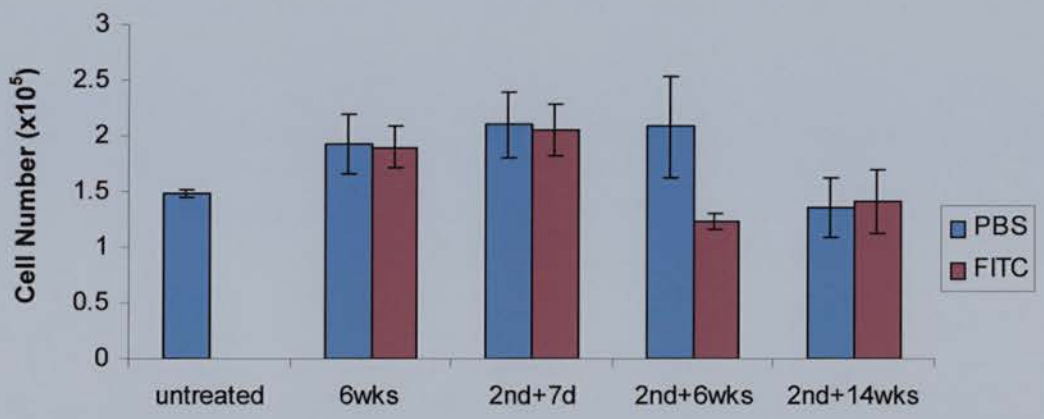

Figure 4.12 Total BAL fluid cell counts measured from untreated mice, and at six weeks after the first intratracheal dose of FITC or PBS, seven days, six weeks and 14 weeks after the second dose. BAL fluid was collected and processed as described from untreated, and both FITC- and PBS-treated mice. Cells were centrifuged and counted as described. Data represent means ± SEM (untreated, n=6; 6wks, n=9; 2nd+7d, n=11; 2nd+6wks, n=3; 2nd+14wks, n=9).

4.3.2 Differential Cell Counts

To assess the cell types present in the BAL fluid of FITC-treated vs. control mice in Series 3, cytospin preparations were made as described in section 2.2, and differential counts were performed as described in section 3.4.2. At all time points except for 2nd dose + 6 weeks, BAL macrophages comprised over 96% of the total cell population, and there were no differences between the FITC- or PBS-treated mice (Figure 4.13). The rest of the cell population consisted of either lymphocytes or neutrophils, but neither was particularly dominant. At six weeks after the second dose, although there was no difference between the FITC- or PBS-treated mice, macrophages made up 90.4 ± 1.9 % of the total population in the BAL fluid of FITC-treated mice, as compared to 91.5 ± 1.5 % for the PBS control mice. In both cases, the majority of the remaining cell population was comprised of lymphocytes. This suggests that the cause was not the FITC treatment, but was an anomaly of this particular group of mice. However, other possibilities, such as infection, or cells moving to the tissues or draining lymph nodes, cannot be ruled out.

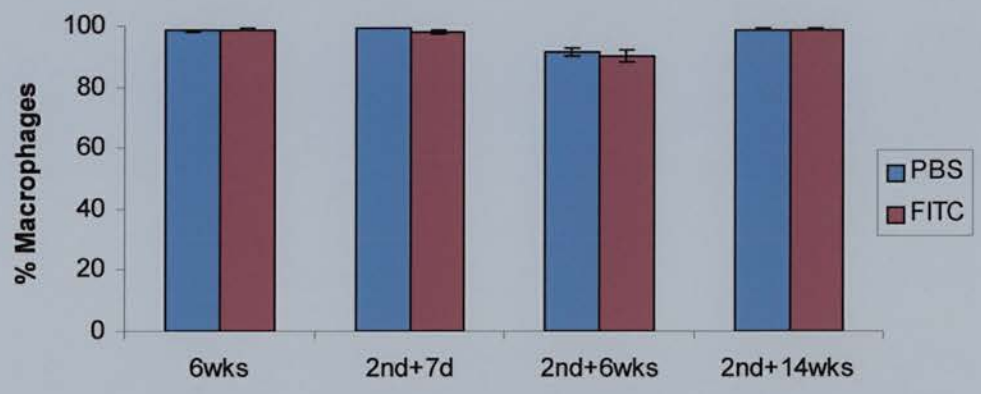

Figure 4.13 Percentage of BAL fluid macrophages counted on cytospin preparations from FITC- or PBS-treated mice over four time points. Three hundred cells per slide were counted over random fields at x100 magnification. Data represent means ± SEM (6wks, n=9; 2nd+7d, n=11; 2nd+6wks, n=3; 2nd+14wks, n=9).

4.3.3 Cytokine Production

BAL fluid was collected, processed and assayed as described. As for the short-term time points, the BAL fluid was assayed for TNF-α, IFN-γ, and TGF-β from the mice in Series 1 and 2.

4.3.3.1 TNF-α

Levels of TNF-α in mice at acute time points were increased in FITC-treated mice as compared to PBS-treated mice at Days 1 and 2 after instillation, with levels becoming undetectable in both groups from Day 3 (Figure 3.17).

The results from Series 1 (Figure 4.14) can only be interpreted with caution as cytokine levels all fall around the 15.625 pg/ml lower detection limit of the R&D DuoSet mouse TNF-α ELISA assay. In Series 1 long-term mice, levels of TNF-α in the BAL fluid remained undetectable at all time points except six weeks after the second dose. In this case, the TNF-α levels were significantly higher than those of the FITC-treated mice at the same time point ($p < 0.01$). Apart from this, although the levels of TNF-α did seem to increase slightly over the five months, there were no significant changes between the FITC- and PBS-treated mice, or between any of the time points.

In Series 2, however, a different pattern emerged (Figure 4.15). In this series of mice, all of which were set up at the same time, levels of TNF-α in the BAL fluid were well above the lower detection limit of the ELISA. At six weeks after the first dose, levels were detectable in both groups of mice, although they were slightly higher in the FITC-treated mice. Seven days after the second dose, TNF-α levels had risen in the BAL fluid of the PBS-treated mice (67.4 ± 10.9 pg/ml), but although considerably higher than those of the FITC-treated mice (31.1 ± 8.5 pg/ml), the difference was not statistically significant. Six weeks after the second dose the levels

in the FITC-treated mice had increased above those of the PBS controls, although again, not significantly. Finally, at 14 weeks after the second dose TNF-α levels in the BAL fluid of both FITC-treated mice and controls remained elevated, but there was no significant difference between them. As with Series 1 mice, there were no significant differences between any of the time points.

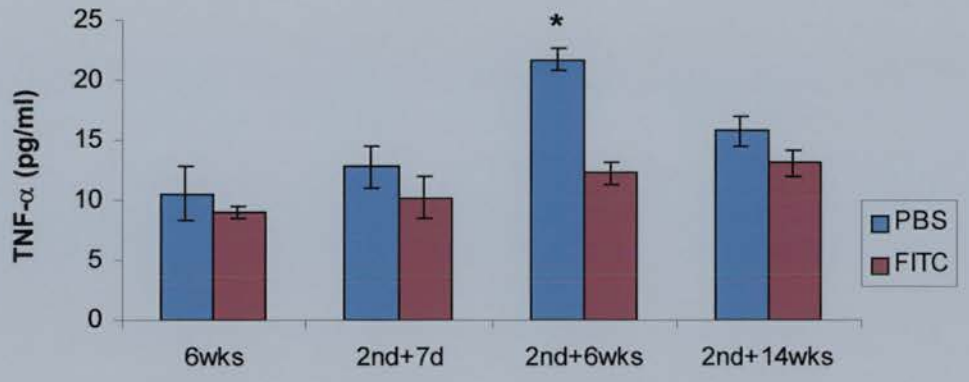

Figure 4.14 TNF-α production measured in BAL fluid from FITC-treated mice and PBS controls over four time points in Series 1 mice. BAL fluid was collected, processed, and assayed as described. BAL fluid from FITC- and PBS-treated mice was collected at six weeks after the first dose, seven days, six weeks or 14 weeks after the second dose. Data are presented as the mean ± SEM (6wks, n=2 sets of four FITC- and four PBS-treated mice; 2^{nd}+7d, n=5 sets; 2^{nd}+6wks, n=2 sets; 2^{nd}+14wks, n=8 sets). *p<0.01 by paired Student's *t*-test.

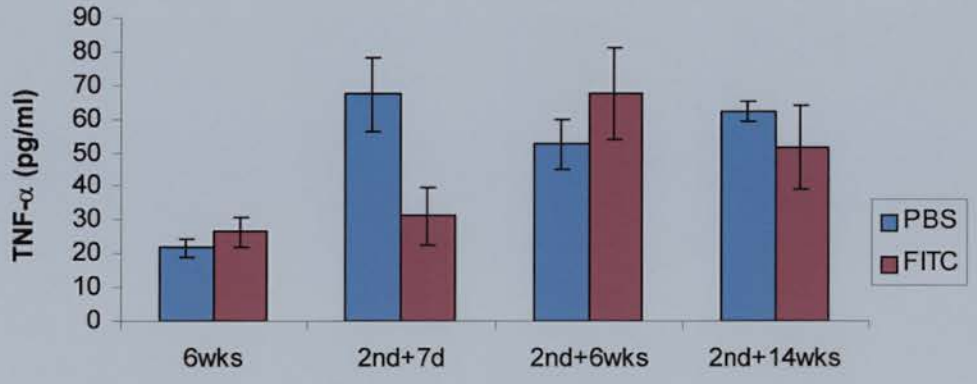

Figure 4.15 TNF-α production in BAL fluid from FITC-treated and PBS control mice over four time points in Series 2 mice. Data are presented as means ± SEM (n=1 set of four FITC-treated and four PBS-treated mice at each time point).

4.3.3.2 *IFN-γ*

IFN-γ was measured in the BAL fluid from mice in Series 1 and 2 as described. The lower detection limit for this R&D ELISA is 31.25 pg/ml and therefore the levels of IFN-γ measured in the BAL fluid from mice in Series 1 (Figure 4.16) must be interpreted with caution as they all fall below this limit. IFN-γ levels in the BAL fluid of mice assessed at acute time points were all undetectable (Figure 3.18).

In Series 1 mice, the levels of IFN-γ in the BAL fluid were similar six weeks after the first dose in both FITC-treated and PBS control mice. At seven days after the second dose, however, IFN-γ levels decreased in the FITC-treated mice as compared to the levels at six weeks after the first dose, and this decrease became significant at six weeks after the second dose ($p < 0.04$). IFN-γ levels had increased by 14 weeks after the second dose in the FITC-treated mice. IFN-γ measured in the BAL fluid of PBS-treated control mice did not change significantly over any of the time points, and in fact was significantly higher than the paired FITC levels for each of the last three time points ($p < 0.02$), however, as all levels fell below the lower detection limit for this assay, any increases in levels of the cytokine may not have any biological effect, and further investigation is required.

A different pattern was seen in the BAL fluid from mice in Series 2 (Figure 4.17). Although the difference in levels of IFN-γ between the FITC-treated and PBS control mice was not significant at any time point, the levels of the cytokine had fallen by seven days after the second dose. A significant increase to detectable levels was then seen six weeks after the second dose, as compared to the previous time point ($p < 0.02$), again for both groups of mice, with levels dropping back down below the level of detection by 14 weeks after the second dose. This may reflect a possible infection in the animal house at the time.

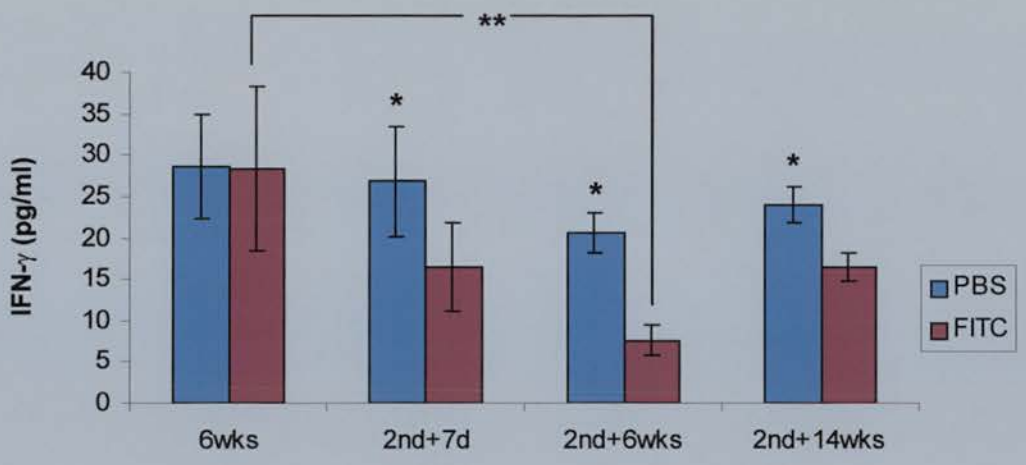

Figure 4.16 IFN-γ production measured in BAL fluid from FITC-treated mice and PBS controls over four time points in Series 1 mice. BAL fluid was collected, processed, and assayed as described. BAL fluid from FITC- and PBS-treated mice was collected at six weeks after the first dose, seven days, six weeks or 14 weeks after the second dose. Data are presented as the mean ± SEM (6wks, n=2 sets; 2^{nd}+7d, n=5 sets; 2^{nd}+6wks, n=2 sets; 2^{nd}+14wks, n=8 sets).
**p<0.04 by Student's *t*-test; *p<0.02 by paired Student's *t*-test.

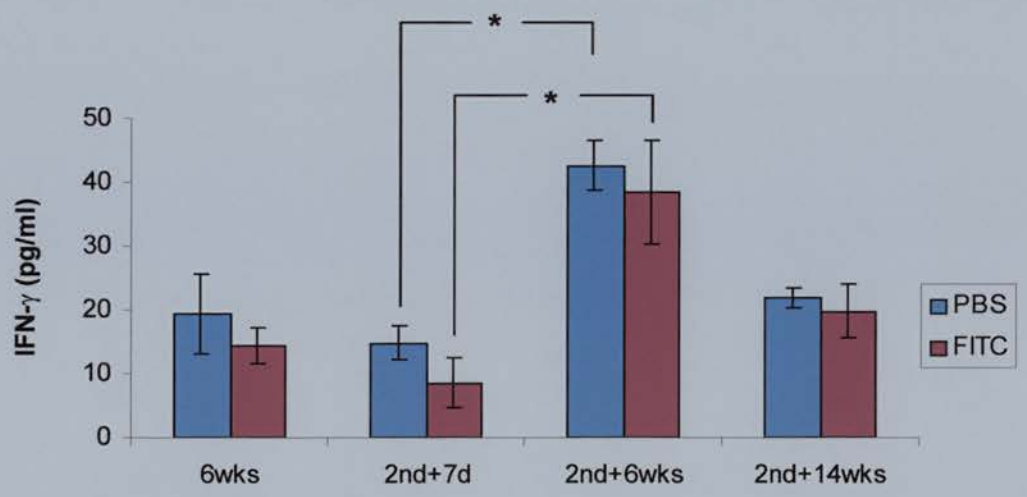

Figure 4.17 IFN-γ production in BAL fluid from FITC-treated and PBS control mice over four time points in Series 2 mice. Data are presented as means ± SEM (n=1 set of four FITC-treated and four PBS-treated mice at each time point).
*p<0.02 by Student's *t*-test.

4.3.3.3 TGF-β

As previously described, both active and total TGF-β were measured in the BAL fluid of mice in Series 1 and 2. At acute time points, total TGF-β levels in the BAL fluid were increased at Day 2 in the FITC-treated mice (32.7 ± 5.8 pg/ml) as compared to the PBS controls (19.4 ± 1.5 pg/ml), although not significantly (Figure 3.19). A significant increase in active TGF-β was seen at the same time point, however (31.3 ± 3.4 pg/ml FITC vs. 14.5 ± 2.4 pg/ml PBS) (Figure 3.20). All other values at all other acute time points were below the level of detection for this assay (31.25 pg/ml).

BAL fluid from mice in Series 1 showed total TGF-β levels below the lower limit of detection for this assay at all long-term time points examined (Figure 4.18). Also, no significant differences were detected between the levels measured for FITC-treated mice and the PBS control mice. There did appear to be a slight increase in the total TGF-β levels in FITC-treated mice at seven days after the second dose compared to the previous time point, which had then decreased by six weeks after the second dose to a level slightly below that of the PBS controls, and by 14 weeks after the second dose, levels of the total cytokine had increased in both groups of mice.

Similarly, the active form of the cytokine was present at similar levels in the BAL fluid of the FITC-treated and PBS control mice over all the time points evaluated (Figure 4.19). However, levels did increase above the lower detection limit at six weeks after the first dose, falling again seven days after the second dose, and only reaching detectable levels again 14 weeks after the second dose. Six weeks after the second dose active TGF-β had increased again, significantly in the FITC-treated mice ($p < 0.02$) although not significantly more than the paired PBS value. Five months after the first dose, active TGF-β levels in both FITC-treated and PBS control mice had significantly increased as compared to seven days post-second dose ($p < 0.005$), and were detectable above the lower detection limit of the assay (43.9 ± 5.5 pg/ml FITC, 42.0 ± 4.1 pg/ml PBS). It would be possible then, that in Series 1

mice the intratracheal instillation of FITC or PBS may have caused a decrease in the production of active TGF-β in the BAL fluid, and that this level increased afterwards. This change, however, is not attributable to the instillation of the FITC itself.

BAL fluid from mice in Series 2 showed overall higher levels of total TGF-β than in Series 1, however there were no significant differences between the FITC-treated mice and PBS control mice at any time point (Figure 4.20). Measured total cytokine levels remained slightly above or below the lower detection limit of the assay, although at six weeks after the first dose the levels in the BAL fluid of the FITC-treated mice seem marginally higher than the rest. A significant reduction in the measured total TGF-β levels in the FITC-treated mice was seen at the 2^{nd}+14 week time point, as compared to both the 2^{nd} + 7 day time point ($p < 0.04$).

Active TGF-β measured in the BAL fluid from the mice in Series 2 was generally undetectable, falling only slightly above or below the assay's lower detection limit (Figure 4.21). The levels in the three later time points are marginally higher than in the earliest time point. As in the total TGF-β assay, no significant differences between the FITC- or PBS-treated mice were seen at any time point.

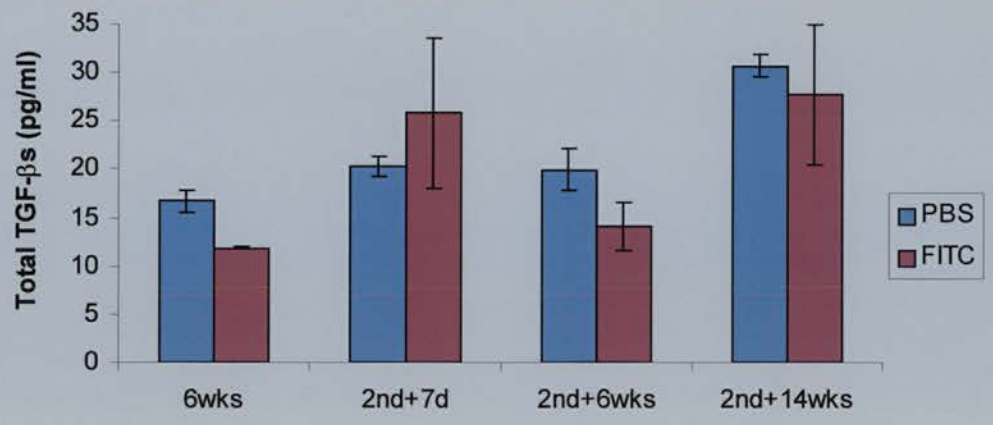

Figure 4.18 Total TGF-β levels measured in BAL fluid from Series 1 mice treated with FITC or PBS and examined at various time points. Data are presented as means ± SEM (6wks, n=2 sets of four FITC- and four PBS-treated mice; 2^{nd}+7d, n=5 sets; 2^{nd}+6wks, n= 2 sets; 2^{nd}+14wks, n=8 sets).

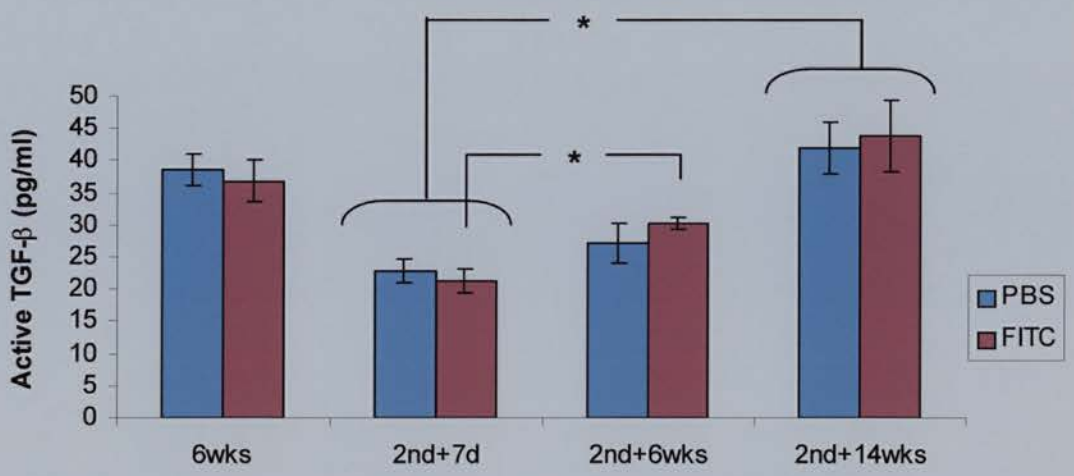

Figure 4.19 Active TGF-β levels measured in BAL fluid from Series 1 mice treated with FITC or PBS and examined at various time points. Data are presented as means ± SEM.
*p<0.03 by Student's *t*-test.

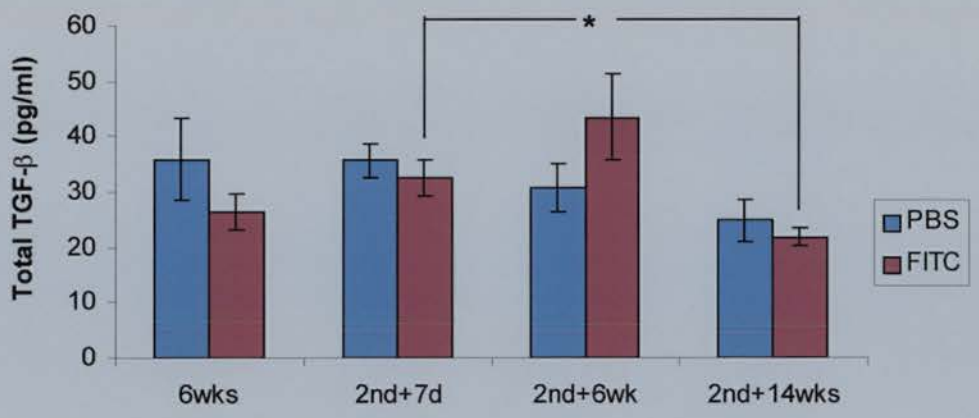

Figure 4.20 Total TGF-β levels measured in BAL fluid from Series 2 mice treated with FITC or PBS and examined at various time points. Data are presented as means ± SEM (n=1 set of 4 FITC- and 4 PBS-treated mice per time point).
*p<0.04 by Student's *t*-test.

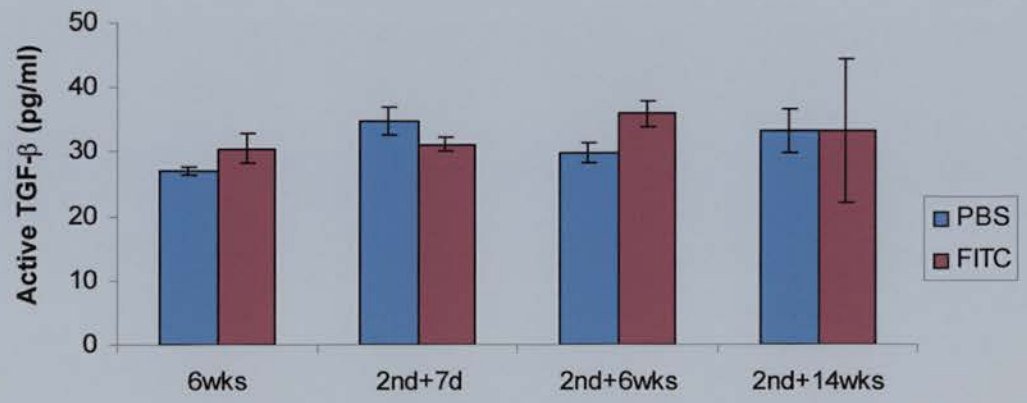

Figure 4.21 Active TGF-β levels measured in BAL fluid from Series 2 mice treated with FITC or PBS and examined at various time points. Data are presented as means ± SEM.

4.4 Conclusions and Discussion

Chapters 3 and 4 have described the disease pattern seen in the modified murine FITC model of pulmonary fibrosis originally described by Roberts *et al.* [243]. In the modified model, a two-dose nonsurgical method of intratracheal instillation was used rather than the original single surgical dose. Chapter 3 described the acute effects of the FITC in the lung tissue and the BAL fluid in this modified model from one day to seven days, while Chapter 4 has described the long-term effects from six weeks after the initial dose, to seven days, six weeks, and 14 weeks after the second dose.

4.4.1 Responses to FITC in the Tissue

As described in Chapter 3, examination of the mouse lungs up to one week after the initial dose showed an acute inflammatory response characterised by alveolar wall oedema and a granulocytic infiltrate which disappeared over a week, and in some areas was replaced by a chronic mononuclear infiltrate. FITC deposition was found surrounding the large and smaller airways and blood vessels, and in the alveolar walls. Much of the FITC, however, was presumably removed by the resident macrophages.

In order to obtain quantitative data enabling the comparison of acute inflammation between FITC- and PBS-treated animals after the first dose, a method of scoring was devised. Four different compartments in the lung were scored and the scores then combined to form an overall score. The overall scores clearly demonstrated that the inflammation present in the lungs of the FITC-treated mice was significantly greater than that measured in the PBS control mice, which had little, if any, signs of an inflammatory response. A second intratracheal dose of FITC, or PBS, was given to the remaining mice six weeks after the first dose. By this method, 14 weeks after the

second dose, up to 75% of the animals had developed fibrotic changes in the lungs in response to the administration of two doses of FITC, while no changes were seen in the lungs of any of the PBS-treated mice (Table 4.1).

The acute granulocytic inflammatory cell infiltrate evident from Day 1 became predominantly mononuclear by six weeks after the initial dose as apoptotic granulocytes would be mainly cleared by macrophages. The mononuclear infiltrate remained over the subsequent long-term time points, indicating a chronic state of inflammation. A patchy distribution of FITC was visible on immunohistochemically stained lung sections, and persisted until the final time point at 14 weeks after the second dose. Areas in which the FITC was visible often showed thickening of the alveolar walls, deposition of fibrous tissue, and occasionally mononuclear cell aggregates while adjacent areas remained normal.

Immunohistochemical staining showed that lymphocytes did not become prominent in the tissues until Day 5 after the first dose of FITC, and that they remained present at all subsequent time points. Although T cell differentiating antibodies were not available, CD3 protein staining showed that T cells were the predominant lymphocytes present in the tissues, while B cells predominated in the mononuclear cell aggregates that can develop in the later stages, suggesting the potential for an immunological basis for the continuing inflammation. This is supported by the finding of anti-FITC antibodies in the serum up to six weeks after a single, surgical intratracheal dose of FITC [243]. Christensen *et al.* [244] reported that the induction of fibrosis in the original model was not T-cell dependent, but did agree that T cell immunity could be important in later stages (Galen Toews, personal communication).

Alterations in T lymphocytes may be of particular interest in determining the pathogenesis of CFA, given that recruitment of lymphocytes to the lung is a well-documented feature of the disease [447]. As lymphocytes tend to be underrepresented in BAL fluid, the extent to which they may contribute to the pulmonary inflammatory response may be underestimated [407,448]. T cells secrete

chemoattractants for a variety of cell types including neutrophils, monocytes, and eosinophils [449], and it has been proposed that *in vivo* secretion of macrophage-derived growth factors may be locally driven by interaction with T cells participating in the inflammation elicited by fibrogenic injury [450].

However, as discussed in Chapter 1, the role of T cells in the pathogenesis of bleomycin-induced pulmonary fibrosis has not been fully elucidated. *In vivo* T cell depletion with anti-T cell antibodies has been shown to completely abrogate bleomycin-induced pulmonary fibrosis [220], while Helene *et al.* [451] have reported that bleomycin-induced pulmonary fibrosis is T cell-independent. Studies in athymic nude mice, which lack functional T cells, have been equally unclear. One study demonstrated that bleomycin was not fibrogenic in nude mice [215], and another showed the same in mice with silica-induced pulmonary fibrosis [452], while a third reported histologically similar fibrosis in nude and euthymic mice after bleomycin treatment [364], with a the same finding in asbestos-induced pulmonary fibrosis [453].

Similar studies in the single-dose FITC model are also conflicting. Christensen *et al.* [244], reported that depletion of CD4 T cells from FITC-treated BALB/c mice ablated the development of a specific immune response to FITC, but that these mice had similar increases in lung collagen content compared to control mice. They found the same responses in both BALB/c severe combined immunodeficiency (SCID) mice and C57BL/6 mice carrying a selective deletion of the recombination activating gene. However Roberts *et al.* [243], who developed the original FITC model, found that while FITC-treated SCID mice showed severe inflammation seven days after instillation similar to that seen in immunocompetent FITC-treated mice, although without the presence of T cells, by three months no scarring or infiltrate was seen despite the presence of fluorescent FITC. This was in direct contrast to the scarring and infiltrate found in the immunocompetent mice at the same time point (unpublished data). This is illustrated by the figures in Appendix 2.

Further examination of the T lymphocyte population in the FITC model is required. Immunohistochemical staining for Th1 and Th2 cytokines would be beneficial in determining whether FITC-induced pulmonary fibrosis resembles a Th1-type or more likely, a Th2-type immune response, and whether the T cells present are major sources of those cytokines. Staining for $CD8^+$ and $CD4^+$ T cells subsets would also be useful, if such antibodies for use on paraffin sections become available. CFA is associated with a predominantly $CD8^+$ T cell infiltrate [368], and preliminary experiments performed on the single surgical dose FITC model, in which 50% of $CD4^+$ or $CD8^+$ T cells were depleted 24 hours before FITC instillation, suggested that $CD8^+$ cells may cause most of the epithelial cell damage. $CD4^+$ T cells, however, may promote anti-self epithelial cell antibody production [119,120], which could also perpetuate the epithelial cell damage. The use of anti-T cell antibodies, or possibly setting up the FITC model in athymic nude mice may also help to elucidate the role of T lymphocytes in FITC-induced pulmonary fibrosis.

The lymphocyte aggregates seen in the later stages in the FITC model are similar to the B lymphocyte aggregates observed in patients with CFA as reported in the literature [105,370]. They were described most recently by Wallace *et al.* [371], who found evidence of a local humoral immune response associated with these aggregates. They described the presence of follicular DCs in the aggregates, which are associated with antigen presentation to B lymphocytes, indicating that a humoral response had occurred in the lungs of these patients. The B cell aggregates seen in the FITC model also showed cells that stained positively for MHC class II (Figure 4.8D), which may indicate the presence of DCs and possibly a local humoral immune reaction.

Wallace *et al.* [371] proposed that these B cell aggregates may be involved in the pathogenesis of CFA for two reasons. First, that the aggregates were not found to be topographically associated with large honeycomb spaces, nor near any evidence of infection. The B cell aggregates found in the FITC model appear to be similarly removed from such areas. Second, a link between increased B cells in biopsy

specimens and poor prognosis in CFA patients, as suggested previously [105], might suggest that the humoral response is significant in CFA pathogenesis.

Turner-Warwick and Doniach [113] described the presence of non-organ-specific circulating autoantibodies in approximately 40% of patients with CFA, which have since been shown to include antinuclear antibodies, anti-DNA topoisomerase II antibodies, and anti-cytokeratin 8 antibodies [112,115,116,118]. Moreover, immune complexes have been identified in the blood, BAL fluid and tissue of patients with CFA [108,110]. Although it has been suggested that autoantibodies are secondary to lung injury and inflammation [106], Wallace *et al.* [119,120] have reported the presence of autoantibodies against alveolar lining cells in the serum of patients with CFA, thus identifying the suspected autoantigen as being endogenous and specific to the lung. Further study into these B cell aggregates is essential to determine the role of both B cells and the humoral immune response in FITC-induced pulmonary fibrosis. Most important, perhaps, is establishing the presence of these same anti-self antibodies in the plasma of FITC-treated mice. Comparing the severity of FITC-induced disease after administration of B cell-depleting antibodies, or in a B cell knockout mouse, could also provide useful information.

The cell surface proteins CD11c and MHC class II are both found on lung macrophages and DCs although, as will be shown in Chapter 5, they were expressed at different levels on the two cell types from the mice examined. Immunohistochemical staining of lung sections from the FITC-treated mice at all time points showed cells expressing varied levels of both CD11c and MHC class II. CD11c is known to be expressed on both neutrophils and monocytes in the lung [454,455], and high expression of CD11c has been reported on bronchial epithelium, particularly in the acute phase of influenza A virus infection after ovalbumin challenge [456]. Interestingly in this study, CD11c expression was not detectable in the recovery phase, while expression seemed fairly constant in the progressive FITC model. As anti-CD11c antibody stained other structures in the FITC-treated lung, it is difficult to comment on the distribution of CD11c-expressing cells. However, some individual cells stained very strongly for cell surface CD11c protein,

suggesting they may be macrophages. Kumar *et al.* [450] have proposed that *in vivo* secretion of macrophage-derived growth factors may be locally driven by interaction with the T cells participating in the inflammation elicited by fibrogenic injury. The cell surface protein F4/80, often used as macrophage marker although its expression is not exclusive to these cells, was not suitable for use on mouse paraffin sections.

The MHC class II antibody, however, was very specific, and showed that cells positive for this protein were present from Day 1 after the initial dose, and persisted throughout the five months. Often, very strongly MHC class II^+ cells, bearing dendritic-like processes, were found in and around the mononuclear cell aggregates, suggesting a possible role for DCs in antigen presentation to the lymphocytes, and a possible humoral immune reaction.

Cell surface TGF-β appeared to be highly expressed in the lungs of the FITC-treated mice, particularly at the earlier time points, but also in the later stages. Although this correlates well with published data showing that TGF-β is produced by type II epithelial cells in the lung [250], and plays a major role in the pathogenesis of lung fibrosis [235,267,279,281,434], it was not corroborated in the BAL fluid, as will be discussed in the following section. Interestingly, in a murine Th2-type model of allergic airway inflammation induced by group 1 allergen, Der p 1, only very weak TGF-β staining was detected on lung sections [457].

The measurement of hydroxyproline content of hydrolyzed lung as a marker of collagen content is the most widely accepted method of quantifying lung fibrosis biochemically, although other methods for obtaining semi-quantitative data could be used, such as reverse transcription-polymerase chain reaction for selected genes. As the methodology for measuring hydroxyproline content was not available, a system of scoring the pathology was devised, based on the method of Ashcroft *et al.* [435] (Table 4.2). The fibrosis scores for all time points examined after the second FITC dose were significantly more severe in areas of FITC deposition as compared to areas of no FITC on the same sections, and as compared to the PBS controls (Figure 4.10), and the severity of fibrosis increased with the later time points (Figure 4.11). By this

method, it was clearly shown that the administration of two intratracheal doses of FITC lead to pulmonary fibrosis in the majority of mice. One of the shortfalls of this model, however, is that not all the mice given FITC intratracheally developed pulmonary fibrosis. This will be discussed in detail in Section 4.4.3. In the future, image analysis could also be considered as an alternative method of quantifying fibrosis in the lungs.

4.4.2 Responses to FITC in the BAL

In the BAL, evidence of a granulocytic infiltrate was seen in the high PMN count and correspondingly decreased macrophage count at Day 1, gradually returning to normal over seven days (Figures 3.13, 3.14). Little change, if any, was seen in the lungs of the PBS control mice.

MIP-1α is a member of the C-C chemokine family and increased expression has been demonstrated in BAL immune cells of patients with CFA [458]. MIP-1α protein has also been found in the lungs of mice with bleomycin-induced injury, and it has been proposed that it is regulated by TNF-α and IL-6 [219,459]. However, BAL fluid from FITC- and PBS-treated mice collected between Day 1 and Day 7 did not show any MIP-1α. This may have been because tissue levels are not reflected in the BAL, and should be confirmed by other methods, such as gene expression in the lung tissue.

4.4.2.1 TNF-α

Cytokine production in the BAL fluid was measured at both acute and long-term time points after FITC instillation. Levels of TNF-α were increased to 29.1 ± 6.5 pg/ml in the FITC-treated mice immediately after they were given the first dose of

FITC, and gradually decreased to levels similar to those of the PBS control mice over seven days (Figure 3.17). TNF-α is a potent proinflammatory mediator that plays a critical role in acute pulmonary injury and in the regulation of fibroblast growth [75]. The increased levels of TNF-α found in the BAL fluid of the FITC-treated mice at the acute time points are consistent with the initiation of inflammation in response to acute injury.

Over the long-term time points, the BAL fluid from two series of mice was analysed for the presence of TNF-α. In Series 1 mice, TNF-α was only detectable at six weeks after the second dose, and only in the PBS control mice (Figure 4.14). In Series 2 mice, TNF-α was detectable at all time points measured, and although there were no significant differences between the treated and control mice, levels were higher in the PBS control mice at seven days after the second dose of FITC (Figure 4.15). One possible reason for the discrepancy between the two series is that perhaps the Series 2 mice had an underlying infection causing an inflammatory reaction. Regardless, examination of the differences in levels of TNF-α between the FITC-treated and PBS control mice in both series showed that, apart from the 2^{nd} + 6 weeks time point in Series 1, no significant differences were found. Again, the possibility of an underlying infection may be the reason for the anomaly in Series 1. Notably, Fujita *et al.* [288] demonstrated that overexpression of TNF-α in mouse lungs results in increased levels of TNF-α protein in the BAL fluid, measured between 60 and 90 ng/ml, while control mice had levels of approximately 1-3 ng/ml. This group found, however, that these mice did not develop pulmonary fibrosis. The TNF-α protein levels in the BAL fluid of the FITC- and PBS-treated Series 2 mice did not rise above 75 pg/ml. Even if tissue levels are found to be much higher, and despite its role in the acute inflammation caused by FITC instillation, it seems unlikely that TNF-α by itself plays a major role in the pathogenesis of FITC-induced pulmonary fibrosis, although it may work in concert with other cytokines, as discussed below.

The role of TNF-α in the development of pulmonary fibrosis has not been fully elucidated, although its importance has been highlighted in many studies. TNF-α

mRNA is increased in the lungs of patients with CFA [296]. Anti-TNF-α antibody administration prevents the development of both bleomycin-induced pulmonary fibrosis [220] and silica-induced pulmonary fibrosis [460]. TNF-α overexpression has been shown to lead to the development of pulmonary fibrosis, while deficiency can confer resistance [461].

However, there is evidence to suggest that TNF-α by itself may not produce pulmonary fibrosis. Another murine model of TNF-α overexpression produced mice with severe alveolitis and progressive pulmonary fibrosis [292], however further study revealed that TNF-α alone was unable to produce significant pulmonary fibrosis in these mice in the long term [288]. Maeda *et al.* [236] were unable to detect any differences in TNF-α expression in BAL cells between mice given intraperitoneal bleomycin and controls. Furthermore, gene transfer studies with TNF-α revealed an induction of limited pulmonary fibrosis compared to that with TGF-β [293]. There is also evidence to suggest that TNF-α may even inhibit fibrosis by enhancing the production of fibroblast collagenases and PGE_2 [290,462].

Most likely, however, TNF-α acts indirectly by stimulating diverse lung cells to produce certain fibrogenic cytokines, such as TGF-β, which has more direct fibrogenic activity [246,277,293]. In the modified FITC-induced model of pulmonary fibrosis it would appear that while TNF-α did contribute to the acute inflammation that occurred after the first dose of intratracheal FITC, either its presence was not required for the fibrotic changes that occurred in the later stages, or more likely, it was involved in the initiation of fibrosis. The role of TNF-α in this model requires further study. Immunohistochemical staining of tissue sections with anti-TNF-α would be useful, as the tissue concentrations of cytokines are not necessarily reflected in the BAL fluid. Other possible routes of investigation include the use of TNF-α receptor knockout mice, or anti-TNF-α antibody administration.

4.4.2.2 IFN-γ

IFN-γ measured in the BAL fluid of mice was not found at detectable levels at any of the acute time points evaluated, nor were there any differences found in the levels between the FITC-treated and PBS control mice (Figure 3.18). The long-term time points were evaluated in Series 1 and 2 mice. In Series 1, levels of IFN-γ remained below the level of detection, although there was a trend in which PBS control mice had higher levels than the FITC-treated mice (Figure 4.16). Although the differences were statistically significant at the three later time points, levels were still below the detection limit of the assay. In Series 2, there were no differences in IFN-γ levels between the treated and control mice at any time point, although again, there was a trend showing slightly higher levels in the PBS control mice (Figure 4.17). There was a significant increase in IFN-γ levels in both treated and control mice at six weeks after the second dose of FITC, as compared to the previous time point, but as this occurred in both groups of mice it was not attributable to the either the FITC or PBS treatments.

IFN-γ is a Th1 cytokine, while the inflammation in CFA is most often characterised as being Th2-like [16]. IFN-γ has been shown to inhibit fibroblast collagen synthesis, and diminished production may also enhance collagen deposition in pulmonary fibrosis [247,250]. As discussed in Chapter 1, it is thought that decreased Th1-type IFN-γ may occur concomitantly with a rise in Th2 cytokines such as IL-4 and IL-5, thus shifting the cytokine balance towards a profibrotic response [74,100,101]. Studies of blood and lung tissue from CFA patients have found absolute and relative deficits in IFN-γ as compared with other Th2 cytokines [74,250,251,257]. Administration of IFN-γ has been used therapeutically to treat bleomycin-induced pulmonary fibrosis [96,255,256], and has even shown promising results in clinical trials [103].

The low levels of IFN-γ found in the BAL in the FITC-induced model of pulmonary fibrosis suggest the inflammation may resemble a more Th2-type response, and

indicate a limited or an indirect role for this cytokine. As for TNF-α, the use of immunohistochemical staining, IFN-γ knockout mice, or anti-IFN-γ antibodies would help to provide a much clearer picture of the perhaps indirect role IFN-γ may play.

4.4.2.3 TGF-β

TGF-β is a multifunctional cytokine that is synthesised in a latent form covalently bound to a latency-associated peptide [283]. The presence of the latency-associated peptide protein renders the TGF-β biologically inactive, and acts to facilitate transit of TGF-β from the cell [259]. Signaling through TGF-β receptors requires exposure of the active site of the ligand through conformational change or through cleavage of the latency-associated peptide [259,283]. Both total (consisting of active and latent) and active TGF-β were measured in the BAL fluid from the FITC-treated mice and PBS controls over both acute and long-term time points. No significant differences were found in the levels of total TGF-β between treated and control mice over the first seven days after FITC or PBS instillation, and levels were generally below the limit of detection for the assay (Figure 3.19). This was also true of active TGF-β in these same samples with the exception of Day 2, at which detectable levels were measured in the BAL fluid of FITC-treated mice, and were found to be significantly higher than those of the PBS controls (Figure 3.20).

Long-term time points were assessed in Series 1 and 2 mice. In Series 1 mice, although there was some variation in levels, total TGF-β was not found at detectable levels in the BAL fluid, nor were there any significant differences between FITC-treated mice and PBS controls (Figure 4.18). Active TGF-β was present at detectable levels at six weeks after the first intratracheal instillation, and again at 14 weeks after the second instillation, and while significant differences were seen between the different time points, levels between the FITC- and PBS-treated mice were not significantly different, and therefore any changes could not be attributed to the FITC treatment (Figure 4.19). In Series 2 mice, as for Series 1 mice, there were

no significant differences in the levels of active or total TGF-β between the FITC-treated and PBS control mice (Figures 4.20, 4.21).

The above data suggest that TGF-β has only minimal involvement in the pathogenesis of FITC-induced pulmonary fibrosis, and possibly only in the acute stages, although TGF-β is thought to be responsible for repair rather than acute damage in bleomycin-induced pulmonary fibrosis [265]. Immunohistochemical staining of tissue sections from FITC-treated mice, however, showed a relative increase in extracellular TGF-β as compared to PBS controls. Tissue TGF-β is not quantifiable, and even if an increase did exist it may not be pathogenic. Such discrepancies, however, have been reported in the literature, and it has been suggested that BAL fluid cytokine levels may not represent tissue concentrations [429].

The gene coding for TGF-β is expressed by type II pneumocytes [276], and the detection of extracellular TGF-β by immunohistochemistry and collagen gene expression by *in situ* hybridisation are found in the same areas of fibrosis in the human lung, which suggests that TGF-β is directly involved in mesenchymal cell production of ECM [275,287]. However, the production of TGF-β by AMs in humans with fibrosis has been reported to be decreased, while BAL levels remained normal [282], and BAL cells from bleomycin-treated mice were reported to express decreased levels of TGF-β on Day 1 after treatment, which returned to only normal levels by Day 15 and on to Day 29 [236].

Overexpression of active TGF-β has been shown to induce severe and progressive pulmonary fibrosis in both the rat and in C57BL/6 mice [67,463]. Recently, Kolb *et al.* [464] compared the response of "fibrosis-resistant" BALB/c mice and "fibrosis-prone" C57BL/6 mice [465] to the overexpression of active TGF-β1 using adenoviral gene transfer. They reported that despite having higher levels of the transgene protein in the lung, the BALB/c mice developed significantly less fibrosis than the C57BL/6 mice in response to active TGF-β1, and that this difference seemed to be

downstream from TGF-β1. Several studies demonstrating strain differences in TGF-β expression upon stimulation have led to the hypothesis that the reduction in TGF-β upregulation in the lung tissue of BALB/c mice results in their inability to develop pulmonary fibrosis. The most relevant of these studies demonstrated an increase in TGF-β mRNA by bleomycin treatment in fibrosis-prone C57BL/6 mice but not in fibrosis-resistant BALB/c mice [270,465].

The results of Kolb *et al.* [464] and those presented in this thesis are discordant with this hypothesis, however. Pulmonary fibrosis induced by the surgical method of FITC instillation develops in both BALB/c and C57BL/6 mice, and is more severe in the BALB/c mice [244]. The work presented in this thesis has shown that the two dose nonsurgical method of FITC instillation also produced a severe, progressive pulmonary fibrosis that did not appear to be dependent on the increased production of TGF-β in the BAL fluid or possibly in the tissues.

The development of a TGF-β-independent model of pulmonary fibrosis could have important implications in the study of CFA, providing insight into new pathways involved in the pathogenesis of this disease. Indeed, recently Moore *et al.* [62] reported that the absence of CCR2 signaling confers protection from pulmonary fibrosis in mice given FITC by the surgical method. Although they postulate that alterations in TGF-β may contribute to the protection seen in the absence of CCR2, evidence to the contrary may lead to novel pathways in the disease pathogenesis, and ultimately, to novel treatments.

The absence of increased TGF-β levels in the BAL fluid of FITC-treated mice is only a preliminary finding, however, and requires more investigation. The assay used to detect TGF-β is intended for human samples, and although the manufacturer approved its use for murine samples (R&D, personal communication), it may lack sensitivity. Also, as discussed above, the BAL fluid cytokine levels may not represent tissue concentrations. Several methods have been developed to examine the role TGF-β plays in the pathogenesis of pulmonary fibrosis that could be applied to the FITC-induced model. Systemic administration of TGF-β neutralising

antibodies reduced the degree of collagen accumulation in both a model of glomerulonephritis and a bleomycin model of pulmonary fibrosis [273,274]. More recently, intranasal administration of an adenoviral vector carrying the gene for decorin, a ubiquitous proteoglycan known to be an important negative regulator of TGF-β [466,467], effectively blocked the fibrogenic response to bleomycin in mice [429].

4.4.3 Evaluation of the Modified FITC Model of Pulmonary Fibrosis

The fibrosis measured in the FITC-treated mice over a total of five months, and with two intratracheal doses of FITC, appeared chronic and progressive, giving this model an advantage over other rodent models, such as bleomycin, which cause a transient fibrosis after acute injury that kills the animals after a short period of time or leads to complete resolution. As the FITC-treated animals appeared healthy even after five months, this model could be extended in order to draw further parallels with the human disease. It would also be interesting to see if these animals eventually developed adenocarcinomas, as did nine out of 15 BALB/c mice in the original model [243] at 18 months (unpublished data). The chronic inflammation remained evident until 14 weeks after the second dose of FITC, lending support to the hypothesis that persistent inflammation plays a vital role in the development of pulmonary fibrosis.

Measurement of BAL cytokines suggests that this model may resemble a Th2-like immune response. As discussed in Chapter 1, it has been suggested that an imbalance between Th1 and Th2 cytokine responses may lead to abnormal responses to injury, and may thus be involved in the pathogenesis of CFA [6]. Expression of the Th2 cytokines IL-4 and IL-5 appears to be increased with a concomitant reduction in expression of the Th1 cytokine IFN-γ [74,100,101]. As IFN-γ expression was very low in the FITC-treated mice (although also in the controls), measurement of IL-4 and IL-5 in the FITC model could be very useful, particularly if

increased expression could be shown in only the FITC-treated mice. Based on the evidence presented in this thesis, the FITC model of pulmonary fibrosis could possibly be TGF-β-independent, opening up unique avenues for investigation into CFA pathogenesis. However as local microenvironments in the tissue are not reflected in the BAL fluid, which is diluted as part of the collection procedure, cytokine levels may be significantly higher in the tissues and thus require further investigation, ideally through knockout mice or the administration of anticytokine antibodies. B lymphocyte aggregates containing MHC class II^+ cells suggest that antigen presentation may be occurring, leading to a local humoral immune response that may be an important factor in the pathogenesis of FITC-induced pulmonary fibrosis.

Problems with this model of murine pulmonary fibrosis are still evident, however. At the long-term time points, the nonsurgical intratracheal instillation of FITC failed in approximately 25% of the animals (Table 4.1), and of those that did receive the FITC dose, not all had the same amount deposited in the lungs, and not all developed pulmonary fibrosis to the same degree. The success rate, in terms of actual FITC deposition, appeared to be higher in animals assessed at the acute time points (Table 3.1), however as discussed below, this could be due to some animals being able to clear the FITC more quickly, particularly if they received a smaller dose.

The variations in dose and disease severity may be caused by several factors. First, the investigator is not able to see exactly where the blunted needle delivers the dose. Indeed, upon dissection FITC has occasionally been found in the trachea walls. Second, the weights of the mice can vary, and since only a standard dose of anaesthetic was given, some of the mice may have recovered the cough reflex and expelled the FITC in this way. Again occasionally, FITC was seen around the mouths of some of the mice. Finally, FITC is insoluble in PBS and remains fairly particulate in solution. This can be beneficial as it ensures a patchy deposition, and may even be essential, as Christensen *et al.* [244] found that dose reductions below the solubility threshold resulted in no fibrosis. However it can also mean that some mice get a much higher dose than others if the solution is not mixed thoroughly.

Also worth considering, however, is the role host defense may play in the pathogenesis of FITC-induced pulmonary fibrosis. Mice for this project were pathogen-free upon arrival, and usually received the first FITC or PBS dose within days. Some mice did not, however, and since none of the mice were isolated in any way, it is possible that some may have contracted an infection before the intratracheal instillation that could have had an effect on their response to the FITC, or even their ability to clear the FITC deposits. Ideally, the mice would have been kept in isolator cages for the duration of the experiment, and further work could take this into consideration. This could be an explanation as to why some mice developed pulmonary fibrosis on exposure to FITC while others did not. However, it would also be useful to investigate the effects an underlying infection, which may induce a Th1- or a Th2-type response, may have on the response of the mice to FITC. Would an underlying Th2-type infection predispose mice to the Th2-type response associated with pulmonary fibrosis? Conversely, would an underlying infection with a Th1-type response confer some degree of protection from FITC-induced pulmonary fibrosis? These questions would ideally be addressed when continuing this work.

The use of other substances in which FITC is soluble, such as DMSO, were examined while investigating the original model, however they resulted in a very high rate of death. Christensen *et al.* [244], who extended the surgical FITC method, used sonication to disperse the particulate nature of FITC, although they then had to reduce the dose by 50%. Sonication of the FITC at lower doses could be further investigated in this two-dose model.

Standardisation of the dose of FITC is essential for this model of pulmonary fibrosis, however the consistent finding that PBS-treated mice do not develop any lung pathology is the most conclusive evidence of the effectiveness of FITC as a pulmonary fibrosis-inducing agent. Once standardised, this model has great potential for studying novel pathways in the pathogenesis of pulmonary fibrosis, and further investigation should be pursued in the anticipation of novel and effective treatments for patients with CFA.

CHAPTER 5

Isolation of Antigen Presenting Cells from Murine Lungs

5.1 Introduction: Methods for Isolation of Lung APCs

In normal lung, DCs represent less than 1% of all lung cells and both the isolation and purification of enriched populations require multiple steps [137,158]. Lung DCs have no specific differentiation markers, and thus cannot be isolated by direct immunoselection [137]. However, as discussed in Chapter 1, their various cell surface markers, including products encoded by the MHC class I and II genes, costimulatory molecules, adhesion molecules, and FcRs, can be used to differentiate DCs from other cell types, and to characterise their phenotype and function [137].

While methods for the isolation of DCs from other tissues were in place in the laboratory at the outset of this project, the methodology of DC isolation from mouse lung had not been developed. Thus, in order to study the function of murine lung-derived DCs, it was necessary to optimise methods for obtaining enriched populations of these cells.

5.1.1 Alveolar Macrophage Isolation

The isolation of AMs by BAL is a fairly standard and straightforward technique. Macrophages obtained by lavage include resident AMs and intraluminal macrophages (those that reside within the lumen of the bronchi and bronchioles). Although a distinction between these two cell populations cannot be made, in rats and mice the typical procedure of placing a catheter in the trachea results in obtaining a majority of AMs [184].

The general outline of the BAL technique for mice involves cannulating the trachea, filling the lungs with fluid, and then withdrawing the fluid. This is repeated several times and the lavage fluid is pooled and centrifuged. The technique is usually optimised by adjusting the volume, and/or temperature, of fluid used to lavage the lungs, the lavage fluid itself (i.e. saline or tissue culture medium), and the number of

lavages, and so can differ between investigators [185]. Yields from the BAL of normal mice can range from 0.06 – 1.36 x 10^6 AMs, and typically more than 95% of the BAL cells are AMs [179,468,469].

5.1.2 Dendritic Cell Isolation

"*...as DC are only a trace population in all tissues their preparation in sufficient numbers is extremely tedious.*" [470]

No one technique to isolate DCs from whole lung results in a completely pure population and thus a combination of techniques is used. The isolation procedure typically has two stages. The purpose of the first stage is to obtain a single-cell suspension of lung cells, and the methods involved are, for the most part, consistent among groups who isolate these cells. The second stage, in which a DC-enriched population is sought, varies greatly among groups, and involves any number of techniques that exploit the various properties of contaminating cells; for instance, the phagocytic or autofluorescent properties of the main contaminant, lung interstitial macrophages.

5.1.2.1 DC Isolation - Stage 1: Single Lung Cell Suspension

The first stage of the isolation procedure requires BAL, perfusion of the pulmonary vasculature, enzymatic digestion of the tissue, and density fractionation [155,471,472]. Perfusion is required to remove peripheral blood cells from the pulmonary vasculature. BAL removes a large proportion of resident AMs which, like DCs, express the cell surface molecule CD11c [137,157], and have been shown to suppress DC-initiated T cell proliferation [182,194,473-475]. Enzymatic digestion of the lung tissue to extract viable interstitial lung cells is most often accomplished with collagenase, although there are a number of different types of this enzyme

available that vary in their effectiveness [155]. DNase is usually included in the enzyme solution to minimize cell loss due to DNA-induced clumping. Proteolytic enzymes such as elastase and hyaluronidase are not recommended as they can damage structures on the cell surface, such as FcRs [471]. Density fractionation separates pulmonary mononuclear cells from the dissociated cells, resulting in low density DC- and interstitial macrophage-enriched lung cells [137]. Table 5.1 compares the methods used by various groups in the first stage of the isolation procedure.

To further enrich the DC population and eliminate the interstitial macrophages, many groups include a short adherence step to separate nonadherent lymphocytes from adherent cells, and subsequently an overnight adherence step to separate the loosely adherent cells from the firmly adherent macrophages [154,183]. The adherence step, however, has two disadvantages. First, DC function and phenotype may be affected significantly by either the time in overnight culture, which has been shown to down-regulate skin DC antigen-processing capacity [476,477] and increase accessory molecule expression [478], or as a result of interacting with other cells from the pulmonary interstitium which are still present. For example, interstitial macrophages, which continue to contaminate the loosely adherent fraction, have been shown to enhance the ability of DCs to present antigen [154,479]. Second, the overnight enrichment requires a very high number of cells initially, as many are lost due to nonadherence in the first step, or firmer adherence after the overnight culture.

Reference	Tissue Source	BAL	Perfusion	Enzyme Digestion	Density Fractionation	DC yield
Armstrong *et al.*, 1994 [479]	rat whole lung	yes	yes	Collagenase/DNase I	yes	$1x10^5$ per rat
Masten & Lipscomb, 1997 [137]	murine whole lung	yes	yes	Collagenase/DNase I	yes	$2.5x10^3$ per mouse
Gong *et al.*, 1994 [183]	rat whole lung	yes	yes	Collagenase/DNase I	yes	$1x10^5$ per 10 rats
Holt *et al.*, 1985 [471]	rat trachea / lung tissue	yes	yes	Collagenase A	yes (5-step)	$8\text{-}14x10^7$ cells /gram lung tissue
Vermaelen *et al.*, 2001 [138]	murine whole lung	yes	yes	Collagenase/DNase I	no	*not reported*
Gonzalez-Juarrero & Orme, 2001 [158]	murine whole lung	no	yes	Collagenase XI / DNase IV	no	*not reported*

Table 5.1 Comparison of published methods for the first stage of isolation of DCs from rodent lung.

5.1.2.2 DC Isolation - Stage 2: Enrichment for DCs

In the rat, Gong *et al.* [151,183] used a novel microdissection method to separate the lung parenchyma from the airway epithelium in order to study separately airway epithelial DCs and interstitial lung DCs. After perfusing the pulmonary vasculature, the lungs were inflated with a solution containing agarose, dispase, DNase and FCS. The lungs and attached trachea were removed and placed in ice-cold PBS to solidify the agarose. This allowed for the lung parenchyma to be dissected from the tracheobronchial tree. The lung tissue was then cut into pieces and digested with collagenase and DNase I, and the resulting cell suspension subjected to density fractionation.

The cells were then separated into FcR^+ and FcR^- cells by rosetting with antibody-coated sheep erythrocytes. The FcR^- cells were incubated overnight in GM-CSF to improve survival, and with Dynabeads that would be taken up by any remaining phagocytic cells. The Dynabead-containing phagocytic cells were subsequently removed with a magnetic particle concentrator, and the nonphagocytic cells spun over a metrizamide gradient to remove B and natural killer cells. Finally, residual FcR^+ cells were removed by immunopanning for MHC class II^+ cells. This technique yielded a population that was >98% pure for interstitial lung DCs, however the final cell yield was only $1x10^5$ DC from 10 rats.

Holt *et al.* [141,471] also described a method to extract DCs from rat lungs, which involved perfusion, repeated endobronchial lavage, and removal of the lungs. The lungs were then sliced mechanically to 500 μm, and digested in collagenase/DNase for 90 minutes. Rapid filtration through cotton wool was followed by a five-step discontinuous Percoll gradient, plastic adherence, and finally rosetting, to remove the majority of FcR^+ cells. Although absolute numbers were not indicated, their yield was approximately 15% MHC class II^+ cells per gram of rat lung, from this final cell suspension.

Armstrong *et al.* [479] isolated lung DCs from the rat as well, finely mincing the lung tissue and digesting in collagenase/DNase I. Interstitial cells were released by vigorous stirring of the mixture at 37°C for 90 minutes, followed by nylon wool filtration and density fractionation. Phagocytic cells were removed by magnetic separation following incubation with carbonyl iron particles, and the nonphagocytic pulmonary DCs were isolated by flow cytometric cell sorting based on MHC class II expression. Their final cell yield was $1x10^5$ DCs per rat.

Using murine lungs, Lipscomb and colleagues [137,155] described a multistep enrichment protocol that gave a 92-99% pure population. Following density fractionation, lung cells underwent a short adherence step to remove non-adherent B cells, and then an overnight adherence step to remove firmly adherent macrophages from the loosely adherent (LAd) cells.

Masten and Lipscomb [137] (and personal communication) report that DCs represent 11±3% of the total LAd population. LAd cells were next incubated with FITC-latex beads (to identify and eliminate phagocytic cells), and FcRs were blocked by preincubation with anti-CD16/CD32. The cells were also stained with anti-I-A^d/I-E^d antibodies (to identify MHC class II-expressing cells) and anti-CD45R/B220 antibodies (to identify B cells). Lung DCs were then obtained in high purity by flow cytometry, sorting for FITC-bead$^-$ (nonphagocytic), B220$^-$, MHC class II-expressing cells. This method yielded $2.5x10^3$ lung DCs per mouse.

More recently, Vermaelen *et al.* [138] described a different method for murine lung DC isolation. After perfusing, mincing, enzymatic digestion and red blood cell lysis, they labelled their lung cells with a variety of antibodies and used cell sorting to purify the lung DCs, among other populations. They selected for CD11c$^+$/low autofluorescence, and found that >90% of these cells were also MHC class II$^+$. As they had manipulated these cells very little before analysing, they found that the DCs showed an immature phenotype, but overnight culture of these DCs in GM-CSF resulted in a more mature phenotype, with upregulation of CD40, MHC class II, CD86, ICAM-1.

Gonzalez-Juarrero and Orme [158] also described a method using mouse lungs. They did not perform a BAL, but perfused directly. Lungs were minced and enzyme digested, then subjected to red cell lysis treatment. $CD11c^+$ cells were then selected from the single cell suspension after incubation with CD11c MACS microbeads, giving a purity of 80-90% $CD11c^+$ cells. Macrophages were removed by overnight plastic adherence. Although cell numbers were not reported, they found that lung DCs constituted <1% of the total number of cells in the lung.

As discussed in Chapter 1, lung DCs show considerable phenotypic heterogeneity, and each of the groups whose methods are described above obtained one or more populations of lung DCs showing different cell surface phenotypes.

5.1.3 Aims of Chapter

The aims of this chapter are:

- To explain the choice of methods of isolation used in this body of work
- To describe the method used for the isolation of BAL cells
- To describe the development of the isolation method for DCs used throughout this thesis
- To discuss the phenotyping of the two cell populations

5.2 Choice of Method for APC Isolations

In order to study the biology of DCs in the lung it was necessary to develop a protocol that would combine maximum cell yield with minimum disruption of function. As only one investigator performed the perfusions and isolations, there also had to be low numbers of mice in the experimental groups to avoid excessive processing time and consequent cell death.

It was decided that the first stage of the isolation should follow the standard protocol of BAL, perfusion, enzymatic digestion and gradient centrifugation, although with a unique modification. For the second stage, various methods used by other groups were evaluated. Plastic adherence to remove contaminating macrophages was attempted several times, however since the starting number of cells was low, the final yield from this method was extremely low. The agarose/rosetting/immunopanning methods of Gong *et al.* [151] were not attempted as their cell yield ($1x10^5$ DCs per 10 rats) indicated that it was not a practical method for a small number of mice. The methods of Holt *et al.* [471] used similar multiple steps on rat lungs which, again, were not deemed practical in this case. Cell sorting to select for appropriately stained lung DCs, as used by Armstrong *et al.* [479] was the most attractive method, however this technology was not available. Finally, the methods described by Vermaelen *et al.* [138] and Gonzalez-Juarrero and Orme [158] were not published at the time this project was being developed.

Thus, the method described hereafter was developed to obtain a minimally manipulated population of cells that contained APCs from the lung, including DCs, which could be used to examine their function in a murine model of pulmonary fibrosis. The method is adapted from a method described for the isolation of Clara cells from the mouse lung [480].

5.3 Development of Method for Lung APC Isolation

5.3.1 Lung Perfusion

Female BALB/c mice, between six and eight weeks old, were killed by intraperitoneal injection of 0.5 ml Sagatal. The mouse was laid on its back, and the ventral surface skin removed. A midline incision was made to enter the peritoneal cavity, the folds of the peritoneum were lifted back, the gastrointestinal tract displaced to the right, and the major dorsal blood vessels were cut to allow drainage of blood. The diaphragm was punctured just below the xiphisternum and opened, and the rib cage removed to expose the lungs. The trachea was separated from the covering muscle and underlying oesophagus. Once exposed, forceps were pushed under and left in place to extend the trachea. A scalpel was used to create a small hole on the anterior surface near the top of the trachea, between the rings of cartilage. A 0.96 mm cannula (Portex, Ltd., Hythe, Kent, UK) attached to a 2 ml syringe was inserted into the trachea, stopping approximately 2/3 of the way down, well away from the main bronchi. The cannula was secured in place with surgical silk.

The apex of the heart was gripped with a haemostat and the tip cut off with scissors, exposing the right ventricle. A second cannula with a diameter of 1.7 mm (SLS, Ltd., Coatbridge, Lanarkshire, Scotland), attached to a gravity feed of sterile 0.15M saline, was inserted into the left ventricle. The flow of saline, which was maintained at a steady drip so as not to overinflate the heart, caused the right atrium to swell, and subsequently the right atrium was cut to allow the fluid to exit. Using the syringe attached to the intratracheal cannula, the lungs were artificially ventilated 3 or 4 times with approximately 0.8 – 1.2 ml of air, until they were free of blood and appeared completely white. Figure 5.1 illustrates the dissection and perfusion techniques.

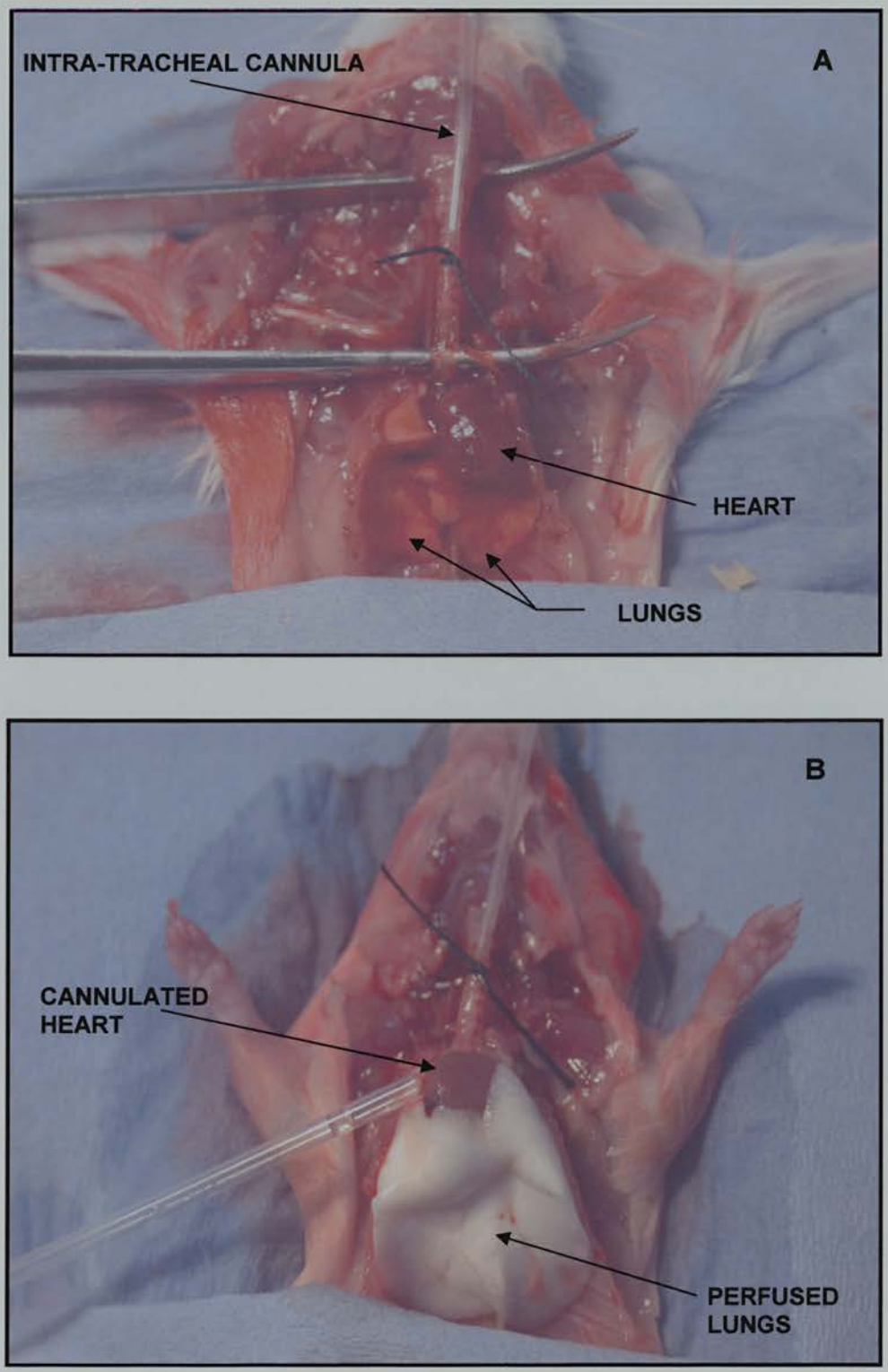

Figure 5.1 Perfusion of murine lungs. (A) Uninflated murine lungs cannulated *in situ*, before perfusion. (B) After perfusion, showing partial inflation of lungs, and complete clearing of blood.

5.3.2 Collection of BAL Fluid and Cells

Collection of BAL fluid was typically performed after the perfusion, however it was found that collecting BAL fluid prior to perfusing made no difference to the quantity or content.

While still *in situ*, the lungs were lavaged with two washes of 0.8 ml and 0.6 ml ice cold PBS, which were collected in a sterile Eppendorf tube and stored on ice. BAL fluid was then spun at 300g for seven minutes. The supernatant volume was estimated and recorded, pipetted into a new Eppendorf, and spun again at 1000g for five minutes to remove all trace cellular debris and contaminants. This second supernatant was then collected, aliquoted and stored at $-70^{\circ}C$. Recovered BAL fluid volumes were typically between 1 - 1.3 ml. The cells remaining from the first spin were pooled and counted, and used for cytospins or as APCs in T cell proliferation assays. BAL cell counts from normal BALB/c mice averaged $1.41 \pm 0.15 \times 10^5$ cells/mouse (n=20). For cytospins, BAL cells were resuspended at 1×10^6/ml in PBS or medium containing 10% FCS, and cytospins were prepared as per the protocol described in section 2.3. BAL cells destined for T cell proliferation assays were resuspended in complete RPMI and plated onto 96 well round-bottomed tissue culture plates and cultured overnight in complete RPMI. T cells were added the following day, as per the protocol described in section 2.1.2.1.

5.3.3 Lung Inflation/Enzymatic Digestion

After perfusing the pulmonary vasculature to remove peripheral blood cells, and collection of BAL fluid, the lungs were carefully excised, and those that were to be used for immunohistochemistry were immediately inflated with 1.2 ml 4% formalin and immersed in 4% formalin for 24 hours before processing. Lungs to be used for cell isolation were placed in RPMI prior to further processing. A maximum of four mice per treatment or control group could be processed as larger numbers required more time, and thus leading to increased cell death, and lower cell yields.

Several different enzymes, enzyme concentrations and combinations, and digestion times were investigated to maximise cell yield in the subsequent steps (Figure 5.2). The initial protocol involved incubating minced lung in a warmed (37°C) RPMI solution containing 0.4 mg/ml collagenase type IV for 90 minutes. Cell yields were quite low however, averaging $2.7 \pm 0.5 \times 10^5$ cells/mouse (n=8).

As lung tissue is extremely difficult to digest, a solution of 2.5 mg/ml trypsin was substituted for the collagenase IV. The trypsin solution was also used to inflate the lungs before mincing, thus maximizing the enzyme's contact with as much of the lung as possible. In this way, it was also possible, and necessary, to decrease the digestion time from 90 minutes to 45 minutes. These changes increased cell yields 63%, to $3.4 \pm 0.3 \times 10^5$ per mouse (n=17).

As cell yields were still very low, it was decided to use collagenase IV (at 0.7 mg/ml) instead of the trypsin in the digestion solution. Trypsin is a very strong proteolytic enzyme, and as inflation of the lungs with enzyme made it possible to digest the lung tissue more thoroughly, trypsin's action was perhaps too harsh, particularly considering the cells were to be used in functional assays. Collagenase IV is routinely used to digest lung tissue as it has low tryptic activity and thus maintains receptor integrity. This modification of the method increased cell yields to $4.0 \pm 0.4 \times 10^5$ per mouse (n=13).

Cell numbers were still limited, however, as a maximum of four mice per treatment group could be used. Dispase is a mixture of neutral proteases that cleave at the level of the basement membrane, and is recommended for the gentle dissociation of animal tissues to release individual cells. In combination with the collagenase IV, and at a concentration of 2 μg/ml, it was found that dispase increased cell yields significantly to $6.6 \pm 0.6 \times 10^5$ per mouse (n=14), as compared to all previous combinations.

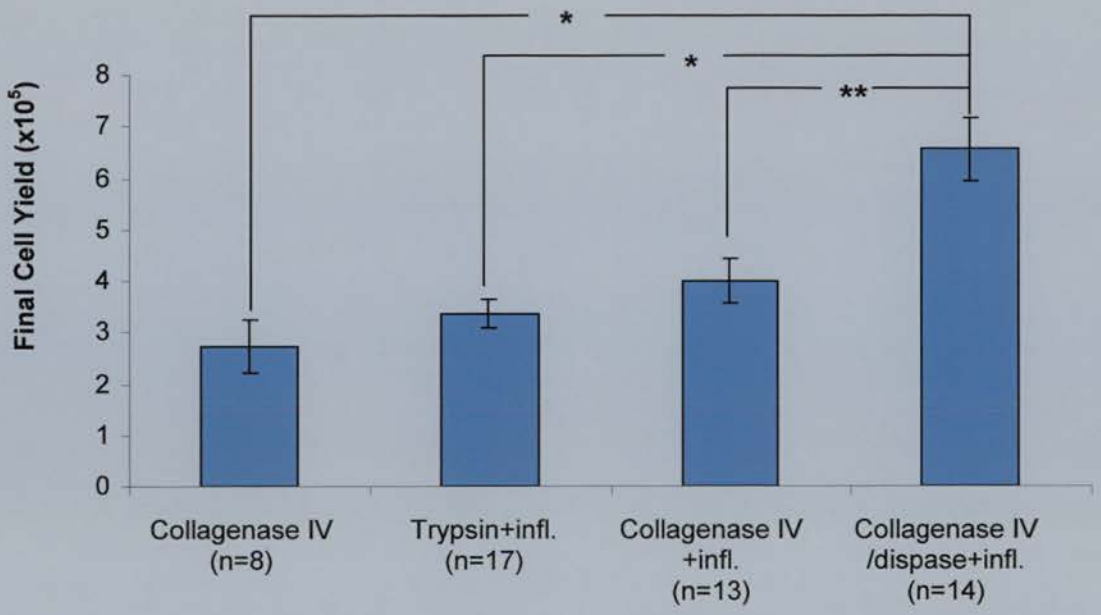

Figure 5.2 Comparison of methods of enzymatic digestion of murine lung tissue used in the isolation of DCs. Murine lungs were perfused and lavaged before removal. Infl. = inflation of lungs with enzyme solution. Each experiment (n) represents the final cell count from between 3-6 mice. Data are presented as mean±SEM of each experiment.
*p<0.001, **p<0.01, as determined by one-way ANOVA with Tukey-Kramer multi-comparison tests

Although cell yields were improved considerably, phenotyping of these cells indicated that purity was very low, with the APCs being only a minor subpopulation. In an attempt to improve cell purity, the enzyme solution was changed again to one containing 0.7 mg/ml collagenase A (Roche Diagnostics GmbH, Mannheim, Germany) and 30 μg/ml type IV bovine pancreatic DNase I, as recommended by B.J. Masten (personal communication) of the University of Albuquerque, New Mexico, USA whose group routinely isolates highly purified populations of lung DCs [137]. Although the final cell yields dropped to $3.2 \pm 0.2 \times 10^5$ per mouse (n=38), the purity had greatly improved, with the APCs representing the majority of the cells in the population.

Therefore, the final protocol called for the lungs to be inflated with the warmed enzyme solution (collagenase A/DNase I) and then minced and incubated in more warmed enzyme solution in a tissue culture dish for 45 minutes at 37°C. Tissue from

no more than 2 sets of lungs was combined at any one time as pooling more resulted in loss of cells.

5.3.4 Isolation of CD11c$^+$-Enriched APCs from Digested Lung Tissue

The digested lung tissue was coarsely strained by passing it through a metal strainer using a syringe plunger, and then finely strained through a 40 μm filter (BD Biosciences, Heidelberg, Germany) directly into a 50 ml polypropylene tube. The cells were washed twice in incomplete RPMI that was supplemented with 10% FCS, 2 mM L-glutamine, 100 U/ml penicillin and 100 μg/ml streptomycin, but no β-2-mercaptoethanol. This additive, necessary for optimal murine lymphocyte proliferation, was added to the medium at $5x10^{-5}$M just before culture as it inhibits the enzymatic action of collagenase (as stated in Roche data sheet). The anti-protease action of FCS was not found to significantly reduce the action of the collagenase.

Percoll gradients were prepared by mixing 4 ml PBS with 2.675 ml Percoll (Amersham Pharmacia Biotech, Little Chalfont, Buckinghamshire, UK) and filter sterilising this mixture into one 50 ml Falcon tube. One gradient was prepared for each pair of lungs. Cells from each set of two lungs were resuspended after the final wash in 10 ml incomplete RPMI, and 5 ml of this cell suspension was layered onto a gradient. The gradients were spun for 30 minutes at room temperature, at 1000g. The upper layers were then removed leaving a pellet enriched for mononuclear cells, and the contents from no more than two gradients were pooled.

The cells were washed once and resuspended in 400 μl ice cold MACS buffer and 100 μl CD11c microbeads (Miltenyi Bitoec) as per the manufacturer's protocol. The cells were incubated for 15 minutes at 4-6°C, then washed in 10-20X the volume of MACS buffer. As the cell count at this stage was consistently less than 10^7 per tube, the cells in each tube, derived from two pairs of lungs, were resuspended in 500 μl

MACS buffer and run over a single MACS column primed with 500 µl MACS buffer. As per the manufacturer's protocol, the columns were then washed three times with 500 µl MACS buffer, and each column was eluted with 1 ml complete RPMI, and the cells counted.

This method consistently yielded between $1x10^5$ - $5x10^5$ $CD11c^+$-enriched APCs per mouse, which showed >99% viability as determined by trypan blue dye exclusion. Figure 5.3 illustrates the final isolation protocol.

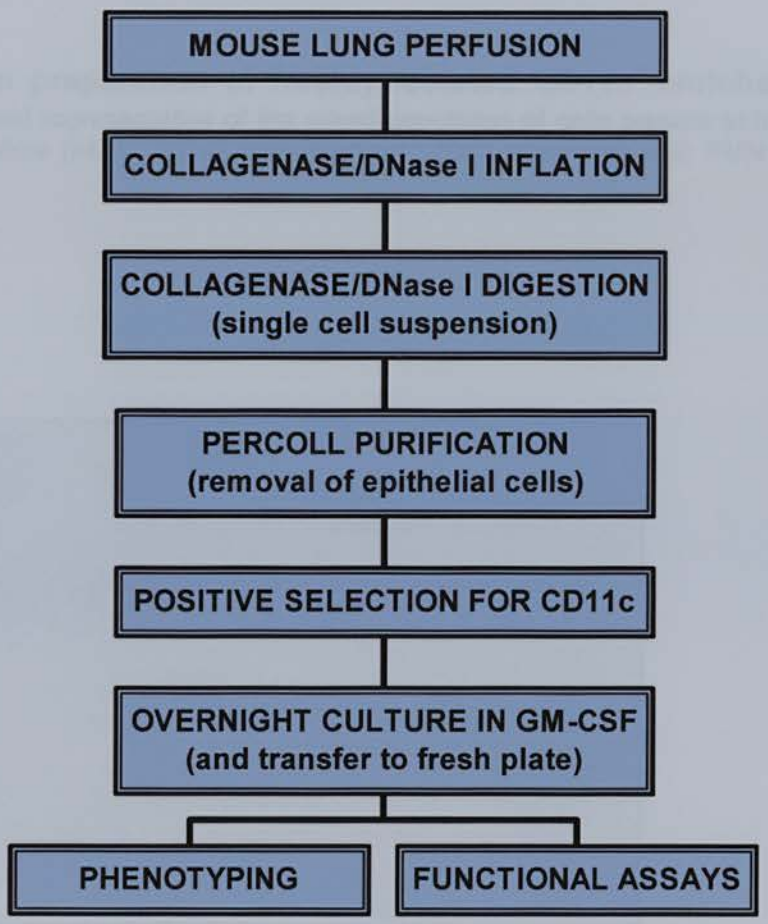

Figure 5.3 Final protocol for the isolation of $CD11c^+$-enriched APCs from murine lungs.

5.4 Phenotypic Characterisation of CD11c$^+$-Enriched DCs and BAL Cells

Cell surface marker expression on CD11c$^+$-enriched DCs and BAL cells was characterised by flow cytometry using the monoclonal antibodies detailed in Table 2.1 following the protocol described in section 2.4. Cytospin preparations were made following the protocol described in section 2.2.

5.4.1 Freshly Isolated Cells

Freshly isolated cells from both the BAL and the lung tissue were examined only by microscopy as they were not used in any functional analyses. Figure 5.4 shows a typical field from a cytospin preparation of pooled, freshly isolated CD11c$^+$-enriched cells from the lungs of four wild-type BALB/c mice. The isolated population was mixed, and was comprised of, on average, 44±8% mononuclear cells, 29±9% granulocytes, and 27±7% lymphocytes (n=13). Also present were the occasional epithelial cell and red blood cell.

Figure 5.4 shows a typical field from a cytospin preparation of pooled, freshly isolated BAL cells from the lungs of four wild-type BALB/c mice. The isolated population showed 98 ± 1% (n=11) mononuclear cells, with the remaining cells being PMNs, and rarely, lymphocytes. Many of the cells showed dendritic-like processes similar to those seen on the lung DCs (Figure 5.4).

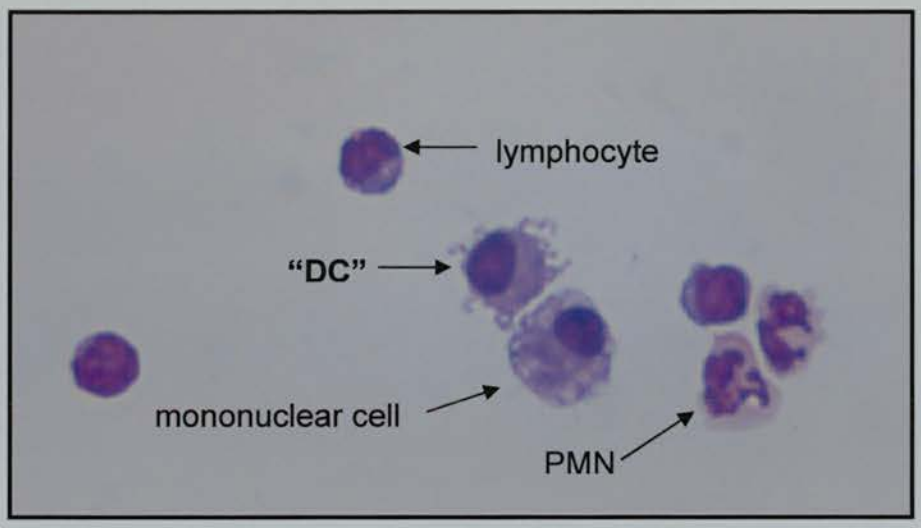

Figure 5.4 Cytospin preparation of freshly isolated CD11c^{+}-enriched lung cells. A typical field representative of the mixed population of cells present at the end of the isolation procedure (x400 original magnification). "DC" = dendritic cell; PMN = polymorphonuclear cell.

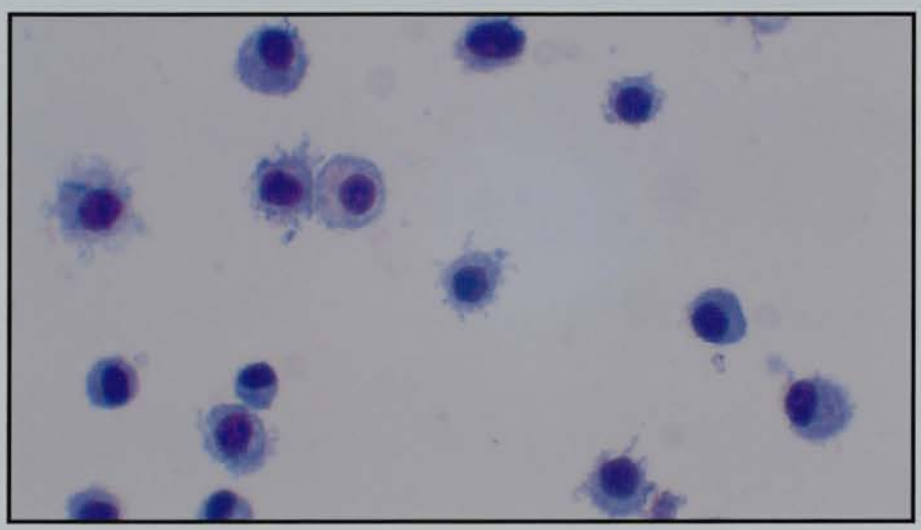

Figure 5.5 Cytospin preparation of freshly isolated mouse BAL cells. A typical field representative of the homogenous population of cells in the BAL fluid of normal BALB/c mice (x400 original magnification).

5.4.2 Cultured Cells

All cells used for functional analyses were cultured overnight in 96-well plates.

5.4.2.1 BAL Cells

BAL cells were prepared as described in section 5.3.2. Figure 5.6 shows a cytospin preparation of BAL cells after overnight culture in complete medium. The population consists of primarily large mononuclear cells, with fewer cells showing the dendritic-like processes. As with the freshly isolated BAL cells, the population was comprised of 98% mononuclear cells.

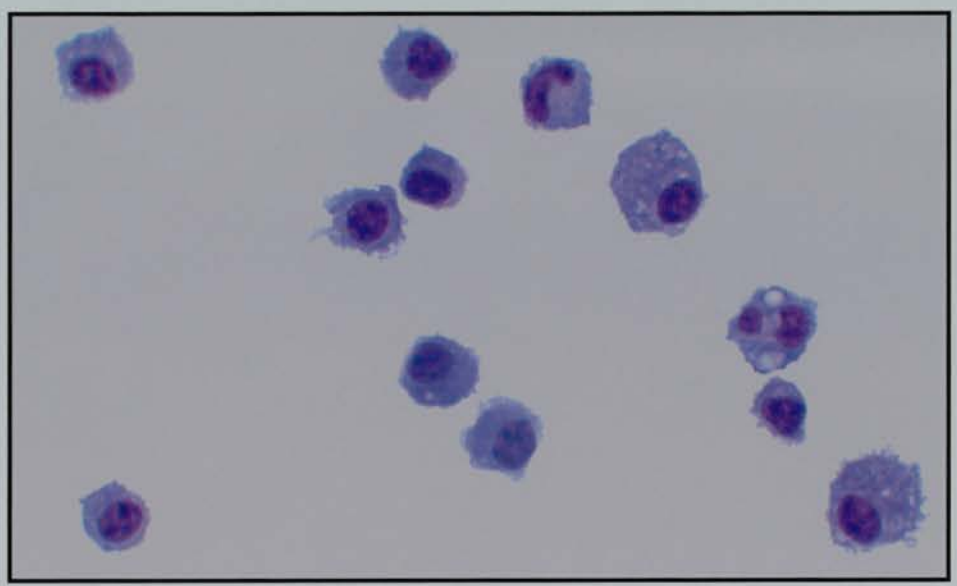

Figure 5.6 Cytospin preparation of BAL cells cultured overnight in medium. A typical field, at x400 original magnification.

BAL cells were also stained for flow cytometric analysis, as described in section 2.4. In order to distinguish live from dead cells, TO-PRO-3 (TP3) (Molecular Probes, Inc., Eugene, Oregon, USA) staining was used. The TP3 fluorophore is a cyanine nucleic acid stain that is impermeable to living cells, but intercalates with the DNA of dead/dying cells. It is almost nonfluorescent unless bound to DNA or RNA. Figure 5.7(A) shows the dot plot histogram of TP3 (in FL4) vs. forward scatter (fs) of these cells. Back-gating on the whole unstained population revealed where the live cells lay. Figure 5.7(B) shows the dot plot histogram of forward scatter (fs) vs. ss of the whole, unstained population, with the gate R1 surrounding the live cells, comprising 39% of the total population, which was subsequently analysed.

The BAL cells were stained for CD11c, MHC class II, CD80, CD86, ICAM-1, CD11b, CD40. Antibodies to detect contaminating B cells (CD19) and T cells (CD3) were also included. Figure 5.8 shows the corresponding single-stain histograms. After overnight culture in medium alone, the BAL cells were 73 ± 6% $CD11c^+$, 16 ± 4% MHC class II^+, 61 ± 8% $CD80^+$, 22 ± 3% $CD86^+$, 91 ± 2% ICAM-1^+, 47 ± 6% $CD11b^+$, and 34.5 ± 8% $CD40^+$ (n=4). Contaminating T and B cells were negligible (1.0 ± 0.3% and 0.8 ± 0.1%, respectively).

When BAL cells were double stained for both CD11c and MHC class II (Figure 5.9), the histogram showed a population in which the majority of cells (87.6%) were highly $CD11c^+$, and expressed mid-range MHC class II. These findings are consistent with murine BAL macrophages, which have been reported to highly express CD11c, but only express low levels of MHC class II [131,190].

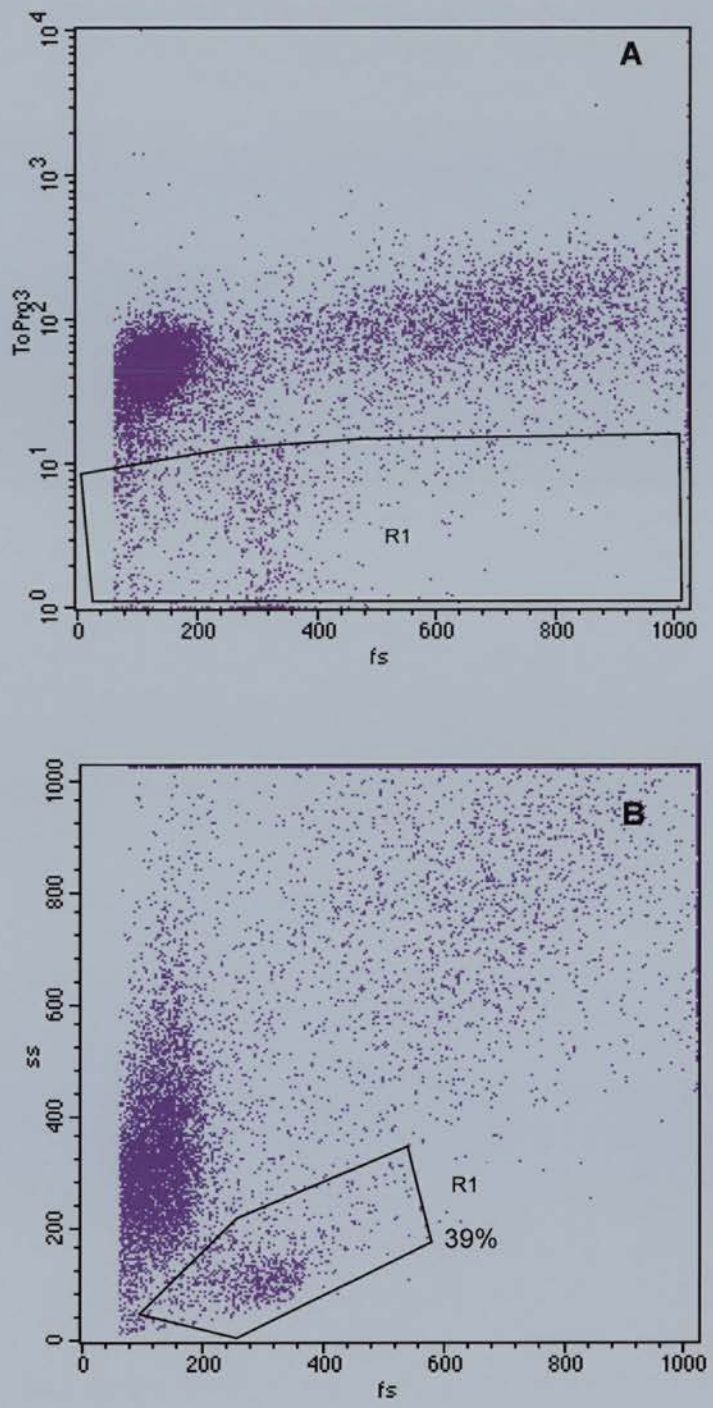

Figure 5.7 Dot plot representations of typical BAL cell preparation. (A) Dot plot of BAL cell population stained with TP3 showing fluorescence versus forward scatter. Gate R1 surrounds the live cell population. (B) Light scatter plot of whole, unstained BAL population. Gate R1, obtained by back gating from plot A, surrounds the live cell population.

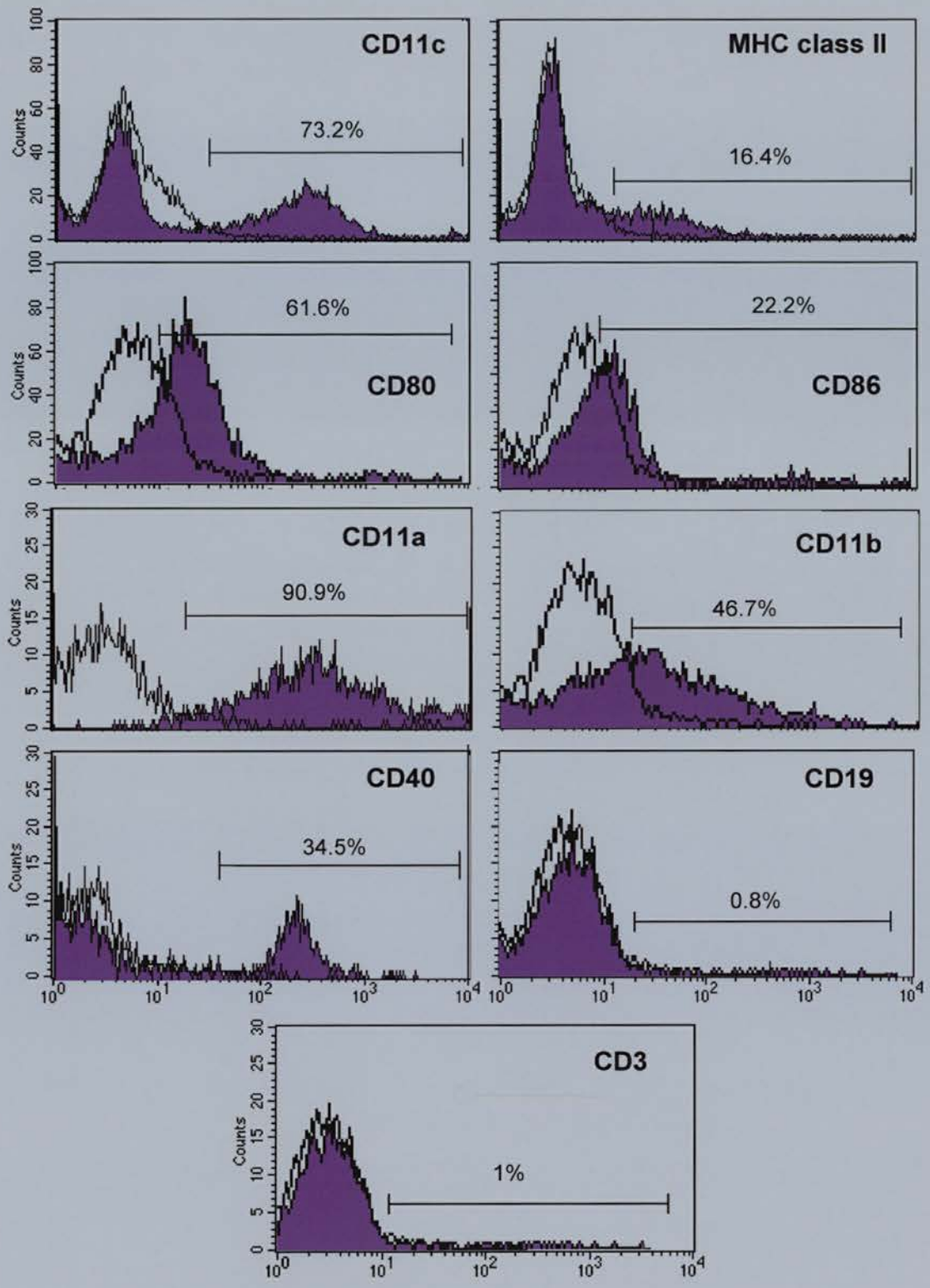

Figure 5.8 Cell surface phenotype of murine BAL cells. Flow cytometry histograms showing live BAL cells, which were isolated as described above and stained for various cell surface markers. Open histograms represent isotype-matched control monoclonal antibodies. The numbers shown on each histogram represent the percent positive cells relative to the isotype control.

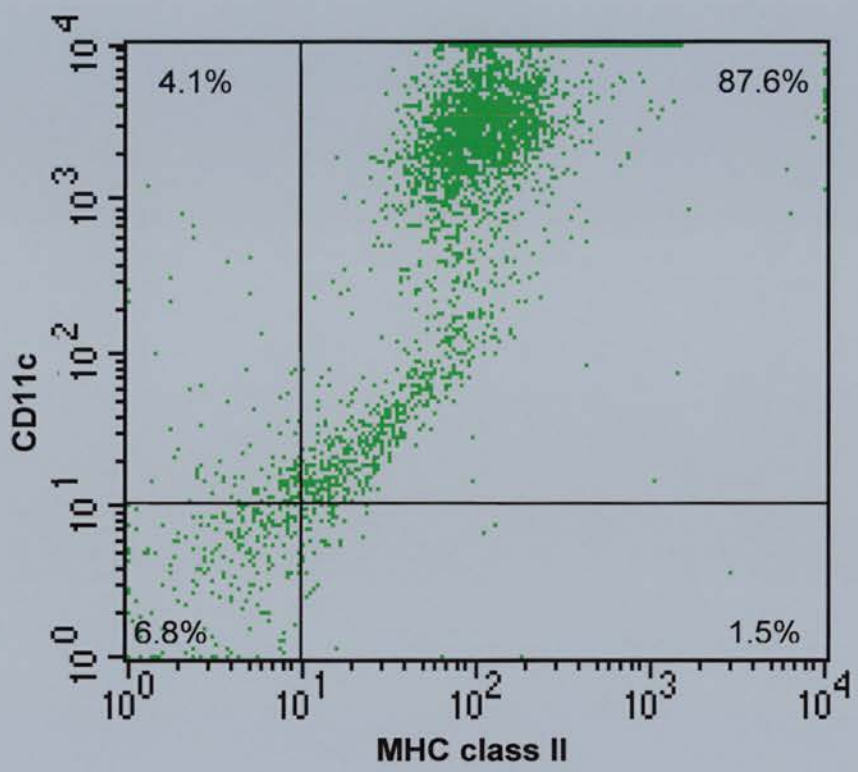

Figure 5.9 Murine BAL cells stain for both CD11c and MHC class II surface markers. BAL cells were stained with both CD11c and MHC class II antibodies and assessed by flow cytometry. Percentages of cells in each quadrant of the dot plot are shown.

5.4.2.2 *CD11c$^+$-Enriched Lung Cells*

CD11c$^+$-enriched lung cells were prepared as described in section 5.3.3. Figure 5.10 shows a cytospin preparation of these cells after overnight culture in complete medium supplemented with 20 ng/ml recombinant GM-CSF (R&D Biosystems). Although the population was still a mixed one, there were a higher proportion of mononuclear cells, including those with dendritic-like processes, than seen in the freshly isolated population.

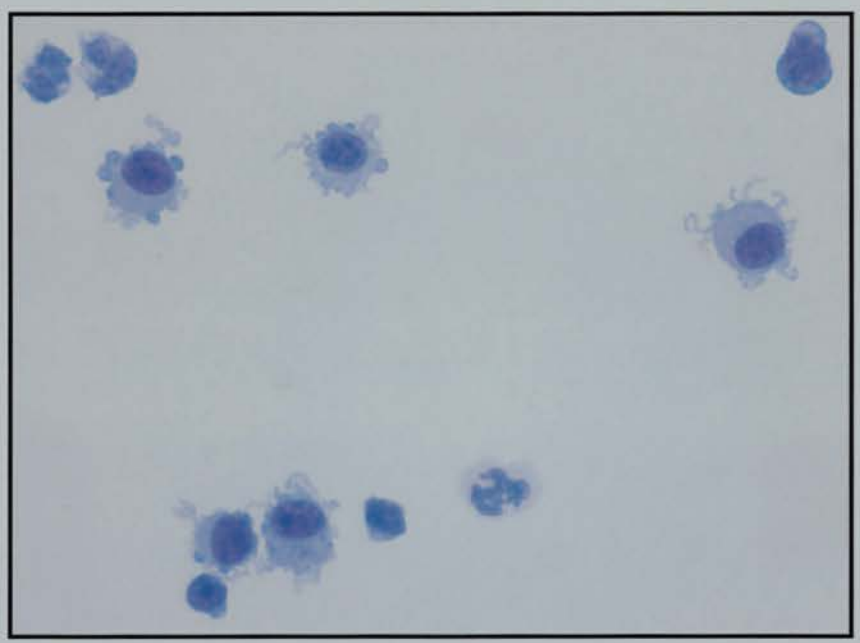

Figure 5.10 Cytospin preparation CD11c$^+$-enriched lung cells after overnight culture in GM-CSF. A typical field representative of the mixed population of cells present, but with a higher percentage of mononuclear cells than the freshly isolated population (Fig. 5.3) (x400 original magnification)

CD11c$^+$-enriched lung cells were also stained for flow cytometric analysis, as described in section 2.4. As for the BAL cells, TP3 was used to distinguish live from dead cells. Figure 5.11 shows the dot plots for these cells. The live cells comprised approximately 28% of the total population, and it was these cells that were analysed for cell surface marker expression.

The lung cells were stained for CD11c, MHC class II, CD80, CD86, ICAM-1, CD11b, and CD40. Antibodies to detect contaminating granulocytes (Gr-1), T cells, and B cells were also included in the panel. Figure 5.12 shows representative corresponding single stain histograms. In four separate experiments, the percent positivity for each surface marker was as follows: CD11c, 85 ± 5; MHC class II, 51 ± 4; CD80, 16 ± 4; CD86, 78 ± 6; ICAM-1, 97 ± 2; CD11b, 45 ± 5; CD40, 33 ± 4; Gr-1, 22 ± 6; CD3, 41 ± 4; CD19, 34 ± 5. These results reflect the mixed population of cells obtained by this method, and show considerable contamination by granulocytes, T cells, and B cells. However, as DCs represent less than 1% of the total cells in the lung, the surface levels of CD11c, MHC class II, and accessory cell markers were reasonably high.

In order to identify the APCs in this mixed population, the lung cells were also stained with both CD11c and MHC class II, as this would eliminate other contaminating cells. Figure 5.13 shows the corresponding dot plot. The three populations of cells which were identified are (i) MHC class II^{high}, $CD11c^{low}$ (lower right quadrant); (ii) MHC class II^{low}, $CD11c^{low}$ (upper left quadrant); (iii) MHC class II^{high}, $CD11c^{mid}$ (upper right quadrant). Interestingly, the first two populations are the same as those reported by Gonzalez-Juarrero and Orme [158], although the third population differs.

The MHC class II and CD11c double staining showed different patterns on the dot plots for the BAL macrophages and the $CD11c^{+}$-enriched APCs (Figures 5.9 and 5.13, respectively). The BAL macrophages are larger cells that expressed high levels of CD11c and mid-range MHC class II, while the smaller $CD11c^{+}$-enriched APCs expressed low levels of CD11c, and generally high levels of MHC class II.

However, to determine if the APCs were, in fact, free from macrophages, freshly isolated lung cells were also examined by flow cytometry. The dot plot of CD11c versus MHC class II is shown in Figure 5.14. Interestingly, the large population of cells that stain MHC class II^{mid}, $CD11c^{high}$ (upper right quadrant) is not present in the APC dot plot, but appears to match that of the BAL cells, suggesting that the

majority of cells in the APC population are, indeed, DCs. The most likely explanation for this is that contaminating macrophages adhere firmly to plastic after overnight incubation, while DCs are only loosely adherent [154]. When pipetting the cells out of the wells for flow cytometric analysis, the macrophages would not have loosened and would remain attached to the plate, while the DCs would have become unattached. Thus, for further study of the DCs, lung cell isolates were routinely cultured overnight in GM-CSF, and subsequently removed to fresh 96-well plates by pipetting. This resulted in fewer overall cells, but a population devoid of contaminating macrophages.

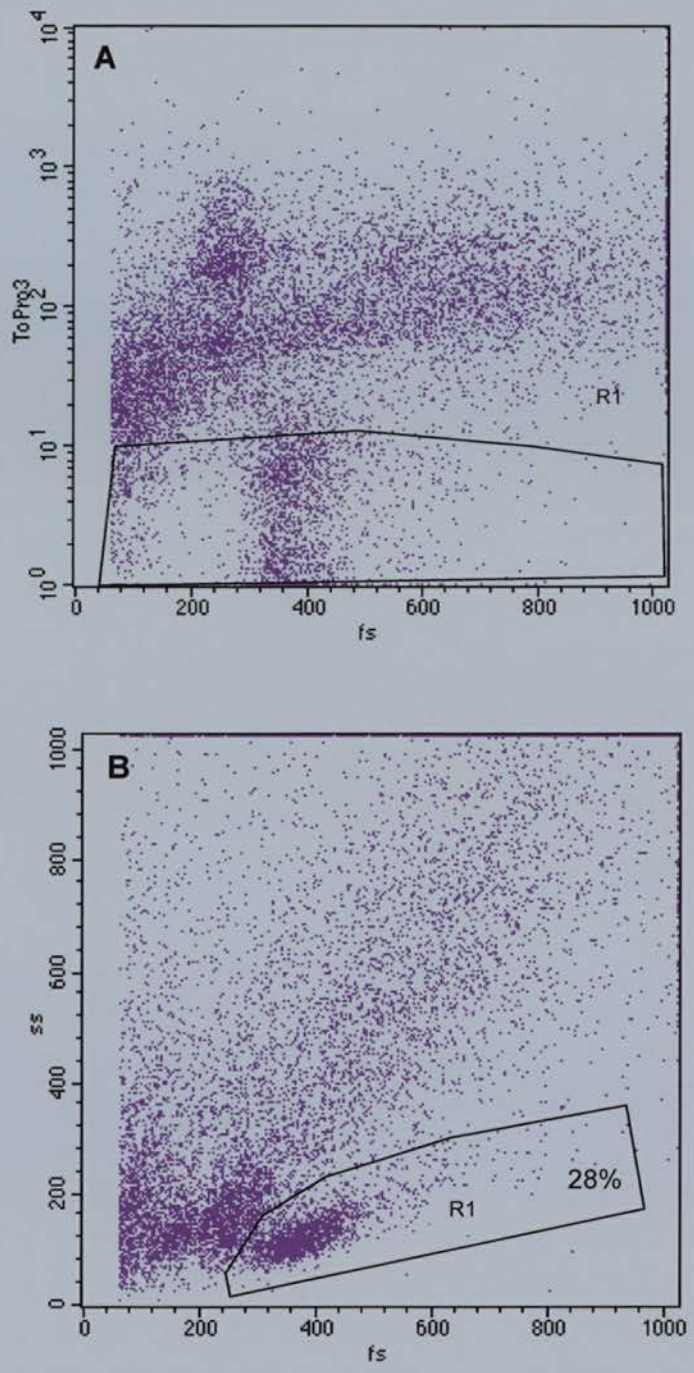

Figure 5.11 Dot plot representations of a typical CD11c$^+$-enriched APC (DC) preparation. (A) Dot plot of TP3 staining, gated around live cell population (R1). (B) Light scatter plot of whole, unstained population, back-gated on the live cell population (R1), corresponding to that in (B).

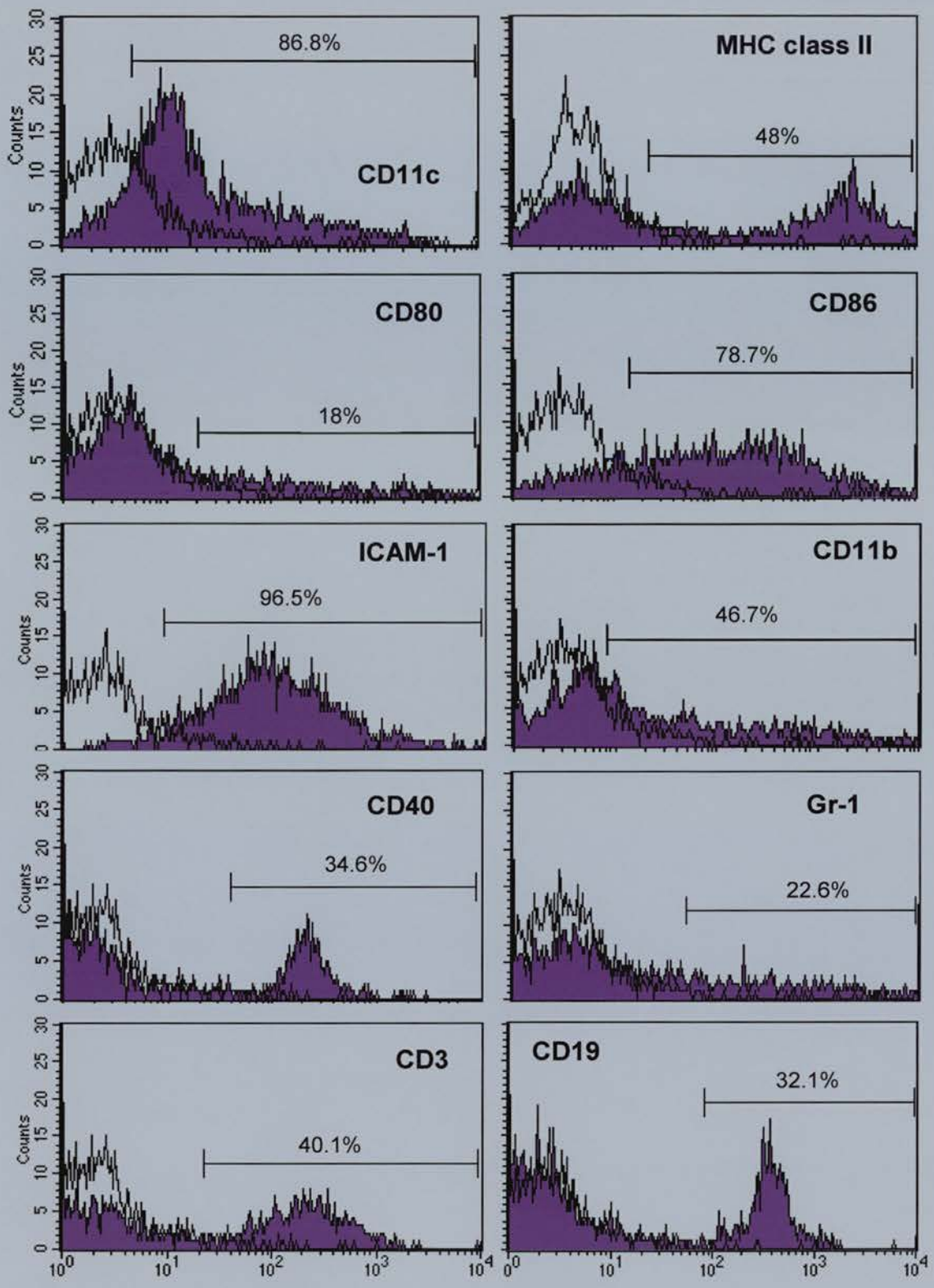

Figure 5.12 Cell surface phenotype of murine lung CD11c$^+$-enriched APCs (DCs). Flow cytometry histograms showing single staining for cell surface markers on APCs cultured overnight in medium and GM-CSF. Open histograms represent isotype-matched control monoclonal antibodies.

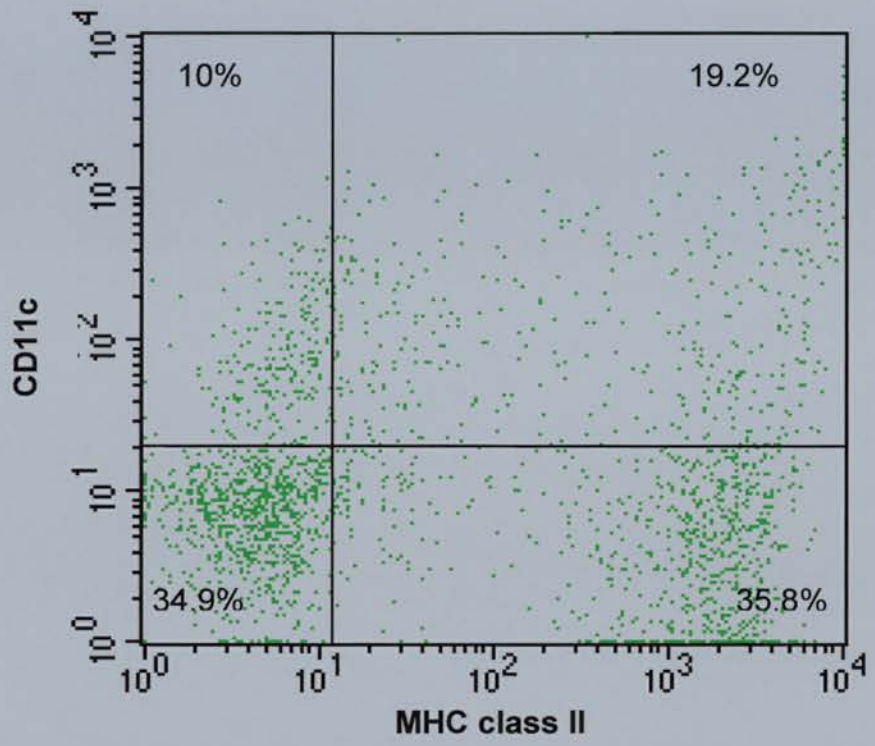

Figure 5.13 Dot plot representation of murine lung CD11c$^+$-enriched APCs (DCs) stained for both CD11c and MHC class II surface markers after overnight culture in GM-CSF. Isolated lung cells were stained with both CD11c and MHC class II antibodies and assessed by flow cytometry. Percentages of cells in each quadrant of the dot plot are shown.

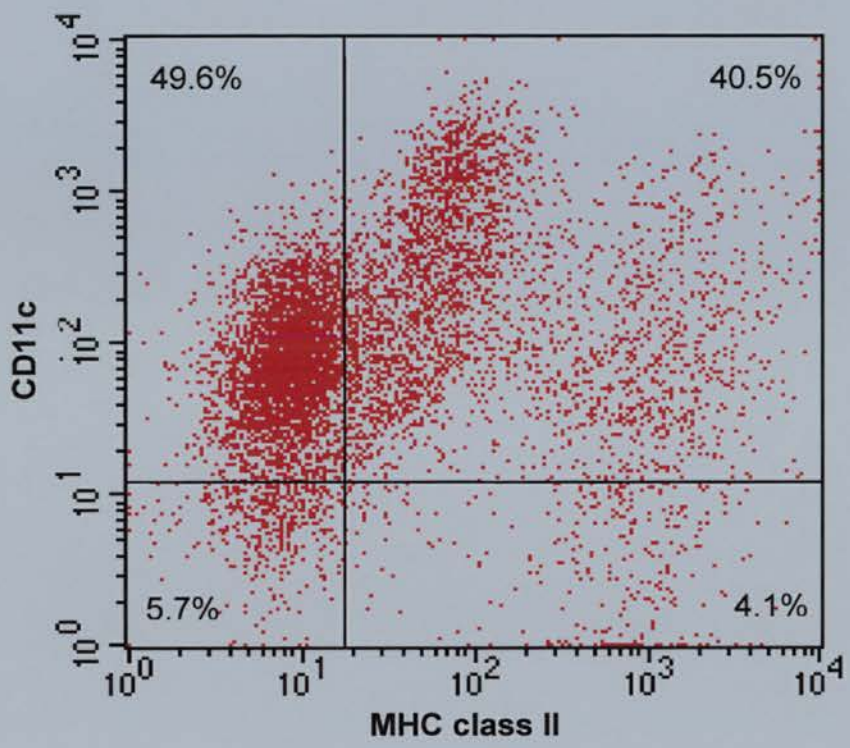

Figure 5.14 Dot plot representation of freshly isolated murine lung CD11c$^+$-enriched APCs (DCs) stain for both CD11c and MHC class II surface markers. Isolated lung cells were stained with both CD11c and MHC class II antibodies and assessed by flow cytometry immediately after isolation. Percentages of cells in each quadrant of the dot plot are shown.

5.5 Conclusions and Discussion

DCs in the lung constitute an extremely small proportion of the total number of cells, and require multiple steps for isolation, enrichment and purification. Ideally, effective procedures for isolating fairly pure populations of lung DCs take advantage of the phagocytic properties of lung macrophages, and the high MHC class II expression of DCs [137].

Ideal separation, however, was not possible for this project as only a limited number of animals could be used at one time. Higher numbers resulted in increased cell death, as the lungs could not be processed immediately. Attempts to delay cell death by keeping extracted lungs on ice or in warmed medium did not resolve the problem. The optimal cell yield was obtained by using a maximum of four mice per experimental group. The main contaminant in the isolated population was macrophages, however again, the low starting number of cells meant that plastic adherence, the method of choice to remove macrophages, was not possible as the final cell yield was negligible. Fluorescence-activated cell sorting to separate DCs from macrophages was not available at the time.

The final protocol used to isolate DCs from murine lungs thus made a number of modifications to the published methods: the lungs were perfused using a modified protocol by Oreffo *et al.* [480]; BAL was collected using standard methods; in a unique addition to published methods, the lungs were inflated with warmed collagenase A/DNase I solution before being minced and digested further in the solution to obtain a single cell suspension; Percoll purification to remove epithelial cells and other cellular debris; positive selection for $CD11c^+$ cells, having removed the $CD11c^+$ BAL cells; overnight culture in GM-CSF, with removal to new tissue culture plates.

Flow cytometric analysis revealed that the majority of cells in the BAL formed a distinct macrophage population. The $CD11c^+$-enriched lung cells, however, showed contamination by other cell populations, and considerable heterogeneity. Although

heterogeneity of lung DCs is well documented [138,154,158], the contamination needed to be addressed.

As the cells would mainly be used for functional studies, other contaminating cells, such as neutrophils and T lymphocytes, which do not possess antigen-presenting capacity, would not be a problem. B cells, though, are capable of antigen presentation, and when activated can stimulate a mixed lymphocyte reaction [481,482]. Masten and Lipscomb [157], however, showed that lung DCs were far superior to B cells at stimulating antigen-specific $CD4^+$ T cell proliferation when given $OVA_{323-339}$ peptide, and that B cells presented very little peptide when administered in a short pulse, as compared to peptide being present continuously in the cultures. Therefore this protocol would be followed for future functional assays.

The main concern however, was that there were still contaminating macrophages present which would affect subsequent functional studies. However, flow cytometric analysis of freshly isolated lung cells compared to those cultured overnight indicated that the main population missing in the latter seemed to correspond to the BAL macrophage population. Since macrophages are known to adhere firmly to plastic, while DCs are only loosely adherent and are easily dislodged with pipetting [155,472,483], removing the cells for phenotypic analysis resulted in a population of cells that was only minimally contaminated by macrophages. Removing the cells from the wells in which they were cultured overnight in GM-CSF became a routine addition to the method. Thus, in terms of antigen presentation, the population of cells isolated by the method described above could, for the body of this work, justifiably be called DCs.

Finally, it was necessary to determine the extent of maturation of the DCs, some of which is inevitable during the multiple isolation steps. Vremec *et al.* [484] suggested that CD11b is a marker of DC maturation, and this was supported by Masten and Lipscomb [157], who also found that the level of CD11b and MHC class II expression on lung DCs correlated with one another. Similar levels of expression of both these markers were found on the lung DCs isolated in this project suggesting

that, while they may have been partially activated by the isolation process, they were still not completely mature, and thus ideal for further functional studies.

CHAPTER 6

Functional Analysis of Murine Lung APCs from FITC-treated Lungs

6.1 Introduction

The aim of this chapter was to determine if the biological ability of lung APCs was modulated in FITC-induced pulmonary fibrosis. In order to do so, the ability of lung APCs to present antigen to T cells, and the cytokine response induced under these conditions, were evaluated.

The investigation of the paradigm that $CD4^+$ Th2 cells may play a major role in the pathogenesis of CFA [6,16,74,257] overlooks the fact that antigen processing and presentation by APCs is an initial step in immune recognition that eventually leads to the development of Th2-like responses. Following capture, APCs process and present antigenic peptides bound to MHC molecules to naïve T cells. In addition, they express costimulatory molecules that are required to provide a "second signal" for optimal induction of T cell activation, clonal expansion and differentiation. Without this second signal, the outcome of ligation of the T cell receptor is anergy rather than immunity [485].

There are a number of professional APCs, such as DCs, macrophages, and B cells, capable of capturing and processing foreign antigen for presentation to T cells, however DCs are the most specialised of the APCs. In this chapter, the ability of both lung DCs and AMs to stimulate T cell proliferation in the context of the FITC model of pulmonary fibrosis will be examined together with the cytokine responses that they induce in T cells.

6.1.1 Aims of Chapter

The aims of the experiments described in this chapter are:

- To determine if both $CD11c^+$-enriched DCs and BAL AMs from FITC-treated mice differ in their ability to induce T cell proliferation from APCs from PBS control mice

- To determine if IL-13, IFN-γ, IL-10, and IL-12 are produced in the cell cultures described above

- To discuss the significance of these results, and the relevant key scientific questions that remain to be answered

6.2 T Cell Proliferation Assays

T cell proliferation assays, described in detail in sections 2.1.1 and 2.1.2, were used to assess how FITC treatment affected the ability of lung APCs to present antigen. Antigen-specific T cell proliferation assays were used to give a relatively easy measure of APC-dependent T cell activation. It was decided to pulse APCs with peptide before introducing T cells rather than with whole OVA protein, as the APCs were not as efficient at presenting whole protein (data not shown). In addition, while DCs are efficient presenters of peptide after only brief pulsing, B cells require nonlimiting peptide to demonstrate antigen presenting activity [157], and this helped to ensure that T cell stimulation was directed by APCs in the cultures, without interference from contaminating B cells. Briefly, purified lung APCs were pre-incubated with $OVA_{323-339}$ peptide for two hours, and then subsequently washed to remove the peptide. The optimum dose of peptide was determined for each batch from a dose-response curve (section 2.1.2). Purified antigen-specific $CD4^+$ DO11.10 T cells, expressing T cell receptor-$\alpha\beta$ specific for $OVA_{323-339}$, were isolated from the spleens of DO11.10 transgenic mice, and were cultured together with the APCs for four days. BSA was added as a negative control for antigen specificity, or the T cell mitogen conA as a positive control for cell viability. [^{3}H]-thymidine was added to the cultures 18 hours before the end of the stimulation. The cells were then harvested and counts per minute (cpm), reflecting T cell proliferation, were obtained using a liquid scintillation counter.

Since the predominant interest was in APCs from fibrotic lungs, APCs from only long-term time points, plus the Day 7 time point, were used in the assays. $CD11c^+$-enriched lung DCs were isolated at each time point for use in these assays, and AMs from the BAL fluid were isolated at six weeks after the first dose of FITC, one week after the second dose, and six weeks after the second dose. AMs were not available from a sufficient number of experiments at Day 7 or 14 weeks after the second dose for a suitable number of repetitions, but the individual experiments are shown.

Because the purity of DCs was quite variable, as described in Chapter 5, the actual number of DCs was not consistent between preparations, and thus T cell proliferation also varied. This may also have occurred because of the heterogeneity of lung DCs, making it possible that the different subtypes of DCs were present in different numbers in each preparation. For these reasons, the data were first evaluated and compared as individual experiments before being combined in order to compare time points.

6.2.1 CD11c$^+$-enriched DCs

6.2.1.1 Day 7 DCs

CD11c$^+$-enriched DCs isolated from mouse lungs seven days after the first dose of FITC or PBS, pre-incubated with $OVA_{323-339}$ peptide, and cultured together with antigen-specific DO11.10 CD4$^+$ T cells induced T cell proliferation that was variable in magnitude (Figure 6.1). Out of six separate experiments, two showed that DCs from FITC-treated mouse lungs ("FITC DCs") stimulated significantly more T cell proliferation than DCs from PBS control lungs ("PBS DCs") (Figure 6.1A, $p<0.04$; Figure 6.1B, $p<0.02$), however the remaining four showed no significant differences between the two groups. Combining the data from all six experiments showed no significant differences between the DCs from either PBS- or FITC-treated mice.

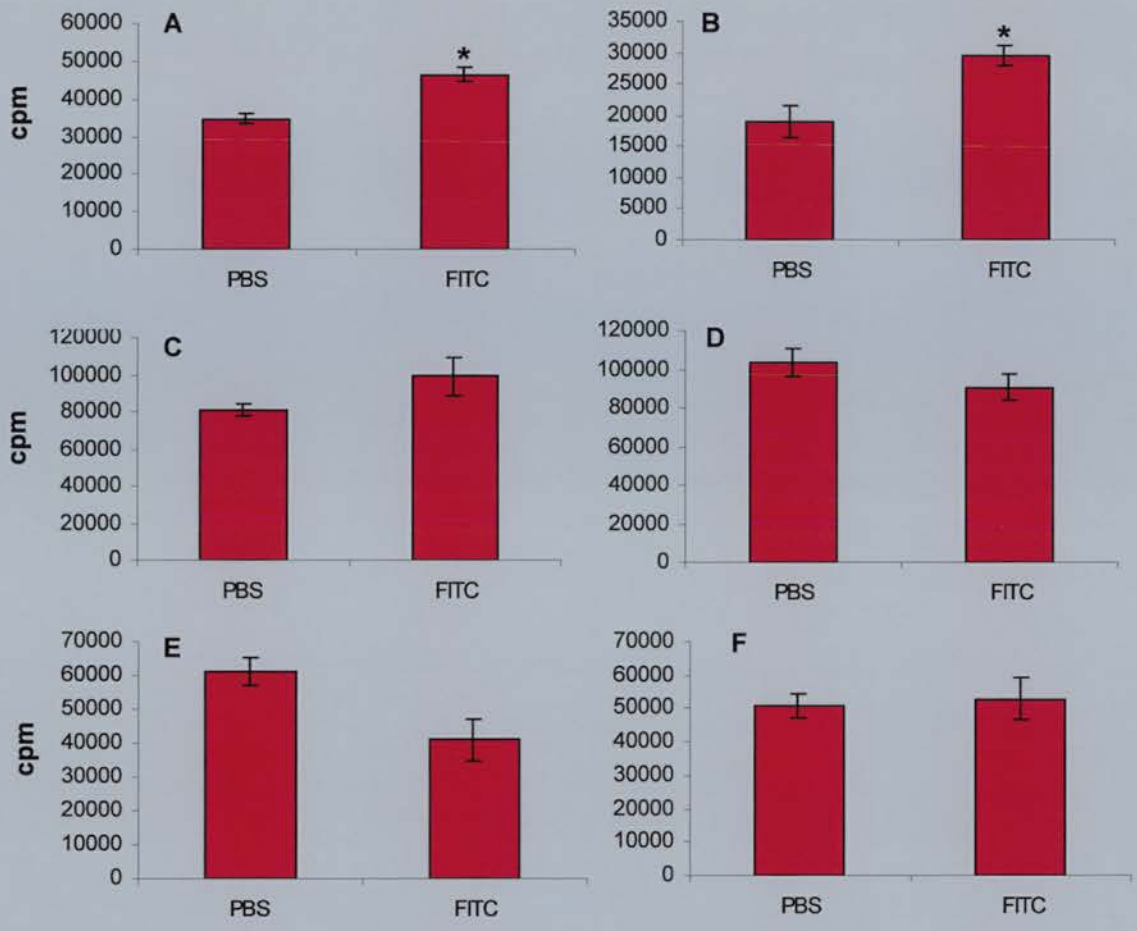

Figure	Time point / cell type	T only (cpm)	T + $OVA_{323-339}$ peptide (cpm)	APC + T + BSA (cpm) (neg. control)	APC + T + conA (cpm) (pos. control)
6.1A	7d DCs	189±23	290±226	616±75	80922±3368
6.1B	"	146±33	133±27	274±78	20447±2983
6.1C	"	462±153	328±26	494±48	60490±7945
6.1D	"	1693±366	1818±162	6001±1682	61022±4113
6.1E	"	257±20	370±11	837±145	65914±3431
6.1F	"	332±59	223±16	958±61	37446±4926

Figure 6.1 Day 7 $OVA_{323-339}$-pulsed DCs from FITC-treated mice stimulate similar levels of $CD4^+$ DO11.10 T cell proliferation as DCs from PBS control mice. Freshly isolated $CD11c^+$-enriched DCs (3 x 10^4 cells/well) from Day 7 mice were pulsed for two hours with $OVA_{323-339}$ peptide, washed, then cultured in round-bottom 96-well plates with $CD4^+$ DO11.10 T cells (1 x 10^5 cells/well). After three days, [^{3}H]thymidine (1 μCi/well) was added for the final 18 hours of culture to assess T cell proliferation, depicted as counts per minute (cpm). The data shown are the mean ± SEM of minimum triplicate wells from six independent experiments. Control values are shown in the accompanying table.
*$p<0.04$ (A), $p<0.02$ (B) as compared to paired PBS value, by paired Student's *t*-test.

6.2.1.2 Six Week DCs

$OVA_{323-339}$-pulsed $CD11c^+$-enriched DCs isolated from mouse lungs six weeks after the first dose of FITC were cultured together with DO11.10 $CD4^+$ T cells. These DCs appeared to be less efficient at stimulating T cell proliferation than those isolated from PBS-treated mice (Figure 6.2). This trend was repeated in all five separate experiments, although statistical significance was only seen in one of those (Figure 6.2A, $p<0.01$).

6.2.1.3 2^{nd} Dose + 7 Day DCs

$CD11c^+$-enriched DCs isolated from FITC-treated mice one week after a second dose of FITC induced less $CD4^+$ T cell proliferation than DCs from the lungs of PBS control mice at the same time point (Figure 6.3). Although the difference between the two groups was not significant, this trend was consistent in four out of five individual experiments, while the fifth showed no difference between groups (Fig.6.3D).

6.2.1.4 2^{nd} + 6 Week DCs

At six weeks after the second dose of FITC, $OVA_{323-339}$-pulsed $CD11c^+$-enriched DCs from mouse lungs did not stimulate $CD4^+$ DO11.10 T cells to proliferate significantly more or less than DCs from the lungs of PBS control mice at the same time point in three out of four T cell proliferation assays (Figure 6.4B,C,D). In only one experiment, DCs from FITC-treated lungs stimulated significantly less T cell proliferation than DCs from PBS control lungs (Fig.6.4A, $p<0.008$), and as such this experiment must be viewed as the exception to the trend of similar levels of proliferation.

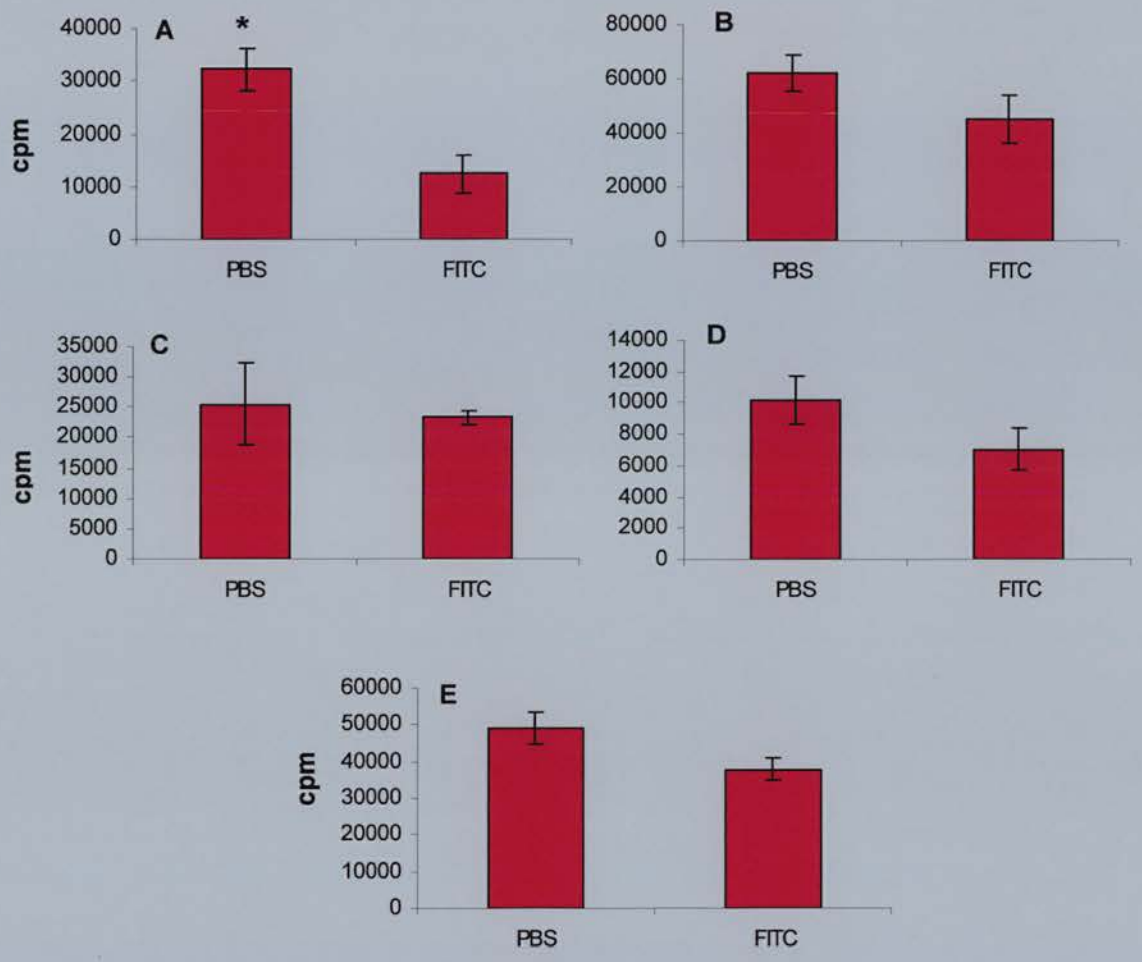

Figure	Time point / cell type	T only (cpm)	T + $OVA_{323-339}$ peptide (cpm)	APC + T + BSA (cpm) (neg. control)	APC + T + conA (cpm) (pos. control)
6.2A	6wk DCs	1064±110	1735±87	2468±181	15043±3959
6.2B	"	1471±415	1071±116	1240±227	11838±2095
6.2C	"	2251±182	3315±1033	1989±633	43043±4932
6.2D	"	1426±239	2866±1235	2452±269	16333±2299
6.2E	"	678±91	877±79	643±157	17498±1609

Figure 6.2 Week 6 $OVA_{323-339}$-pulsed DCs from FITC-treated mice stimulate less $CD4^+$ DO11.10 T cell proliferation than DCs from PBS control mice. Freshly isolated $CD11c^+$ enriched DCs (3 x 10^4 cells/well) from six week mice were pulsed for two hours with $OVA_{323-339}$ peptide, washed, then cultured in round-bottom 96-well plates with $CD4^+$ DO11.10 T cells (1 x 10^5 cells/well). After three days, [^{3}H]thymidine (1 μCi/well) was added for the final 18 hours of culture to assess T cell proliferation, depicted as counts per minute (cpm). The data shown are the mean ± SEM of minimum triplicate wells for five independent experiments. Control values are shown in accompanying table.
*$p<0.01$ by paired Student's *t*-test

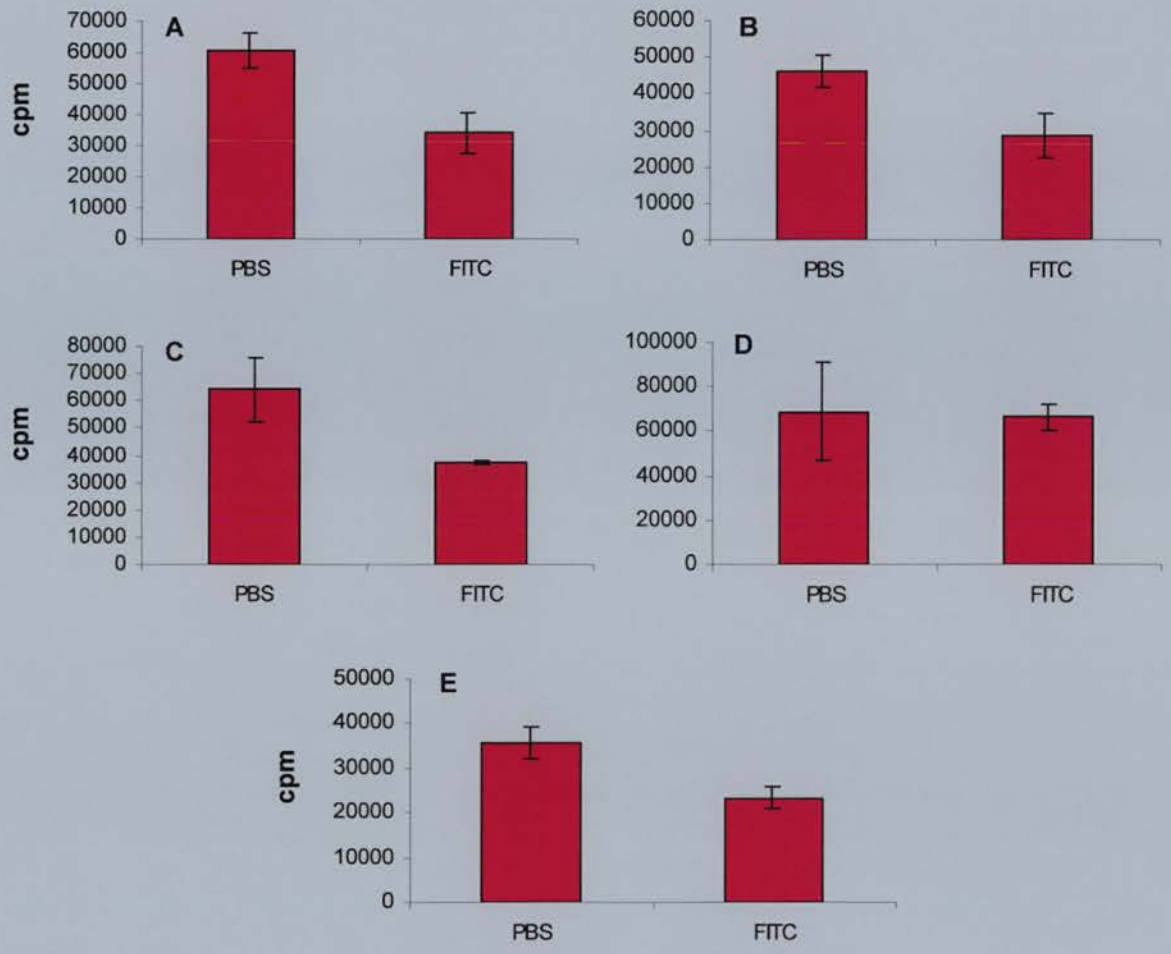

Figure	Time point / cell type	T only (cpm)	T + $OVA_{323-339}$ peptide (cpm)	APC + T + BSA (cpm) (neg. control)	APC + T + conA (cpm) (pos. control)
6.3A	2^{nd}+7d DCs	4705±1565	5841±262	6248±681	64283±12420
6.3B	"	3700±712	4402±1784	4071±590	63477±8993
6.3C	"	2075±1745	2344±638	4992±799	39593±9835
6.3D	"	2098±367	3632±880	2230±86	35536±6130
6.3E	"	3428±745	3977±94	3106±425	25369±815

Figure 6.3 2^{nd} Dose + 7 Day $OVA_{323-339}$-pulsed DCs from FITC-treated mice stimulate less $CD4^+$ DO11.10 T cell proliferation than DCs from PBS control mice. Freshly isolated $CD11c^+$-enriched DCs (3 x 10^4 cells/well) from 2^{nd} Dose + 7 Day mice were pulsed for two hours with $OVA_{323-339}$ peptide, washed, then cultured in round-bottom 96-well plates with $CD4^+$ DO11.10 T cells (1 x 10^5 cells/well). After three days, [^{3}H]thymidine (1 μCi/well) was added for the final 18 hours of culture to assess T cell proliferation, depicted as counts per minute (cpm). The data shown are the mean ± SEM of minimum triplicate wells of five independent experiments. Control values are shown in the accompanying table.

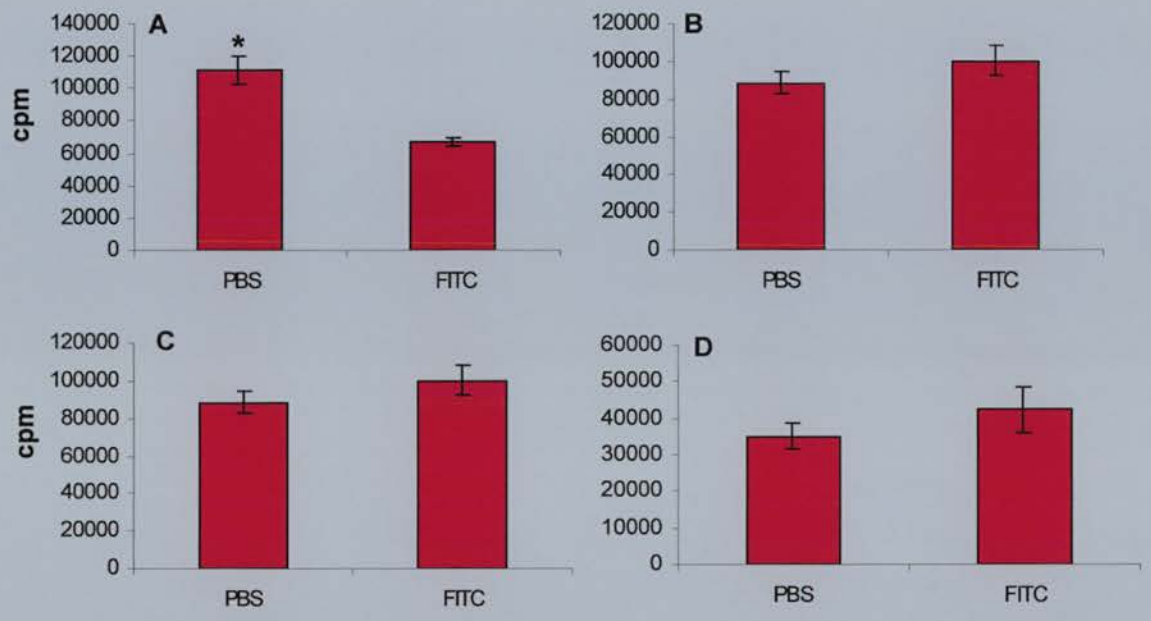

Figure	Time point / cell type	T only (cpm)	T + $OVA_{323-339}$ peptide (cpm)	APC + T + BSA (cpm) (neg. control)	APC + T + conA (cpm) (pos. control)
6.4A	2^{nd}+6wk DCs	2084±357	2288±137	2958±428	18598±2500
6.4B	"	1398±182	743±73	1929±129	22818±4576
6.4C	"	3565±546	3561±105	3732±537	107245±12921
6.4D	"	2183±83	2298±873	5992±1071	26143±7765

Figure 6.4 2^{nd} Dose + 6 Week $OVA_{323-339}$-pulsed DCs from FITC-treated mice stimulate similar levels of $CD4^+$ DO11.10 T cell proliferation as DCs from PBS control mice. Freshly isolated $CD11c^+$-enriched DCs (3 x 10^4 cells/well) from 2^{nd} Dose + 6 Week mice were pulsed for two2 hours with $OVA_{323-339}$ peptide and, washed, then cultured in round-bottom 96-well plates with $CD4^+$ DO11.10 T cells (1 x 10^5 cells/well). After three days, [^{3}H]thymidine (1 μCi/well) was added for the final 18 hours of culture to assess T cell proliferation, depicted as counts per minute (cpm). The data shown are the mean ± SEM of minimum triplicate wells of four independent experiments. Control values are shown in the accompanying table.
*$p < 0.008$ as compared to paired FITC value, by paired Student's *t*-test

6.2.1.5 2^{nd} Dose + 14 Week DCs

In three out of five separate experiments, $OVA_{323-339}$-pulsed $CD11c^+$-enriched DCs from the lungs of mice isolated 14 weeks after the second dose of FITC were poorer stimulators of $CD4^+$ DO11.10 T cell proliferation than DCs from PBS control mice at the same time point (Figure 6.5A,C,E). In one of these experiments, the difference between groups was statistically significant (Fig6.5A, $p<0.04$). Again, however, this can only be identified as a trend as the remaining two experiments for this time point did not show a difference in proliferation between the two groups (Figure 6.5B,D).

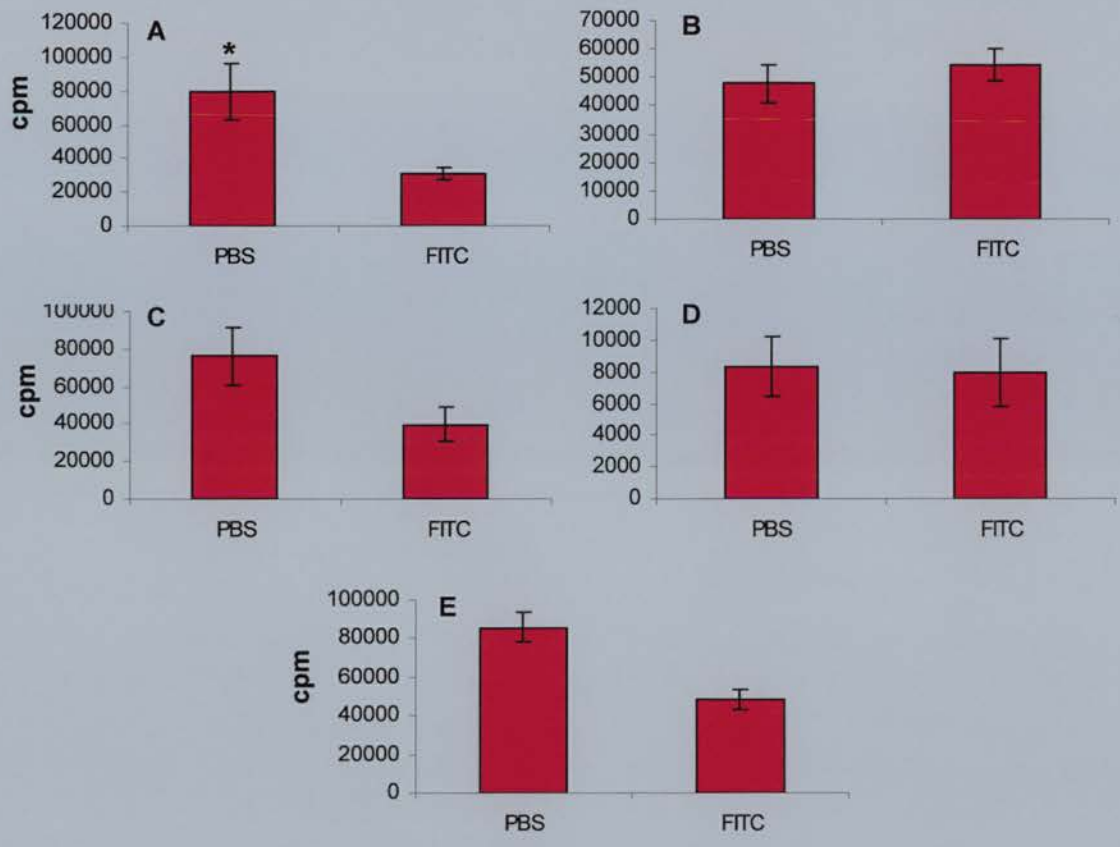

Figure	Time point / cell type	T only (cpm)	T + $OVA_{323-339}$ peptide (cpm)	APC + T + BSA (cpm) (neg. control)	APC + T + conA (cpm) (pos. control)
6.5A	2^{nd}+14wk DCs	3322±1554	3450±1682	2796±705	21618±5635
6.5B	"	2239±396	2907±254	2925±445	136614±12473
6.5C	"	1848±695	1831±382	2457±768	78617±22997
6.5D	"	1332±230	1515±235	1441±153	29860±2961
6.5E	"	1332±21	2288±401	2340±216	40025±4789

Figure 6.5 2^{nd} Dose + 14 Week $OVA_{323-339}$-pulsed DCs from FITC-treated mice stimulate similar levels of $CD4^+$ DO11.10 T cell proliferation as DCs from PBS control mice. Freshly isolated $CD11c^+$-enriched DCs (3 x 10^4 cells/well) from 2^{nd} Dose + 14 Week mice were pulsed for two hours with $OVA_{323-339}$ peptide, washed, then cultured in round-bottom 96-well plates with $CD4^+$ DO11.10 T cells (1 x 10^5 cells/well). After three days, [^{3}H]thymidine (1 μCi/well) was added for the final 18 hours of culture to assess T cell proliferation, depicted as counts per minute (cpm). The data shown are the mean ± SEM of minimum triplicate wells of five independent experiments. Controls are shown in the accompanying table.
*$p < 0.04$ as compared to paired FITC value, by paired Student's *t*-test.

6.2.1.6 Combined DC Results

As it was difficult to see a trend between time points, and because of the variation in cpm between experiments, a method of normalising the data was developed in order to compare the results of the T cell proliferation assays (Figure 6.6). For each experiment, proliferation (cpm) for the replicate wells was averaged to obtain a final value. This was done for wells containing DCs from both PBS- and FITC-treated mice. The final FITC count was subtracted from the final PBS count, and this value was expressed as either a positive or negative percentage of the PBS value. All the percentages for each experiment were then combined to obtain a final percentage, indicative of the percentage of the greater or reduced T cell proliferation induced by DCs from FITC-treated mice as compared to those from PBS control mice. This process was repeated for the acute Day 7 time point, and for each of the long-term time points.

At Day 7 after the first FITC dose, DCs from the lungs of FITC-treated mice stimulated, on average, more T cell proliferation than DCs from PBS control mice. By six weeks, however, this trend changed dramatically, with FITC DCs stimulating less proliferation than PBS DCs. This difference between the two time points was significant ($p<0.03$). One week after the second dose of FITC was administered, FITC DCs again stimulated less T cell proliferation than PBS DCs, although their ability to stimulate the T cells had improved. Six weeks after the second FITC dose, FITC and PBS DCs had similar abilities to stimulate T cell proliferation, although FITC DCs were still not as efficient. Finally, 14 weeks after the second dose of FITC, although not significant, the efficiency of FITC DCs as T cell proliferation stimulators had dropped dramatically, nearing the six week levels.

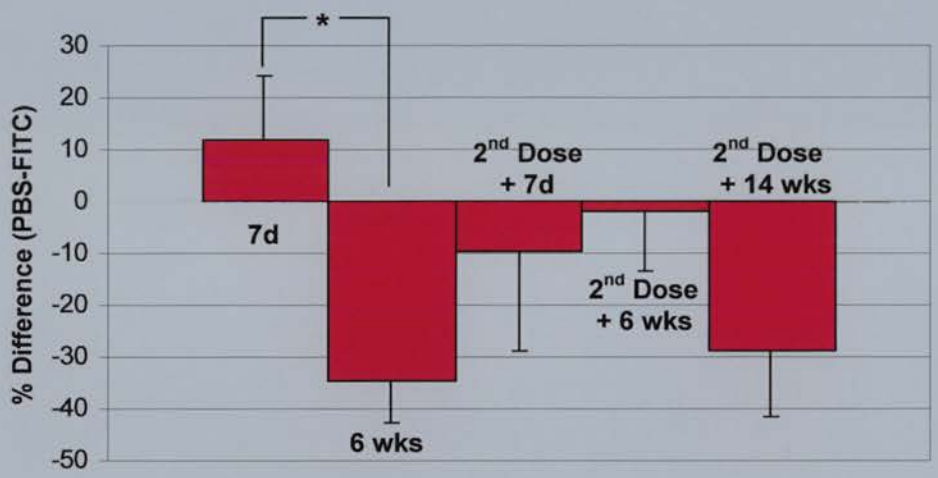

Figure 6.6 Difference in ability of CD11c$^+$-enriched DCs from the lungs of FITC-treated mice to stimulate T cell proliferation at different time points, expressed as a percentage of the value for DCs from PBS control mice. Freshly isolated CD11c$^+$-enriched DCs (3 x 10^4 cells/well) from mice at each time point were pulsed for two hours with $OVA_{323-339}$ peptide, washed, then cultured in round-bottom 96-well plates with CD4$^+$ DO11.10 T cells (1 x 10^5 cells/well). After three days, [^{3}H]thymidine (1 μCi/well) was added for the final 18 hours of culture to assess T cell proliferation, and was measured as counts per minutes (cpm). For each separate experiment, the combined cpm from replicate wells with DCs from FITC-treated mice was subtracted from the combined cpm from those with DCs from PBS-treated mice. This value was then expressed as a percentage of the PBS cpm, and all percentages were then combined to obtain the final value shown above. These calculations were made for each time point (7d, n=6 separate experiments; 6 wks, n=5; 2nd+7d, n=5; 2nd+6wks, n=4; 2nd+14wks, n=5).
*$p<0.03$ by Student's *t*-test.

6.2.2 BAL Alveolar Macrophages

The T cell proliferation was much lower in all experiments using BAL AMs than they were in experiments using DCs. This finding is consistent with reports in the literature of AMs being less efficient at stimulating T cell proliferation than lung DCs [181,486], although it must be noted that AMs were not cultured with GM-CSF as were the DCs, which may have also been a factor in the lower stimulating abilities of the AMs.

6.2.2.1 Day 7 BAL AMs

There was no significant difference in the abilities of $OVA_{323-339}$-pulsed BAL AMs from FITC- or PBS-treated mice to stimulate DO11.10 T cells to proliferate (Figure 6.7). This statement is based on the results from only two independent experiments, however, and ideally should be repeated to determine if this is, in fact, the trend.

6.2.2.2 6 Week BAL AMs

Interestingly, $OVA_{323-339}$-pulsed AMs isolated from the BAL fluid of mice six weeks after the first FITC dose were more efficient at stimulating DO11.10 T cells to proliferate than AMs from PBS control mice at the same time point (Figure 6.8). This trend was found consistently over three independent experiments, although it was not significant.

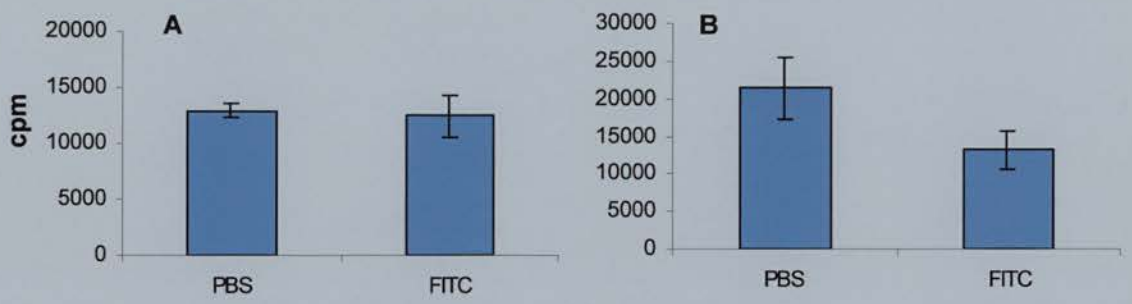

Figure	Time point / cell type	T only (cpm)	T + $OVA_{323-339}$ peptide (cpm)	APC + T + BSA (cpm) (neg. control)	APC + T + conA (cpm) (pos. control)
6.7A	7d AMs	462±153	328±26	657±218	11710±12657
6.7B	"	2886±535	2760±310	1663±186	13959±3835

Figure 6.7 Day 7 $OVA_{323-339}$-pulsed AMs from the BAL of FITC-treated mice stimulate more $CD4^+$ DO11.10 T cell proliferation than DCs from PBS control mice. Freshly isolated BAL AMs (3 x 10^4 cells/well) from Day 7 mice were pulsed for two hours with $OVA_{323-339}$ peptide, washed, then cultured in round-bottom 96-well plates with $CD4^+$ DO11.10 T cells (1 x 10^5 cells/well). After three days, [^{3}H]thymidine (1 μCi/well) was added for the final 18 hours of culture to assess T cell proliferation, depicted as counts per minute (cpm). The data shown are the mean ± SEM of minimum triplicate wells of two independent experiments. Control values are shown in accompanying table.

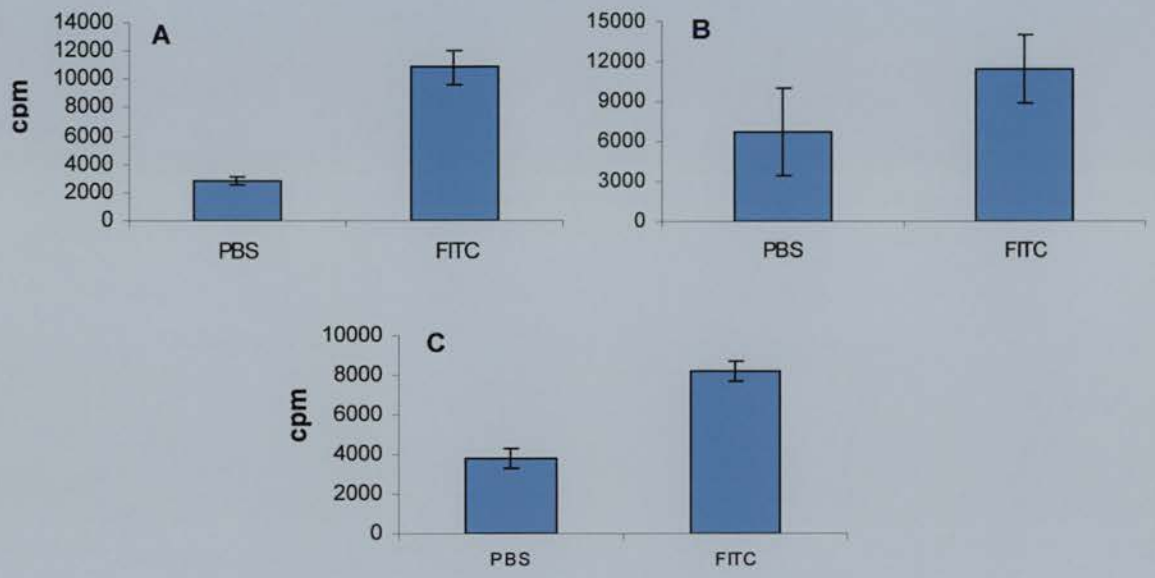

Figure	Time point / cell type	T only (cpm)	T + $OVA_{323-339}$ peptide (cpm)	APC + T + BSA (cpm) (neg. control)	APC + T + conA (cpm) (pos. control)
6.8A	6wk AMs	1226±144	1703±207	1655±344	15453±1479
6.8B	"	1560±145	958±109	2071±320	8982±822
6.8C	"	281±45	265±64	2078±219	43122±3286

Figure 6.8 Week 6 $OVA_{323-339}$-pulsed AMs from the BAL of FITC-treated mice stimulate more $CD4^+$ DO11.10 T cell proliferation than DCs from PBS control mice. Freshly isolated BAL AMs (3 x 10^4 cells/well) from six week mice were pulsed for two hours with $OVA_{323-339}$ peptide, washed, then cultured in round-bottom 96-well plates with $CD4^+$ DO11.10 T cells (1 x 10^5 cells/well). After three days, [^{3}H]thymidine (1 μCi/well) was added for the final 18 hours of culture to assess T cell proliferation, depicted as counts per minute (cpm). The data shown are the mean ± SEM of minimum triplicate wells of three independent experiments. Control values are shown in the accompanying table.

6.2.2.3 2nd Dose + 7 Day BAL AMs

As was seen at the six week time point for the same cells, at one week after the second dose of FITC, $OVA_{323-339}$-pulsed AMs from the BAL are more efficient stimulators of the proliferation of DO11.10 $CD4^+$ T cells than AMs from the BAL of PBS-treated mice (Figure 6.9). This trend was consistent over three separate experiments, but was not significant.

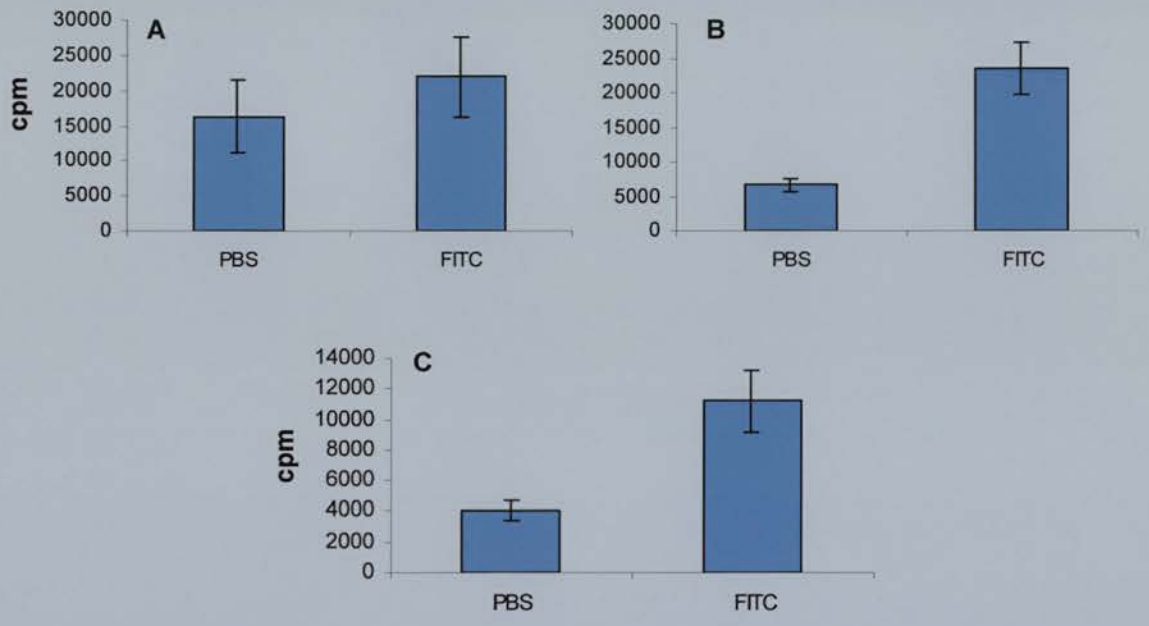

Figure	Time point / cell type	T only (cpm)	T + $OVA_{323-339}$ peptide (cpm)	APC + T + BSA (cpm) (neg. control)	APC + T + conA (cpm) (pos. control)
6.9A	2nd+7d AMs	1493±150	2357±807	1584±164	46167±10999
6.9B	"	2908±471	3583±815	3907±682	41682±8127
6.9C	"	1585±84	2098±367	2230±86	35536±6130

Figure 6.9 2nd Dose + 7 Day $OVA_{323-339}$-pulsed AMs from the BAL of FITC-treated mice stimulate more $CD4^+$ DO11.10 T cell proliferation than DCs from PBS control mice. Freshly isolated BAL AMs (3 x 10^4 cells/well) from 2nd Dose + 7 Day mice were pulsed for two hours with $OVA_{323-339}$ peptide, washed, then cultured in round-bottom 96-well plates with $CD4^+$ DO11.10 T cells (1 x 10^5 cells/well). After three days, [^{3}H]thymidine (1 μCi/well) was added for the final 18 hours of culture to assess T cell proliferation, depicted as counts per minute (cpm). The data shown are the mean ± SEM of minimum triplicate wells, and are representative of the trend seen in three independent experiments. Control values are shown in the accompanying table.

6.2.2.4 2nd Dose + 6 Week BAL AMs

Again, $OVA_{323-339}$-pulsed AMs from the BAL of FITC-treated mice, at six weeks after the second FITC dose, were more potent stimulators of $CD4^+$ DO11.10 T cell proliferation than PBS control BAL AMs at the same time point (Figure 6.10). In two out of three separate experiments, the level of proliferation was significantly greater with the FITC BAL AMs than with the PBS BAL AMs (Fig.6.10B, $p<0.01$; Fig.6.10C, $p<0.001$), but as the third experiment showed no difference between the two groups, these findings can only be reported as a possible trend.

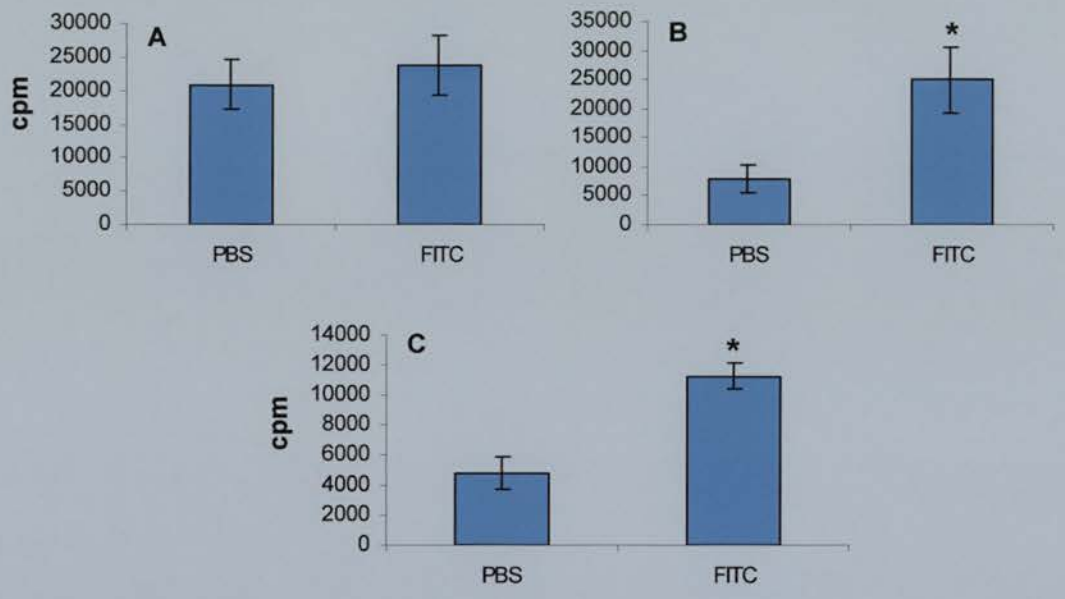

Figure	Time point / cell type	T only (cpm)	T + $OVA_{323-339}$ peptide (cpm)	APC + T + BSA (cpm) (neg. control)	APC + T + conA (cpm) (pos. control)
6.10A	2nd+6wk AMs	1639±196	2879±898	1224±158	21184±5181
6.10B	"	2000±236	1652±255	5224±926	27223±2951
6.10C	"	1223±130	1740±170	2361±294	34207±2471

Figure 6.10 2nd Dose + 6 Week $OVA_{323-339}$-pulsed AMs from the BAL of FITC-treated mice stimulate more $CD4^+$ DO11.10 T cell proliferation than DCs from PBS control mice. Freshly isolated BAL AMs (3×10^4 cells/well) from 2nd Dose + 6 Week mice were pulsed for two hours with $OVA_{323-339}$ peptide, washed, then cultured in round-bottom 96-well plates with $CD4^+$ DO11.10 T cells (1×10^5 cells/well). After three days, [^{3}H]thymidine (1 μCi/well) was added for the final 18 hours of culture to assess T cell proliferation, depicted as counts per minute (cpm). The data shown are the mean ± SEM of minimum triplicate wells of three independent experiments. Control values are shown in the accompanying table.
*$p<0.01$ (B), $p<0.001$ (C), as compared to paired PBS value, by paired Student's *t*-test.

6.2.2.5 2nd Dose + 14 Week BAL AMs

There were insufficient BAL AMs from this time point to perform more than one T cell proliferation experiment, which showed that $OVA_{323-339}$-pulsed BAL AMs from FITC-treated mice were less efficient at stimulating T cell proliferation than BAL AMs from PBS control mice (Figure 6.11). More assays are required to identify a trend.

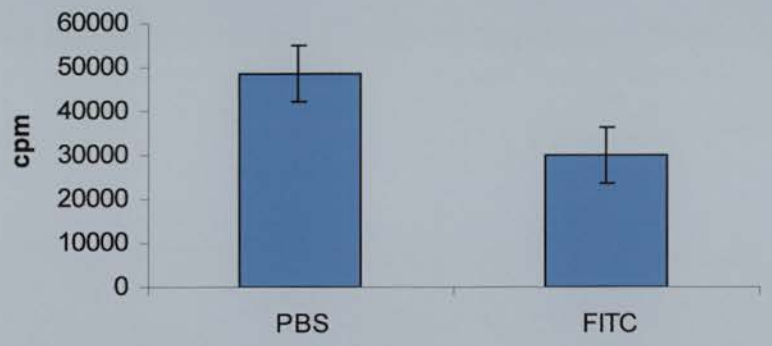

Figure	Time point / cell type	T only (cpm)	T + $OVA_{323-339}$ peptide (cpm)	APC + T + BSA (cpm) (neg. control)	APC + T + conA (cpm) (pos. control)
6.11	2nd+ 14wk AMs	1022±240	994±194	2279±485	25361±1643

Figure 6.11 2nd Dose + 14 Week $OVA_{323-339}$-pulsed AMs from the BAL of FITC-treated mice may stimulate less $CD4^+$ DO11.10 T cell proliferation than DCs from PBS control mice. Freshly isolated BAL AMs (3×10^4 cells/well) from 2nd Dose + 14 Week mice were pulsed for two hours with $OVA_{323-339}$ peptide, washed, then cultured in round-bottom 96-well plates with $CD4^+$ DO11.10 T cells (1×10^5 cells/well). After three days, [^{3}H]thymidine (1 μCi/well) was added for the final 18 hours of culture to assess T cell proliferation, depicted as counts per minute (cpm). The data shown are the mean ± SEM of minimum triplicate wells of one experiment. Control values are shown in the accompanying table.

6.2.2.6 Combined BAL AM Results

The method for analysing the T cell proliferation assay results obtained from the BAL AMs was the same as that used for the DCs (Figure 6.12). Interestingly, the DCs and BAL AMs behaved reciprocally. At Day 7 after the initial dose of FITC, FITC AMs induced slightly less T cell proliferation than PBS AMs at the same time point, although this value was obtained from only two experiments. By six weeks, although not signficant, the ability of FITC AMs to stimulate T cell proliferation had increased dramatically. FITC AMs remained considerably more efficient at T cell stimulation than PBS AMs at both one and six weeks after the second dose of FITC. Only a single T cell proliferation assay was performed with BAL AMs obtained from mice 14 weeks after the second dose of FITC, so the result can only be interpreted with caution as several more repeats should be performed to identify any trend. This single assay showed that at this late time point, FITC AMs were able to induce less T cell proliferation than PBS AMs, suggesting reversal of the trend seen at previous time points, and contrary to the results obtained with the lung DCs.

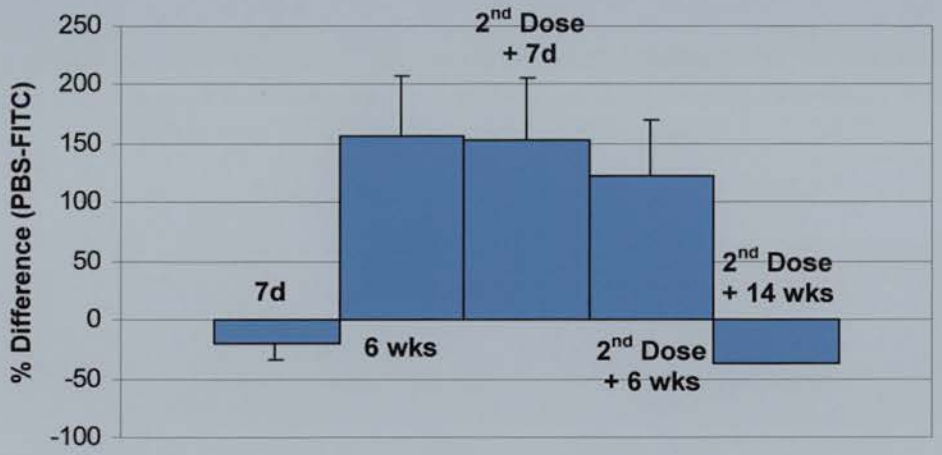

Figure 6.12 Difference in ability of AMs from the BAL of FITC-treated mice to stimulate T cell proliferation at different time points, expressed as a percentage of the value for DCs from PBS control mice. Freshly isolated AMs (3 x 10^4 cells/well) from the BAL of mice at each time point were pulsed for two hours with $OVA_{323-339}$ peptide, washed, then cultured in round-bottom 96-well plates with $CD4^+$ DO11.10 T cells (1 x 10^5 cells/well). After three days, [^{3}H]thymidine (1 μCi/well) was added for the final 18 hours of culture to assess T cell proliferation, and was measured as counts per minute (cpm). For each separate experiment, the combined cpm from replicate wells with AMs from FITC-treated mice was subtracted from the combined cpm from those with AMs from PBS-treated mice. This value was then expressed as a percentage of the PBS cpm, and all percentages were then combined to obtain the final value shown above. These calculations were made for each time point (7d, n=2 separate experiments; 6 wks, n=3; 2^{nd}+7d, n=3; 2^{nd}+6wks, n=3; 2^{nd}+14wks, n=1).

6.3 Cytokine Production

To measure cytokine protein production, supernatants were taken from the wells of the T cell proliferation assays 72 hours after the addition of the APCs. The supernatants were processed as described in section 2.1.2.1, and assayed by ELISA as described in section 2.3. In many experiments, protein expression was found in wells containing APCs from both treated and non-treated animals. The levels measured in the wells containing APCs from PBS control animals may reflect cytokine expression by the activated T cells or background expression by the APCs themselves. However, since the purpose of these preliminary studies was to examine the effect that FITC treatment had on the APCs compared to the controls, it was the difference between the two groups that was of interest.

The cytokines chosen for evaluation were firstly IL-12, a Th1-type cytokine known to be a potent inducer of IFN-γ from T cells [487], shown to attenuate bleomycin-induced pulmonary fibrosis in mice [97], and which has the potential to switch the response from a fibrotic Th2 phenotype to a more favourable Th1 phenotype [488,489]. Secondly IL-10, a Th2-type cytokine known to be a potent inhibitor of IL-12 production [490], and whose expression is thought to be delayed compared to that of IL-12 *in vivo,* making it a possible downregulator of the IL-12 response [491]. IL-10 produced by lung DCs has also been shown to mediate tolerance induced by respiratory exposure to antigen [492], and AMs have been shown to have increased expression of the IL-10 gene in interstitial lung disease [86]. Thirdly, supernatants were analysed for the presence of IFN-γ, a Th1-type cytokine known to have profound suppressive effects on the production of ECM proteins [247], has been shown to ameliorate effects of bleomycin-induced fibrosis in mouse lungs [255], and has been used in preliminary clinical trials as a treatment for CFA [103,493]. Finally IL-13, which has similar biological properties to IL-4, and has been implicated in the pathogenesis of fibroproliferative disorders, was also chosen for analysis [85,91,335,494].

6.3.1 DCs

6.3.1.1 DCs: IL-13

Seven days after the first dose of FITC, supernatants taken from wells to which $CD11c^+$-enriched DCs from FITC-treated mice were added ("FITC DC supernatants") had significantly more IL-13 protein than supernatants from wells to which $CD11c^+$-enriched DCs from PBS-treated mice were added ("PBS DC supernatants") ($p<0.0006$, $n=9$) (Figure 6.13). At six weeks after the first dose, levels of cytokine expression were much lower, and there was no significant difference between either group of supernatants. Seven days after the second dose of FITC, a significant difference was seen between the two groups again, with protein levels in the FITC DC supernatants again being higher ($p<0.05$, $n=13$), and at six weeks after the second FITC dose ($p<0.04$, $n=15$). The trend continued at 14 weeks after the second dose, although the difference in IL-13 expression between the two groups of supernatants was not significant.

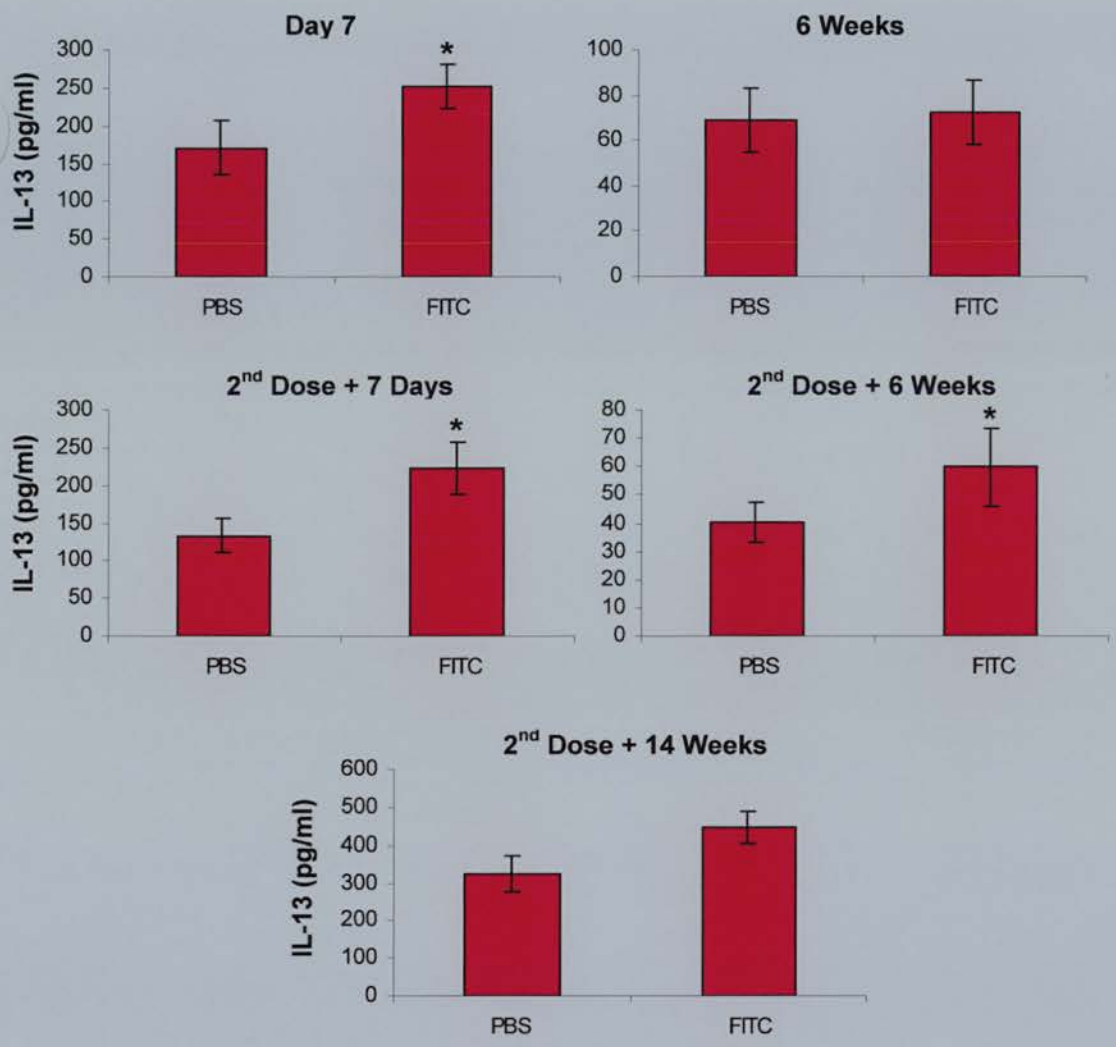

Figure 6.13 IL-13 protein production in supernatants from T cell proliferation assays containing CD11c$^+$-enriched DCs. T cell proliferation assays were prepared as described. In each separate experiment, after 72 hours in culture, 0.2 ml of supernatant was removed from each well, centrifuged to remove any remaining cells, and protein expression was measured by ELISA. "PBS" = supernatant from wells to which CD11c$^+$-enriched DCs from PBS-treated mice were added. "FITC" = supernatant from wells to which CD11c$^+$-enriched DCs from FITC-treated mice were added. (Day 7, *$p<0.0006$, n=9; 6 Weeks, n=12; 2nd Dose + 7 Days, *$p<0.05$, n=13; 2nd Dose + 6 Weeks, *$p<0.04$, n=15; 2nd Dose + 14 Weeks, n=9).
*Statistical significance as compared to paired PBS value, as determined by paired Student's *t*-test.

6.3.1.2 DCs: IFN-γ

No significant difference was seen in IFN-γ protein expression between Day 7 FITC or PBS DC supernatants (Figure 6.14) but six weeks after the first FITC dose, PBS DC supernatants had higher levels of the cytokine than FITC DC supernatants ($p<0.002$, $n=17$). By seven days after the second dose of FITC, however, this trend was reversed with significantly more IFN-γ found in the FITC DC supernatants than in the PBS DC supernatants ($p<0.05$, $n=13$), and was continued at six weeks after the second dose ($p<0.03$, $n=15$), and at 14 weeks after the second dose, although the difference at this time point was not significant.

6.3.1.3 DCs: IL10, IL-12p70

No IL-10 or IL-12p70 protein was found in the supernatants of wells to which DCs from FITC- or PBS-treated DCs were added.

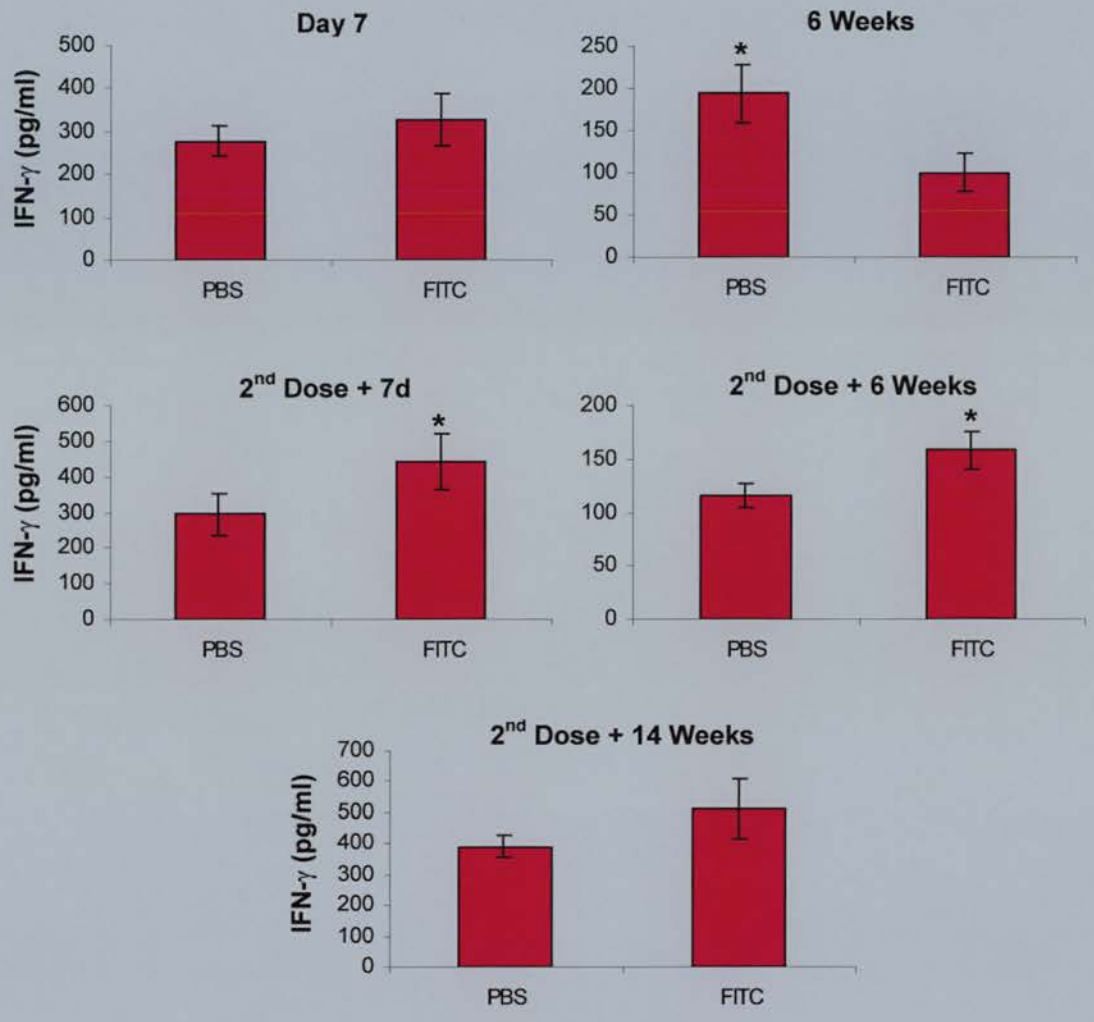

Figure 6.14 IFN-γ protein production in supernatants from T cell proliferation assays containing CD11c$^+$-enriched DCs. T cell proliferation assays were prepared as described. In each separate experiment, after 72 hours in culture, 0.2 ml of supernatant was removed from each well, centrifuged to remove any remaining cells, and protein expression was measured by ELISA. "PBS" = supernatant from wells to which CD11c$^+$-enriched DCs from PBS-treated mice were added. "FITC" = supernatant from wells to which CD11c$^+$-enriched DCs from FITC-treated mice were added. (Day 7, n=9; 6 Weeks, *$p<0.002$, n=17; 2nd Dose + 7 Days, *$p<0.05$, n=13; 2nd Dose + 6 Weeks, *$p<0.03$, n=15; 2nd Dose + 14 Weeks, n=11).
* Statistical significance as compared to paired value, as determined by paired Student's *t*-test.

6.3.2 BAL AMs

6.3.2.1 BAL AMs: IL-13

Supernatants from T cell proliferation assays containing BAL AMs were only available for the 6 Weeks, 2nd Dose + 7 Days, and 2nd Dose + 6 Weeks time points for the IL-13 assays (Figure 6.15). At six weeks after the first dose, although very little protein is present (lower detection limit of the R&D IL-13 ELISA is 39.1 pg/ml), the supernatants from wells to which BAL AMs from FITC-treated mice were added ("FITC AM supernatants") expressed significantly more IL-13 protein than supernatants from wells to which BAL AMs from PBS control mice were added ("PBS AM supernatants") ($p<0.03$, $n=15$). At the next two time points, however, at seven days and six weeks after the second dose of FITC, no difference was seen between the two groups of supernatants.

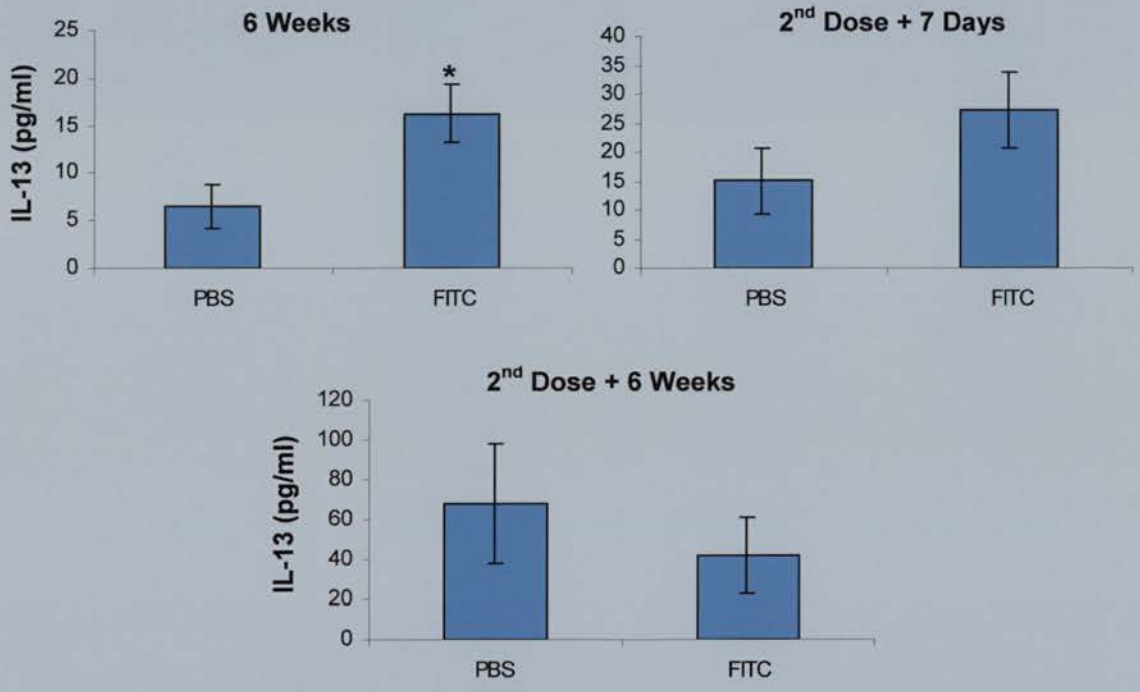

Figure 6.15 IL-13 protein production in supernatants from T cell proliferation assays containing BAL AMs. T cell proliferation assays were prepared as described. In each separate experiment, after 72 hours in culture, 0.2 ml of supernatant was removed from each well, centrifuged to remove any remaining cells, and protein expression was measured by ELISA. "PBS" = supernatant from wells to which $CD11c^+$-enriched DCs from PBS-treated mice were added. "FITC" = supernatant from wells to which $CD11c^+$-enriched DCs from FITC-treated mice were added. (6 Weeks, *$p<0.03$, $n=15$; 2^{nd} Dose + 7 Days, $n=6$; 2^{nd} Dose + 6 Weeks, $n=9$).
*Statistical significance as compared to paired PBS value, as determined by paired Student's *t*-test.

6.3.2.2 BAL AMs: IFN-γ

PBS and FITC AM supernatants were available for the 6 Weeks, 2nd Dose + 6 Weeks, and 2nd Dose + 14 Weeks time points only. At six weeks after the first dose of FITC, and at six weeks after the second dose, no significant difference was seen between the FITC AM and PBS AM supernatants (Figure 6.16). At 14 weeks after the second dose, however, PBS AM supernatants had significantly more IFN-γ protein than FITC AM supernatants ($p<0.04$, $n=3$), although it should be noted that this result was based on fewer experiments than the other time points.

6.3.2.3 BAL AMs: IL-10, IL-12

No IL-10 or IL-12p70 protein expression was detected in FITC or PBS, DC or AM supernatants at any time point

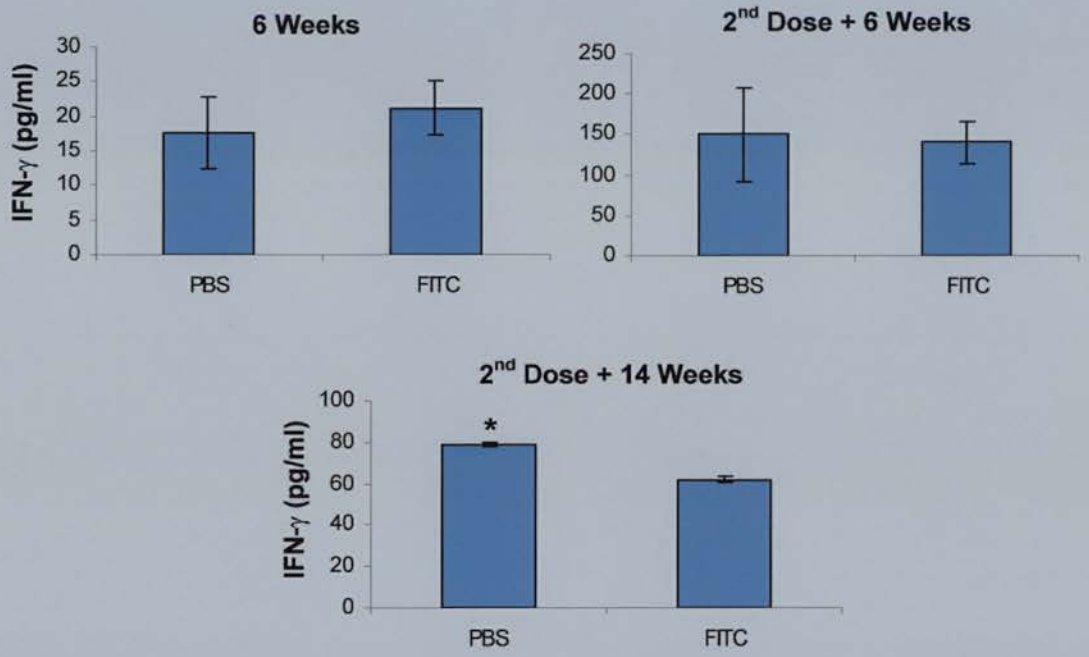

Figure 6.16 IFN-γ protein production in supernatants from T cell proliferation assays containing BAL AMs. T cell proliferation assays were prepared as described. In each separate experiment, after 72 hours in culture, 0.2 ml of supernatant was removed from each well, centrifuged to remove any remaining cells, and protein expression was measured by ELISA. "PBS" = supernatant from wells to which $CD11c^+$-enriched DCs from PBS-treated mice were added. "FITC" = supernatant from wells to which $CD11c^+$-enriched DCs from FITC-treated mice were added. (6 Weeks, n=15; 2^{nd} Dose + 6 Weeks, n=9; 2^{nd} Dose + 14 Weeks, $p<0.04$, n=3).
*Statistical significance as compared to paired FITC value, as determined by paired Student's *t*-test.

6.4 Conclusions and Discussion

6.4.1 DCs in T Cell Proliferation Assays

Much of the available functional data on DCs in the lung has been obtained from studies of asthma, which is regarded as a Th2-mediated disease. As discussed in detail in Chapter 1, these functional studies have revealed that while DCs have inherent Th1-promoting activity [495-498], DCs at mucosal surfaces such as the lung induce responses that are polarised towards Th2-type immunity [499-502], possibly because the uptake and subsequent presentation of antigen by the airway DCs occurs within an environment rich in IL-10 and PGE_2, which are known to suppress IL-12 production, a Th1 cytokine, in DCs [165,503].

There is no published data on the *in vitro* functional abilities of lung DCs from a fibrotic environment, so while the experiments presented in this chapter are preliminary, they provide insight into this neglected area.

6.4.1.1 FITC DCs May Be Less Efficient In Vitro T Cell Stimulators

The results of the T cell proliferation assays evaluated singly at each time point suggest a trend for FITC DCs to be less efficient T cell stimulators than PBS DCs from control mice (Figures 6.1-5). When the results from each time point were calculated as the difference between the two groups (PBS-FITC) and expressed as a percentage of the PBS value, and then combined, this trend became more prominent (Figure 6.6). At all time points, with the exception of Day 7, FITC DCs stimulated less T cell proliferation than PBS DCs. At Day 7 this trend was reversed, and there was a significant difference between this time point and the 6 Week time point. It would appear that it is only once the acute phase has passed that FITC DCs become

less efficient T cell stimulators, as the difference was greatest at six weeks after the first dose and at 14 weeks after the second dose.

There could be several explanations as to why FITC DCs present antigen less efficiently. Certainly this could be a protective mechanism as it would prevent local maturation of DCs leading to increased T cell activation and subsequent damage. As discussed in Chapter 1, murine DCs have been classified into two subsets: mature (DC1) and immature (DC2), although it is not clear if these cells are derived from one common progenitor, or if they represent two distinct lineages. The mature DCs express high levels of MHC class II on their surface and produce IL-12, which drives Th1 differentiation. The immature DCs express low levels of MHC class II and produce IL-10, which favours Th2 differentiation [171]. Resting, steady-state lung DCs preferentially prime for low-level Th2 immunity, and under normal circumstances, this response would be expected to resolve towards a protective Th1 response as antigen exposure continued unless, as in the case of some allergic responses, incomplete immune deviation leads to a persistent pathogenic Th2 response [165]. Therefore, FITC DCs may be held in the "DC2" lineage, maintaining their immature status, and thus their poor T cell stimulatory abilities *in vitro*, and contributing to the continuing pathogenic Th2 response *in vivo*.

In addition, the potent capacity of DCs to activate immunologically naïve T cells is related to their high constitutive expression of MHC class II and T cell costimulatory molecules, such as CD40, CD80 and CD86. Deficiency or absence of expression of these molecules reduces the antigen presenting function of DCs, and may render them potentially tolerogenic; presentation of antigen to T cells by APCs in the absence of costimulatory molecules induces T cell anergy [485]. Studies of tolerance have shown that immature DCs, expressing low levels of CD86, are able to induce tolerance [504], and thus the FITC DCs may also be maintained in a tolerogenic state. Thus, nontolerogenic DCs may become tolerogenic in FITC-induced fibrosis by blocking their ability to provide costimulatory signals, by modification with suppressive cytokines such as IL-4 [505], or TGF-β which has been shown to induce tolerance in splenic DCs [178], or by preventing their maturation.

However, the DCs isolated from the lungs of treated and control mice for these experiments were exposed to GM-CSF overnight before contact with the T cells. GM-CSF matures DCs, and leads to a marked increase in their overall potency as APCs [149,165,479], yet the FITC DCs appeared to respond poorly to GM-CSF *in vitro*. As the mucosal immune system has a unique immunological milieu that acts, in part, via the DCs to induce different T cell phenotypes, the following question has arisen: does the milieu act to irreversibly differentiate DCs or are the DCs tolerogenic only in the mucosal environment [506]? It would appear, from the results discussed in this section, that the immunological milieu induced by the instillation of FITC prevents the DCs from maturing, irreversibly differentiates them, or perhaps induces a permanent, or long-term, tolerogenic effect. At the very least, the FITC DCs are being altered in this fibrotic milieu in such a way as to be unresponsive to GM-CSF.

A variety of experimental systems have provided evidence for the supposition that immunological homeostasis in the lung and airways is maintained primarily by endogenous immunosuppressive mechanisms that regulate local induction of T cell responses [507]. NO secretion by the AMs is thought to be a major contributing factor in this phenomenon [194]. AMs can also downmodulate the antigen-presenting capacities of DCs in the bronchial and alveolar environment [196]. In mice, NO production by AMs is the major source of the downmodulation of both T cells and DCs [508]. Interestingly, production of NO by AMs has been shown to inhibit the ability of lung DCs to respond to maturation factors such as GM-CSF, thus essentially holding them in an immature state in terms of T cell stimulating activity [182,195]. NO-mediated suppression of DC function may also contribute to the Th2-promoting activity of lung epithelial DCs, a notion consistent with the proposed Th2-promoting activity of this mediator [163,509]. Thus, in the FITC-treated mice, the production of NO by the AMs could be either terminally differentiating them to a DC2 phenotype, or otherwise maintaining them in this state, thereby decreasing their T cell stimulating abilities and contributing to the pathogenic Th2 response in the lungs, and thus rendering them unable to respond to the GM-CSF *in vitro*.

Interestingly, although there are many similarities between the Th2-driven asthma response and CFA, and indeed, NO has also been implicated in the pathogenesis of asthma [510,511], the hypothesis presented above is in direct contrast to a proposed scenario for the aetiology of asthma which suggests that unregulated *in situ* maturation of respiratory tract DC functional activity may lead to excessive T cell activation within the airway mucosa, and to damaging local pathology [163,164].

Another possibility is the idea proposed by Stein *et al.* [512] of alternative activation, in which APCs can participate in anti-inflammatory processes, tolerance and healing. Although this was originally applied to macrophages, it has been suggested that DCs may also be alternatively activated and may be induced to exert suppressive effects [513]. IL-10-treated immature DCs induce tolerance in naïve T cells, and IL-10 induces tolerance *in vivo* [514]. Although IL-10 was not detected in the supernatants, it may well be present in the tissues.

Finally, CD80 and CD86 have been shown to play a role in allogeneic T cell proliferation by murine lung DCs, with CD80 being the more crucial costimulatory molecule, as anti-CD80 antibody was more suppressive of T cell proliferation in a mixed lymphocyte reaction than anti-CD86 antibody [154]. Also, CD80 and CD86 appear, in some models, to have different roles in skewing T cells towards a Th1 or Th2 response. For example, Kuchroo *et al.* [515] and Freeman *et al.* [516] showed that CD86 more effectively directed the differentiation of T cells toward a Th2-like phenotype, where CD80 favoured Th1 development. Masten *et al.* [154] suggest that by using CD80 as a dominant costimulatory ligand, lung DCs normally favour the development of a Th1 response over a Th2 response in the lung after injury. Therefore, in a pathogenic state like pulmonary fibrosis, if CD80 expression were being suppressed a Th2 response would predominate, and *in vitro* T cell proliferation would be decreased. Phenotyping the FITC and PBS lung DCs would be necessary to explore this possibility.

6.4.1.2 *FITC DCs May Polarise T Cells Towards a Th2-type Response In Vitro*

Cytokine measurements of supernatants taken from the T cell proliferation assays revealed that FITC DCs induced T cells to produce more IL-13 protein, a Th2 cytokine, than PBS DCs (Figure 6.13). This trend was seen at all time points, with the exception of week six, and was significant at seven days after the first dose, and seven days and six weeks after the second dose. It is possible that FITC does induce DCs to polarise T cells to produce increased amounts of IL-13, but that while one dose was not sufficient to sustain this effect, the second dose induced a longer-lasting effect. This may be due to the complexity of the *in vivo* cytokine microenvironment in which APCs, lymphocytes, lung epithelial cells and fibroblasts all contribute.

As discussed in Chapter 1, IL-13 has been implicated in the pathogenesis of asthma, which is a Th2-mediated disease, causing subepithelial airway fibrosis [79,333,517]. IL-13 is also a potent stimulator of fibroblast proliferation and collagen production *in vitro* [332,335], and its potential as a mediator of CFA progression is being recognised.

Lee *et al.* [91], using a transgenic CC10-IL-13 mouse in which the overexpression of IL-13 causes airway and parenchymal fibrosis, demonstrated that the fibrotic effects of IL-13 are mediated to a great extent by its ability to selectively induce and activate TGF-β1 in the lung. Although macrophages were the major site of production and deposition in the tissue, TGF-β1 mRNA and protein were also found in bronchiolar epithelial cells, alveolar type II cells, and eosinophils.

Further studies by this group [494] assessed the roles of MCP and its major receptor, CCR2, in the effector pathways of IL-13. They demonstrated that IL-13 is a potent inducer of MCPs *in vivo*, although this stimulation is not MCP-specific. They showed that many of the features of IL-13 overexpression in the lung, including inflammation, hyaluronic acid accumulation, pulmonary fibrosis and respiratory failure and death are mediated by mechanisms that are, at least partially, CCR2-

dependent, indicating that MCP-mediated signaling via CCR2 plays a key role in the pathogenesis of IL-13-induced inflammatory, fibrotic and proteolytic effector responses *in vivo*. Additionally, they reported that the diminished fibrogenic and hyaluronic acid stimulating effects of IL-13 in the absence of CCR2 are associated with the diminished production and activation of TGF-β1, thus demonstrating that CCR2 signaling is a critical event in cytokine induction and activation of TGF-β1 *in vivo*.

Interestingly, specific CCR2 signaling has been shown to promote a profibrotic cytokine cascade in the original single dose surgical model of FITC-induced pulmonary fibrosis [62], and the authors speculate that alterations in TGF-β may contribute to the protection conferred to mice in the absence of CCR2 signaling.

Finally, both IL-13 and C-10, a novel C-C chemokine that is chemotactic for mononuclear phagocytes, are increased in the pathogenesis of bleomycin-induced pulmonary fibrosis [102]. IL-13 is a potent inducer of C-10 *in vivo*, and neutralisation of C-10 attenuated bleomycin-induced pulmonary fibrosis and intrapulmonary macrophage numbers. Belperio *et al.* [102] suggest, therefore, that IL-13 has a profibrotic role in the development of pulmonary fibrosis that is independent of its known direct effects on fibroblasts, and is evidence for a cooperative interaction between Th2 cytokines and specific C-C chemokines.

IL-10 and IL-12 were not detected in the supernatants from the T cell proliferation assays, but interestingly production of IFN-γ, a Th1 cytokine, was increased in the wells containing FITC DCs (Figure 6.14). As IFN-γ was not detected in the BAL fluid, it demonstrates that these two environments are not reflective of each other. The increase was significant at one week and six weeks after the second FITC dose, and the trend present at seven days after the first dose and 14 weeks after the second dose. As with IL-13, the trend was not seen at six weeks after the first dose of FITC, confirming the requirement for a second dose of FITC in this model. Although this result may seem contradictory to the IL-13 production, possibly increased IFN-γ

production *in vivo* may be a secondary response in an attempt to balance the increased Th2-type response to FITC.

Another possibility could be drawn from Rissoan *et al.* [168] who have described a negative feedback mechanism to maintain the balance between Th1 and Th2 responses. They demonstrated that IFN-γ seemed to promote the survival and maturation of DC2 cells. If, however, the FITC DCs are being held in a constant immature state by NO production that overrides that aspect of IFN-γ regulation, perhaps the IFN-γ acts solely to promote the survival of the DC2s, thus contributing to the ongoing Th2-like response.

Finally, the production of IFN-γ could be a feature unique to the FITC model. Sime and O'Reilly [6] observe that although Th2 cytokines are important in the development of fibrosis in CFA, and models of the disease suggest a shift in the cytokine response towards a Type 2 response, this response clearly does not occur in isolation, and is certainly more complex than initially appreciated. Therefore, it is not surprising that Type 1 cytokines have been identified in fibrotic conditions. Indeed, increased IFN-γ production by lymphocytes has been noted in a mouse model of silicosis [205]. Additionally, IFN-γ production has been found in bleomycin-induced pulmonary fibrosis in C57BL/6J and A/J mice, but not in bleomycin-resistant BALB/c mice, and that the potential for IFN-γ to enhance proinflammatory processes was noted [258]. BALB/c mice are susceptible to FITC-induced pulmonary fibrosis, however, and perhaps accordingly, IFN-γ production is increased.

IFN-γ production in the absence of IL-12 is curious, as IL-12 is essential for stimulating IFN-γ production [518]. Culturing lung DCs in GM-CSF, as was done in the experiments discussed here, has been shown to shut down IL-10 mRNA production and markedly upregulate IL-12p35 [165]. However if, as suggested previously, the DCs are resistant to maturation by GM-CSF, perhaps IL-10 production is reduced, certainly below the levels of detection for the assay used in these experiments, but not enough to allow the upregulation of IL-12, thus explaining

the lack of either cytokine in the cultures. Certainly, mRNA analysis of both the DCs and T cells would provide much more information.

6.4.2 BAL AMs in T Cell Proliferation Assays

AMs are the prominent cell population obtained from the alveoli of CFA patients [75], and it is well established that resting AMs help to create an immunosuppressive environment in the lung that serves to limit immune response initiation, and activation of antigen-specific T cells [126,194]. Although their role in CFA pathogenesis has been examined extensively, the focus has mainly been on cytokine secretion by these cells.

As with DCs, although these results are preliminary, there are no available studies examining the *in vitro* antigen presenting abilities of AMs from fibrotic lungs, and so the results of these experiments could have implications for the study of CFA.

6.4.2.1 FITC BAL AMs May Be More Efficient In Vitro T Cell Stimulators than PBS BAL AMs

The [^{3}H]thymidine incorporation, which reflects T cell proliferation, for all experiments involving BAL AMs were considerably lower than those involving DCs. This correlates well with published data showing that DCs are far superior at stimulating T cell proliferation than BAL AMs [181,486], however as mentioned previously, the lack of GM-CSF in the overnight AM cultures may have contributed to this effect.

Although the data sets were not complete due to insufficient numbers of cells, the results from the single experiments performed at each time point suggested a trend for BAL AMs from FITC-treated mice to be more efficient T cell stimulators than

PBS BAL AMs (Figures 6.7-11). This trend, reciprocal to that of the DCs, was confirmed when the data were analysed as described above, in order to compare between groups, although there were no significant differences (Figure 6.12). The first and last time points, however, would need to be repeated in order to make conclusive remarks regarding the results.

Despite their apparent end-stage differentiation state, AMs can express markers thought to be rather specific for DCs [131]; indeed, in the interstitial lung disease sarcoidosis, AMs express high levels of CD86 and CD40 [192], just as do mature DCs. Similar changes have been found in mice when AMs were exposed to bleomycin [193]. GM-CSF is produced by several cell types in the lung (activated T cells, epithelial cells, fibroblasts) and modulates the cytokine production of AMs and enhances their antigen-presenting capacity [75], although as discussed in Chapter 1, its role in the pathogenesis of pulmonary fibrosis is controversial [300-303,305]. Therefore, if GM-CSF expression is upregulated in the lungs of FITC-treated mice, it could be inducing high levels of costimulatory molecules on the AMs, resulting in higher levels of T cell proliferation than induced by PBS control AMs, while the DCs appeared to be resistant to the effects of this cytokine.

Another possibility to explain the increased T cell stimulatory abilities of FITC BAL AMs could be related to the increased levels of IFN-γ detected in the FITC-treated mice. IFN-γ is produced by lymphocytes and is able to activate macrophages [519,520]. If this were the case, then the enhanced T cell-stimulating abilities of the FITC BAL AMs would be a feature limited to the FITC model.

Finally, as described for the DCs, the concept of alternative activation of BAL AMs could provide an explanation for the results described in this section. Stein *et al.* [512] found that alternatively activated macrophages express a special set of molecules that enables them to actively participate in anti-inflammatory processes, tolerance induction, and healing. As such, they found that IL-4 enhanced the capacity of macrophages for endocytosis and antigen presentation. Measurement of

levels of this cytokine in the supernatants from these T cell proliferation assays may be revealing, as would testing the hypothesis with the closely-related IL-13.

6.4.2.2 FITC BAL AMs May Polarise T Cells Towards a Th2-type Response In Vitro

Although the results from the measurement of IL-13 in the supernatants from T cell proliferation assays with BAL AMs do not form a complete data set, and are preliminary due to insufficient cell numbers, they suggest that BAL AMs do contribute to polarising the T cells towards a Th2 response by inducing IL-13 production in the T cells, but that this contribution may be transitory (Figure 6.15). This would need to be confirmed by measuring IL-13 production at seven days after the first FITC dose, and at 14 weeks after the second dose.

As with the DCs, no IL-10 or IL-12p70 production was detected in the supernatants. IFN-γ production however, was detected, although only the time points at six weeks after the first FITC dose, and at six and 14 weeks after the second dose were evaluated (Figure 6.16). No difference between the FITC- and PBS-treated groups was detected at the first two time points evaluated, but at 14 weeks after the second dose, BAL AMs from FITC-treated mice stimulated significantly less IFN-γ production than those from PBS-treated mice. Although the time points for seven days after the first dose and seven days after the second dose need to be evaluated, this result correlates with the lack of IL-12 production, and suggests that the Th2 polarisation in FITC-induced pulmonary fibrosis is still important even in the late stages of the disease.

6.4.3 Future Directions for DC and BAL AM Work

The results of the experiments reported in this chapter show that while FITC DCs stimulated less T cell proliferation than PBS DCs, FITC BAL AMs were better

stimulators. As discussed above, the increased stimulating abilities of the FITC BAL AMs could be explained by the cytokine milieu, possibly by the presence of IFN-γ or GM-CSF [75,86,287,519,520]. The FITC DCs however, have been altered by the FITC environment in a fashion not reversible, or only partially reversible, by *in vitro* culture with GM-CSF. This may be a terminally differentiated state, or related to tolerance. Thus, the cytokine milieu affecting the BAL AMs *in vivo* would have little or no effect on the FITC DCs. Perhaps the most important next step is to phenotype both freshly isolated and cultured FITC- and PBS-treated DCs and BAL AMs to establish the pattern of upregulation of MHC class II and costimulatory molecules.

The cytokine analyses of the supernatants from the T cell proliferation assays with both DCs and BAL AMs indicated that the APCs were stimulating IL-13 production by the T cells. As discussed, IL-13 is a profibrotic cytokine, that has potential as a mediator of pulmonary fibrosis [85,91,102,336]. Neither IL-10 or IL-12 were detected in the supernatants, but IFN-γ appeared to be upregulated in the FITC DC supernatants.

Cytokine expression analysis at the mRNA level would be extremely beneficial, as the ELISAs used for the experiments in this section may not have been sensitive enough to detect low levels of cytokines. This would depend, however, on being able to obtain larger numbers of cells on which to work. It would also be interesting to examine the T cells for the presence of IL-4, the prototypic Th2 cytokine.

In summary, the key scientific questions that remain to be answered are: are the FITC APCs skewing the response in the FITC-induced fibrotic lungs towards a Th2 phenotype? If so, is this response dominated by either IL-13 or IL-4, or do they act in concert? Is IFN-γ upregulated in the FITC lungs, and if so, is this specific to the FITC model? Is the poor stimulating ability of the FITC DCs a protective or a pathogenic mechanism? And finally, if the cytokine milieu induced by FITC acts to alter the antigen presenting capacity of DCs, what is the mechanism? These questions could form the basis for continuing the work detailed in this chapter.

CHAPTER 7

In Vitro Response of Lung Epithelial Cell Lines to FITC

7.1 Introduction

As discussed in Chapter 1, there are two proposed routes for the development of CFA following injury to the alveolar epithelium: the more traditional "inflammatory" route, or the "epithelial-fibroblastic" route, a new hypothesis suggesting that fibrosis results from primarily epithelial injury and abnormal wound healing with minimal contribution from inflammation [48,266]. Regardless of the route, it is becoming increasingly apparent that injured and activated AECs both synthesise and respond to a variety of enzymes, cytokines and growth factors, thereby contributing to the outcome of the profibrogenic processes [266].

The alveolar epithelium consists of type I and type II epithelial cells in an almost balanced numerical proportion. While type I cells cover approximately 90% of the alveolar surface, type II cells represent the stem cell population [2]. Following injury and damage to, or loss of, the highly vulnerable type I epithelial cells, proliferation of type II cells results in alveolar re-epithelialisation. The lungs of CFA patients, however, exhibit several significant changes in the alveolar epithelium. These include the presence of hyperplastic type II pneumocytes, microscopical areas of epithelial denudation, and areas of honeycomb lesions lined by bronchiolar epithelium [64]. Thus, it would appear that in CFA the ability of type II alveolar epithelial cells to restore damaged type 1 cells is seriously affected [2,64].

This chapter will present the results from a preliminary examination of the *in vitro* response of two murine lung epithelial cell lines to FITC treatment. The cell line CMT64/61 is a mouse lung carcinoma alveolar epithelial type II-like cell line, while mtCC1-2 cells are a murine Clara cell-like line, generated from the lungs of a transgenic mouse expressing the SV40 large T antigen under the control of a Clara cell-specific promoter [420]. Cultured cells exposed to FITC were examined for signs of damage, such as peeling or shape change, assessed for viability/cell death, and the cytokine profiles were evaluated by assaying supernatants.

7.1.1 Aims of Chapter

The principal aims of this chapter are:

- To describe the morphological *in vitro* effects FITC treatment had on the two epithelial cell lines
- To examine the effects of FITC treatment on the viability of the two cell lines
- To examine the effects of FITC treatment on the epithelial cell lines in terms of cytokine production
- To discuss the relevance of these *in vitro* findings in the context of CFA pathogenesis, and suggest directions for future *in vitro* study

7.2 Confluence of Plated Cell Lines

Epithelial cells in damaged lungs are often found at varying levels of confluence, due to denudation of the alveolar surface following injury, and the subsequent re-epithelialisation by the type II cells [2]. Therefore, in order to gauge the response of the epithelial cells to FITC at different levels of confluence, cells from the two cell lines were plated at three densities each, to achieve low, moderate, and complete confluence after overnight culture. This procedure involved trypsinising the cells, as described in sections 2.1.4 and 2.1.5, and plating them onto 24 well tissue culture plates containing 1 ml complete medium. CMT64/61 cells were plated at densities of $5x10^4$, 10^5, and $5x10^5$ cells/well, while slower-growing mtCC1-2 cells were plated at densities of 10^5, $5x10^5$, and 10^6 cells/well. Plates were incubated at 37°C in 5% CO_2 overnight. Table 7.1 shows the plating densities and estimated level of confluence achieved after overnight culture for both cell lines. Figures 7.1 and 7.2 demonstrate the level of confluence in the wells for each cell line at different plating densities.

Cell Line	Plating Density	Confluence	Corresponding Figure
mtCC1-2	10^5	LOW: 40-50%	7.1A
	$5x10^5$	MID: 70-80%	7.1B
	10^6	COMPLETE: 90-100%	7.1C
CMT64/61	$5x10^4$	LOW: 30-35%	7.2A
	10^5	MID: 50-60%	7.2B
	$5x10^5$	COMPLETE: 90-100%	7.2C

Table 7.1 Plating densities and resulting confluence of epithelial cell lines. Cells from each cell line were trypsinsed and plated onto 24 well plates at the densities indicated in the table. After overnight incubation at 37°C and 5% CO_2, confluence was estimated visually as a percentage of the area of the plate. Corresponding figures are provided.

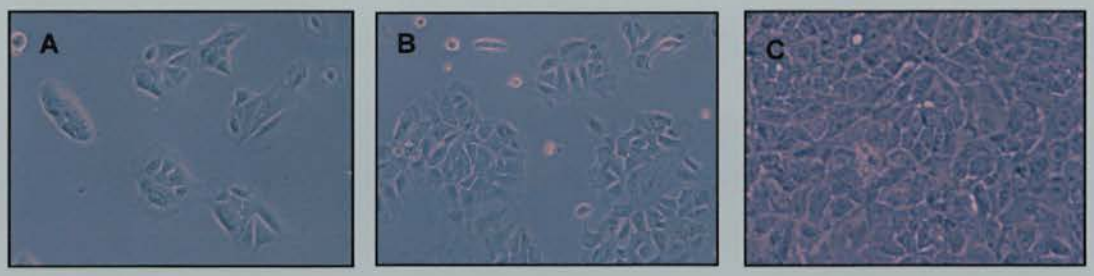

Figure 7.1 Confluence of mtCC1-2 cells after overnight incubation. Cells from the mtCC1-2 cell line were trypsinised and plated at 10^5 (A), $5x10^5$ (B), or 10^6 cells/well (C) of a 24 well plate, and cultured overnight at 37°C in 5% CO_2. Confluence was estimated visually. Original magnification x200.

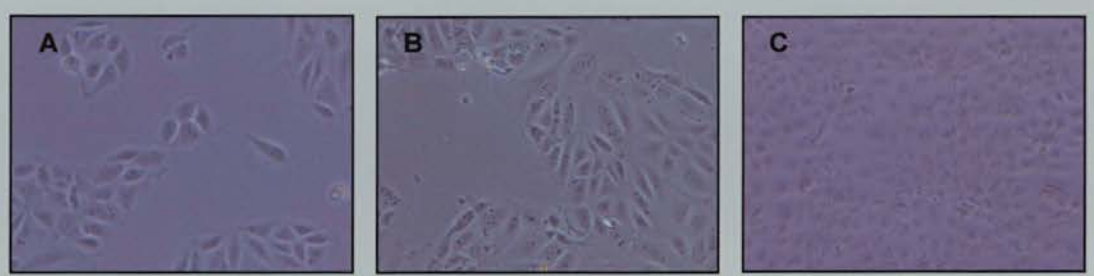

Figure 7.2 Confluence of CMT64/61 cells after overnight incubation. Cells from the CMT64/61 cell line were trypsinised and plated at $5x10^4$ (A), 10^5 (B), or $5x10^5$ cells/well (C) of a 24 well plate, and cultured overnight at 37°C in 5% CO_2. Confluence was estimated visually. Original magnification x200.

7.3 FITC Damage Assays

7.3.1 Method of Damaging Cells

After overnight incubation, medium was removed from all wells, and the cells were washed by pipetting 500 µl of warmed, serum-free medium onto the cells, swirling the plate, and removing the medium. Next, 500 µl of serum-free medium with the necessary additives was added to each well. Serum-free medium was used to avoid the possibility of FITC binding to the serum proteins. These additives were: no additives (serum-free medium alone), 1:80 dilution of DMSO, 2 µg/ml BSA as a negative control, 0.0003% H_2O_2 as a positive control, and FITC, dissolved in a 1:80 dilution of DMSO, at 0.05 mg/ml, 0.1 mg/ml, and 0.5 mg/ml. This was determined to be the optimal concentration of DMSO as it dissolved the FITC, but did not appear to alter the cells in any fashion. The high dose of FITC was chosen after preliminary experiments as it caused the most visible damage without excessive cell death. The plates were then incubated at 37°C and 5% CO_2 for 30 minutes, which was sufficient time to cause damage to the cells with the least amount of cell death, and the solutions then removed. Cells were washed once in complete medium, and 1 ml fresh, warmed complete medium was added to each well. The plates were then returned to the incubator for one, 12, or 24 hours.

7.3.2 FITC Damage Assay Results

Initial FITC damage assays were performed with FITC prepared as a colloidal suspension in PBS, as described in Appendix 1, and as used for *in vivo* administration. In the cell lines, however, the FITC particulates adhered to the cells and could not be washed off (Figure 7.3). Thus, for subsequent *in vitro* studies, FITC was dissolved in DMSO before being diluted 1:80 with medium. Appropriate controls (see below) showed that this dilution of DMSO did not affect either cell line.

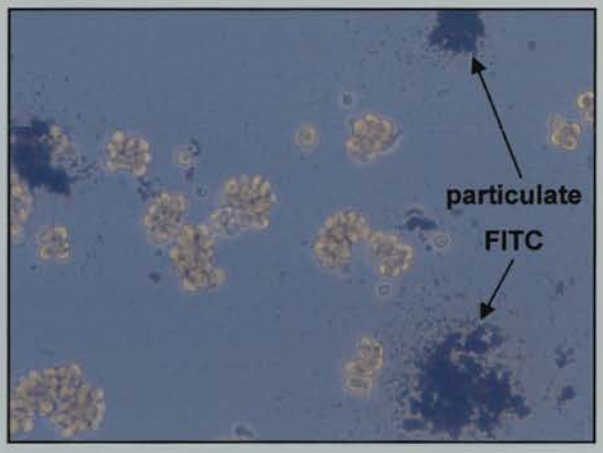

Figure 7.3 FITC in colloidal suspension (0.05 mg/ml) administered to CMT64/61 cells, after washing in an attempt to remove the FITC. FITC was suspended in PBS and administered to the cell line as described. After 30 minutes in culture, cells were washed to remove residual FITC. In colloidal suspension, FITC could not be removed from the wells, and caused extensive cell death to occur (cells rounded and lifting from wells). Original magnification x200.

7.3.3 MTS Assays for Cell Death

The CellTiter 96® AQ_{ueous} One Solution Cell Proliferation Assay (Promega Corporation, Madison, Wisconsin, USA) is a colorimetric method for determining the number of viable cells in proliferation or cytotoxicity assays. The MTS tetrazolium compound is bioreduced by cells into a formazan product that is soluble in tissue culture medium. The quantity of formazan product as measured by the amount of 490 nm absorbance is directly proportional to the number of living cells in culture.

After damaging the cells as described in the section above, 200 µl MTS tetrazolium compound was added to each well after one hour, 12 hours, and 24 hours. Plates were then incubated for a further two to three hours (manufacturer's instructions, one to four hours). From each well, 100 µl supernatant was added and pipetted into a single well of a 96 well plate. This was repeated a further two times for each well.

The absorbance of each well was then read at 490 nm on a Revelation 3.04 microplate reader (Dynex Tecnologies, Billinghurst, West Sussex, UK).

7.3.3.1 FITC Reduces Viability of CMT64/61 Cells

Figure 7.4 shows that CMT64/61 cells had increased viability over time, at all degrees of confluence. This viability was not affected by BSA, the DMSO solution in which FITC was dissolved, or FITC solution at 0.05 or 0.1 mg/ml, at any degree of confluence. Microscopically, there were also no visible changes apparent.

Cells at low confluence (Fig. 7.4A) showed greatly decreased viability when treated with H_2O_2, and this was also seen with FITC treatment at 0.5 mg/ml. The viability of the FITC-treated cells did not improve over time. This same pattern was seen for cells at mid confluence (Fig. 7.4B). Microscopically, most of the cells appeared rounded, and many had become detached from the plates (Figure 7.5).

When CMT64/61 cells had achieved complete confluence before treatment, H_2O_2 did reduce viability, but only to the same extent at one hour (Fig. 7.4C). This was seen as peeling around the edges of some of the cells, although most appeared normal. There was reduced viability at 12 and 24 hours after treatment, but it appears that the cells were able to recover and continue proliferating to some degree. Microscopically, however, the cells appeared normal. FITC treatment at 0.5 mg/ml caused slightly decreased viability at one hour, with many cells looking very rounded having become detached from the wells (Fig. 7.6).

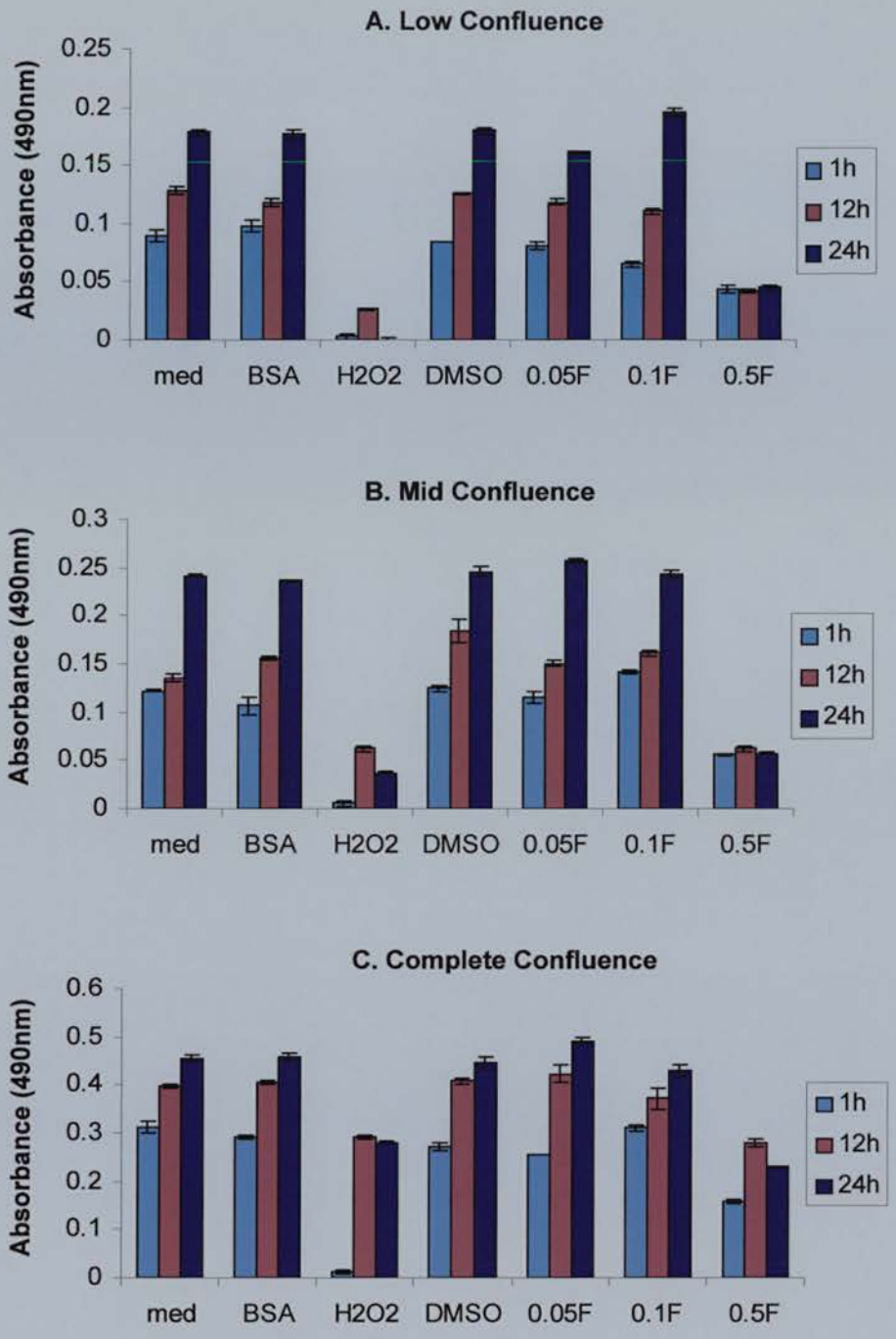

Figure 7.4 MTS assay for cellular respiration on treated CMT64/61 cells at low, mid and complete confluence. Cells were seeded into 24 well plates at $5x10^4$ cells/well (A), 10^5 cells/well (B), and $5x10^5$ cells/well (C) and cultured overnight at 37°C and 5% CO_2. Cells were treated as described, then given MTS 1 hour, 12 hours or 24 hours after treatment. Absorbance of the supernatants was then read at 490nm. Data are representative of three separate experiments, and are presented as mean ± SEM of triplicate wells. Med = serum-free medium alone, BSA = 2 μg/ml BSA (neg. control), H_2O_2 = 0.0003% H_2O_2 (positive control), DMSO = 1:80 dilution of DMSO in serum-free medium, 0.05F = 0.05 mg/ml FITC in DMSO/serum-free medium, 0.1F = 0.1 mg/ml FITC in DMSO/serum-free medium, 0.5F = 0.5 mg/ml FITC in DMSO/serum-free medium.

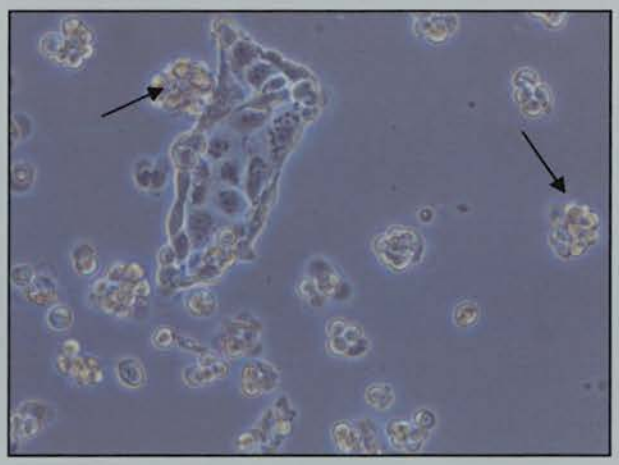

Figure 7.5 CMT64/61 cells at mid confluence, 12 hours after exposure to 0.5 mg/ml FITC. Many cells appear rounded, and are no longer adherent (arrows). CMT64/61 cells were plated at 10^5 cells/well in a 24 well plate and cultured overnight to achieve a mid level of confluence as described. After washing cells in serum-free medium, FITC solution (0.5 mg/ml in a 1:80 dilution of DMSO in serum-free medium) was applied for 30 minutes. Cells were washed again and incubated for 12 hours in medium containing serum.

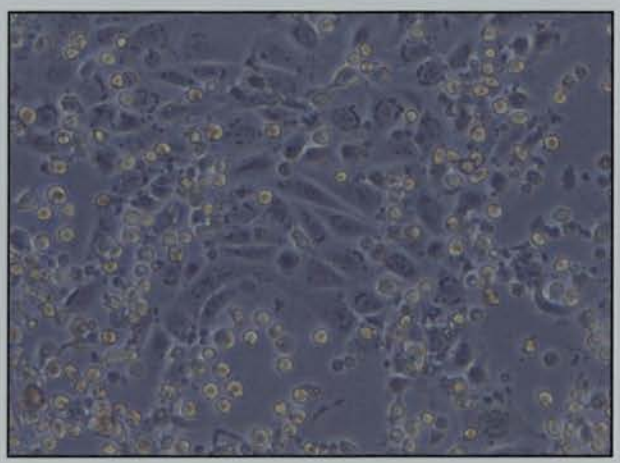

Figure 7.6 CMT64/61 cells at complete confluence, one hour after exposure to 0.5 mg/ml FITC. Many cells appear rounded, and are no longer adherent. CMT64/61 cells were plated at $5x10^5$ cells/well in a 24 well plate and cultured overnight to achieve a mid level of confluence as described. After washing cells in serum-free medium, FITC solution (0.5 mg/ml in a 1:80 dilution of DMSO in serum-free medium) was applied for 30 minutes. Cells were washed again and incubated for one hour in medium containing serum.

At 12 and 24 hours after treatment however, cell viability was again slightly reduced, but higher than at one hour, in contrast to the low and mid levels of confluence. Microscopically at these time points, there was still some rounding and detachment the FITC-treated cells.

7.3.3.2 FITC Does Not Affect Viability of mtCC1-2 Cells

The viability of mtCC1-2 cells treated at low and mid confluence levels was only affected by H_2O_2 (Figure 7.7A,B). Even 24 hours after treatment, cell viability was still low. Microscopically, most of these cells were rounded, with many to most having detached from the wells. Treatment of these cells with FITC, however, did not affect cell viability. At complete confluence, the addition of H_2O_2 had no effect on cell viability one hour after treatment, and only slightly decreased viability at 12 and 24 hours, although no visible changes could be seen in any of the cells (Figure 7.7C). None of the other treatments had an effect.

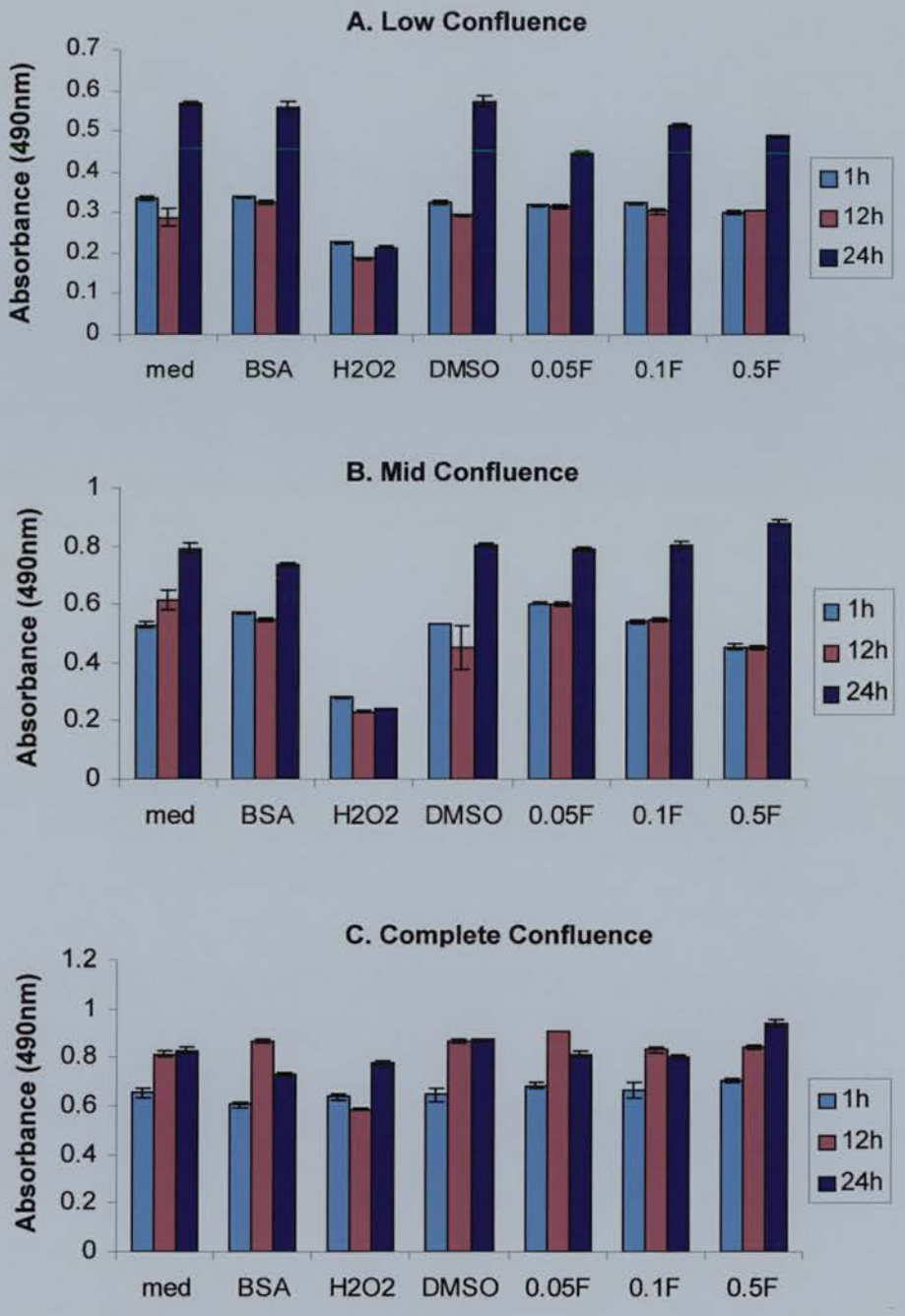

Figure 7.7 MTS assay for cellular respiration on treated mtCC1-2 cells at low, mid and complete confluence. Cells were seeded into 24 well plates at 10^5 cells/well (A), $5x10^5$ cells/well (B), and 10^6 cells/well (C) and cultured overnight at 37°C and 5% CO_2. Cells were treated as described, then given MTS 1 hour, 12 hours or 24 hours after treatment. Absorbance of the supernatants was then read at 490nm. Data are representative of three separate experiments, and are presented as mean ± SEM of triplicate wells. Med = serum-free medium alone, BSA = 2 μg/ml BSA (neg. control), H_2O_2 = 0.0003% H_2O_2 (positive control), DMSO = 1:80 dilution of DMSO in serum-free medium, 0.05F = 0.05 mg/ml FITC in DMSO/serum-free medium, 0.1F = 0.1 mg/ml FITC in DMSO/serum-free medium, 0.5F = 0.5 mg/ml FITC in DMSO/serum-free medium.

7.3.4 *In Vitro* FITC-treated Epithelial Cell Cytokine Production

Supernatants were collected at each time point (1h, 12h and 24h) after the damage experiments and were assayed for the presence of GM-CSF, TNF-α, IFN-γ, TGF-β, IL-1β, and MIP-1α as described in section 2.4.

7.3.4.1 FITC Does Not induce GM-CSF Production In Vitro

GM-CSF plays a complex role in the processes of both tissue repair and fibrosis at epithelial surfaces [305]. Transgenic overexpression of GM-CSF in the lung results in enhanced lung growth and alveolar type II epithelial cell hyperplasia [303]. Administration of GM-CSF-neutralising antisera to mice with bleomycin-induced pulmonary fibrosis increases hydroxyproline deposition in the lung, while in contrast, overexpression of GM-CSF using a recombinant replication-defective adenoviral vector results in fibrogenesis [301]. Following bleomycin-induced lung injury in mice, GM-CSF has a protective effect on repair processes [300,305]. GM-CSF also affects the maturation of dendritic cells and thus may affect their function [521].

No GM-CSF protein was detected in the supernatants from the CMT64/61 cell line. The addition of H_2O_2 did induce GM-CSF production in the mtCC1-2 cell line (Figure 7.8), however treatment with FITC did not induce cytokine production at any concentration or time point.

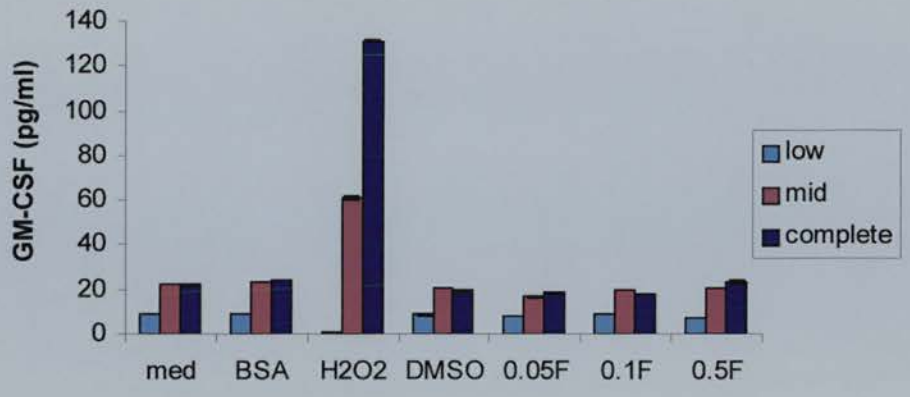

Figure 7.8 GM-CSF production by mtCC1-2 cells 24 hours after various treatments. Cells from the mtCC1-2 cell line were trypsinised and plated in 24 well plates at required densities to achieve low (10^5 cells/well), mid ($5x10^5$), or complete (10^6) confluence after overnight culture, as described previously. Cells were then subjected to various treatments and supernatants were collected after 1h, 12h or 24h and assayed for GM-CSF protein. The figure is representative of three individual experiments. Data are presented as mean ± SEM of triplicate wells. Med = serum-free medium alone, BSA = 2 μg/ml BSA (neg. control), H_2O_2 = 0.0003% H_2O_2 (positive control), DMSO = 1:80 dilution of DMSO in serum-free medium, 0.05F = 0.05 mg/ml FITC in DMSO/serum-free medium, 0.1F = 0.1 mg/ml FITC in DMSO/serum-free medium, 0.5F = 0.5 mg/ml FITC in DMSO/serum-free medium.

7.3.4.2 FITC Does Not Induce TNF-α Production In Vitro

Several studies have shown that hyperplastic type II AECs in fibrotic lungs constitute the main site of synthesis of TNF-α and TGF-β [276,277,393]. In human CFA, compared with cells from normal lungs, TNF-α immunoreactivity is increased in hyperplastic type II AECs lining the thickened septae, compared with cells from normal lungs [296]. In mice, TNF-α can stimulate fibroblast replication and collagen synthesis *in vitro*, and pulmonary TNF-α gene expression increases after administration of bleomycin [220]. Transgenic mice overexpressing TNF-α in alveolar epithelium have also been shown to develop pulmonary fibrosis [292]. However, it has also been demonstrated that overexpression of TNF-α alone in mouse lungs was unable to produce significant pulmonary fibrosis [288]. In the

context of the abnormal wound-healing model of CFA therefore, TNF-α release from damaged AECs could have considerable profibrotic effects and be a major contributor to the pathogenesis of CFA [266].

No TNF-α production was detected in the supernatants from either cell line, at any time point, with any treatment.

7.3.4.3 FITC Does Not Induce IFN-γ Production In Vitro

As discussed in Chapter 1, IFN-γ is a Th1-type cytokine that can be produced by type II AECs, and may have antifibrotic effects [255,258]. It inhibits fibroblast collagen synthesis *in vitro*, and attenuates bleomycin-induced lung fibrosis when administered to mice [256]. IFN-γ mRNA has been shown by *in situ* hybridisation to be present in human lung biopsies of patients with CFA, but the protein is not translated, as shown by immunohistochemistry [100]. Diminished IFN-γ reported in patients with CFA therefore could enhance collagen accumulation [250]. This supports the suggestion that a balance of positively and negatively regulating cytokines might modulate the fibrotic response to injury [83].

No IFN-γ protein was detected in the supernatants from either cell line, at any time point, with any treatment.

7.3.4.4 FITC Does Not Induce IL-1β Production In Vitro

IL-1 is an important cytokine in both acute and chronic inflammation. The IL-1 gene family has three known constituents, of which IL-1β is the most prominent in the propagation of inflammation [306].

There are several human and animal studies which have demonstrated the presence of IL-1β in chronic inflamed tissues and in tissues undergoing fibrogenesis [230,307-309]. Adenoviral IL-1β gene transfer causing transient overexpression of IL-1β in the epithelial cells of rodent lung induces acute inflammation with alveolar tissue destruction resulting in progressive interstitial fibrosis, which coincides with sustained induction of the TGF-β [306]. Together, these data could indicate a critical role for IL-1β in the induction of acute and chronic inflammation, and potentially, in CFA.

No IL-1β protein was detected in the supernatants from either cell line, at any time point, with any treatment.

7.3.4.5 FITC Does Not Induce MIP-1α Production In Vitro

As discussed in Chapter 1, MIP-1α is a member of the C-C chemokine supergene family, and has been found to be associated with interstitial lung disease [337]. There are several roles MIP-1α could play in CFA, including recruiting and activating macrophages which subsequently secrete profibrotic factors or it may be directly stimulating fibroblasts to proliferate and deposit ECM [222].

No MIP-1α protein was detected in the supernatants from either cell line, at any time point, with any treatment.

7.3.4.6 FITC Does Not Affect TGF-β1 Production In Vitro

TGF-β1 is well known to be important in the pathogenesis of animal models of pulmonary fibrosis and in human fibrotic lung diseases [262]. *In vitro*, conversion of latent to active TGF-β1 during epithelial wound repair occurs quickly, and TGF-β1

speeds epithelial repair in 16HBE 14o$^-$ bronchial epithelial-derived cells after damage by multiple scoring [261].

TGF-β1 is a directly fibrogenic cytokine, based on studies demonstrating that TGF-β1 protein, when overexpressed locally within the lung, can lead directly to fibrogenesis with induction of myofibroblasts, which is histologically very reminiscent of CFA [67,272]. In a study of several different interstitial lung disorders, TGF-β1 was shown to be expressed mainly in AMs in early fibrotic lungs, characterised by inflammation and minimal fibrosis, but in advanced fibrotic honeycomb lesions primarily seen in CFA, it was mainly present in epithelial cells [278]. Selman *et al.* [48] therefore speculate that fibrosis occurs where there is epithelial expression of TGF-β1.

FITC treatment had no effect on the production of total (latent + active) or active TGF-β1 protein, in the supernatants from either cell line, at any time point.

7.4 Conclusions and Discussion

The body of work presented in this chapter was a preliminary investigation into the *in vitro* effects of FITC on lung epithelial cells.

7.4.1 MTS Assays for Cell Death

The MTS assays for cell death and viability showed that for the CMT64/61 cell line, an alveolar epithelial type II-like cell line, FITC caused the most cell death when the cells were at low and mid confluence (Figure 7.4A, B), and this did not change over time. At complete confluence, however, while cell viability was slightly reduced at one hour, at 12 and 24 hours there was relatively increased viability, and microscopically fewer cells had rounded and lifted from the plates. These results suggest that while FITC appears able to damage and/or kill type II-like mouse lung epithelial cells, when they are at a high level of confluence, as would be expected in normal mouse lung, either the damaged cells are able to recover and proliferate, or surrounding, undamaged cells proliferate in their place.

As discussed in Chapter 4, a single intratracheal dose of FITC was not sufficient to induce pulmonary fibrosis in mice. It would therefore be interesting to administer a second dose of FITC to the treated CMT64/61 epithelial cells to determine if they are able to recover as efficiently as after the first dose of FITC. It would also be beneficial to continue these studies beyond the 24 hour time point.

Interestingly, FITC treatment did not affect the cell viability or microscopic appearance of the Clara cell-like mtCC1-2 cell line (Figure 7.7). Clara cells are the nonciliated secretory cells lining the bronchiolar epithelium and are involved in the repair of damaged airways [420]. It may be that Clara cells, being found higher up in the airways, are more resistant to damage than the fragile AECs.

The mtCC1-2 cell line appeared to be more resistant to the effects of FITC than the type II-like cell line, suggesting that this may also be the case *in vivo*. While Clara cells may contribute to the repair processes after FITC administration *in vivo*, these results suggest that FITC may not affect the bronchiolar epithelium at the dose used, but instead causes critical damage deeper in the airways at the level of the alveolar epithelium. Future *in vitro* work could involve administering higher doses of FITC to the mtCC1-2 cells and, as with the CMT64/61 cells, examining later time points after damage.

The particulate nature of the *in vivo* FITC solution appeared to contribute to the patchy nature of the disease, making it particularly relevant to the study of human CFA. However, it was not possible to use the particulate solution of FITC on these cells lines, as was used in the *in vivo* experiments, and thus it is difficult to draw parallels between the two systems.

It is also important to note that these cell lines may not completely accurately represent the behaviour of normal lung epithelial cells, perhaps being more protective than *in vivo* cells, and these experiments would ideally be repeated on primary cell cultures in the future.

7.4.2 Cytokine Production

Although FITC treatment did not induce the production of any of the cytokines for which the supernatants were examined in either cell line, this avenue of investigation is still worth pursuing. The cells were not completely unresponsive, as shown by the production of GM-CSF from the H_2O_2-treated mtCC1-2 cell line, although further controls, such as TNF administration, or assaying for lactate dehydrogenase, may prove useful.

Although the cytokine assays were negative, this does not mean cytokines were not being produced. It may be that the cytokines were simply too diluted to be detected

by the assays used, and these experiments could be repeated while culturing the cell lines in a lower volume of medium. Examining the supernatants at later time points may also provide different results. Finally, mRNA analysis of the cell lines would perhaps also be even more useful, as protein production may not necessarily reflect expression of cytokine mRNA [101,522]. Ideally however, as mentioned above, primary cultures of lung epithelial cells would provide the most useful information in future work.

CHAPTER 8

Final Summary and Discussion

"If our knowledge of medicine were sufficient, the diagnostic process, starting with assessment of the clinical symptoms and signs, should progress through elucidation of the underlying structural abnormalities and disturbances of function to knowledge of the cause or causes of all these phenomena. Unfortunately, it is only in a few contexts that knowledge is sufficient to permit this process to be carried to completion...."

John Guyett Scadding, 1970 [523]

This final chapter will briefly summarise the results, discuss possible implications in terms of application to CFA, and suggest directions for future work.

8.1 Summary of Results

The following results have arisen from the work detailed in this thesis:

- A single FITC dose administered nonsurgically into the trachea was not sufficient to induce fibrosis in BALB/c mice, but a second dose administered six weeks after the first induced fibrosis in the majority of mice (Chapters 3 and 4).

- A single intratracheal FITC dose induced a pattern consistent with acute lung injury that persisted for up to five days. This was characterised by acute inflammation in the lungs that resolved by seven days after FITC administration. Cellular infiltrate in the tissues was initially granulocytic, becoming monocytic by Day 5 when T lymphocytes became prominent, particularly in areas of alveolar wall oedema. Few B cells were apparent, although at Day 7 they appeared to localise to areas with dense collections of cells. FITC deposition had become patchy by Day 5, and was localised around bronchi and blood vessels and in AMs (Chapter 3).

- The method devised to score the inflammatory response confirmed that the FITC-induced inflammation was mild initially, becoming moderate by Day 7, as compared to the control mice (Chapter 3).

- PMNs were significantly increased in the BAL fluid from FITC-treated mice one day after the initial FITC dose, and gradually returned to normal levels by Day 7. TGF-β protein was expressed throughout the lung on structural and immune cells, particularly AMs, peaking at Day 5. MHC class II^+ cells with dendritic-like processes were present and were often localised to areas of alveolar wall oedema and cell aggregation (Chapter 3).

- Increased levels of the proinflammatory cytokine TNF-α were found in the BAL fluid of acute phase FITC-treated mice, peaking at Day 1 and gradually decreasing over the seven days, but were consistently higher than those of control mice. No significant changes in IFN-γ or TGF-β levels were seen in the BAL fluid (Chapter 3).

- The long-term response to FITC, gauged from six weeks after the first dose up to 14 weeks after the second dose, was characterised by a predominantly mononuclear cell infiltrate after the second dose, which was present at all subsequent time points. Fewer lymphocytes were present, although the infiltrate still consisted mostly of T cells, with some B cells. A small number of strongly staining MHC class II^+ cells were evident in the tissues, and in the B cell aggregates present from six weeks after the second dose of FITC. At 14 weeks after the second dose of FITC there were areas of severe fibrosis with obliteration of alveolar wall architecture and large fibrous deposits next to areas of normal tissue. Patchy FITC distribution was evident at all time points, and was often found in conjunction with alveolar wall thickening, fibrous tissue deposition, and B cell aggregates (Chapter 4).

- The severity of fibrosis in FITC-positive fields increased with time, as determined by the modified Ashcroft scoring method for quantifying fibrosis (Chapter 4).

- TGF-β staining was present in the lung tissue at all long-term time points, although at a lower intensity than at acute time points (Chapter 4).

- TGF-β, IFN-γ and TNF-α levels were not detected in the BAL fluid of mice at long-term time points (Chapter 4).

- Cell isolates obtained from murine lung tissue by adapting several methods from other groups were phenotypically consistent with DCs (Chapter 5). Although they were in a mixed population, contaminating cells did not interfere with proliferation assay results. BAL isolates were phenotypically consistent with AMs.

- FITC DCs appeared to be less efficient at stimulating T cell proliferation *in vitro* than PBS DCs at later time points, and induced the production of IL-13, suggesting they may polarise towards a Th2-type cytokine response in FITC-treated lungs (Chapter 6). IFN-γ was also detected in the supernatants, which may enhance the inflammatory response, or be an attempt to redress the Th2 cytokine imbalance.

- FITC BAL AMs appeared to be more efficient at stimulating T cell proliferation *in vitro* than PBS BAL AMs, and preliminary results showed they also induced IL-13 production (Chapter 6). IFN-γ production was decreased at 14 weeks after the second dose, possibly supporting a role for BAL AMs to contribute to the Th2 response.

- The addition of FITC to epithelial cell lines *in vitro* decreased viability of the type II AEC-like line, but had no effect on viability of the Clara cell-type

line, possibly because cells higher up in the airways are less susceptible to injury (Chapter 7).

8.2 General Discussion and Suggestions for Future Work

Because CFA is, by definition, of unknown aetiology, induced animal models have an intrinsic fault. However, each animal model has its own unique features that allow for multiple avenues of investigation, and help to partly establish pathways of lung injury leading to fibrosis.

The two-dose, nonsurgical model of FITC-induced pulmonary fibrosis characterised in this thesis has proved to be a useful model for examining the role of chronic inflammation in the mechanisms that lead to pulmonary fibrosis. The initial lung injury with accompanying acute inflammation appeared to shift to a more chronic pattern, but was prevented from resolving by the second dose of FITC. This second dose eventually led to a chronic, progressive disease state with a moderate, persistent inflammation and increasing severity of fibrotic changes in areas of FITC deposition. As well, the presence of B cell aggregates suggests a humoral response may also be present and indeed likely, as anti-FITC antibodies have been demonstrated in the original single-dose surgical model [243,244].

As discussed, this model requires optimisation in terms of physical accuracy of dosing, and in terms of accuracy in amount of FITC delivered, to ensure consistency between animals. Ideally, it should also be extended to later time points in order to better determine the nature of the long-term response. Further immunohistochemical staining for CD4 and CD8 T cells would also be beneficial to establish the nature of the lymphocytic infiltration.

Although the presence of chronic inflammation is subject to debate when considering the pathogenesis of CFA [5], an unremitting profibrotic inflammatory response is a

cause of dysregulated fibrogenesis, and an animal model of pulmonary fibrosis that also has localised injury, is progressive in nature and may be immunologically mediated has great potential and application to the human disease.

Although TGF-β was not detected in the BAL fluid, it seems highly unlikely that this profibrotic cytokine would not be involved in the fibrotic process, and indeed, the presence of TGF-β in the tissues, demonstrated by immunohistochemistry, suggests otherwise. As discussed, BAL protein levels are not necessarily reflective of tissue processes, and ideally, mRNA analysis of BAL AMs and lung tissue should be performed for all cytokines mentioned to develop an accurate cytokine profile. The use of specific antibodies to cytokines and transgenic mouse strains deficient in certain cytokines would also provide clues to the pattern of cytokine involvement in FITC-induced pulmonary fibrosis.

The finding that lung DCs and AMs from FITC-treated mice may polarise T cells towards a Th2-type response by the induction of IL-13 production is particularly exciting, given the "Th2 cytokine hypothesis" of lung fibrosis [6,83], and the growing interest in the role of IL-13 in pulmonary fibrosis [79,85,102,327,332]. An interesting avenue of investigation in this respect would be the MCP-mediated CCR2-dependent proinflammatory and profibrotic functions of IL-13 and TGF-β [494], particularly as the importance of CCR2 in the profibrotic cytokine cascade of FITC-induced pulmonary fibrosis has been demonstrated [62].

The reciprocal T cell-stimulating abilities of lung DCs vs. AMs are intriguing. Certainly, the preliminary results obtained for the FITC AMs should be repeated to establish if they are indeed more efficient stimulators, and most importantly, both cell types from FITC- and PBS-treated mice should be phenotyped. The lack of IL-10 or IL-12 in the supernatants from DC experiments seems unlikely, and mRNA analysis would be the logical next step.

It is likely that the cytokine milieu in the FITC-treated lungs is altering the antigen-presenting capacities of both APC types, and for the DCs, in a GM-CSF-independent

fashion. The apparent immature state of the DCs fits well with the Th2 cytokine hypothesis, as immature DCs, or DC2s, are known to skew T cells towards Th2-type responses [171]. It has been suggested that DCs could be responsible for maintaining a chronic localised immune response in asthmatic airways [372], and this may also hold true for FITC-induced fibrotic lungs. Chronic inflammation and structural changes in the airways could lead to local DC maturation and antigen presentation occurring in the asthmatic airways [372], but equally, perhaps chronic inflammation could participate in maintaining the DCs in an immature state, particularly in fibrotic lungs, suggesting a point of divergence for these two disease states.

DCs, but not AMs, were seen in B cell aggregates, and it may be that this local microenvironment could contribute to the behaviour of the DCs. It has been shown that chronic antigen presentation by DCs leads to neoformation of organized lymphoid structures within peripheral tissues, such as the pancreas [524], and Lambrecht [372] speculates that repetitive presentation of antigen to Th2 cells by DCs in asthmatic airways could also lead to formation of these aggregates; perhaps again, this could apply to the fibrotic lung as well. Additionally, DCs might directly interact with B cells in the airways to enhance immunoglobulin production [372].

However, if TGF-β and/or IL-10 levels are revealed to be increased in the tissue of FITC-treated mice, the concept of "tolerogenic" DCs could also be explored, as both these cytokines have been shown to induce tolerance in DCs [492,525].

Although the cell line experiments were largely unrevealing, the decreased viability of the type II AEC-like line is interesting, and should be repeated on primary type II cell cultures. If Clara cells are more resistant to the injurious effects of FITC, this could be another avenue for investigation. Certainly, all the experiments described for the cell lines would bear repeating on primary cell cultures.

In conclusion, the key question in CFA is why do some lungs heal with fibrosis, whereas others are restored to a virtually normal state? Appropriate therapy relies on

the correct understanding of the nature of the lung's response to injury, and although the mechanisms remain elusive, some facts are becoming clearer. Pulmonary inflammation and fibrosis in the FITC-induced model and indeed, in CFA, most likely occur via more than one pathway. These processes are undoubtedly very complex and involve multiple interactions among inflammatory cells, lung parenchymal cells, and their products. Animal models of this disease play an essential role in directing research towards the understanding of the mechanisms of pulmonary fibrosis in humans, and with advances such as the recent cloning of the entire mouse genome [526], will hopefully lend significant insight into these processes with the aim of improving therapeutic strategies and halting the downward clinical progression of human CFA.

APPENDICES

Appendix 1: Reagent Recipes

A1.1 Avertin (tribromoethanol anaesthetic)

For 200 ml:

- 2.5g 2,2,2-tribromoethanol (Aldrich)
- 5 ml 2 methy-2-butanol (tertiary amyl alcohol))
- 200 ml dH_2O

Tribromoethanol and tertiary amyl alcohol were mixed on a heated stirrer until all crystals dissolved, then distilled H_2O was added until totally dispersed. This solution is stored at 4°C protected from light, and warmed to 37°C before use. Dose: 0.2 ml up to10g body weight given intraperitoneally.

A1.2 Flow Cytometry

A1.2.1 Flow buffer

- PBS
- 1% (w/v) BSA
- 0.05% (w/v) NaN_3
- Stored at 4°C.

A1.2.2 Flow fix

- PBS
- 2% (w/v) formaldehyde
- Stored at room temperature.

A1.3 MACS Buffer

- 0.5% BSA in PBS
- Filter sterilised and stored at 4°C.

A1.4 Particulate FITC Solution

- 2 mg/ml FITC in sterile PBS

FITC powder was weighed out, then diluted with sterile PBS, and pipetted vigorously until no remaining particles were visible. The solution was always prepared fresh.

Appendix 2: Unpublished Data from Original FITC Model

The following images are unpublished data from the work of Roberts *et al.* [243] on the original one-dose surgical FITC-induced model of pulmonary fibrosis.

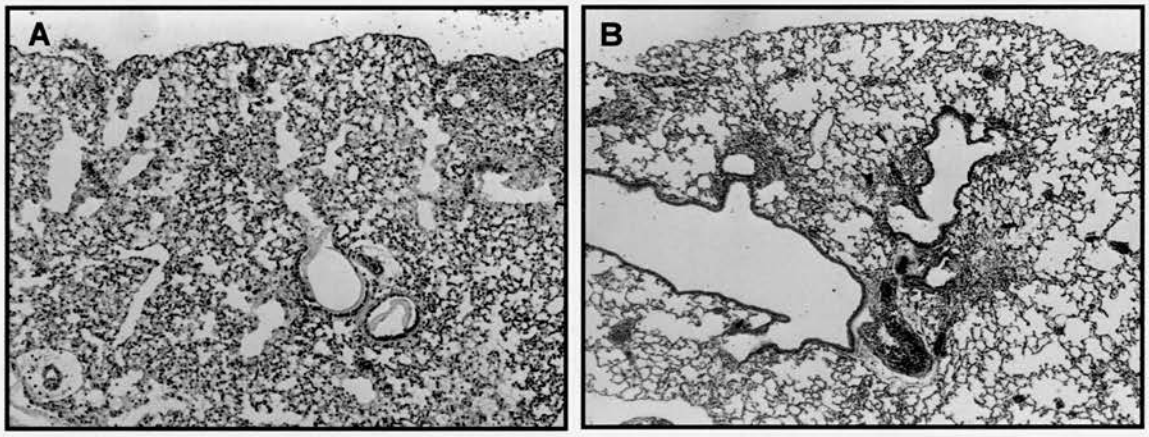

Figure A2.1 FITC-treated SCID mice (A) show severe inflammation three days after instillation similar to that seen in immunocompetent FITC-treated mice (B). Original magnification x100.

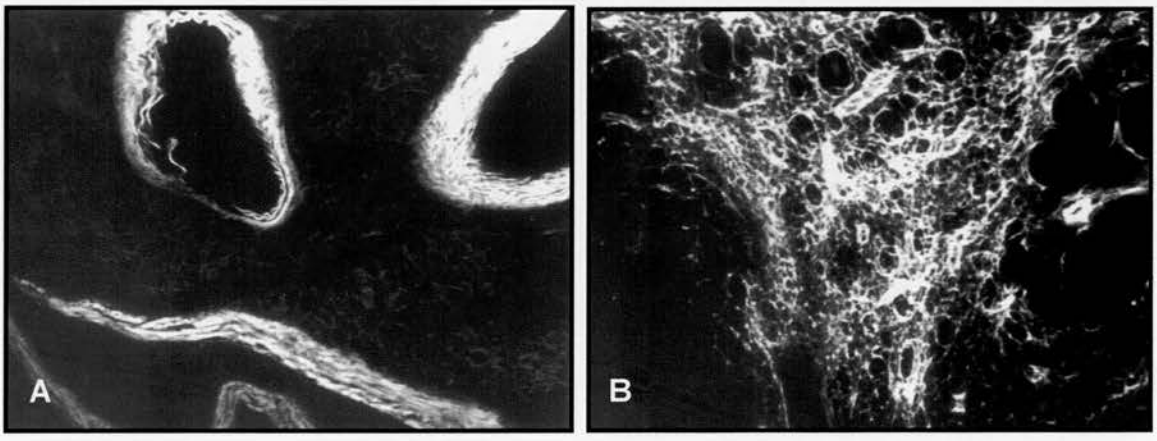

Figure A2.2 Three months after FITC instillation, fluorescent FITC was visible in the lungs of both SCID (A) and immunocompetent (B) mice. Original magnification x100.

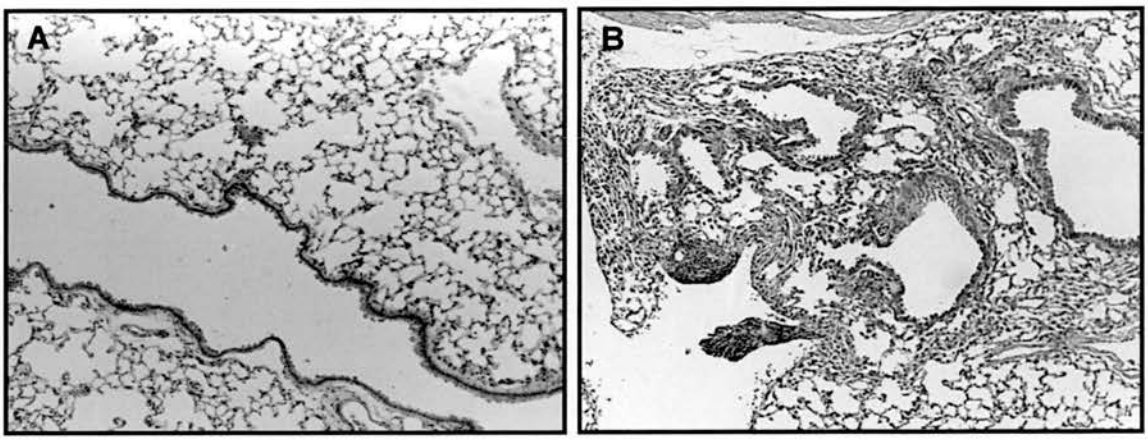

Figure A2.3 Despite the presence of FITC, three months after FITC instillation, no scarring or infiltrate was seen in the lungs of SCID mice (A), in direct contrast to the scarring and infiltrate found in the lungs of the immunocompetent mice (B) at the same time point. Original magnification x100.

Appendix 3: Publications Arising from the Work Detailed in this Thesis

1. Ahmad SA, Lamb JRL, Howie SEM. Differential induction of Th1 and Th2 cytokines by dendritic cells and alveolar macrophages from fibrotic lungs [in preparation].

2. Stewart GA, Hoyne GF, Ahmad SA, Jarman E, Wallace WA, Harrison DJ, Haslett C, Lamb JR, Howie SE. Expression of the developmental Sonic hedgehog (Shh) signalling pathway is upregulated in chronic lung fibrosis and the Shh receptor patched 1 is present in circulating T lymphocytes. *J Pathol* 2002 [in press].

3. Ahmad SA, Stewart G, McBride S, Hoyne GF, Lamb JR, Howie SEM. Dendritic cells in a murine model of lung fibrosis. *Keystone Symposium. Dendritic cells: interfaces with immunobiology and medicine 2001* [abstract].

4. Ahmad SA, McBride S, Lamb JR, Howie SEM. Lung APC from a murine model of lung fibrosis induce less antigen-specific T cell proliferation than controls. *Immunology* 2001;*104Supplement1*:71 [abstract].

5. Ahmad SA, McBride S, Howie SEM. Isolation of dendritic cells from murine lungs. *Immunology* 1999;*98Supplement1*:38 [abstract].

REFERENCES

1. **Crystal RG, Bitterman PB, Rennard SI, Hance AJ, Keogh BA**. Interstitial lung diseases of unknown cause. Disorders characterized by chronic inflammation of the lower respiratory tract. *N Engl J Med* 1984;*310*:235-44.

2. **Kasper M, Haroske G**. Alterations in the alveolar epithelium after injury leading to pulmonary fibrosis. *Histol Histopathol* 1996;*11*:463-83.

3. **Mercer RR, Crapo JD**. Normal anatomy and defense mechanisms of the lung. In: Baum GL, Crapo JD, Celli BR, Karlinsky JB. eds. *Textbook of pulmonary diseases*. 6 Ed. Philadelphia: Lippincott-Raven Publishers, 1998:23-45.

4. **Martinet Y, Menard O, Vaillant P, Vignaud JM, Martinet N**. Cytokines in human lung fibrosis. *Arch Toxicol* 1996;*Supplement. 18*:127-39.

5. **Gauldie J, Strieter RM**. Pro/con editorial: inflammatory mechanisms are/are not a minor component of the pathogenesis of idiopathic pulmonary fibrosis. *Am J Respir Crit Care Med* 2002;*165*:1205-8.

6. **Sime PJ, O'Reilly KMA**. Fibrosis of the lung and other tissues: new concepts in pathogenesis and treatment. *Clin Immunol* 2001;*99*:308-19.

7. **Gauldie J, Kolb M, Sime PJ**. A new direction in the pathogenesis of idiopathic pulmonary fibrosis? *Respir Res* 2002;*3*:1-3.

8. **Crouch E**. Pathobiology of pulmonary fibrosis. *Am J Physiol* 1990;*259*:L184

9. **Cherniack RM, Crystal RG, Kalica AR**. Current concepts in idiopathic pulmonary fibrosis: a road map for the future. *Am Rev Respir Dis* 1991;*143*:680-3.

10. **Katzenstein AL, Myers JL**. Idiopathic pulmonary fibrosis: clinical relevance of pathologic classification. *Am J Respir Crit Care Med* 1998;*157*:1301-15.

11. **American Thoracic Society**. Idiopathic pulmonary fibrosis: diagnosis and treatment. International consensus statement. *Am J Respir Crit Care Med* 2000;*161*:646-64.

12. **Crystal RG, Bitterman PB, Mossman BT, Schwarz MI, Sheppard D, Almasy L, Chapman HA, Friedman SL, King TE, Jr., Leinwand LA, Liotta L, Martin GR, Schwartz DA, Schultz GS, Wagner CR, Musson RA**. Future research directions in idiopathic pulmonary fibrosis. Summary of a National Heart, Lung, and Blood Institute working group. *Am J Respir Crit Care Med* 2002;*166*:236-46.

13. **Selman M, Pardo A**. Pathogenic mechanisms in the development of diffuse pulmonary fibrosis. *Braz J Med Biol Res* 1996;*29*:1117-26.

14. **Ward PA, Hunninghake GW**. Lung inflammation and fibrosis. *Am J Respir Crit Care Med* 1998;*157*:S123-S129

15. **Cook DN, Brass DM, Schwartz DA** . A matrix for new ideas in pulmonary fibrosis. *Am J Respir Cell Mol Biol* 2002;*27*:122-4.

16. **Gross TJ, Hunninghake GW**. Idiopathic pulmonary fibrosis. *N Engl J Med* 2001;*345*:517-25.

17. **Hamman L, Rich AR**. Fulminating diffuse interstitial fibrosis of the lungs. *Trans Am Clin Climatol Assoc* 1935;*51*:154-63.

18. **Scadding JG**. Fibrosing alveolitis. *Br Med J* 1964;*2*:686

19. **Ryu JH, Colby TV, Hartman TE**. Idiopathic pulmonary fibrosis: current concepts. *Mayo Clin Proc* 1998;*73*:1085-101.

20. **Liebow AA**. Definiton and classification of interstitial pneumonias in human pathology. *Prog Respir Res* 1975;*8*:1-31.

21. **Crystal RG, Fulmer JD, Roberts WC, Moss ML, Line BR, Reynolds HY**. Idiopathic pulmonary fibrosis: clinical, histologic, radiographic, physiologic, scintigraphic, cytologic and biochemical aspects. *Ann Intern Med* 1976;*85*:769-188.

22. **Winterbauer RH, Hammar SP, Hallman KO**. Diffuse interstitial pneumonitis: clinicopathologic correlations in 20 patients treated with prednisone/azathioprine. *Am J Med* 1978;*65*:661-72.

23. **Turner-Warwick M, Burrows B, Johnson A**. Cryptogenic fibrosing alveolitis: clinical features and their influence on survival. *Thorax* 1980;*35*:171-80.

24. **Cherniack RM, Colby TV, Flint A, Thurlbeck WM, Waldron JA, Jr., Ackerson L, Schwarz MI, King TE, Jr.** Correlation of structure and function in idiopathic pulmonary fibrosis. *Am J Respir Crit Care Med* 1995;*151*:1180-8.

25. **Nicholson AG, Colby TV, du Bois RM, Hansell DM, Wells AU**. The prognostic significance of the histologic pattern of interstitial pneumonia in patients presenting with the clincal entity of cryptogenic fibrosing alveolitis. *Am J Respir Crit Care Med* 2000;*162*:2213-7.

26. **Flaherty KR, Travis WD, Colby TV, Toews GB, Kazerooni EA, Gross BH, Jain A, Strawderman III RL, Flint A, Lynch III JP, Martinez FJ**. Histopathologic variablility in usual and nonspecific interstitial pneumonias. *Am J Respir Crit Care Med* 2001;*164*:1722-7.

27. **Nicholson AG**. Classification of idiopathic interstitial pneumonias: making sense of the alphabet soup. *Histopathology* 2002;*41*:381-91.

28. **Demedts M, Wells AU, Costabel U, Hubbard R, Cullinan P, Slabbynck H, Rizzato G, Poletti V, Verbeken EK, Thomeer MJ, Kokkarinen J, Dalphin JC, Taylor AN**. Interstitial lung diseases: an epidemiological overview. *Eur Respir J* 2001;*18*:2s-16s.

29. **Scott J, Johnston I, Britton J** . What causes cryptogenic fibrosing alveolitis? A case-control study of environmental exposure to dust. *Br Med J* 1990;*301*:1015-7.

30. **Coultas DB, Zumwalt RE, Black WC, Sobonya RE**. The epidemiology of interstitial lung diseases. *Am J Respir Crit Care Med* 1994;*150*:967-72.

31. **Schwartz DA, Helmers RA, Galvin JR, Van Fossen DS, Frees KL, Dayton CS, Burmeister LF, Hunninghake GW**. Determinants of survival in idiopathic pulmonary fibrosis. *Am J Respir Crit Care Med* 1994;*149*:450-4.

32. **Mannino DM, Etzel RA, Parrish RG**. Pulmonary fibrosis deaths in the United States. *Am J Respir Crit Care Med* 1996;*153*:1548-52.

33. **Johnston I, Britton J, Kinnear W, Logan R**. Rising mortality from cryptogenic fibrosing alveolitis. *Br Med J* 1990;*301*:1017-21.

34. **Johnston ID, Prescott RJ, Chalmers JC, Rudd RM**. British Thoracic Society study of cryptogenic fibrosing alveolitis: current presentation and initial management. *Thorax* 1997;*52*:38-44.

35. **Bjoraker JA, Ryu JH, Edwin MK, Myers JL, Tazelaar HD, Schroeder DR, Offord KP**. Prognostic significance of histopathologic subsets in idiopathic pulmonary fibrosis. *Am J Respir Crit Care Med* 1998;*157*:199-203.

36. **Mageto YN, Raghu G**. Genetic predisposition of idiopathic pulmonary fibrosis. *Curr Opin Pulm Med* 1997;*3*:336-40.

37. **Marshall RP, McAnulty RJ, Laurent GJ**. The pathogenesis of pulmonary fibrosis: is there a fibrosis gene?. *Int J Biochem Cell Biol* 1997;*29*:107-20.

38. **Marshall RP, Puddicombe A, Cookson WO, Laurent GJ**. Adult familial cryptogenic fibrosing alveolitis in the United Kingdom. *Thorax* 2000;*55*:143-6.

39. **Bitterman PB, Rennard SI, Keogh BA, Wewers MD, Adelberg S, Crystal RG**. Familial idiopathic pulmonary fibrosis: evidence of lung inflammation in unaffected family members. *N Engl J Med* 1986;*314*:1343-7.

40. **Raghu G, Mageto YN**. Genetic predisposition of interstitial lung disease. In: Schwarz MI, King TE, Jr. eds. *Interstitial Lung Disease*. Hamilton, Ontario: BC Decker, 1998:

41. **Bitterman PB, Crystal RG**. Is there a fibrotic gene? *Chest* 1980;*78*:549-50.

42. **Fujita J, Yoshinouchi T, Ohtsuki Y, Tokuda M, Yang Y, Yamadori I, Bandoh S, Ishida T, Takahara J, Ueda R**. Non-specific interstitial pneumonia as pulmonary involvement of systemic sclerosis. *Ann Rheum Dis* 2001;*60*:281-3.

43. **White B, Moore WC, Wigley FM, Xiao HQ, Wise RA**. Cyclophosphamide is associated with pulmonary function and survival benefit in patients with scleroderma and alveolitis. *Ann Intern Med* 2000;*132*:947-54.

44. **Korfhagen TR, Swantz RJ, Werts E**. Respiratory epithelial cell expression of human transforming growth factor-alpha induces lung fibrosis in trangenic mice. *J Clin Invest* 1994;*93*:1691-9.

45. **Sanderson N, Factor V, Nagy P, Kopp JB, Kondaiah P, Wakefield L, Roberts AB, Sporn MB, Thorgeirsson SS**. Hepatic expression of mature transforming growth factor β results in multiple tissue lesions. *Proc Natl Acad Sci USA* 1995;*92*:2572-6.

46. **Briggs DC, Vaughan RW, Welsh KI, Myers A, du Bois RM, Black CM**. Immunogenetic prediction of pulmonary fibrosis in systemic sclerosis. *Lancet* 1991;*338*:661-2.

47. **Whyte M, Hubbard R, Meliconi R, Whidborne M, Eaton V, Bingle C, Timms J, Duff G, Facchini A, Pacilli A, Fabbri M, Hall I, Britton J, Johnston I, Di Giovine F**. Increased risk of fibrosing alveolitis associated with interleukin-1 receptor antagonist and tumor necrosis factor-alpha gene polymorphisms. *Am J Respir Crit Care Med* 2000;*162*:755-8.

48. **Selman M, King TE, Jr., Pardo A**. Idiopathic pulmonary fibrosis: prevailing and evolving hypotheses about its pathogenesis and implications for therapy. *Ann Intern Med* 2001;*134*:136-51.

49. **Baumgartner KB, Samet J, Stidley CA, Colby TV, Waldron J**. Cigarette smoking: a risk factor for idiopathic pulmonary fibrosis. *Am J Respir Crit Care Med* 1997;*155*:242-8.

50. **Saag KG, Kline JN**. Interstitial lung diseases. In: Baum BJ, Crapo JD, Celli BR, Karlinsky JB. eds. *Textbook of pulmonary diseases*. 6 Ed. Philadelphia: Lippincott-Raven Publishers, 1998:341-365.

51. **du Bois RM, Wells AU**. Cryptogenic fibrosing alveolitis/idiopathic pulmonary fibrosis. *Eur Respir J* 2001;*18*:43S-55S.

52. **Irving WL, Day S, Johnston ID**. Idiopathic pulmonary fibrosis and hepatitis C virus infection. *Am Rev Respir Dis* 1993;*148*:1683-4.

53. **Meliconi R, Andreone P, Fasano L, Galli S, Pacilli A, Minieiro R**. Incidence of hepatitis C virus infection in Italian patients with idiopathic pulmonary fibrosis. *Thorax* 1996;*51*:315-7.

54. **Egan JJ, Woodcock AA, Stewart JP**. Viruses and idiopathic pulmonary fibrosis. *Eur Respir J* 1997;*10*:1433-7.

55. **Turner-Warwick M**. In search of a cause of cryptogenic fibrosing alveolitis (CFA): one initiating factor or many?. *Thorax* 1998;*53 Suppl 2*:S3-S9

56. **Stewart JP, Egan JJ, Ross AJ, Kelly BG, Lok SS, Hasleton PS, Woodcock AA**. The detection of Epstein-Barr virus DNA in lung tissue from patients with idiopathic pulmonary fibrosis. *Am J Respir Crit Care Med* 1999;*159*:1336-41.

57. **Hubbard R, Venn A, Smith C, Cooper M, Johnston I, Britton J**. Exposure to commonly prescribed drugs and the etiology of cryptogenic fibrosing alveolitis: a case-control study. *Am J Respir Crit Care Med* 1998;*157*:743-7.

58. **Cooper JAJ, Zitnik RJ, Matthay RA**. Mechanisms of drug-induced pulmonary disease. *Annu Rev Med* 1988;*39*:395-404.

59. **Tobin RW, Pope CE, Pellegrini CA, Emond MJ, Sillery J, Raghu G**. Increased prevalence of gastroesophageal reflux in patients with idipathic pulmonary fibrosis. *Am J Respir Crit Care Med* 1998;*158*:1804-8.

60. **Billings CG, Howard P**. Hypothesis: exposure to solvents may cause fibrosing alveolitis. *Eur Respir J* 1994;*7*:1172-6.

61. **Verleden GM, du Bois RM, Bouros D, Drent M, Millar A, Müller-Quernheim J, Semenzato G, Johnson S, Sourvinos G, Olivieri D, Pietinalho A, Xaubet A**. Genetic predisposition and pathogenetic mechanisms of interstitial lung diseases of unknown origin. *Eur Respir J* 2001;*18*:17S-29S.

62. **Moore BB, Paine R, Christensen PJ, Moore TA, Sitterding S, Ngan R, Wilke CA, Kuziel WA, Toews GB**. Protection from pulmonary fibrosis in the absence of CCR2 signaling. *J Immunol* 2001;*167*:4368-77.

63. **Sheppard D**. Pulmonary fibrosis: a cellular overreaction or a failure of communication? *J Clin Invest* 2001;*107*:1501-2.

64. **Selman M, Pardo A**. Idiopathic pulmonary fibrosis: an epithelial/fibroblastic cross-talk disorder. *Respir Res* 2002;*3*:3-10.

65. **Kuhn III C**. An immunohistochemical study of architectural remodeling and connective tissue synthesis in pulmonary fibrosis. *Am Rev Respir Dis* 1989;*140*:1693-703.

66. **Adamson IY, Young L, Bowden DH** . Relationship of alveolar epithelial injury and repair to the induction of pulmonary fibrosis. *Am J Path* 1988;*130*:377-83.

67. **Sime PJ, Xing Z, Graham FL, Csaky G, Gauldie J**. Adenovector-mediated gene transfer of active transforming growth factor-β1induces prolonged severe fibrosis in rat lung. *J Clin Invest* 1997;*100*:768-76.

68. **Huaux F, Louahed J, Hudspith B, Meredith C, Delos M, Renauld J, Lison D**. Role of interleukin-10 in the lung response to silica in mice. *Am J Respir Cell Mol Biol* 1998;*18*:51-9.

69. **Douglas WW, Ryu JH, Swensen SJ, Offord KP, Schroeder DR, Caron GM, DeRemee RA**. Colchicine versus prednisone in the treatment of idiopthic pulmonary fibrosis. A randomized prospective study. *Am J Respir Crit Care Med* 1998;*158*:220-5.

70. **Selman M, Carrillo G, Salas J, Pérez-Padilla, Pérez R, Sansores R**. Colchicine, D-penicillamine, and prednisone in the treatment of idiopathic pulmonary fibrosis: a controlled clinical trial. *Chest* 1998;*114*:507-12.

71. **Douglas WW, Ryu JH, Schroeder DR**. Idiopathic pulmonary fibrosis. Impact of oxygen and colchicine, prednisone, or no therapy on survival. *Am J Respir Crit Care Med* 2000;*161*:1172-8.

72. **Infante-Duarte C, Kamradt T**. Th1/Th2 balance in infection. *Springer Semin Immunopathol* 1999;*21*:317-38.

73. **Shurin MR, Lu L, Kalinski P, Stewart-Akers AM, Lotze MT**. Th1/Th2 balance in cancer, transplantation and pregnancy. *Springer Semin Immunopathol* 1999;*21*:339-59.

74. **Majumdar S, Li D, Ansari T, Pantelidis P, Black CM, Gizycki M, du Bois RM, Jeffrey PK**. Different cytokine profiles of cryptogenic fibrosing alveolitis and fibrosing alveolitis associated with systemic sclerosis. A quantitative study of open lung biopsies. *Eur Respir J* 1999;*14*:251-7.

75. **Agostini C, Siviero M, Semenzato G**. Immune effector cells in idiopathic pulmonary fibrosis. *Curr Opin Pulm Med* 1997;*3*:348-55.

76. **Hogaboam CM, Steinhauser ML, Chensue SW, Kunkel SL**. Novel roles for chemokines and fibroblasts in interstitial fibrosis. *Kidney Int* 1998;*54*:2152-9.

77. **Paine R, Ward PA**. Cell adhesion molecules and pulmonary fibrosis. *Am J Med* 1999;*107*:268-79.

78. **Hosken NA, Shibuya K, Heath AW, Murphy KM, O'Garra A**. The effect of antigen dose on CD4+ T helper cell phenotype development in a T cell receptor-α-transgenic model. *J Exp Med* 1995;*182*:1579-84.

79. **Zhu Z, Homer RJ, Wang Z, Chen Q, Geba GP, Wang J, Zhang Y, Elias JA**. Pulmonary expression of interleukin-13 causes inflammation, mucus hypersecretion, subepithelial fibrosis, physiologic abnormalities, and eotaxin production. *J Clin Invest* 1999;*103*:779-88.

80. **Kunkel SL, Lukacs NW, Strieter RM, Chensue SW**. Th1 and Th2 responses regulate experimental lung granuloma development. *Sarcoidosis Vasc Diffuse Lung Dis* 1996;*13*:120-8.

81. **Romagnani S**. Induction of Th1 and Th2 responses: a key role for the natural immune response? *Immunol Today* 1992;*13*:379-81.

82. **Romagnani S**. Th1/Th2 cells. *Inflamm Bowel Dis* 1999;*5*:285-94.

83. **Coker RK, Laurent GJ**. Pulmonary fibrosis: cytokines in the balance. *Eur Respir J* 1998;*11*:1218-21.

84. **Furuie H, Yamasaki H, Suga M, Ando M**. Altered accessory cell function of alveolar macrophages: a possible mechanism for induction of Th2 secretory profile in idiopathic pulmonary fibrosis. *Eur Respir J* 1997;*10*:787-94.

85. **Hancock A, Armstrong L, Gama R, Millar A**. Production of interleukin 13 by alveolar macrophages from normal and fibrotic lung. *Am J Respir Cell Mol Biol* 1998;*18*:60-5.

86. **Martinez JA, King TE, Jr., Brown K**. Increased expression of the interleukin-10 gene by alveolar macrophages in interstitial lung disease. *Am J Physiol* 1997;*273*:L676-L683

87. **Chensue SW, Terebuh PD, Warmington K**. Role of IL-4 and IFN-γ in *Schistosoma mansoni* egg-induced hypersensitivity granuloma formation. *J Immunol* 1992;*148*:900-10.

88. **Sher A, Fiorentino DF, Caspar P**. Production of IL-10 by CD4+ T lymphocytes correlates with down-regulation of Th1 cytokine synthesis in helminth infection. *J Immunol* 1991;*147*:2713-6.

89. **Lukacs NW, Hogaboam CM, Chensue SW, Blease K, Kunkel SL**. Type 1/type 2 cytokine paradigm and the progression of pulmonary fibrosis. *Chest* 2001;*120*:5S-8S.

90. **Hogaboam CM, Blease K, Mehrad B, Steinhauser ML, Standiford TJ, Kunkel SL, Lukacs NW**. Chronic airway hyperreactivity, goblet cell hyperplasia, and peribronchial fibrosis during allergic airway disease induced by *Aspergillus fumigatus*. *Am J Path* 2000;*156*:723-32.

91. **Lee CG, Homer RJ, Zhu Z, Lanone S, Wang X, Koteliansky V, Shipley JM, Gotwals P, Noble P, Chen Q, Senior RM, Elias JA**. Interleukin-13 induces tissue fibrosis by selectively stimulating and activating transforming growth factor β_1. *J Exp Med* 2001;*194*:809-21.

92. **Gharaee-Kermani M, McGarry B, Lukacs N, Huffnagle G, Egan RW, Phan SH**. The role of IL-5 in bleomycin-induced pulmonary fibrosis. *J Leukoc Biol* 1998;*64*:657-66.

93. **Gharaee-Kermani M, Phan SH**. Lung interleukin-5 expression in murine bleomycin-induced pulmonary fibrosis. *Am J Respir Cell Mol Biol* 1997;*16*:438-47.

94. **Zhang K, Gharaee-Kermani M, Jones ML, Warren JS, Phan SH**. Lung monocyte chemoattractant protein-1 gene expression in bleomycin-induced pulmonary fibrosis. *J Immunol* 1994;*153*:4733-41.

95. **Gharaee-Kermani M, Nozaki Y, Hatano K, Phan SH**. Lung interleukin-4 gene expression in a murine model of bleomycin-induced pulmonary fibrosis. *Cytokine* 2001;*15*:138-47.

96. **Keane MP, Belperio JA, Arenberg DA, Burdick MD, Xu ZJ, Xue YY, Strieter RM**. IFN-gamma-inducible protein-10 attenuates bleomycin-induced pulmonary fibrosis via inhibition of angiogenesis. *J Immunol* 1999;*163*:5686-92.

97. **Keane MP, Belperio JA, Burdick MD, Strieter RM**. IL-12 attenuates bleomycin-induced pulmonary fibrosis. *Am J Physiol (Lung Cell Mol Physiol)* 2001;*281*:L92-L97

98. **Antoniades HN, Neville-Golden J, Galanopoulos T, Kradin RL, Valente AJ, Graves DT**. Expression of monocyte chemoattractant protein 1 mRNA in human idiopathic pulmonary fibrosis. *Proc Natl Acad Sci USA* 1992;*89*:5371-5.

99. **Car BD, Meloni F, Luisetti M, Semenzato G, Gialdroni-Grassi G, Walz A**. Elevated IL-8 and MCP-1 in the bronchoalveolar lavage fluid of patients with idiopathic pulmonary fibrosis and pulmonary sarcoidosis. *Am J Respir Crit Care Med* 1994;*149*:655-9.

100. **Wallace WA, Howie SE**. Immunoreactive interleukin 4 and interferon-γ expression by type II alveolar epithelial cells in interstitial lung disease. *J Pathol* 1999;*187*:475-80.

101. **Wallace WA, Ramage EA, Lamb D, Howie SE**. A type 2 (Th2-like) pattern of immune response predominates in the pulmonary interstitium of patients with cryptogenic fibrosing alveolitis (CFA). *Clin Exp Immunol* 1995;*101*:436-41.

102. **Belperio JA, Dy M, Burdick MD, Xue YY, Li K, Elias JA, Keane MP**. Interaction of IL-13 and C-10 in the pathogenesis of bleomycin-induced pulmonary fibrosis. *Am J Respir Cell Mol Biol* 2002;*27*:419-27.

103. **Ziesche R, Hofbauer E, Wittman K, Petkov V, Block L-H**. A preliminary study of long-term treatment with interferon gamma-1b and low-dose prednisolone in patients with idiopathic pulmonary fibrosis. *N Engl J Med* 1999;*341*:1264-9.

104. **Reynolds HY, Fulmer JD, Kazamierowski JA**. Analysis of cellular and protein content of bronchoalveolar lavage fluid from patients with idiopathic pulmonary fibrosis and chronic hypersensitivity pneumonitis. *J Clin Invest* 1977;*59*:165-75.

105. **Haslam PL**. Evaluation of alveolitis by studies of lung biopsies. *Lung* 1990;*168(Suppl)*:984-92.

106. **Singh S, du Bois RM**. Autoantibodies in cryptogenic fibrosing alveolitis. *Respir Res* 2001;*2*:61-3.

107. **Emura M, Nagi S, Takeuchi M, Kitaichi M, Izumi T**. In vitro production of B cell growth factors and B cell differentiation factors by peripheral blood mononuclear cells and bronchoavleolar lavage T lymphocytes from patients with idiopathic pulmonary fibrosis. *Clin Exp Immunol* 1990;*82*:133-9.

108. **Dreisen RB, Schwarz MI, Theofilopoulos AN, Stanford RE**. Circulating immune complexes in the idiopathic interstitial pneumonias. *N Engl J Med* 1978;*298*:353-8.

109. **Haslam PL, Thompson B, Mohammed I, Townsend PJ, Hodson ME, Holborow EJ, Turner-Warwick M**. Circulating immune complexes in patients with cryptogenic fibrosing alveolitis. *Clin Exp Immunol* 1979;*37*:318

110. **Dall'Aglio PP, Pesci A, Bertorelli G, Brianti E, Scarpa S**. Study of immune complexes in bronchoalveolar lavage fluids. *Respiration* 1988;*54(Suppl 1)*:36-41.

111. **Dobashi N, Fujita J, Murota M, Ohtsuki Y, Yamadori I, Yoshinouchi T, Ueda R, Bandoh S, Kamei T, Nishioka M, Ishida T, Takahara J**. Elevation of anti-cytokeratin 18 antibody and circulating cytokeratin 18: anti-cytokeratin 18 antibody immune complexes in sera of patients with idiopathic pulmonary fibrosis. *Lung* 2000;*178*:171-9.

112. **Dobashi N, Fujita J, Ohtsuki Y, Yamadori I, Yoshinouchi T, Kamei T, Tokuda M, Hojo S, Bandou S, Ueda Y, Takahara J**. Circulating cytokeratin 8:anti-cytokeratin 8 antibody immune complexes in sera of patients with pulmonary fibrosis. *Respiration* 2000;*67*:397-401.

113. **Turner-Warwick M, Doniach D**. Autoantibody studies in interstitial pulmonary fibrosis. *Br Med J* 1965;*1*:886-91.

114. **Holgate ST, Haslam PL, Turner-Warwick M**. The significance of antinuclear and DNA antibodies in cryptogenic fibrosing alveolitis. *Thorax* 1983;*38*:67-70.

115. **Chapman JR, Charles PJ, Venables PJW, Thompson PJ, Haslam PL, Maini RN, Turner-Warwick M**. Definition and clinical relevance of antibodies to nuclear ribonucleoprotein and other nuclear antigens in patients with cryptogenic fibrosing alveolitis. *Am Rev Respir Dis* 1984;*130*:439-43.

116. **Meliconi R, Bestagno M, Sturani C, Negri C, Galavotti V, Sala C, Facchini A, Ciarrocchi G, Gasbarrini G, Astaldi-Ricotti GC**. Autoantibodies to DNA topoisomerase II in cryptogenic fibrosing alveolitis and connective tissue disease. *Clin Exp Immunol* 1989;*76*:184-9.

117. **Grigolo B, Mazzetti I, Borzi RM, Hickson LD, Fabbri M, Fasano L, Meliconi R, Facchini A**. Mapping of topoisomerase II α epitopes recognized by autoantibodies in idiopathic pulmonary fibrosis. *Clin Exp Immunol* 1998;*114*:339-46.

118. **Dobashi N, Fujita J, Ohtsuki Y, Yamadori I, Yoshinouchi T, Kamei T, Tokuda M, Hojo S, Okada H, Takahara J**. Detection of anti-cytokeratin 8 antibody in the serum of patients with cryptogenic fibrosing alveolitis and pulmonary fibrosis associated with collagen vascular disorders. *Thorax* 1998;*53*:969-74.

119. **Wallace WA, Roberts SN, Caldwell H, Thornton E, Greening AP, Lamb D, Howie SE**. Circulating antibodies to lung protein(s) in patients with cryptogenic fibrosing alveolitis. *Thorax* 1994;*49*:218-22.

120. **Wallace WA, Schofield JA, Lamb D, Howie SE**. Localisation of a pulmonary autoantigen in cryptogenic fibrosing alveolitis. *Thorax* 1994;*49*:1139-45.

121. **Schwartz MI, Dreisen RB, Pratt DS, Stanford RE**. Immunofluroescent pattern in idiopathic interstitial pneumonia. *J Lab Clin Med* 1978;*91*:929-35.

122. **Wallace WA, Howie SE**. Upregulation of tenascin and TGFβ production in a type II alveolar epithelial cell line by antibody against a pulmonary auto-antigen. *J Pathol* 2001;*195*:251-6.

123. **Wallace WA, Howie SE, Lamb D, Salter DM**. Tenascin immunoreactivity in cryptogenic fibrosing alveolitis. *J Pathol* 1995;*175*:415-20.

124. **Adamson IYR, Hedgecock C, Bowden DH**. Epithelial cell-fibroblast interactions in lung injury and repair. *Am J Path* 1990;*137*:385-92.

125. **Kimura RH, Hu H, Stein-Streilein J**. Delayed type hypersensitivity (DTH) responses regulate collagen depostion in the lung. *Immunology* 1992;*77*:550-5.

126. **Zhang-Hoover J, Sutton A, van Rooijen N, Stein-Streilein J**. A critical role for alveolar macrophages in elicitation of pulmonary immune fibrosis. *Immunology* 2001;*101*:501-11.

127. **Adawi A, Zhang Y, Baggs R, Rubin P, Williams J, Finkelstein J, Phipps RP**. Blockade of CD40-CD40 ligand interactions protects against radiation-induced pulmonary inflammation and fibrosis. *Clin Immunol Immunopathol* 1998;*89*:222-30.

128. **Zhang Y, Cao HJ, Graf B, Meekins H, Smith TJ, Phipps RP**. CD40 engagement up-regulates cyclooxygenase-2 expression and prostaglandin E_2 production in human lung fibroblasts. *J Immunol* 1998;*160*:1053-7.

129. **Zhang-Hoover J, Sutton A, Stein-Streilein J**. CD40/CD40 ligand interactions are critical for elicitation of autoimmune-mediated fibrosis in the lung. *J Immunol* 2001;*166*:3556-63.

130. **Kaneko Y, Kuwano K, Kunitake R, Kawasaki M, Hagimoto H, Hara N**. B7-1, B7-2 and class II MHC molecules in idiopathic pulmonary fibrosis and bronchiolitis obliterans-organizing pneumonia. *Eur Respir J* 2002;*15*:49-55.

131. **Nicod LP, Cochand L, Dreher D** . Antigen presentation in the lung: dendritic cells and macrophages. *Sarcoidosis Vasc Diffuse Lung Dis* 2000;*17*:246-55.

132. **Tsang JY, Chai JG, Lechler R**. Antigen presentation by mouse CD4+ T cells involving acquired MHC class II:peptide complexes: another mechanism to limit clonal expansion? *Blood* 2002;*[in press]*:

133. **Lanzavecchia A**. Receptor-mediated antigen uptake and its effect on antigen presentation to class II-restricted T lymphocytes. *Annu Rev Immunol* 1990; *8*:773-93.

134. **Zhong G, Reis e Sousa C, Germain RN**. Antigen-unspecific B cells and lymphoid dendritic cells both show extensive surface expression of processed antigen-major histocompatibility complex class II complexes after soluble protein exposure in vivo or in vitro. *J Exp Med* 1997;*186*:673-82.

135. **Holt PG**. Antigen presentation in the lung. *Am J Respir Crit Care Med* 2000;*162*:S151-S156

136. **Steinman RM**. The dendritic cell system and its role in immunogenicity. *Annu Rev Immunol* 1991;*9*:271-96.

137. **Masten BJ, Lipscomb MF**. Methods to isolate and study lung dendritic cells. In: Lipscomb MF, Russell SW. eds. *Lung macrophages and dendritic cells in health and disease*. New York: Marcel Dekker, Inc., 1997:223-238.

138. **Vermaelen KY, Carro-Muino I, Lambrecht BN, Pauwels RA**. Specific migratory dendritic cells rapidly transport antigen from the airways to the thoracic lymph nodes. *J Exp Med* 2001;*193*:51-60.

139. **Gallucci S, Lolkema M, Matzinger P**. Natural adjuvants: endogenous activators of dendritic cells. *Nat Med* 1999;*5*:1249-55.

140. **Holt PG, Schon-Hegrad MA**. Localization of T cells, macrophages and dendritic cells in rat respiratory tract tissue: implications for immune function studies. *Immunology* 1987;*62*:349-56.

141. **Holt PG, Schon-Hegrad MA, Oliver J**. MHC class II antigen-bearing dendritic cells in pulmonary tissues of the rat. *J Exp Med* 1988;*167*:262-74.

142. **Sertl K, Takemura T, Tschachler E, Ferrans VJ, Kaliner MA, Shevach EM**. Dendritic cells with antigen-presenting capability reside in airway epithelium, lung parenchyma, and visceral pleura. *J Exp Med* 1986;*163*:436-51.

143. **Holt PG**. Ia-positive dendritic cells form a tightly meshed network within the human airway epithelium. *Clin Exp Allergy* 1989;*6*:597-601.

144. **Nicod LP, Cochand L**. Dendritic cells in the respiratory tract. In: Lotze MT, Thomson AW. eds. *Dendritic cells: biology and clinical applications*. 2 Ed. London: Academic Press, 2001:315-323.

145. **Holt PG, Haining S, Nelson DJ, Sedgwick JD**. Origin and steady-state turnover of class II MHC-bearing dendritic cells in the epithelium of the conducting airways. *J Immunol* 1994;*153*:256-61.

146. **Xia WJ, Pinto C, Kradin RL**. The antigen-presenting activities of Ia^+ dendritic cells shift dynamincally from lung to lymph node after an airway challenge with soluble antigen. *J Exp Med* 1995;*181*:1275-83.

147. **McWilliam AS, Napoli S, Marsh AM**. Dendritic cells are recruited into the airway epithelium during the inflammatory response to a broad spectrum of stimuli. *J Exp Med* 1996;*184*:2429-32.

148. **Power CA, Church DJ, Meyer A, Alouani S, Proudfoot AE, Clark-Lewis I, Sozzani S, Mantovani A, Wells TN**. Cloning and characterization of a specific receptor for the novel CC chemokine MIP-3alpha from lung dendritic cells. *J Exp Med* 1997;*186*:825-35.

149. **Banchereau J, Briere F, Caux C, Davoust J, Lebecque S, Liu YJ, Pulendran B, Palucka K**. Immunobiology of dendritic cells. *Annu Rev Immunol* 2000;*18*:767-811.

150. **Lambrecht BN, Prins J-B, Hoogsteden HC**. Lung dendritic cells and host immunity to infection. *Eur Respir J* 2001;*18*:571-88.

151. **Gong JL, McCarthy KM, Telford J, Tamatani T, Miyasaka M, Schneeberger EE**. Intraepithelial airway dendritic cells: a distinct subset of pulmonary dendritic cells obtained by microdissection. *J Exp Med* 1992;*175*:797-807.

152. **Pulendran B, Lingappa J, Kennedy MK, Smith J, Teepe M, Rudensky A, Maliszewski CR, Maraskovksy E**. Developmental pathways of dendritic cells in vivo: distinct function, phenotype, and localization of dendritic cells subsets in FLT3 ligand-treated mice. *J Immunol* 1997;*159*:2222-31.

153. **Vremec D, Shortman K**. Dendritic cell subtypes in mouse lymphoid organs: cross-correlation of surface markers, changes with incubation, and differences among thymus, spleen, and lymph nodes. *J Immunol* 1997;*159*:565-73.

154. **Masten BJ, Yates JL, Pollard Koga A.M., Lipscomb MF**. Characterization of accessory molecules in murine lung dendritic cell function: roles for CD80, CD86, CD54, and CD40L. *Am J Respir Cell Mol Biol* 1997;*16*:335-42.

155. **Pollard AM, Lipscomb MF**. Characterization of murine lung dendritic cells: similarities to Langerhans cells and thymic dendritic cells. *J Exp Med* 1990;*172*:159-67.

156. **Salomon B, Cohen JL, Masurier C, Klatzmann D**. Three populations of mouse lymph node dendritic cells with different origins and dynamics. *J Immunol* 1998;*160*:708-17.

157. **Masten BJ, Lipscomb MF**. Comparison of lung dendritic cells and B cells in stimulating naive antigen-specific T cells. *J Immunol* 1999;*162* :1310-7.

158. **Gonzalez-Juarrero M, Orme IM**. Characterization of murine lung dendritic cells infected with *Mycobaterium tuberculosis*. *Infection and Immunity* 2001;*69*:1127-33.

159. **Pierre P, Turley SJ, Gatti E, Hull M, Meltzer J, Mirza A, Inaba K, Steinman RM, Mellman I**. Developmental regulation of MHC class II transport in mouse dendritic cells. *Nature* 1997;*388*:787-92.

160. **Wilson HL, Ni K, O'Neill HC**. Identification of progenitor cells in long-term spleen stromal cultures that produce immature dendritic cells. *Proc Natl Acad Sci USA* 2000;*97*:4784-9.

161. **Cella M, Salusto F, Lanzavecchia A**. Origin, maturation and antigen presenting function of dendritic cells. *Curr Opin Immunol* 1997;*9*:10-6.

162. **Reischl IG**. Dendritic cells and lung antigen responses. *Clin Exp Allergy* 2000;*30*:160-3.

163. **Stumbles PA**. Regulation of T helper cell differentiation by respiratory tract dendritic cells. *Immunol Cell Biol* 1999;*77*:428-33.

164. **Semper AE, Hartley JA**. Dendritic cells in the lung: what is their relevance to asthma? *Clin Exp Allergy* 1996;*26*:485-90.

165. **Stumbles PA, Thomas JA, Pimm CL, Lee PT, Venaille TJ, Proksch S, Holt PG**. Resting respiratory tract dendritic cells preferentially stimulate T helper cell type 2 (Th2) responses and require obligatory cytokine signals for induction of Th1 immunity. *J Exp Med* 1998;*188*:2019-31.

166. **Pulendran B, Smith JL, Caspary G, Brasel K, Pettit D, Maraskovksy E, Maliszewski CR**. Distinct dendritic cell subsets differentially regulate the class of immune response *in vivo*. *Proc Natl Acad Sci USA* 1999;*96*:1036-41.

167. **Maldonado-Lopez R, De Smedt T, Michel P, Godfroid J, Pajak B, Heirman C, Thielemans K, Leo O, Urbain J, Moser M**. $CD8\alpha^+$ and $CD8\alpha^-$ subclasses of dendritic cells direct the development of distinct T helper cells in vivo. *J Exp Med* 1999;*189*:587-92.

168. **Rissoan MC, Soumelis V, Kadowaki N, Grourad G, Briere F, de Waal-Malefyt R, Liu YJ**. Reciprocal control of T helper cell and dendritic cell differentiation. *Science* 1999;*283*:1183-6.

169. **Kalinski P, Schuitemaker JH, Hilkens CM, Kapsenberg M**. Prostaglandin E_2 induces the final maturation of IL-12-deficient $CD1a^+CD83^+$ dendritic cells: the levels of IL-12 are determined during the final dendritic cell maturation and are resistant to further modification. *J Immunol* 1998;*161*:2804-9.

170. **Constant S, Lee KS, Bottomly K**. Site of antigen delivery can influence T cell priming: pulmonary environment promtoes preferential Th2-type differentiation. *Eur J Immunol* 2000;*30*:840-7.

171. **Ray A, Cohn L**. Th2 cells and GATA-3 in asthma: new insights into the regulation of airway inflammation. *J Clin Invest* 1999;*104*:985-93.

172. **van der Pouw Kraan TCTM, Boeije LCM, Smeenk RJT, Wijdenes J, Aarden LA**. Prostaglandin-E2 is a potent inhibitor of human interleukin-12. *J Exp Med* 1995;*181*:775-9.

173. **Panina-Bordignon P, Mazzeo D, DiLucia P, D'Ambrosio D, Lang R, Fabbri L, Self C, Sinigaglia F**. Beta(2)-agonists prevent Th1 development by selective inhibition of interleukin 12. *J Clin Invest* 1997;*100*:1513-9.

174. **van der Pouw Kraan TCTM, Snijders A, Boeije LCM, de Groot AE, Alewijnse AE, Leurs R, Aarden LA**. Histamine inhibits the production of interleukin-12 through interaction with H_2 receptors. *J Clin Invest* 1998;*102*:1866-73.

175. **Huang FP, Niedbala W, Wei XQ, Xu DM, Feng GJ, Robinson JH, Lam C, Liew FY**. Nitric oxide regulates Th1 cell development through the inhibition of IL-12 synthesis by macrophages. *Eur J Immunol* 1998;*28*:4062-70.

176. **Sinigaglia F, D'Ambrosio D**. Regulation of helper T cell differentiation and recruitment in airway inflammation. *Am J Respir Crit Care Med* 2000;*162*:S157-S160

177. **Dupuis M, McDonald DM**. Dendritic-cell regulation of lung immunity. *Am J Respir Cell Mol Biol* 1997;*17*:284-6.

178. **Lu L, Thomson AW**. Dendritic cell tolerogenicity and prospects for dendritic cell-based therapy of allograft rejection and autoimmune disease. In: Lotze MT, Thomson AW. eds. *Dendritic cells: biology and clinical applications*. 2 Ed. London: Academic Press, 2000:587-607.

179. **Hu B, Sonstein J, Christensen PJ, Punturieri A, Curtis JL**. Deficient in vitro and in vivo phagocytosis of apoptotic T cells by resident murine alveolar macrophages. *J Immunol* 2000;*165*:2124-33.

180. **Brody AR**. Whither goes the alveolar macrophage? Another small chapter is written on the localized response of this crucial cell. *J Lab Clin Med* 1998;*131*:391

181. **Lipscomb MF, Lyons CR, Nunez G, Ball EJ, Stanstny P, Vial W, Lem V, Weissler JC, Miller LM, Toews GB**. Human alveolar macrophages: HLA-DR-positive cells that are poor stimulators of a primary mixed leukocyte reaction. *J Immunol* 1986;*136*:497-504.

182. **Holt PG, Oliver J, Bilyk N, McMenamin C, McMenamin PG, Kraal G, Thepen T**. Downregulation of the antigen presenting cell function(s) of pulmonary dendritic cells in vivo by resident alveolar macrophages. *J Exp Med* 1993;-397

183. **Gong JL, McCarthy KM, Rogers RA, Schneeberger EE**. Interstitial lung macrophages interact with dendritic cells to present antigenic peptides derived from particulate antigens to T cells. *Immunology* 1994;*81*:343-51.

184. **Lipscomb MF, Bice DE, Lyons CR, Schuyler MR, Wilkes D**. The regulation of pulmonary immunity. *Adv Immunol* 1995;*59*:369-455.

185. **Kobzik L**. Methods to isolate and study lung macrophages. In: Lipscomb MF, Russell SW. eds. *Lung macrophages and dendritic cells in health and disease*. New York: Marcel Dekker, Inc., 1997:111-129.

186. **Murphy MA, Herscowitz HB**. Heterogeneity among alveolar macrophages in humoral and cell-mediated responses: separation of functional subpopulations by density gradient centrifugation on Percoll. *J Leukoc Biol* 1984;*35*:39-54.

187. **Shellito J, Kaltreider HB**. Heterogeneity of immunologic function among subfractions of normal rat alveolar macrophages. II. Activation as a determinant of functional activity. *Am Rev Respir Dis* 1985;*131*:678-83.

188. **Oghiso Y**. Morphologic and functional heterogeneity among rat alveolar macrophage fractions isolated by centrifugation on density gradients. *J Leukoc Biol* 1987;*42*:188-96.

189. **Gordon S, Hughes D**. Macrophages and their origins. Heterogeneity in relation to tissue microenvironment. In: Lipscomb MF, Russell SW. eds. *Lung macrophages and dendritic cells in health and disease*. New York: Marcel Dekker, Inc., 1997:3-32.

190. **Weinberg DS, Unanue ER**. Antigen-presenting function of alveolar macrophages: uptake and presentation of *Listeria moncytogenes*. *J Immunol* 1981;*126*:794-9.

191. **Chelen CJ, Fang Y, Freeman GJ** . Human alveolar macrophages present antigen ineffectively due to defective expression of B7 costimulatory cell surface molecules. *J Clin Invest* 1995;*95*:1415-21.

192. **Nicod LP, Isler P**. Alveolar macrophages in sarcoidosis coexpress high levels of CD86 (B7.2), CD40 and CD30L. *Am J Respir Cell Mol Biol* 1997;*17*:91-6.

193. **Tager AM, Luster AD, Leary CP, Sakamoto H, Zhao LH, Preffer F, Kradin RL**. Accessory cells with immunophenotypic and functional features of monocyte-derived dendritic cells are recruited to the lung during pulmonary inflammation. *J Leukoc Biol* 1999;*66*:901-8.

194. **Strickland DH, Kees UR, Holt PG**. Regulation of T-cell activation in the lung: alveolar macrophages induce reversible T-cell anergy *in vitro* associated with inhibition of interleukin-2 receptor signal transduction. *Immunology* 1996;*87*:250-8.

195. **Bilyk N, Holt PG**. Cytokine modulation of the immunosuppressive phenotype of pulmonary alveolar macrophages via regulation of nitirc oxide production. *Immunology* 1995;*86*:231-7.

196. **Bilyk N, Holt PG**. Inhibition of the immunosuppressive activity of resident pulmonary alveolar macrophages by granulocyte/macrophage colony-stimulating factor. *J Exp Med* 1993;*177*:1773-7.

197. **Boehringer N, Hagens G, Songeon F**. Differential regulation of tumour necrosis factor-α (TNF-α) and interleukin-10 (IL-10) secretion by protein kinase and phosphatase inhibition in human alveolar macrophages. *Eur Cytokine Netw* 1999;*10*:211-7.

198. **Beckett W, Abraham J, Becklake M, Christiani D, Cowle R, Davis GS, Jones R, Kreiss K, Parker J, Wagner G**. Adverse effects of crystalline silica exposure. *Am J Respir Crit Care Med* 1997;*155*:761-5.

199. **Hunninghake GW, Garrett KC, Richerson HB, Fantone JC, Ward PA, Rennard SI, Bitterman PB, Crystal RG**. Pathogenesis of the granulomatous lung diseases. *Am Rev Respir Dis* 1984;*130*:476-96.

200. **Faffe DS, Silva GH, Kurtz PMP, Negri EM, Capelozzi VL, Rocco PRM, Zin WA**. Lung tissue mechanics and extracellular matrix composition in a murine model of silicosis. *J Appl Physiol* 2001;*90*:1400-6.

201. **Hubbard AK, Timblin CR, Shukla A, Rincón M, Mossman BT**. Activation of NK-κB-dependent gene expression by silica in lungs of luciferase reporter mice. *Am J Physiol (Lung Cell Mol Physiol)* 2001;*282*:L968-L975

202. **Mossman BT, Churg A**. Mechanisms in the pathogenesis of asbestosis and silicosis. *Am J Respir Crit Care Med* 1998;*157*:1666-80.

203. **Huaux F, Lardot C, Arras M, Delos M, Many M, Coutelier J, Renauld J, Lison D**. Lung fibrosis induced by silica particles in NMRI mice is associated with an upregulation of the p40 subunit of interleukin-12 and Th-2 manifestations. *Am J Respir Cell Mol Biol* 1999;*20*:561-72.

204. **Arras M, Huaux F, Vink A, Delos M, Coutelier J, Many M, Barbain V, Renauld J, Lison D**. Interleukin-9 reduces lung fibrosis and type 2 immune polarization induced by silica particles in a murine model. *Am J Respir Cell Mol Biol* 2001;*24*:368-75.

205. **Davis GS, Pfeiffer LM, Hemenway DR**. Interferon-gamma production by specific lung lymphocyte phenotypes in silicosis in mice. *Am J Respir Cell Mol Biol* 2000;*22*:491-501.

206. **Adamson IY, Bowden DH**. Endothelial injury and repair in radiation-induced pulmonary fibrosis. *Am J Path* 1983;*112*:224-30.

207. **Pickrell JA, Abdel-Mageed AB**. Radiation-induced pulmonary fibrosis. In: Phan SH, Thrall RS. eds. *Pulmonary fibrosis*. New York: Marcel Dekker, 1995:363-381.

208. **Büttner C, Skupin A, Reimann T, Rieber EP, Unteregger G, Geyer P, Frank KH**. Local production of interleukin-4 during radiation-induced pnuemonitis and pulmonary fibrosis in rats: macrophages as a prominent source of interleukin-4. *Am J Respir Cell Mol Biol* 1997;*17*:315-25.

209. **Westermann W, Schobl R, Rieber EP, Frank KH**. Th2 cells as effectors in postirradiation pulmonary damage preceding fibrosis in the rat. *Int J Radiat Biol* 1999;*75*:629-38.

210. **Haston CK, Travis EL**. Murine susceptibility to radiation-induced pulmonary fibrosis is influenced by a genetic factor implicated in susceptibility to belomycin-induced pulmonary fibrosis. *Cancer Res* 1997;*57*:5286-91.

211. **Haston CK, Zhou X, Gumbiner-Russo L, Irani R, Dejournett R, Gu X, Weil M, Amos CI, Travis EL**. Universal and radiation-specific loci influence mruine susceptibility to radiation-induced pulmonary fibrosis. *Cancer Res* 2002;*62*:3782-8.

212. **Luna MA, Bedrossian CWM, Lichtiger B, Salem P**. Interstitial pneumonitis associated with bleomycin therapy. *Am J Clin Pathol* 1972;*58*:501-10.

213. **Chandler DB**. Possible mechanisms of bleomycin-induced fibrosis. *Clin Chest Med* 1990;*11*:21-30.

214. **Adamson IYR, Bowden DH**. The pathogenesis of bleomycin-induced pulmonary fibrosis in mice. *Am J Path* 1974;*77*:185-98.

215. **Schrier DJ, Phan SH, McGarry B**. The effects of nude (*nu/nu*) mutation on bleomycin induced pulmonary fibrosis. A biochemical evaluation. *Am Rev Respir Dis* 1983;*127*:614-7.

216. **Bowden DH**. Unraveling pulmonary fibrosis: the bleomycin model. *Lab Invest* 1984;*50*:487-8.

217. **Oberly LW, Buettner GR**. The production of hydroxyl radical by bleomycin and iron(II). *FEBS Lett* 1979;*97*:47-9.

218. **Chandler DB, Hyde DM, Gin SN**. Morphometric estimates of infiltrative cellular changes during the development of bleomycin-induced pulmonary fibrosis in hamsters. *Am J Path* 1983;*112*:170-7.

219. **Smith RE, Strieter RM, Phan SH, Lukacs NW, Huffnagle G, Wilke CA, Burdick MD, Lincoln P, Evanoff H, Kunkel SL** . Production and function of murine macrophage inflammatory protein-1α in bleomycin-induced lung injury. *J Immunol* 1994;*153*:4704-12.

220. **Piguet PF, Collart MA, Grau GE, Kapanci Y, Vassalli P**. Tumor necrosis factor/cachectin plays a key role in bleomycin-induced pneumopathy and fibrosis. *J Exp Med* 1989;*170*:655-63.

221. **Eitzman DT, McCoy RD, Zheng X, Fay WP, Shen T, Ginsburg D, Simon RH**. Bleomycin-induced pulmonary fibrosis in transgenic mice that either lack or overexpress the murine plasminogen activator inhibitor-1 gene. *J Clin Invest* 1996;*97*:232-7.

222. **Smith RE, Strieter RM, Phan SH, Kunkel SL**. C-C chemokines: novel mediators of the profibrotic inflammatory response to bleomycin challenge. *Am J Respir Cell Mol Biol* 1996;*15*:693-702.

223. **Borzone G, Moreno R, Urrea R, Meneses M, Oyarzún M, Lisboa C**. Bleomycin-induced chronic lung damage does not resemble human idiopathic pulmonary fibrosis. *Am J Respir Crit Care Med* 2001;*163*:1648-53.

224. **Phan SH, Thrall RS, Williams C**. Bleomycin-induced pulmonary fibrosis: effects of steroids on lung collagen metabolism. *Am Rev Respir Dis* 1981;*124*:428-34.

225. **Azuma A, Furuta T, Enomoto T, Hashimoto Y, Uematsu K, Nukariya N, Murata A, Kudoh S**. Preventive effect of erythromycin on experimental bleomycin-induced acute lung injury in rats. *Thorax* 1998;*53*:186-9.

226. **Chandler DB, Fulmer JD**. The effect of deferoxamine on bleomycin-induced lung fibrosis in the hamster. *Am Rev Respir Dis* 1985;*131*:596-8.

227. **Oyarzún M, Dussaubat N, Capetillo M, Rocco V, Mendoza R, Lathrop ME**. Pharmacological inhibition of bleomycin-induced pulmonary fibrosis in the rat. *Eur Respir J* 1995;*8*:544s

228. **Zhu J, Kaplan AM, Goud SN**. Immunologic alterations in bleomycin-treated mice: role of pulmonary fibrosis in the modulation of immune responses. *Am J Respir Crit Care Med* 1996;*153*:1924-30.

229. **Lossos IS, Or R, Ginzburg V, Christensen TG, Mashriki Y, Breuer R**. Cyclosporin A upmodulates bleomycin-induced pulmonary fibrosis in BALB/c mice. *Respiration* 2001;*69*:344-9.

230. **Phan SH, Kunkel SL**. Lung cytokine production in bleomycin-induced pulmonary fibrosis. *Exp Lung Res* 1992;*18*:29-43.

231. **Santana A, Saxena B, Noble NA, Gold LI**. Increased expression of transforming growth factor β isoforms (β1, β2, β3) in bleomycin-induced pulmonary fibrosis. *Am J Respir Cell Mol Biol* 1995;*13*:34-44.

232. **Zhang K, Flanders KC, Phan SH** . Cellular localization of transforming growth factor-β expression in bleomycin-induced pulmonary fibrosis. *Am J Path* 1995;*147*:352-61.

233. **Khalil N, Corne S, Whitman C, Yacyshyn H**. Plasmin regulates the activation of all associated latent TGF-β_1 secreted by rat alveolar macrophages after *in vivo* bleomycin injury. *Am J Respir Cell Mol Biol* 1996;*15*:252-9.

234. **Khalil N, Whitman C, Zuo L, Danielpour D, Greenberg AH**. Regulation of alveolar macrophage transforming growth factor-β secretion by corticosteroids in bleomycin-induced pulmonary inflammation in the rat. *J Clin Invest* 1993;*92*:1812-8.

235. **Coker RK, Laurent GJ, Shahzeidi S, Lympany PA, du Bois RM, Jeffery PK, McAnulty RJ**. Transforming growth factors-β_1, -β_2, and -β_3 stimulate fibroblast procollagen production *in vitro* but are differentially expressed during bleomycin-induced lung fibrosis. *Am J Path* 1997;*150*:981-91.

236. **Maeda A, Ishioka S, Taooka Y, Hiyama K, Yamakido M**. Expression of transforming growth factor-β1 and tumour necrosis factor-α in bronchoalveolar lavage cells in murine pulmonary fibrosis after intraperitoneal administration of bleomycin. *Respirology* 1999;*4*:359-63.

237. **Tokuda A, Itakura M, Onai N, Kimura H, Kuriyama T, Matsushima K**. Pivotal role of CCR-1-positive leukocytes in bleomycin-induced lung fibrosis in mice. *J Immunol* 2000;*164*:2745-51.

238. **Hamaguchi Y, Nishizawa Y, Yasui M, Hasegawa M, Kaburagi Y, Komura K, Nagaoka T, Saito E, Shimada Y, Takehara K, Kadono T, Steeber DA, Tedder TF, Sato S.** Intercellular adhesion molecule-1 and L-selectin regulate bleomycin-induced lung fibrosis. *Am J Path* 2002;*161*:1607-18.

239. **Sato N, Suzuki Y, Nishio K, Suzuki K, Naoki K, Takeshita K, Kudo H, Miyao N, Tsumura H, Serizawa H, Suematsu M, Yamaguchi K.** Roles of ICAM-1 for abnormal leukocyte recruitment in the microcirculation of bleomycin-induced pulmonary fibrosis. *Am J Respir Crit Care Med* 2000;*161*:1681-8.

240. **Schrier DJ, Kunkel RG, Phan SH.** The role of strain variation in murine bleomycin-induced pulmonary fibrosis. *Am Rev Respir Dis* 1983;*127*:63-6.

241. **Filderman AE, Lazo JS.** Murine strain differences in pulmonary bleomycin metabolism. *Biochem Pharmacol* 1991;*42*:195-8.

242. **Gur I, Or R, Segel MJ, Shriki M, Izbicki G, Breuer R.** Lymphokines in bleomycin-induced lung injury in bleomcyin-sensitive C57BL/6 and -resistant BALB/c mice. *Exp Lung Res* 2000;*26*:521-34.

243. **Roberts SN, Howie SE, Wallace WA, Brown DM, Lamb D, Ramage EA, Donaldson K.** A novel model for human interstitial lung disease: hapten-driven lung fibrosis in rodents. *J Pathol* 1995;*176*:309-18.

244. **Christensen PJ, Goodman RE, Pastoriza L, Moore B, Toews GB.** Induction of lung fibrosis in the mouse by intratracheal instillation of fluorescein isothiocyanate is not T-cell-dependent. *Am J Path* 1999;*155*:1773-9.

245. **Moore BB, Christensen PJ, Wilke C, Sitterding S, Paine R, Toews GB.** Fluorescein isothiocyanate-induced pulmonary fibrosis is regulated by monocyte chemoattractant protein-1 and chemokine receptor 2. *Chest* 2001;*120*:4S

246. **Zhang K, Phan SH.** Cytokines and pulmonary fibrosis. *Biological Signals* 1996;*5*:232-9.

247. **Duncan MR, Berman B.** γ Interferon is the lymphokine and β interferon the monokine responsible for inhibition of fibroblast collagen production and late but not early fibroblast proliferation. *J Exp Med* 1985;*162*:516-27.

248. **Elias JA.** Tumor necrosis factor interacts with interleukin-1 and interferons to inhibit fibroblast proliferation via fibroblast prostaglandin-dependent and -independent mechanisms. *Am Rev Respir Dis* 1988;*138*:652-8.

249. **Elias JA, Jimenez SA, Freundlich B.** Recombinant gamma, alpha and beta interferon regulation of human lung fibroblast proliferation. *Am Rev Respir Dis* 1987;*135*:62-5.

250. **Prior C, Haslam PL.** *In vivo* levels and *in vitro* production of interferon-gamma in fibrosing interstitial lung diseases. *Clin Exp Immunol* 1992;*88*:280-7.

251. **Gurujeyalakshmi G, Giri SN.** Molecular mechanisms of antifibrotic effect of interferon gamma in bleomycin-mouse model of lung fibrosis: downregulation of TGF-beta and procollagen I and III gene expression. *Exp Lung Res* 1995;*21*:791-808.

252. **Sempowski GD, Derdak S, Phipps RP.** Interleukin-4 and interferon-gamma discordantly regulate collagen biosynthesis by functionally distinct lung fibroblast subsets. *J Cell Physiol* 1996;*167*:290-6.

253. **Jaffe HA, Gao Z, Mori Y, Li L, Varga J**. Selective inhibition of collagen gene expression in fibroblasts by an interferon-gamma transgene. *Exp Lung Res* 1999;*25*:199-215.

254. **Diaz A, Jimenez SA**. Interferon-gamma regulates collagen and fibronectin gene expression by transcriptional and post-transcriptional mechanisms. *Int J Biochem Cell Biol* 1997;*29*:251-60.

255. **Giri SN, Hyde DM, Marafino BJ** . Ameliorating effect of murine interferon-γ on bleomcyin-induced lung collagen fibrosis in mice. *Biochem Med Metab Biol* 1986;*36*:194-7.

256. **Hyde DM, Henderson TS, Giri SN**. Effect of murine-gamma interferon on the cellular responses to bleomycin in mice. *Exp Lung Res* 1988;*14*:686-704.

257. **Tamura R, Sato K, Chida K, Suganuma H**. Fibroblasts as target and effector cells in Japanese patients with sarcoidosis. *Lung* 1998;*176*:75-87.

258. **Chen ES, Greenlee BM, Wills-Karp M, Moller DR**. Attenutation of lung inflammation and fibrosis in interferon-γ-deficient mice after intratracheal bleomycin. *Am J Respir Crit Care Med* 2001;*24*:545-55.

259. **Khalil N**. TGF-beta: from latent to active. *Microbes & Infection* 1999;*1*:1255-63.

260. **Letterio JJ, Roberts AB**. Molecule of the month. TGFβ; a key modulator of immune cell function. *Clin Immunol Immunopathol* 1997;*84*:244-50.

261. **Howat WJ, Holgate ST, Lackie PM**. TGF-β isoform release and activation during in vitro bronchial epithelial wound repair. *Am J Physiol (Lung Cell Mol Physiol)* 2002;*282*:L115-L123

262. **Border WA, Noble NA**. Transforming growth factor β in tissue fibrosis. *N Engl J Med* 1994;*331*:1286-92.

263. **Varga J, Jimenez SA**. Modulation of collagen gene expression: its relation to fibrosis in systemic sclerosis and other disorders. *Ann Intern Med* 1995;*122*:60-2.

264. **McAnulty RJ, Campa JS, Cambrey AD**. The effect of transforming growth factor β on rates of procollagen synthesis and degradation in vitro. *Biochem Biophys Acta* 1991;*1091*:231-5.

265. **Xing Z, Jordana M, Gauldie J, Wang J**. Cytokines and pulmonary inflammatory and immune diseases. *Histol Histopathol* 1999;*14*:185-201.

266. **Allen JT, Spiteri MA**. Growth factors in idiopathic pulmonary fibrosis: relative roles. *Respir Res* 2002;*3*:13-21.

267. **Mori M, Kida H, Morishita H, Goya S, Matsuoka H, Arai T, Osaki T, Tachibana I, Yamamoto S, Sakatani M, Ito M, Ogura T, Hayashi S**. Microsatellite instability in transforming growth factor-β1 type II receptor gene in alveolar lining epithelial cells of idiopathic pulmonary fibrosis. *Am J Respir Cell Mol Biol* 2001;*24*:398-404.

268. **Breen E, Absher M, Kelley J, Phan SH, Cutroneo KR**. Bleomycin regulation of TGF-β mRNA in lung fibroblasts. *Am J Respir Cell Mol Biol* 1992;*6*:146-52.

269. **Phan SH, Gharaee-Kermani M, Wolber F, Ryan US**. Stimulatino of rat endothelial cell transforming growth factor production by bleomycin. *J Clin Invest* 1991;*87*:148-54.

270. **Hoyt DG, Lazo JS**. Alterations in pulmonary mRNA encoding procollagens, fibronectin and transforming growth factor-beta precede bleomycin-induced pulmonary fibrosis in mice. *J Pharmacol Exp Ther* 1988;*246*:765-71.

271. **Khalil N, Bereznay OH, Sporn MB**. Macrophage production of transforming growth factor β and fibroblast collagen synthesis in chronic pulmonary inflammation. *J Exp Med* 1989;*170*:727-37.

272. **Sime PJ, Xing Z, Foley R, Graham FL, Gauldie J**. Transient gene transfer and expression in the lung. *Chest* 1997;*111*:89S-94S.

273. **Giri SN, Hyde DM, Hollinger MA**. Effect of antibody to TGFβ on bleomycin-induced accumulation of lung collagen in mice. *Thorax* 1993;*48*:959-66.

274. **Border WA, Okuda S, Languino LR, Sporn MB, Ruoslahti E**. Suppression of experimental glomerulonephritis by antiserum against transforming growth factor β1. *Nature* 1999;*346*:371-4.

275. **Broekelmann TJ, Limper AH, Colby TV, McDonald JA**. Transforming growth factor β_1 is present at sites of extracellular matrix gene expression in human pulmonary fibrosis. *Proc Natl Acad Sci USA* 1991;*88*:6642-6.

276. **Khalil N, O'Connor R, Unruh HW, Warren PW, Flanders KC, Kemp A, Bereznay OH, Greenberg AH**. Increased production and immunohistochemical localization of transforming growth factor-β in idiopathic pulmonary fibrosis. *Am J Respir Cell Mol Biol* 1991;*5*:155-62.

277. **Kapanci Y, Desmouliere A, Pache JC, Redard M, Gabbiani G**. Cytoskeletal protein modulation in pulmonary alveolar myofibrobalasts during idiopathic pulmonary fibrosis. Possible role of transforming growth factor beta and tumor necrosis factor alpha. *Am J Respir Crit Care Med* 1995;*152*:2163-9.

278. **Khalil N, O'Connor R, Flanders KC**. TGF-β_1 but not TGF-β_2 or TGF-β_3 is differentially present in epithelial cells of advanced pulmonary fibrosis: an immunohistochemical study. *Am J Respir Cell Mol Biol* 1996;*14*:131-8.

279. **Khalil N, Parekh TV, O'Connor R, Antman N, Kepron W, Yehualaeshet T, Xu YD, Gold LI**. Regulation of the effects of TGF-β1 by activation of latent TGF-β receptors (TβR-I and TβR-II) in idiopathic pulmonary fibrosis. *Thorax* 2001;*56*:907-15.

280. **Yong S, Adlakha A, Limper AH**. Circulating transforming growth factor-β_1. A potential marker of disease activity during idiopathic pulmonary fibrosis. *Chest* 2001;*120*:68S-70S.

281. **Coker RK, Laurent GJ, Jeffery PK, du Bois RM, Black CM, McAnulty RJ**. Localisation of transforming growth factor β_1 and β_3 mRNA transcripts in normal and fibrotic human lung. *Thorax* 2001;*56*:549-56.

282. **Vanhee D, Gosset P, Wallaert B, Voisin C, Tonnel AB**. Mechanisms of fibrosis in coal workers' pneumoconiosis. Increased production of platelet-derived growth factor, insulin-like growth factor type-1, and transforming growth factor-β and relationship to disease severity. *Am J Respir Crit Care Med* 1991;*151*:1965-73.

283. **Grande JP**. Role of transforming growth factor-beta in tissue injury and repair. *Proc Soc Exp Biol Med* 1997;*214*:27-40.

284. **Branton MH, Kopp JB**. TGF-beta and fibrosis. *Microbes & Infection* 1999;*1*:1349-65.

285. **Coker RK, Laurent GJ**. Anticytokine approaches in pulmonary fibrosis: bringing factors into focus. *Thorax* 1997;*52*:294-6.

286. **Raghu G, Johnson WC, Lockhart D, Mageto YN**. Treatment of idiopathic pulmonary fibrosis with a new antifibrotic agent, pirfenidone: results of a prospective , open-label phase II study. *Am J Respir Crit Care Med* 1999;*159*:1061-9.

287. **Vaillant P, Menard O, Vignaud JM, Martinet N, Martinet Y**. The role of cytokines in human lung fibrosis. *Monaldi Archives for Chest Disease* 1996;*51*:145-52.

288. **Fujita M, Shannon JM, Irvin CG, Fagan KA, Cool C, Augustin A, Mason RJ**. Overexpression of tumor necrosis factor-α produces an increase in lung volumes and pulmonary hypertension. *Am J Physiol (Lung Cell Mol Physiol)* 2001;*280*:L39-L49

289. **Bazzoni F, Beutler B**. The tumor necrosis factor ligand and receptor families. *N Engl J Med* 1996;*334*:1717-25.

290. **Mauviel A, Daireaux M, Redini F, Galera P, Loyau G, Pujol JP**. Tumor necrosis factor inhibits collagen and fibronectin synthesis in human dermal fibroblasts. *FEBS Lett* 1988;*236*:47-52.

291. **Piguet PF, Vesin C**. Treatment by human recombinant soluble TNF receptor of pulmonary fibrosis induced by bleomycin or silica in mice. *Eur Respir J* 1994;*7*:515-8.

292. **Miyazaki Y, Araki K, Vesin C, Garcia I, Kapanci Y, Whitsett JA, Piguet PF, Vassalli P**. Expression of a tumor necrosis factor-alpha transgene in murine lung causes lymphocytic and fibrosing alveolitis. A mouse model of progressive pulmonary fibrosis. *J Clin Invest* 1995;*96*:250-9.

293. **Sime PJ, Marr RA, Gauldie D, Xing Z, Hewlett BR, Graham FL, Gauldie J**. Transfer of tumor necrosis factor-α to rat lung induces severe pulmonary inflammation and patchy interstitial fibrogenesis with induction of transforming growth factor-β1 and myofibroblasts. *Am J Path* 1998;*153*:825-32.

294. **Fiers W**. Tumor necrosis factor. *FEBS Lett* 1991;*285*:199-212.

295. **Zissel G, Schlaak J, Müller-Quernheim J**. Regulation of cytokine release by alveolar macrophages treated with interleukin-4, interleukin-10, or transforming growth factor beta. *Eur Cytokine Netw* 1996;*7*:59-66.

296. **Piguet PF, Ribaux C, Karpuz V, Grau GE, Kapanci Y**. Expression and localization of tumor necrosis factor-α and its mRNA in idiopathic pulmonary fibrosis. *Am J Path* 1993;*143*:651-5.

297. **Zhang Y, Lee TC, Guillemin B**. Enchanced IL-1β and tumor necrosis factor α release and messenger RNA expression on macrophages from idiopathic pulmonary fibrosis or after asbestosis exposure. *J Immunol* 1993;*150*:4188-96.

298. **Pantelidis P, McGrath DS, Southcott AM, Black CM, du Bois RM**. Tumour necrosis factor-α production in fibrosing alveolitis is macrophage subset specific. *Respir Res* 2001;*2*:365-72.

299. **Metcalf D**. The molecular biology and functions of the granulocyte-macrophage colony-stimulating factors. *Blood* 1986;*67*:257-67.

300. **Christensen PJ, Bailie M, Goodman RE, O'Brien AD, Toews GB, Paine R**. Role of diminished epithelial cell GM-CSF in the pathogensis of bleomycin-induced pulmonary fibrosis. *Am J Physiol (Lung Cell Mol Physiol)* 2000;*279* :L487-L495

301. **Xing Z, Ohkawara M, Jordana M, Graham FL, Gauldie J**. Transfer of granulocyte-macrophage colony-stimulating factor gene to rat lung induces eosinophilia, monocytosis, and fibrotic reactions. *J Clin Invest* 1996;*97*:1102-10.

302. **Xing Z, Tremblay GM, Sime JS, Gauldie J**. Overexpression of granulocyte-macrophage colony stimulating factor induces pulmonary granulation tissue formation and fibrosis by induction of transforming growth factor-β1 and myofibroblast accumulation. *Am J Path* 1997;*150*:59-66.

303. **Reed JH, Rice W, Zsengeller Z, Wert S, Dranoff G, Whitsett JA**. GM-CSF enhances lung growth and causes alveolar type II epithelial cell hyperplasia in transgenic mice. *Am J Physiol (Lung Cell Mol Physiol)* 1997;*273*:L715-L725

304. **Piguet PF, Grau GE, de Kossodo S**. Role of granulocyte-macrophage colony-stimulating factor in pulmonary fibrosis induced in mice by bleomycin. *Exp Lung Res* 1993;*19*:579-87.

305. **Moore BB, Coffey MJ, Christensen P, Sitterding S, Ngan R, Wilke CA, McDonald R, Phare SM, Peters-Golden M, Paine R, Toews GB**. GM-CSF regulates bleomycin-induced pulmonary fibrosis via a prostaglandin-dependent mechanism. *J Immunol* 2000;*165*:4032-9.

306. **Kolb M, Margetts PJ, Anthony DC, Pitossi F, Gauldie J**. Transient expression of IL-1β induces acute lung injury and chronic repair leading to pulmonary fibrosis. *J Clin Invest* 2001;*107*:1529-36.

307. **Thrall RS, Scalise PJ**. Bleomycin. In: Phan SH. ed. *Pulmonary fibrosis*. New York, New York: Marcel Dekker, 1995:231-292.

308. **Pan LH, Ohtani H, Yamauchi K, Nagura H**. Co-expression of TNF alpha and IL-1beta in human acute pulmonary fibrotic diseases. *Pathol Int* 1996;*46*:91-9.

309. **Johnston CJ**. Early and persistent alterations in the expression of interleukin-1 alpha, interleukin-1 beta and tumor necrosis factor alpha mRNA levels in fibrosis-resistant and sensitive mice after thoracic irradiation. *Radiat Res* 1996;*145*:762-7.

310. **Piguet PF, Vesin C, Grau GE, Thompson RC**. Interleukin-1 receptor antagonist prevents or cures pulmonary fibrosis elicited in mice by bleomycin or silica. *Cytokine* 1993;*5*:57-61.

311. **Smith DR, Kunkel SL, Standiford TJ**. Increased interleukin-1 receptor antagonist in idiopathic pulmoary fibrosis. *Am J Respir Crit Care Med* 1995;*151*:1965-73.

312. **Janson RW, King TE, Hance KR, Arend WP**. Enhanced production of IL-1 receptor antagonist by alveolar macrophages from patients with interstitial lung disease. *Am Rev Respir Dis* 1993;*148*:495-503.

313. **Arend WP**. Interleukin-1 receptor antagonist. *Adv Immunol* 1993;*54*:167-227.

314. **Wilmott RW, Kitzmiller JA, Fiedler MA, Stark JM**. Generation of a transgenic mouse with lung-specific over-expression of the human interleukin-1 receptor antagonist protein. *Am J Respir Cell Mol Biol* 1998;*18*:429-34.

315. **Postlethwaite AE, Holness MA, Katai H, Raghow R**. Human fibroblasts synthesize elevated levels of extracellular matrix proteins in response to interleukin 4. *J Clin Invest* 1992;*90*:1479-85.

316. **Gillery P, Fertin C, Nicolas JF, Chasang F, Kalis B, Banchereau J, Maquart FX**. Interleukin-4 stimulates collagen gene expression in human fibroblast monolayer cultures. *FEBS Lett* 1992;*302*:231-4.

317. **Sempowski GD, Beckmann MP, Derdak S, Phipps RP**. Subsets of murine lung fibroblasts express membrane-bound and soluble IL-4 receptors. Role of IL-4 in enhancing fibroblast proliferation and collagen synthesis. *J Immunol* 1994;*152*:3606-14.

318. **Ong C, Wong C, Roberts CA, Teh HS, Jirik FR**. Anti-IL-4 treatment prevents dermal collagen deposition in the tight-skin mouse model of scleroderma. *Eur J Immunol* 1998;*28*:2619-29.

319. **Izbicki G, Or R, Christensen TG, Segel MJ, Fine A, Goldstein RH, Breuer R**. Bleomycin-induced lung fibrosis in IL-4-overexpressing and knockout mice. *Am J Physiol (Lung Cell Mol Physiol)* 2002;*283*:L1110-L1116

320. **Ziegenhagen MW, Zabel P, Zissel G, Schlaak M, Müller-Quernheim J**. Serum level of interleukin 8 is elevated in idiopathic pulmonary fibrosis and indicates disease activity. *Am J Respir Crit Care Med* 1998;*157*:762-8.

321. **Southcott AM, Jones A, Majumdar S, Cambrey AD, Pantelidis P, Black G, Laurent GJ, Davies P, Jeffery PK, du Bois RM**. Interleukin-8: differential expression in lone fibrosing alveolitis and systemic sclerosis. *Am J Respir Crit Care Med* 1995;*151*:1604-12.

322. **Carré PC, Mortenson RL, King TE, Noble P, Sable CL, Riches DWH**. Increased expression of the interleukin-8 gene by alveolar macrophages in idiopathic pulmonary fibrosis. *J Clin Invest* 1991;*88*:1802-10.

323. **Lynch III JP, Standiford TJ, Rolfe MW, Kunkel SL, Strieter RM**. Neutrophilic alveolitis in idiopathic pulmonary fibrosis. *Am Rev Respir Dis* 1992;*145*:1433-9.

324. **Quattrocchi E, Dallman MJ, Dhillon AP, Quaglia A, Bagnato G, Feldmann M**. Murine IL-10 gene transfer inhibits established collagen-induced arthritis and reduces adenovirus-mediated inflammatory responses in mouse liver. *J Immunol* 2001;*166*:5970-8.

325. **Van Scott MR, Justice JP, Bradfield JF, Enright E, Sigounas A, Sur S**. IL-10 reduces Th2 cytokine production and eosinophilia but augments airway reactivity in allergic mice. *Am J Physiol (Lung Cell Mol Physiol)* 2000;*278*:L667-L674

326. **Arai T, Abe K, Matsuoka H, Yoshida M, Mori M, Goya S, Kida H, Nishino K, Osaki T, Tashibana I, Kaneda Y, Hayashi S**. Introduction of the interleukin-10 gene into mice inhibited bleomycin-induced lung injury in vivo. *Am J Physiol (Lung Cell Mol Physiol)* 2000;*278*:L914-L922

327. **de Vries JE**. The role of IL-13 and its receptor in allergy and inflammatory responses. *J Allergy Clin Immunol* 1998;*102*:165-9.

328. **McKenzie GJ, Emson CL, Bell SE, Anderson S, Fallon PG, Grencis R**. Impaired development of Th2 cells in IL-13-deficient mice. *Immunity* 1998;*9*:423-32.

329. **McKenzie AN, Culpepper JA, de Waal-Malefyt R, Briere F, Punonen J, Aversa G, Sato A, Dang W, Cocks BG, Menon S, de Vries JE, Banchereau J, Zurawski S**. Interleukin-13, a T cell derived cytokine that regulates human monocyte and B-cell function. *Proc Natl Acad Sci USA* 1993;*90*:3735-9.

330. **Minty A, Chalon P, Derocq JM, Dumont X, Guillemot J, Kaghad M, Labit C, Leplatois P, Liauzun P, Muoux b, Minty C, Casellas P, Loison G, Lupker J, Shire D, Ferrara P,**

Caput D. Interleukin-13 is a new human lymphokine regulating inflammatory and immune responses. *Nature* 1993;*362*:248-50.

331. **de Saint-Vis B, Fugier-Vivier I, Massacrier C, Gaillard C, Vanbervliet B, Aît-Yahia S, Banchereau J, Liu YJ, Lebecque S, Caux C**. The cytokine profile expressed by human dendritic cells is dependent on cell subtype and mode of activation. *J Immunol* 1998;*160*:1666-76.

332. **Doucet C, Brouty-Boye D, Pottin-Clemenceau C, Canonica GW, Jasmin C, Azzarone B**. Interleukin (IL)-4 and IL-13 act on human lung fibroblasts. *J Clin Invest* 1998;*101*:2129-39.

333. **Grünig G, Warnock M, Wakil AE, Venkayya R, Brombacher F, Rennick DM, Sheppard D, Mohrs M, Donaldson DD, Locksley RM, Corry DB**. Requirement for IL-13 independently of IL-4 in experimental asthma. *Science* 1998;*282*:2261-3.

334. **Elias JA, Zhu Z, Chupp G, Homer RJ**. Airway remodeling in asthma. *J Clin Invest* 1999;*104*:1001-6.

335. **Fallon PG, Richardson EJ, McKenzie GJ, McKenzie AN**. Schistosome infection of transgenic mice defines distinct and contrasting pathogenic roles for IL-4 and IL-13: IL-13 is a profibrotic agent. *J Immunol* 2000;*164*:2585-91.

336. **Homer RJ, Zheng T, Chupp G, He S, Zhu Z, Chen Q, Ma B, Hite RD, Gobran LI, Rooney SA, Elias JA**. Pulmonary type II cell hypertrophy and pulmonary lipoproteinosis are features of chronic IL-13 exposure. *Am J Physiol (Lung Cell Mol Physiol)* 2002;*283*:L52-L59

337. **Standiford TJ, Rolfe MW, Kunkel SL**. Macrophage inflammatory protein-1α expression in interstitial lung disease. *J Immunol* 1993;*151*:2852-63.

338. **Sakanashi Y, Takeya M, Yoshimura T, Feng L, Morioka T, Takahashi K**. Kinetics of macrophage subpopulations and expression of monocyte chemoattractant protein-1 (MCP-1) in bleomycin-induced lung injury of rats studies by a novel monoclonal antibody against rat MCP-1. *J Leukoc Biol* 1994;*56*:741-50.

339. **Smith RE, Strieter RM, Zhang K, Phan SH, Standiford TJ, Lukacs N, Kunkel SL**. A rolel for C-C chemokines in fibrotic lung disease. *J Leukoc Biol* 1994;*57*:782-7.

340. **Smith RE, Phan SH, Strieter RM, Glass MC, Burdick MD, Lincoln P, Evanoff H, Kunkel SL**. Soluble TNF receptor mediated reduction of MIP-1α expression in bleomycin-induced lung injury. *Third Annual International Cytokine Conference, Banff, Alberta, Canada* 1994;

341. **Strieter RM, Wiggins R, Phan SH, Wharram BL, Showell HJ, Remick DG, Chensue SW, Kunkel SL**. Monocyte chemotactic protein gene expression by cytokine-treated human fibroblasts and endothelial cells. *Biochem Biophys Res Commun* 1989;*162*:694-700.

342. **Chensue SW, Warmington K, Ruth JS, Sanghi PS, Lincoln P, Kunkel SL**. Role of monocyte chemoattractant protein-1 in Th1 (Mycobaterial) and Th2 (Schistosomal) antigen-induced granuloma formation: relationship to local inflammation, Th cell expression and IL-12 production. *J Immunol* 1996;*157*:4602-8.

343. **Karpus WJ, Lukacs NW, Kennedy KJ, Smith WS, Hurst SD, Barrett TA**. Differential CC chemokine-induced enhancement of T helper cell cytokine production. *J Immunol* 1997;*158*:4129-36.

344. **Lukacs NW, Chensue SW, Karpus WJ, Lincoln P, Keefer C, Strieter RM, Kunkel SL.** C-C chemokines differentially alter interleukin-4 production from lymphocytes. *Am J Path* 1997;*150*:1861-8.

345. **Hogaboam CM, Lukacs NW, Chensue SW, Strieter RM, Kunkel SL.** Monocyte chemoattractant protein-1 synthesis by murine lung fibroblasts modulates $CD4^+$ T cell activation. *J Immunol* 1998;*160*:4606-14.

346. **Brieland JK, Fantone JC.** Neutrophils and pulmonary fibrosis. In: Phan SH, Thrall RS. eds. *Pulmonary fibrosis*. New York: Marcel Dekker, Inc., 1995:383-404.

347. **Thrall RS, Phan SH, McCormick JR, Ward PA.** The development of bleomycin-induced pulmonary fibrosis in neutrophil-depleted and complement-depleted rats. *Am J Path* 1981;*105*:76-81.

348. **Clark JG, Kuhn III C.** Bleomycin-induced pulmonary fibrosis in hamsters: effect of neutrophil depletion on lung collagen synthesis. *Am Rev Respir Dis* 1982;*127*:456-9.

349. **Obayashi Y, Yamadori I, Fujita J, Yoshinouchi T, Ueda N, Takahara J.** The role of neutrophils in the pathogenesis of idiopathic pulmonary fibrosis. *Chest* 1997;*112*:1338-43.

350. **King TE, Cherniack RM, Schwarz MI.** Idiopathic pulmonary fibrosis and other interstitial lung diseases of unknown etiology. In: Murray NM. ed. *Textbook of respiratory medicine*. 2 Ed. Philadelphia: W.B.Saunders Company, 1994:1827-1849.

351. **Cantin AM, North SL, Fells GA, Hubbard RC, Crystal RG.** Oxidant mediated epithelial cell injury in idiopathic pulmonary fibrosis. *J Clin Invest* 1987; *79*:1665-73.

352. **Gadeck JE, Kelman JA, Fells GA, Weiberger SE, Horwitz AL.** Collagenase in the lower respiratory tract of patients with idiopathic pulmonary fibrosis. *N Engl J Med* 1979;*301*:737-42.

353. **Mitsuhashi H, Asano S, Nonaka T, Hamamura I, Masuda K, Kiyoki M.** Administration of truncated secretory leukoprotease inhibitor ameliorates bleomycin-induced pulmonary fibrosis in hamsters. *Am J Respir Crit Care Med* 1996;*153*:369-74.

354. **Strausz J, Müller-Quernheim J, Steppling H, Ferlinz R.** Oxygen radical production by alveolar inflammatory cells in idiopathic pulmonary fibrosis. *Am Rev Respir Dis* 1990;*141*:124-8.

355. **Crystal RG, Ferrans VJ, Basset F.** Biologic basis of pulmonary fibrosis. In: Crystal RG, West JB. eds. *The lung: scientific foundations*. New York: Raven Press, Ltd., 1991:2031-2046.

356. **Cassatella MA.** The productin of cyotkines by polymorphonuclear neutrophils. *Immunol Today* 1995;*16*:21-6.

357. **Dunnill MS.** Pulmonary fibrosis. *Histopathology* 1990;*16*:321-9.

358. **Peterson MW, Monick M, Hunninghake GW.** Prognostic role of eosinophils in pulmonary fibrosis. *Chest* 1987;*92*:51-6.

359. **Fujimoto K, Kubo K, Yamaguchi S, Honda T, Matsuzuma Y.** Eosinophil activation in patients with pulmonary fibrosis. *Chest* 1995;*108*:48-54.

360. **Zhang K, Gharaee-Kermani M, McGary B, Remick D, Phan SH**. TNF-α mediated lung cyotkine networking and eosinophil recruitment in pulmonary fibrosis. *J Immunol* 1997;*158*:954-9.

361. **Ohnishi T, Kita H, Weller D, Sur S, Sedgwick JB, Calhoun WJ, Busse WW, Abrams J, Gleich GJ**. IL-5 is the predominant eosinophil-active cytokine in the antigen-induced pulmonary late-phase reaction. *Am Rev Respir Dis* 1993;*147*:901-7.

362. **Bradley B, Azzawi M, Jacobson M, Assoufi B, Collins JV, Irani AAM, Schwartz LB, Durham SR, Jeffery PK, Kay AB** . Eosinophils, T-lymphocytes, mast cells, neutrophils and macrophages in bronchial biopsy specimens from atopic subjects with asthma: comparison with atopic subjects without asthma and normal control subjects. *J Allergy Clin Immunol* 1991;*88*:661-74.

363. **Broide DH, Pains MM, Firestein GS**. Eosinophils express interleukin-5 and granulocyte/macrophage-colony-stimulating factor mRNA at sites of allergic inflammation in asthmatics. *J Clin Invest* 1992;*90*:1414-24.

364. **Szapiel SV, Elson NA, Fulmer JD, Hunninghake GW, Crystal RG**. Bleomycin-induced interstitial pulmonary disease in the nude, athymic mouse. *Am Rev Respir Dis* 1979;*120*:893-9.

365. **Postlethwaite AE, Smith GN, Mainardi CL, Seyer JM, Kang AH**. Lymphocyte modulation of fibroblasts in vitro: stimulation and inhibition of collagen production but different effector molecules. *J Immunol* 1984;*132*:2470-7.

366. **Monroe JG, Haldar S, Prystowsky MB, Lammie P**. Lymphokine regulation of inflammatory processes: interleukin-4 stimulates fibroblast proliferation. *Clin Immunol Immunopathol* 1988;*49*:292-8.

367. **Garlisi CG, Falcone A, Kung TT, Stelts D, Pennline KJ, Beavis AJ, Smith SR, Egan RW, Umland SP**. T cells are necessary for Th2 cytokine production and eosinophil ccumulation in airways of antigen-challenged allergic mice. *Clin Immunol Immunopathol* 1995;*75*:75-83.

368. **Fireman E, Vardinon N, Burke M, Spizer S, Levin S, Endler A, Stav D, Topilsky M, Mann A, Schwarz Y, Kivity S, Greif J**. Predictative value of response to treatment of T-lymphocyte subpopulations in idiopathic pulmonary fibrosis. *Eur Respir J* 1998;*11*:706-11.

369. **Yamadori I, Fujita J, Kajitani H, Bandoh S, Tokuda M, Yang Y, Ohtsuki Y, Yoshinouchi T, Kamei T, Ishida T**. Lymphocyte subsets in lung tissues of non-specific interstitial pneumonia and pulmonary fibrosis associated wtih collagen vascular disorders: correlation with CD4/CD8 ratio in broncholalvelar lavage. *Lung* 2000;*178*:361-70.

370. **Campbell DA, Poulter LW, Janossy G, du Bois RM**. Immunohistological analysis of lung tissue from patients with cryptogenic fibrosing alveolitis suggesting local expression of immune hypersensitivity. *Thorax* 1985;*40*:405-11.

371. **Wallace WA, Howie SE, Krajewski AS, Lamb D**. The immunological architecture of B-lymphocyte aggregates in cryptogenic fibrosing alveolitis. *J Pathol* 1996;*178*:323-9.

372. **Lambrecht BN**. The dendritic cell in allergic airway diseases: a new player to the game. *Clin Exp Allergy* 2001;*31*:206-18.

373. **Caux C, Massacrier C, Vanbervliet B**. Activation of human dendritic cells through CD40 cross-linking. *J Exp Med* 1994;*180*:1263-72.

374. **Björck P, Banchereau J, Flores-Romo L**. CD40 ligation counteracts Fas-induced apoptosis of human dendritic cells. *Int Immunol* 1997;*9*:365-72.

375. **Kawanami O, Ferrans VJ, Fulmer JD**. Ultrastructure of pulmonary mast cells in patients with fibrotic lung disorders. *Lab Invest* 1979;*40*:717-34.

376. **Goto T, Befus D, Low R**. Mast cell heterogeneity and hyperplasia in bleomycin-induced pulmonary fibrosis in rats. *Am Rev Respir Dis* 1984;*130*:797-802.

377. **Aldenborg F, Nilsson K, Jarlshammar B**. Mast cells and biogenic amines in radiation-induced pulmonary fibrosis. *Am J Respir Cell Mol Biol* 1993;*8*:112-7.

378. **Agius RM, Godfrey RC, Holgate ST**. Mast cell and histamine contnet of human bronchoalveolar lavage fluid. *Thorax* 1985;*40*:760-7.

379. **Jordana M**. Mast cells and fibrosis - who's on first? *Am J Respir Cell Mol Biol* 1993;*8*:7-8.

380. **Mahnke K, Bhardwaj RS, Luger TA**. Interaction of murine dendritic cells with collagen up-regulates allostimulatory capacity, surface expression of heat stable antigen, and release of cytokines. *J Leukoc Biol* 1996;*60*:465-72.

381. **Kodaira Y, Nair SK, Wrenshall LE**. Phenotypic and functional maturation of dendritic cells mediated by heparan suflate. *J Immunol* 2000;*165*:1599-604.

382. **Pforte A, Gerth C, Voss A**. Proliferating alveolar macrophages in BAL and lung function changes in interstitial lung disease. *Eur Respir J* 1993;*6*:951-5.

383. **Hunninghake GW, Gadek E, Lawley TJ, Crystal RG**. Mechanisms of neutrophil accumulation in the lungs of patients with idiopathic pulmonary fibrosis. *J Clin Invest* 1981;*68*:259-69.

384. **Zhu S, Manuel M, Tanaka S, Choe N, Kagan E, Matalon S**. Contribution of reactive oxygen and nitrogen species to particulate-induced lung injury. *Environ Health Perspect* 1998;*106*:1157-63.

385. **Martinet Y, Rom WN, Grotendorst GR, Martin GR, Crystal RG**. Exaggerated spontaneous release of platelet-derived growth factor by alveolar macrophages from patients with idiopathic pulmonary fibrosis. *N Engl J Med* 1987;*31*:202-9.

386. **Ward PA**. Phagocytes and the lung. *Ann NY Acad Sci* 1997;*832*:304-10.

387. **Lardot C, Delos M, Lison D**. Upregulation of urokinase in alveolar macrophages and lung tissue in reponse to silica particles. *Am J Physiol* 1998;*274*:L1040-L1048

388. **Gyetko M, Wilkinson C, Sitrin R**. Monocyte urokinase expression: modulation by interleukins. *J Leukoc Biol* 1993;*53*:598-601.

389. **Wilborn J, Crofford L, Burkick M, Kunkel SL, Strieter RM, Peters-Golden M**. Cultured lung fibroblasts isolated from patients with idiopathic pulmonary fibrosis have a diminished capacity to synthesize prostaglandin E_2 and to express cyclooxygenase-2. *J Clin Invest* 1995;*95*:1861-8.

390. **Bitterman PB, Wewers N, Rennard SI, Adelberg S, Crystal RG**. Modulation of alveolar macrophage-driven fibroblast proliferation by alternative macrophage mediators. *J Clin Invest* 1986;*77*:700

391. **Korn J, Halushka P, Leroy E**. Mononculear cell modulation of connective tissue function: suppression of fibroblast growth by stimulation of endogenous prostaglandin production. *J Clin Invest* 1980;*65*:543-54.

392. **Lemjabbar H, Gosset P, Lechapt-Zalcman E, Franco-Montoya M, Wallaert B, Harf A, Lafuma C**. Overexpression of alveolar macrophage gelatinase B (MMP-9) in patients with idiopathic pulmonary fibrosis. *Am J Respir Cell Mol Biol* 1999; *20*:903-13.

393. **Nash JRG, McLaughlin PJ, Butcher D, Corrin B**. Expression of tumour necrosis factor-α in cryptogenic fibrosing alveolitis. *Histopathology* 1993;*22*:343-7.

394. **Vignaud JM, Allam M, Martinet N, Pech M, Plenat F, Martinet Y**. Presence of platelet-derived growth factor in normal and fibrotic lung is specifically associated with interstitial macrophages, while both interstitial macrophages and alveolar epithelial cells express the *c-sis* proto-oncogene. *Am J Respir Cell Mol Biol* 1991;*5*:531-8.

395. **Antoniades HN, Bravo M, Avila R, Galanopoulos T, Neville-Golden J**. Platelet-derived growth factor in idiopathic pulmonary fibrosis. *J Clin Invest* 1990;*86*:1055-64.

396. **Pardo A, Selman M**. Idiopathic pulmonary fibrosis: new insights in its pathogenesis. *Int J Biochem Cell Biol* 2002;*34*:1534-8.

397. **Haschek WM, Brody AR, Klein-Szanto AJ, Witschi H**. Animal model of human disease. Diffuse interstitial pulmonary fibrosis. Pulmonary fibrosis in mice induced by treatment with butylated hydroxytoluene and oxygen. *Am J Path* 1981;*105*:333-5.

398. **Klein J, Adamson IYR**. Fibroblast inhibition and prostaglandin secretion by alveolar epithelial cells exposed to silica. *Lab Invest* 1989;*60*:808-13.

399. **Pan T, Mason RJ, Westcott J, Shannon JM**. Rat alveolar type II cells inhibit lung fibroblast proliferation *in vitro*. *Am J Respir Cell Mol Biol* 2001;*25*:353-61.

400. **Moore BB, Peters-Golden M, Christensen PJ, Lama V, Kuziel WA, Paine III R, Toews GB**. Alveolar epithelial cell inhibition of fibroblast proliferation is regulated by MCP-1/CCR2 and mediated by PGE_2. *Am J Physiol (Lung Cell Mol Physiol)* 2002;*(in press)*:

401. **Lama V, Moore BB, Christensen P, Toews GB, Peters-Golden M**. Prostaglandin E_2 synthesis and suppression of fibroblast proliferation by alveolar epithelial cells is cyclooxygenase-2-dependent. *Am J Respir Cell Mol Biol* 2002;*27*:752-8.

402. **Brody AR, Soler P, Basset F, Haschek WM, Witschi H**. Epithelial-mesenchymal associations of cells in human pulmonary fibrosis and in BHT-oxygen-induced fibrosis in mice. *Exp Lung Res* 1981;*2*:207-20.

403. **Fasske E, Morgenroth K**. Experimental bleomycin lung in mice. A contribution to the pathogenesis of pulmonary fibrosis. *Lung* 1983;*161*:133-46.

404. **Gerritsen ME, Bloor CM**. Endothelial cell gene expression in response to injury. *FASEB J* 1993;*7*:523-32.

405. **Kawamoto M, Fukuda Y**. Cell proliferation during the process of bleomycin-induced pulmonary fibrosis in rats. *Acta Pathol Japan* 1990;*40*:227-38.

406. **McGavran PD, Moore LB, Brody AR**. Inhalation of chrysotile asbestos induces rapid cellular proliferation in small pulmonary vessels of mice and rats. *Am J Path* 1990;*136*:695-705.

407. **Kumar RK, Lykke AW**. Messages and handshakes: cellular interactions in pulmonary fibrosis. *Pathology* 1995;*27*:18-26.

408. **Ramos C, Montano M, Garcia-Alvarez J, Ruiz V, Uhal BD, Selman M, Pardo A**. Fibroblasts from idiopathic pulmonary fibrosis and normal lungs differ in growth rate, apoptosis, and tissue inhibitor of metalloproteinases expression. *Am J Respir Cell Mol Biol* 2001;*24*:594-8.

409. **Venkatesan N, Roughley PJ, Ludwig MS**. Proteoglycan expression in bleomycin lung fibroblasts: role of transforming growth factor-β_1 and interferon-γ. *Am J Physiol (Lung Cell Mol Physiol)* 2002;*283*:L806-L814

410. **Hogaboam CM, Bone-Larson CL, Lipinski S, Lukacs NW, Chensue SW, Strieter RM, Kunkel SL**. Differential monocyte chemoattractant protein-1 and chemokine receptor 2 expression by murine lung fibroblasts derived from Th1- and Th2-type pulmonary granuloma models. *J Immunol* 1999;*163*:2193-201.

411. **Buckley CD, Pilling D, Lord JM, Akbar AN, Scheel-Toellner D, Salmon M**. Fibroblasts regulate the switch from acute resolving to chronic persistent inflammation. *Trends Immunol* 2001;*22*:199-204.

412. **Kuhn III C, McDonald JA**. The roles of the myofibroblast in idiopathic pulmonary fibrosis: ultrastructural and immunohistochemical features of sites of active extracellular matrix synthesis. *Am J Path* 1991;*138*:1257-65.

413. **Fukuda Y, Ishizaki M, Kudoh S, Kitaichi M, Yamanaka N**. Localization of matrix metalloproteinases-1, -2, and -9, and tissue inhibitor of metalloproteinase-2 in interstitial lung diseases. *Lab Invest* 1998;*78*:687-98.

414. **Selman M, Ruiz V, Cabrera S, Segura L, Ramirez R, Barrios R, Pardo A**. TIMP-1, -2, -3 and -4 in idiopathic pulmonary fibrosis. A prevailing non-degradative lung microenvironment? *Am J Physiol* 2000;*279*:L562-L574

415. **Vancheri C, Sortino MA, Tomaselli V, Mastruzzo C, Condorelli F, Bellistri G, Pistorio MP, Canonico PL, Crimi N**. Different expression of TNF-α receptros and prostaglandin E_2 production in normal and fibrotic lung fibroblasts. Potential implications for the evolution of the inflammatory process. *Am J Respir Cell Mol Biol* 2000;*22*:628-34.

416. **Uhal BD, Joshi I, True AL, Mundle S, Raza A, Pardo A, Selman M**. Fibroblasts isolated after fibrotic lung injury induce apoptosis of alveolar epithelial cells in vitro. *Am J Physiol* 1995;*269*:L819-L828

417. **Wang R, Ramos C, Joshi I, Zagariya A, Pardo A, Selman M, Uhal BD**. Human lung myofibroblast-derived inducers of alveolar epithelial apoptosis identified as angiotensin peptides. *Am J Physiol* 1999;*277*:L1158-L1164

418. **Uhal BD, Joshi I, Hughes WF, Ramos C, Pardo A, Selman M**. Alveolar epithelial cell death adjacent to underlying myofibroblasts in advanced fibrotic human lung. *Am J Physiol* 1998;*275*:L1192-L1199

419. **Hsieh CS, Heimberger AB, Gold JS, O'Garra A, Murphy KM**. Differential regulation of T helper phenotype development by interleukins 4 and 10 in an alpha beta T-cell-receptor transgenic system. *Proc Natl Acad Sci USA* 1992;*89*:6065-9.

420. **Magdaleno SM, Wang G, Jackson KJ, Ray MK, Welty S, Costa RH, DeMayo FJ**. Interferon-γ regulation of Clara cell gene expression: in vivo and in vitro. *Am J Physiol (Lung Cell Mol Physiol)* 1997;*272*:L1142-L1151

421. **Gould VE, Miller J**. Sclerosing alveolitis induced by cyclophosphamide: ultrasturctural observations on alveolar injury and repair. *Am J Path* 1975;*81*:513-30.

422. **Smith P, Heath D, Kay JM**. The pathogenesis and structure of paraquat-induced pulmonary fibrosis. *J Pathol* 1974;*114*:57-67.

423. **Taylor RG, McCall CE, Thrall RS, Woodruff RD, O'Flaherty JT**. Histopathologic features of phorbol myristate acetate-iniduced lung injury. *Lab Invest* 1985;*52*:61-70.

424. **Sikic BI, Young DM, Mimnaugh EG, Gram TE**. Quantification of bleomycin pulmonary toxicity in mice by changes in lung hydroxyproline content and morphometric histopathology. *Cancer Res* 1978;*38*:787-92.

425. **Reiser KM, Last JA**. Pulmonary fibrosis in experimental acute respiratory disease. *Am Rev Respir Dis* 1981;*123*:58-63.

426. **Brown RF, Drawbaugh RB, Marrs TC**. An investigation of possible models for the production of progressive pulmonary fibrosis in the rat: the effects of repeated intratracheal instillation of bleomycin. *Toxicology* 1988;*51*:101-10.

427. **Yagoda A, Mukherji B, Young E, Etcubanas E, Lamonte C, Smith JR, Tan CT, Krakoff IH**. Bleomycin: an antitumor antibiotic: clinical experience in 274 patients. *Ann Intern Med* 1972;*77*:861-5.

428. **Unemori EN, Pickford LB, Salles AL, Piercy CE, Grove BH, Erikson ME, Amento EP**. Relaxin induces an extracellular matrix-degrading phenotype in human lung fibroblasts in vitro and inhibits lung fibrosis in a murine model in vivo. *J Clin Invest* 1996;*98*:2739-45.

429. **Kolb M, Margetts PJ, Galt T, Sime PJ, Xing Z, Schmidt M, Gauldie J**. Transient transgene expression of decorin in the lung reduces the fibrotic response to bleomycin. *Am J Respir Crit Care Med* 2001;*163*:770-7.

430. **Macatonia SE, Knight SC, Edwards AJ, Griffiths S, Fryer P**. Localization of antigen on lymph node dendritic cells after exposure to the contact sensitizer fluorescein isothiocyanate: functional and morphological studies. *J Exp Med* 1987;*166*:1654-67.

431. **Nelson S, Bagby GJ, Bainton BG, Wilson LA, Tompson JJ, Summer WR**. Compartmentalization of intra-alveolar and systemic lipopolysaccharide-induced tumor necrosis factor and the pulmonary inflammatory response. *J Infect Dis* 1989;*159*:189-94.

432. **Yehualaeshet T, O'Connor R, Green-Johnson J, Mai S, Silverstein R, Murphy-Ullrich JE, Khalil N**. Activation of rat alveolar macrophage-derived latent transforming growth factor β–1 by plasmin requires interaction with thrombospondin-1 and its cell surface receptor, CD36. *Am J Path* 1999;*155*:841-51.

433. **Yehualaeshet T, O'Connor R, Begleiter A, Murphy-Ullrich JE, Silverstein R, Khalil N**. A CD36 synthetic peptide inhibits bleomycin-induced pulmonary inflammation and connective tissue synthesis in the rat. *Am J Respir Cell Mol Biol* 2000;*23*:204-12.

434. **Gauldie J, Sime PJ, Xing Z, Marr B, Tremblay GM**. Transforming growth factor-beta gene transfer to the lung induces myofibroblast presence and pulmonary fibrosis. *Curr Top Pathol* 1999;*93*:35-45.

435. **Ashcroft T, Simpson JM, Timbrell V**. Simple method of estimating severity of pulmonary fibrosis on a numerical scale. *J Clin Pathol* 1988;*41*:467-70.

436. **Oury TD, Thakker K, Menache M, Chang LY, Crapo JD, Day BJ**. Attenuation of bleomycin-induced pulmonary fibrosis by a catalytic antioxidant metalloporphyrin. *Am J Respir Cell Mol Biol* 2001;*25*:164-9.

437. **Yasui H, Gabazza EC, Tamaki S, Kobayashi T, Hataji O, Yuda H, Shimizu S, Suzuki K, Adachi Y, Taguchi O**. Intratracheal administration of activated protein C inhibits bleomycin-induced lung fibrosis in the mouse. *Am J Respir Crit Care Med* 2001;*163*:1660-8.

438. **Takahashi F, Takahashi K, Okazaki T, Maeda K, Ienaga H, Maeda M, Kon S, Uede T**. Role of osteopontin in the pathogenesis of bleomycin-induced pulmonary fibrosis. *Am J Respir Cell Mol Biol* 2001;*24*:264-71.

439. **Krishna G, Liu KL, Shigemitsu H, Gao MX, Raffin A, Rosen GD**. PG490-88, a derivative of triptolide, blocks bleomycin-induced lung fibrosis. *Am J Path* 2001;*158*:997-1004.

440. **Shimizu Y, Dobashi K, Iizuka K, Horie T, Suzuki K, Tukagoshi H, Nakazawa T, Nakazato Y, Mori M**. Contribution of small GTPase Rho and its target protein ROCK in a murine model of lung fibrosis. *Am J Respir Crit Care Med* 2001;*163*:210-7.

441. **Dohi M, Hasegawa T, Yamamoto K, Marshall BC**. Hepatocyte growth factor attenuates collagen accumulation in a murine model of pulmonary fibrosis. *Am J Respir Crit Care Med* 2000;*162*:2302-7.

442. **Hagiwara S, Ishii Y, Kitamura S**. Aerosolized administration of *N*-acetylcysteine attenuates lung fibrosis induced by bleomycin in mice. *Am J Respir Crit Care Med* 2000;*162*:225-31.

443. **Tamagawa K, Taooka Y, Maeda A, Hiyama K, Ishioka S, Yamakido M**. Inhibitory effects of a lecithinized superoxide dismutase on bleomycin-induced pulmonary fibrosis. *Am J Respir Crit Care Med* 2000;*161*:1279-84.

444. **Wild JS, Sigounas A, Sur N, Siddiqui S, Alam R, Kurimoto M, Sur S**. IFN-gamma-inducing factor (IL-18) increases allergic sensitization, serum IgE, Th2 cytokines, and airway eosinophilia in a mouse model of allergic asthma. *J Immunol* 2000;*164*:2701-10.

445. **Matsuse T, Teramoto S, Katayama H, Sudo E, Ekimoto H, Mitsuhashi H, Uejima Y, Fukuchi Y, Ouchi Y**. ICAM-1 mediates lung leukocyte recruitment but not pulmonary fibrosis in a murine model of bleomycin-induced lung injury. *Eur Respir J* 1999;*13*:71-7.

446. **Yaekashiwa M, Nakayama S, Ohnuma K, Sakai T, Abe T, Satoh K, Matsumoto T, Nakamura T, Takahashi T, Nukiwa T**. Simultaneous or delayed administration of hepatocyte growth factor equally respresses the fibrotic changes in murine lung injury induced by bleomycin - a morphologic study. *Am J Respir Crit Care Med* 1997;*156*:1937-44.

447. **Kradin RL, Divertie MB, Colvin RB, Ramirez J, Ryu JH, Carpenter HA, Bhan AK**. Usual interstitial pneumonitis is a T-cell alveolitis. *Clin Immunol Immunopathol* 1986;*40*:224-35.

448. **Haslam PL, Turton CWG, Heard B**. Broncholaveolar lavage in pulmonary fibrosis: comparison of cells obtained with lung biopsy and clinical features. *Thorax* 1980;*35*:9-18.

449. **Romagnani S, Kapsenberg M, Radbruch A, Adorini L**. Th1 and Th2 cells. *Res Immunol* 1998;*149*:871-3.

450. **Kumar RK, Watkins SG, Lykke AW**. Pulmonary responses to bleomycin-induced injury: an immunomorphologic and electron micropscopic study. *Exp Pathol* 1985;*28*:43

451. **Helene M, Lake-Bullock V, Zhu J, Hao H, Cohen DA, Kaplan AM**. T cell independence of bleomycin-induced pulmonary fibrosis. *J Leukoc Biol* 1999;*65*:187

452. **Suzuki N, Ohta K, Uede T, Ueda T, Ito K, Shiga J**. T lymphocytes and silica-induced pulmonary inflammation and fibrosis in mice. *Thorax* 1996;*51*:1036-42.

453. **Corsini E, Luster MI, Mahler J, Craig WA, Blazka ME, Rosenthal GJ**. A protective role for T lymphocytes in asbestos-induced pulmonary inflammation and collagen deposition. *Am J Respir Cell Mol Biol* 1994;*11*:531-9.

454. **Kidney JC, Proud D**. Neutrophil transmigration across human airway epithelial monolayers. Mechanisms and dependence on electrical resistance. *Am J Respir Cell Mol Biol* 2000;*23*:389-95.

455. **Rosseau S, Selhorst J, Wiechmann K, Leissner K, Maus U, Mayer K, Grimminger F, Seeger W, Lohmeyer J**. Monocyte migration through the alveolar epithelial barrier: adhesion molecule mechanisms and impact of chemokines. *J Immunol* 2000;*164*:427-35.

456. **Yamamoto N, Suzuki S, Suzuki Y, Shirai A, Nakazawa M, Suzuki M, Takamasu T, Nagashima Y, Minami M, Ishigatsubo Y**. Immune response induced by airway sensitization after influenza A virus infection depends on timing of antigen exposure in mie. *J Virol* 2001;*75*:499-505.

457. **Stewart GA, Hoyne GF, Ahmad SA, Jarman E, Wallace WA, Harrison DJ, Haslett C, Lamb JR, Howie SE**. Expression of the developmental Sonic hedgehog (Shh) signalling pathway is upregulated in chronic lung fibrosis and the Shh receptor patched 1 is present in circulating T lymphocytes. *J Pathol* 2002;*(in press)*:

458. **Ziegenhagen MW, Schrum S, Zissel G, Zipfel PF, Schlaak M, Müller-Quernheim J**. Increased expression of proinflammatory chemokines in bronchoalveolar lavage cells of patients with progressing idiopathic pulmonary fibrosis and sarcoidosis. *J Invest Med* 1998;*46*:223-31.

459. **Smith RE, Strieter RM, Phan SH, Lukacs N, Kunkel SL**. TNF and IL-6 mediate MIP-1alpha expression in bleomycin-induced lung injury. *J Leukoc Biol* 1998;*64*:528-36.

460. **Piguet PF, Collart MA, Grau GE, Sappino A, Vassalli P**. Requirement of tumour necrosis factor for development of silica-induced pulmonary fibrosis. *Nature* 1990;*344*:245-7.

461. **Lasky JA, Brody AR**. Intersititial fibrosis and growth factors. *Environ Health Perspect* 2000;*108*:751-62.

462. **Strieter RM**. Mechanisms of pulmonary fibrosis. *Chest* 2001;*120*:77S-85S.

463. **Kolb M, Margetts PJ, Sime PJ, Gauldie J**. Proteoglycans decorin and biglycan differentially modulate TGF-β-mediated fibrotic responses in the lung. *Am J Physiol (Lung Cell Mol Physiol)* 2001;*280*:L1327-L1334

464. **Kolb M, Bonniaud P, Galt T, Sime PJ, Kelly MM, Margetts PJ, Gauldie J**. Differences in the fibrogenic response after transfer of active transforming growth factor-β1 gene to lungs of "fibrosis-prone" and "fibrosis-resistant" mouse strains. *Am J Respir Cell Mol Biol* 2002;*27*:141-50.

465. **Baecher-Allan CM, Barth RK**. PCR analysis of cytokine induction profiles associated with mouse strain variation in susceptibility to pulmonary fibrosis. *Reg Immunol* 1993;*5*:207-17.

466. **Yamaguchi Y, Mann DM, Ruoslahti E**. Negative regulation of TGFβ by the proteoglycan decorin. *Nature* 1990;*346*:281-4.

467. **Hildebrand AM, Romaris M, Rasmussen LM, Heinegard D, Twardzik DR, Border WA, Ruoslahti E**. Interaction of the small proteoglycans biglycan, decorin and fibromodulin with TGFβ. *Biochem J* 1994;*302*:527-34.

468. **Blussé van oud Alblas A, van Furth R**. Origin, kinetics, and characteristics of pulmonary macrophages in the normal steady state. *J Exp Med* 1979;*149*:1504-18.

469. **Warheit D, Overby L, George G, Brody AR**. Pulmonary macrophages are attracted to inhaled particles through complement activation. *Exp Lung Res* 1988;*14*:51-6.

470. **Müller G, Müller A, Jonuleit H, Steinbrink K, Szalma C, Paragnik L, Lingnau K, Schmidt E, Knop J, Enk AH**. Fetal calf serum-free generation of functionally active murine dendritic cells suitable for *in vivo* therapeutic approaches. *J Invest Dermatol* 2000;*114*:142-8.

471. **Holt PG, Degebrodt A, Venaille T, O'Leary C, Krska K, Flexman J, Farrell H, Shellam G, Young P, Penhale J, Robertson T, Papadimitrious JM**. Preparation of interstitial lung cells by enzymatic digestion of tissue slices: preliminary characterization by morphology and performance in functional assays. *Immunology* 1985;*54*:139-47.

472. **Nicod LP, Lipscomb MF, Weissler JC, Lyons CR, Albertson J, Toews GB**. Characterization of a potent accessory cell not obtained by bronchoalveolar lavage. *Am Rev Respir Dis* 1987;*136*:818-23.

473. **Holt PG, Stumbles PA, McWilliam AS**. Functional studies on dendritic cells in the respiratory tract and related mucosal tissues. *J Leukoc Biol* 1999;*66*:272-5.

474. **Thepen T, van Rooijen N, Kraal G**. Alveolar macrophage elimination in vivo is associated with an increase in pulmonary immune response in mice. *J Exp Med* 1989;*170*:499-509.

475. **Lipscomb MF, Pollard AM, Yates JL**. A role for TGF-beta in the suppression by murine bronchoalveolar cells of lung dendritic cell initiated immune responses. *Reg Immunol* 1993;*5*:151-7.

476. **Puré E, Inaba K, Crowley MT, Tardelli L, Witmer-Pack MD, Ruberti G, Garrison F, Steinman RM**. Antigen processing by epidermal Langerhans cells correlates with the level of biosynthesis of major histocompatibility complex class II molecules and expression of invariant chain. *J Exp Med* 1990;*172*:1459-69.

477. **Girolomoni G, Simon JC, Bergstresser PR, Cruz Jr PD**. Freshly isolated spleen dendritic cells and epidermal Langerhans cells undergo similar phenotypic and functional changes during short term culture. *J Immunol* 1990;*145*:2820-6.

478. **Inaba K, Witmer-Pack M, Inaba M, Hathcock KS, Sakuta H, Azuma M, Yagita H, Okumura K, Linsley PS, Ikehara S, Muramatsu S, Hodes RJ, Steinman RM**. The tissue distribution of the B7-2 costimulator in mice: abundant expression on dendritic cells in situ and during maturation in vitro. *J Exp Med* 1994;*180*:1849-60.

479. **Armstrong LR, Christensen PJ, Paine R, Chen GH, McDonald RA, Lim TK, Toews GB**. Regulation of the immunostimulatory activity of rat pulmonary interstitial dendritic cells by cell-cell interactions and cytokines. *Am J Respir Cell Mol Biol* 1994;*11*:682-91.

480. **Oreffo VIC, Morgan A, Richards RJ**. Isolation of Clara cells from the mouse lung. *Environ Health Perspect* 1990;*85*:51-64.

481. **Morris SC, Lees A, Finkelman FD**. In vivo activation of naive T cells by antigen-presenting B cells. *J Immunol* 1994;*152*:3777-85.

482. **Krieger JI, Grammer SF, Grey M, Chesnut RW**. Antigen presentation by splenic B cells: resting B cells are ineffective, whereas activated B cells are effective accessory cells for T cell responses. *J Immunol* 1985;*135*:2937-45.

483. **Xia WJ, Schneeberger EE, McCarthy K, Kradin RL**. Accessory cells of the lung. II. Ia+ pulmonary dendritic cells display cell surface antigen heterogeneity. *Am J Respir Cell Mol Biol* 1991;*5*:276-83.

484. **Vremec D, Zorbas M, Scollay R, Saunders DJ, Ardavin CF, Wu L, Shortman K**. The surface phenotype of dendritic cells purified from mouse thymus and spleen: investigation of the CD8 expression by a subpopulation of dendritic cells. *J Exp Med* 1992;*176*:47-58.

485. **Schwartz RH**. A cell culture model for T lymphocyte clonal anergy. *Science* 1990;*248*:1349-56.

486. **Weissler JC, Lyons CR, Lipscomb MF, Toews GB**. Human pulmonary macrophages: functional comparison of cells obtained from whole lung and by bronchoalveolar lavage. *Am Rev Respir Dis* 1986;*133*:477

487. **Otani T, Nakamura S, Toki M, Motodo R, Kurimoto M, Orita K**. Identification of IFN-gamma-producing cells in IL-12/IL-18-treated mice. *Cellular Immunology* 1999;*198*:111-9.

488. **Trinchieri G, Gerosa F**. Immunoregulation by interleukin-12. *J Leukoc Biol* 1996;*59*:505-11.

489. **Wills-Karp M**. Interleukin-12 as a target for modulation of the inflammatory response in asthma. *Allergy* 1998;*53*:113-9.

490. **D'Andrea A, Aste-Amezaga M, Valiante NM**. Interleukin-10 inhibits human lymphocyte IFN-γ production by suppressing natural killer cell stimulatory factor/interleukin-12 synthesis in accessory cells. *J Exp Med* 1993;*178*:1041-8.

491. **Fiorentino DF, Zlotnik A, Mosmann TR**. IL-10 inhibits cytokine production by activated macrophages. *J Immunol* 1991;*147*:3815

492. **Akbari O, DeKruyff H, Umetsu DT**. Pulmonary dendritic cells producing IL-10 mediate tolerance induced by respiratory exposure to antigen. *Nat Immunol* 2001;*2*:725-31.

493. **du Bois RM**. Interferon gamma-1b for the treatment of idiopathic pulmonary fibrosis. *N Engl J Med* 1999;*341*:1302-4.

494. **Zhu Z, Ma B, Zheng T, Homer RJ, Lee CG, Charo IF, Noble P, Elias JA**. IL-13-induced chemokine responses in the lung: role of CCR2 in the pathogenesis of IL-13-induced inflammation and remodeling. *J Immunol* 2002;*168*:2953-62.

495. **Macatonia SE, Hosken NA, Litton M, Vieira PL, Hsieh CS, Culpepper JA, Wysocka G, Trinchieri G, Murphy KM, O'Garra A**. Dendritic cells produce IL-12 and direct the development of Th1 cells from naive $CD4^+$ T cells. *J Immunol* 1995;*154*:5071-9.

496. **Macatonia SE, Hsieh CS, Murphy KM, O'Garra A**. Dendritic cells and macrophages are required for Th1 development of $CD4^+$ T cells from alpha beta TCR transgenic mice: Il-12

substitution for macrophages to stimulate IFN-gamma production is IFN-gamma-dependent. *Int Immunol* 1993;*5*:1119-28.

497. **Hilkens CM, Kalinski P, de Boer M, Kapsenberg ML**. Human dendritic cells require exogenous interleukin-12-inducing factors to direct the development of naive T-helper cells toward the Th1 phenotype. *Blood* 1997;*90*:1920-6.

498. **Trinchieri G, Scott P**. The role of interleukin 12 in the immune response, disease and therapy. *Immunol Today* 1994;*15*:460-3.

499. **Holt PG, Batty J, Turner K**. Inhibition of specific IgE responses in mice by specific exposure to inhaled antigen. *Immunology* 1981;*42*:409-17.

500. **McMenamin C, Holt PG**. The natural immune response to inhaled soluble protein antigens involves major histocompatibility complex (MHC) class I-restricted $CD8^+$ T cell-mediated but MHC class II-restricted $CD8^+$ T cell-dependent immune deviation resulting in selective suppression of immunoglobulin E production. *J Exp Med* 1993;*178*:889-99.

501. **Sedgwick JD, Holt PG**. Induction of IgE-secreting cells and IgE isotype-specific suppressor T cells in the respiratory lymph nodes of rats in response to antigen inhalation. *Cellular Immunology* 1985;*94*:182-94.

502. **Hoyne GF, Asknonas BA, Hetzel C, Thomas WR, Lamb JR**. Regulation of house dust mite responses by inhaled peptides: transient activation precedes the development of tolerance *in vivo*. *Int Immunol* 1996;*8*:335-42.

503. **Lambrecht BN, De Veerman M, Coyle AJ, Gutierrez-Ramos JC, Thielemans K, Pauwels RA**. Myeloid dendritic cells induce Th2 responses to inhaled antigen, leading to eosinophilic airway inflammation. *J Clin Invest* 2000;*106* :551-9.

504. **Khanna A, Morelli AE, Zhong C, Takayama T, Lu L, Thomson AW**. Effects of liver-derived dendritic cell progenitors on Th1- and Th2-like cytokine responses *in vitro* and *in vivo*. *J Immunol* 2000;*164*:1346-54.

505. **Liu L, Rich BE, Inobe J, Chen W, Weiner HL**. Induction of T_h2 cell differentiation in the primary immune response: dendritic cells isolated from adherent cell culture treated with IL-10 prime naive $CD4^+$ T cells to secrete IL-4. *Int Immunol* 1998;*10*:1017-26.

506. **Weiner HL**. The mucosal milieu creates tolerogenic dendritic cells and T_R1 and T_H3 regulatory cells. *Nat Immunol* 2001;*2*:671-2.

507. **Holt PG**. Regulation of antigen-presenting function(s) in lung and airway tissues. *Eur Respir J* 1993;*6*:120-9.

508. **Strickland DH, Kees UR, Holt PG**. Regulation of T-cell activation in the lung: isolated lung T cells exhibit surface phenotypic characteristics of recent activation in including down-modulated T-cell receptors, but are locked in to the G0/G1 phase of the cell cycle. *Immunology* 1996;*87*:242-9.

509. **Liew FY, Li Y, Severn A**. A possible novel pathway of regulation by murine T helper type-2 (Th2) cells of a Th1 cell activity via the modulation of the induction of nitric oxide synthase on macrophages. *Eur J Immunol* 1991;*21*:2489-94.

510. **Howarth PH, Redington AE, Springall DR, Martin U, Bloom SR, Polak JM**. Epithelially derived endothelin and nitric oxide in asthma. *Int Arch Allergy Immunol* 1995;*107*:228-30.

511. **Bingisser RM, Holt PG.** Immunomodulating mechanisms in the lower respiratory tract: nitric oxide mediated interactions between alveolar macrophages, epithelial cells, and T-cells. *Swiss Med Wkly* 2001;*131*:171-9.

512. **Stein M, Keshav S, Harris N, Gordon S.** Interleukin 4 potently enhances murine macrophage mannose receptor activity: a marker of alternative immunologic macrophage activation. *J Exp Med* 1992;*176*:287-92.

513. **Goerdt S, Orfanos CE.** Other functions, other genes: alternative activation of antigen-presenting cells. *Immunity* 1999;*10*:137-42.

514. **Steinbrink K, Jonuleit H, Knop J, Enk AH.** Induction of tolerance by IL-10-treated dendritic cells. *J Immunol* 1997;*159*:4772-80.

515. **Kuchroo VK, Das MP, Brown JA, Ranger AM, Zamvil SS, Sobel RA, Weiner HL, Nabavi N, Glimcher LH.** B7-1 and B7-2 costimulatory molecules activate differentially the Th1/Th2 developmental pathways: application to autoimmune disease therapy. *Cell* 1995;*80*:707-18.

516. **Freeman GJ, Boussiotis VA, Anumanthan A, Bernstein GM, Ke XY, Rennert PD, Gray GS, Gribben JG, Nadler LM.** B7-1 and B7-2 do not deliver identical costimulatory signals, since B7-2 but not B7-1 preferentially costimulates the initial production of IL-4. *Immunity* 1995;*2*:523-32.

517. **Wills-Karp M, Luyimbazi J, Xu X, Schofield B, Neben TY, Karp CL, Donaldson DD.** Interleukin-13: central mediator of allergic asthma. *Science* 1998;*282*:2288-61.

518. **Lambrecht BN, Hoogsteden HC, Pauwels RA.** Dendritic cells as regulators of the immune response to inhaled allergen: recent findings in animal models of asthma. *Int Arch Allergy Immunol* 2001;*124*:432-46.

519. **Kovacs EJ, Kumar RK, O'Grady R.** Lymphokine regulation of macrophage derived growth factor secretion following pulmonary injury. *Am J Path* 1985;*121*:261-8.

520. **Kemmerich B, Rossing RH, Pennington JE.** Comparative oxidative microbicidal activity of human blood monocytes and alveolar macrophages and activation by recombinant gamma interferon. *Am Rev Respir Dis* 1987;*136*:266-70.

521. **Miller G, Pillarisetty VG, Shah AB, Lahrs S, Xing Z, DeMatteo RP.** Endogenous granulocyte-macrophage colony-stimulating factor overexpression in vivo results in the long-term recruitment of a distinct dendritic cell population with enhances immunostimulatory function. *J Immunol* 2002;*169*:2875-85.

522. **Gordon JR, Burd PR, Galli SJ.** Mast cells as a source of multifunctional cytokines. *Immunol Today* 1990;*11*:458-64.

523. **Sulavik SB.** A clinician's view. In: Phan SH, Thrall RS. eds. *Pulmonary fibrosis*. New York: Marcel Dekker, Inc., 1995:1-57.

524. **Ludewig B, Odermatt B, Landmann S.** Dendritic cells induce autoimmune diabetes and maintain disease via de novo formation of lymphoid tissue. *J Exp Med* 1998;*188*:1493-501.

525. **Strobl H, Knapp W.** TGF-beta1 regulation of dendritic cells. *Microbes & Infection* 1999;*1*:1283-90.

526. **Mouse Genome Sequencing Consortium.** The mouse genome. *Nature* 2002;*420*: